

A Macmillan Physics Text

Consulting Editor: Professor P. A. Matthews, F.R.S.

Other titles

MODERN ATOMIC PHYSICS: FUNDAMENTAL PRINCIPLES: B. Cagnac and
J.-C. Pebay-Peyroula
WAVES: D. R. Tilley

Nature-Macmillan Series

AN INTRODUCTION TO SOLID STATE PHYSICS AND ITS APPLICATIONS: R. J. Elliott
and A. F. Gibson
THE SPECIAL THEORY OF RELATIVITY: H. Muirhead
FORCES AND PARTICLES: A. B. Pippard

Forthcoming

AN INTRODUCTION TO NUCLEAR PHYSICS: D. M. Brink, G. R. Bishop and G. R.
Satchler
SYMMETRY IN PHYSICS: J. P. Elliott and P. G. Dawber
ELECTRICITY AND MAGNETISM: B. L. Morgan and R. W. Smith

MODERN ATOMIC PHYSICS: QUANTUM THEORY AND ITS APPLICATIONS

B. CAGNAC

Faculty of Science, University of Paris VI

J.-C. PEBAY-PEYROULA

Faculty of Science, University of Grenoble

Translated by J. S. Deech

J. J. Thomson Physical Laboratory

University of Reading

M

© Dunod 1971

© English language edition
The Macmillan Press 1975

All rights reserved. No part of this publication may be reproduced or transmitted, in any form or by any means, without permission.

Authorised English language edition of *Physique Atomique*, Tome 2
first published by Dunod, Paris, in 1971

First published in the United Kingdom 1975 by
THE MACMILLAN PRESS LTD
London and Basingstoke
Associated companies in New York Dublin
Melbourne Johannesburg and Madras

SBN 333 15082 1

Printed in Great Britain by
WILLIAM CLOWES & SONS, LIMITED
London, Colchester and Beccles

Contents

<i>Preface to the English Edition</i>	ix
<i>Glossary</i>	xi
<i>Introduction</i>	xvii
1 A Single Electron without Spin in a Central Potential—Quantum Treatment	1
1.1 Introduction	1
1.2 The Case of the Coulomb Field. Quantum Numbers and Energy	2
1.3 Position Probability of the Electron in a Hydrogen-like Atom	9
1.4 Comparison with the Bohr–Sommerfeld Model	13
1.5 The Non-Coulomb Central Potential—Lifting the Degeneracy in l	16
2 Independent Electron Approximation in a Central Potential. Electronic Configurations	22
2.1 The Various Interactions in a Complex Atom	22
2.2 The Energy Levels of a System of N Independent Electrons in a Central Potential. Configurations	25
2.3 The Pauli Principle and Degeneracy of a Configuration	28
2.4 The Periodic Classification of the Elements	31

3 Angular Momenta and Enumeration of the Energy Levels	39
3.1 Composition of Angular Momenta	40
3.2 Spin–Orbit Interaction	43
3.3 Principles of the Calculation of Energy Levels in Atoms with Many Electrons	47
3.4 Determination of the Angular Momenta and Enumeration of the Different Energy Levels of a Configuration	53
3.5 Summary	57
4 The Spectroscopy of Systems with One and Two Electrons	58
4.1 Selection Rules	59
4.2 An Atom with One Outer Electron, Taking into Account Electron Spin	61
4.3 Atoms with Two Electrons	65
4.4 Energy Levels of the Hydrogen Atom: Fine Structure of the Lines	75
4.5 X-Ray Spectra	81
5 Atomic Magnetism. The Zeeman and Paschen–Back Effects	85
5.1 The Hamiltonian of a Charged Particle in the Presence of an Electromagnetic Field	86
5.2 The Hamiltonian in the Presence of a Constant, Uniform Magnetic Field	90
5.3 The Zeeman Effect in a Weak Magnetic Field in the Case of L – S Coupling	93
5.4 The Paschen–Back Effect in a Strong Field. The Case of Intermediate Fields	99
5.5 The Zeeman Effect and the Paschen–Back Effect of Atoms with One or Two Electrons	105
6 The Nucleus and the Physics of the Atom	112
6.1 The Nucleus: Magnetic Moment and Angular Momentum	113
6.2 The Magnetic Hyperfine Structure of the Energy Levels	118
6.3 Magnetic Interactions between the Nucleus and the Electrons: Calculation of the Hyperfine Structure Constant	122
6.4 Corrections due to the Electrostatic Interaction between the Electrons and the Nucleus	125
6.5 The Hyperfine Structure of Spectral Lines	128
6.6 The Magnetism of an Atom Possessing Nuclear Spin. The Zeeman and Back–Goudsmit Effects	131
6.7 Energy Diagrams in the Intermediate Field Region. Effective Magnetic Moments	135
7 Experimental Methods in Atomic Physics	139
7.1 Introduction	139

CONTENTS	vii
7.2 Optical Spectroscopy	142
7.3 Radiofrequency Spectroscopy	154
7.4 Lifetimes and Oscillator Strengths	170
7.5 Electronic and Atomic Collisions	178
7.6 The Electric Dipole Moment of the Neutron and of the Electron	187
7.7 Muonium, Mesic Atoms and Positronium	191
Appendixes	200
<i>Appendix 1.</i> Electromagnetic Formulae Adaptable to All the Usual Systems of Units	200
<i>Appendix 2.</i> Review of the Classical Theory of Radiation	202
<i>Appendix 3.</i> Multipole Moments	214
<i>Appendix 4.</i> Non-Relativistic Elastic Collisions	229
<i>Appendix 5.</i> The Representation of Vector and Scalar Operators. The Wigner–Eckart Theorem	232
<i>Appendix 6.</i> Historical Summary of Atomic Physics	239
<i>Bibliography</i>	243
<i>Index</i>	246

past three years have been included where they have an important bearing on the subject matter. Alterations, other than corrections and those due to changes of terminology, have been inserted as translator's footnotes.

(4) SI units (rationalised MKS) have been used throughout, though the coefficient κ (see preface to the French edition) is retained in relevant formulae. Thus, despite some spectroscopists' aversion to changing, for example, from ångström units to a subunit of the metre or from gauss to tesla, numerical values are always given in SI.

(5) Important names and dates are given for their historical interest only and accordingly precise references are usually omitted, as in the French edition. Where the French edition refers to textbooks that have not been translated into English, an English substitute has been given.

I should like to express my thanks to Dr M. H. Tinker for reading and commenting on the entire translated manuscript, to my wife who sacrificed much of her time for several months in preparing the final typescript version, and finally to the publishers for their continued encouragement and helpfulness.

J. J. Thomson Physical Laboratory
Reading
December 1973

J.S.D.

Glossary

•

1 Latin Alphabet

a	{	acceleration semi-major axis of an ellipse, or other length
A	{	magnetic vector potential amplitude of a sinusoidal function magnetic moment coupling constant probability of spontaneous emission atomic mass number
\mathcal{A}		atomic mass (approximately equal to A in CGS or to $A/1000$ in MKS)
b	{	impact parameter in collision problems semi-minor axis of an ellipse, or other length
B	{	magnetic induction vector, usually called magnetic field (the excitation vector $H = (1/\mu_0\mu_r) \mathbf{B}$ is hardly ever used) absorption and induced emission probability coefficients (Einstein notation) amplitude of a sinusoidal function
\mathcal{B}		magnetic field vector
c		velocity of light

- C { constant in a Coulomb law of force ($W(r) = C/r$)
Curie constant of magnetic susceptibilities
capacitance
torsion constant of a wire
- d differential
- d symbol for the quantum number $l = 2$ (total orbital angular momentum of an electron)
- D { electric induction vector
probability density
distance
symbol for the quantum number $L = 2$ (total orbital angular momentum of an atom)
- \mathcal{D} intensity of a beam of particles per unit cross-sectional area ($N = \mathcal{D}tS$)
- e elementary positive charge $e = 1.6 \times 10^{-19}$ C
- e base of napierian logarithms $e = 2.7183$
- E { electric field vector
algebraic value of the total energy of an atomic state
- \mathcal{E} complex function associated with the electric field of a wave
- f { a function
force vector
oscillator strength
symbol for the quantum number $l = 3$ (orbital angular momentum of an electron)
- F { resultant vector for a system of forces
symbol for the quantum number $L = 3$ (orbital angular momentum of an atom)
- g { Landé factor
symbol for the quantum number $l = 4$ (orbital angular momentum of an electron)
- G { statistical weight or order of degeneracy
symbol for the quantum number $L = 4$ (total orbital angular momentum of an atom)
- h Planck's constant ($\hbar = h/2\pi$)
- H Hamiltonian operator
- \mathcal{H} Hamiltonian function
- i square root of -1 , the base of imaginary numbers
- i { index number
angle of incidence

I	{	magnitude of an electric current moment of inertia nuclear spin quantum number and the corresponding vector
j	{	the electric current density vector index number quantum number of angular momentum and the corresponding vector
J		total angular momentum quantum number of an atom, and the corresponding vector
k	{	Boltzmann's constant wave vector an integer
K	{	contact potential difference absorption coefficient symbol for the principal quantum number $n = 1$
l	{	a length orbital angular momentum quantum number and the corresponding vector
L	{	luminance the total orbital angular momentum quantum number of an atom and the corresponding vector symbol for the principal quantum number $n = 2$
\mathcal{L}		lagrangian function
m	{	mass, especially mass of the electron magnetic quantum number
M	{	molecular mass mass, especially the mass of an atom or a nucleus intensity of magnetisation vector symbol for the principal quantum number $n = 3$
\mathcal{M}		magnetic moment vector
n	{	number of particles per unit volume principal quantum number
N	{	an integer (dimensionless) unit normal vector symbol for the principal quantum number $n = 4$
\mathcal{N}		Avogadro's number
O		symbol for the principal quantum number $n = 5$

- p { momentum or impulse vector
electric dipole-moment vector
index number
population of an energy level
symbol for the quantum number $l = 1$ (orbital angular momentum of an electron)
- P { power
polarisation vector of a dielectric
symbol for the quantum number $L = 1$ (total orbital angular momentum of an atom)
symbol for the principal quantum number $n = 6$
- \mathcal{P} generalised impulse vector
- q algebraic electric charge (especially charge on the electron $q = -e$)
- Q { electric charge
quality factor of a resonant cavity or a resonant circuit reduced quadrupole moment
- \mathcal{Q} components of the quadrupole tensor
- r radius vector, distance between two points
- R { distance between two points
electric resistance
Rydberg constant for atomic spectra
gas constant for a perfect gas
- \mathcal{R} radial wave function
- s { spin quantum number and the corresponding vector
screening coefficient
symbol for the quantum number $l = 0$ (orbital angular momentum of an electron)
- S { area
total spin quantum number of an atom and the corresponding vector
symbol for the quantum number $L = 0$ (total orbital angular momentum of an atom)
- t time
- T { absolute temperature
period
spectral term
- \mathcal{T} work
- u { energy density
unit vector
transverse component of the magnetisation \mathbf{M} in a rotating frame
- U internal energy

v	{	velocity vector transverse component of the magnetisation M in a rotating frame
V	{	electrostatic potential or electromotive force exceptionally, velocity vector
\mathcal{V}		volume
w		a small energy
W		energy in general, and especially potential energy $W(r)$
x X	}	co-ordinate
y		co-ordinate
Y	{	co-ordinate angular wave functions of hydrogen (spherical harmonics)
z		co-ordinate
Z	{	co-ordinate atomic number of an element statistical partition function

2 Greek Alphabet

α	{	fine structure constant ($\alpha = e^2/4\pi \epsilon_0 \hbar c$) angle direction cosine name of a type of particle
β	{	Bohr magneton angle direction cosine name of a type of particle (β^- and β^+ rays)
γ	{	gyromagnetic ratio direction cosine name of a region of the electromagnetic spectrum
Γ		moment of a force or resultant moment of a system of forces
δ		increment, difference
Δ		Laplacian operation
Δ	{	width of a line correction applied to an energy value following a perturbation calculation
ϵ	{	constant depending on units, ϵ_0 , (in CGS ϵ_0 is replaced by $1/4\pi$) dielectric constant ϵ_r a conical eccentricity

θ	angle, especially latitude in spherical co-ordinates
Θ	{ angular wave function Debye temperature
κ	constant depending on units: $\epsilon_0 \mu_0 c^2 = \kappa^2$ { $\kappa = 1$ in MKSA system $\kappa = c$ in gaussian system
λ	wavelength
Λ	Compton wavelength ($\Lambda = h/mc$)
μ	{ constant depending on units, μ_0 , (in c.g.s., μ_0 is replaced by 4π) magnetic permeability reduced mass
ν	frequency
ξ	co-ordinate
ϖ	{ pressure probability
π	{ 3.1416 . . . symbol for a polarisation of a wave (parallel to a magnetic field)
Π	product
ρ	{ density electric charge density particular values of a radius vector
σ	{ angular momentum vector cross-section symbol for a polarisation of a wave (circular or perpendicular to a field)
Σ	summation
τ	time constant (lifetime, relaxation time)
ϕ	angle, especially longitude in spherical co-ordinates
Φ	{ magnetic flux angular wave function
χ	{ angle magnetic susceptibility
ψ	{ angle total wave function
ω	{ angular velocity of rotation angular frequency of a sinusoidal function
Ω	{ solid angle exceptionally, angular velocity of rotation

Introduction

The first volume of this two-volume series, *Modern Atomic Physics—Fundamental Principles*, dealt with fundamental classical problems by describing experiments involving basic properties of atoms: quantisation of energy, wave-particle duality, the planetary model of the atom, and the magnetic moment and angular momentum of atoms. The great contribution of atomic physics to the birth and development of theoretical physics was stressed in this first volume, but it was designed to be readily understood by those who have not studied quantum mechanics; its language was therefore essentially classical. As a result, we were unable to introduce those aspects of atomic physics that could not be readily understood without the use of quantum theory, or at the very least their results. For this reason a second volume is required.

Two themes will be found in this volume. The first, forming the basis of chapters 1 to 6, is a logically developed account of atomic structure, using the methods of quantum mechanics. It is accordingly assumed that the reader has already studied quantum mechanics, at least at an elementary level. However, the first four chapters do not use the formal aspects of quantum theory and an understanding of the general ideas of quantum mechanics will suffice. We have tried to avoid writing a purely theoretical book, and in order to remain as closely in contact with the real physical world as possible, we have endeavoured to provide a considerable amount of experimental data. The wish

to make this book of use to students at various levels has led us, especially in chapter 5, to provide for these different requirements in that various sections can be omitted without affecting comprehension of the whole.

Chapter 7 presents the second theme of this book. The study of atomic systems has always been of importance in the elaboration and development of physical concepts, and atomic physics is an area where the interaction between the experimentalist and theoretician has been highly beneficial. This mutual co-operation, especially marked in the early part of this century, remains of value. The discovery of the 'Lamb Shift' (see p. 80), opened up the field of quantum electrodynamics which itself is now a well understood and most accurate physical theory. At present, many basic and important problems in quantum electrodynamics are being studied: problems concerning the relationship between the electron and the muon; the evaluation of hadronic corrections; problems of possible symmetry violations in electrodynamics. Furthermore, the study of so-called 'exotic atoms' (muonic, pionic or kaonic atoms) should provide a wealth of information about nuclear structure. We have not attempted to present an exhaustive account of these problems, as this would have required a series of books, but by means of a few examples, we have aimed simply at providing an insight into current research in atomic physics.

In writing this book, we have tried to show the student how to handle for himself the results of an experiment and to give him a sense of orders of magnitude necessary for justifying those approximations without which few calculations in physics would be possible. This prevents us from putting, in the way theoreticians do: $h = c = 1$; so we had to confront the irritating problem of units. Since French students have for several years used SI (rationalised MKS) units, we did not want to interfere with this practice, and we have used rationalised formulae. However, most publications and major works in atomic physics, even the most recent, use the non-rationalised gaussian system and one should be able to convert from one to the other. To this end, we have introduced into our formulae a coefficient κ defined by the relation

$$\kappa = \epsilon_0 \mu_0 c^2$$

- (1) In the SI system, $\kappa = 1$: the coefficient κ can be simply disregarded in all the formulae, which then become normal rationalised formulae, and the numerical values of the constants are

$$4\pi\epsilon_0 = \frac{1}{9 \times 10^9}; \quad \frac{\mu_0}{4\pi} = 10^{-7}$$

- (2) In the gaussian system, where electrical units from the electrostatic CGS system and magnetic units from the electromagnetic CGS system are used simultaneously, the coefficients are determined thus

$$4\pi\epsilon_0 = 1; \quad \frac{\mu_0}{4\pi} = 1 \quad \text{and} \quad \kappa = c$$

Appendix 1 gives a set of electromagnetic formulae showing how the classical formulae should be modified to take account of the coefficient κ . We have taken these modified formulae as the starting point for all our calculations in atomic physics.

Finally, we should like to thank all the staff and research workers in our laboratories, both in Paris and Grenoble, who have helped us to prepare this new presentation of atomic physics, But above all, we must thank Professors Kastler and Brossel for all their inspiration, both by their teaching and in the everyday life of the laboratory.

B. Cagnac
J.-C. Pebay-Peyroula

1

A Single Electron without Spin in a Central Potential—Quantum Treatment

1.1 Introduction

Volume 1 showed that many aspects of atomic physics could be understood in terms of simple models, using methods of analysis very similar to those of classical mechanics. Nevertheless, when a detailed study is required, much less natural and less obvious hypotheses need to be made and it then becomes very difficult to assure good agreement between classical theory and experiment.

The methods of quantum mechanics on the other hand appear eminently suited to atomic physics. Their gradual evolution—non-relativistic wave mechanics, Dirac's relativistic mechanics, quantum field theory—has enabled the understanding and accurate description of many phenomena; furthermore, as will be seen in chapter 4, the concept of electron spin arose as a result of the development of quantum mechanics. However, it should immediately be pointed out that a rigorous treatment is possible only in the case of the hydrogen atom and even this is very difficult. The study of more complex systems could not be undertaken without the help of various methods of approximation. This chapter will show how to describe the behaviour of an electron without spin in a central potential. This study covers the case of the hydrogen atom and of the hydrogen-like atoms, having a single electron as described in volume 1, chapter 6. Nevertheless, the reader should try to find a wider theme in this chapter: a number of assertions made previously should

become clearer and the results for an electron in a central potential will be a basis for the study of atoms with many electrons.

The quantum study of the motion of an electron of a hydrogen-like atom is dealt with in books on quantum mechanics. To ensure this book has the necessary continuity the main points have been reviewed with emphasis on the physics and on the description of the results. The notation is that used in the book on quantum mechanics in this same series from which we have drawn considerably. The reader may often find it convenient to refer to it.†

1.2 The Case of the Coulomb Field. Quantum Numbers and Energy

1.2.1 Schrödinger's equation

The problem concerns an electron of charge $-e$ orbiting in the coulomb electrostatic field of the nucleus. If the nucleus is a proton of positive charge e , the problem studied is that of the hydrogen atom. If the nucleus carries a charge equal to $2e$, $3e$, . . . , the system under consideration would be an ionised atom, known as a hydrogen-like atom. For the sake of generality, we shall take the charge of the nucleus equal to Ze , Z being the atomic number.

The potential energy of the electron in the coulomb potential of the nucleus is

$$W(r) = \frac{C}{r} = -\frac{1}{4\pi\epsilon_0} \times \frac{Ze^2}{r}$$

and by introducing the reduced mass μ of the electron (see volume 1, chapter 6) the hamiltonian for the problem is

$$H = -\frac{\hbar^2}{2\mu} \Delta + W(r) = -\frac{\hbar^2}{2\mu} \Delta + \frac{C}{r}$$

Schrödinger's equation may be written as

$$\Delta\psi + \frac{2\mu}{\hbar^2} \left(E - \frac{C}{r} \right) \psi = 0$$

and by expressing the laplacian operator in spherical polar co-ordinates

$$\begin{aligned} \frac{1}{r^2} \frac{\partial}{\partial r} \left(r^2 \frac{\partial \psi}{\partial r} \right) + \frac{1}{r^2 \sin \theta} \frac{\partial}{\partial \theta} \left(\sin \theta \frac{\partial \psi}{\partial \theta} \right) + \frac{1}{r^2 \sin^2 \theta} \frac{\partial^2 \psi}{\partial \phi^2} \\ + \frac{2\mu}{\hbar^2} \left(E - \frac{C}{r} \right) \psi = 0 \end{aligned} \quad (1.1)$$

† Y. Ayant and E. Belorizky, *Cours de mécanique quantique*. This book has not been translated into English. As an alternative, readers are recommended to consult books by P. T. Matthews, *Introduction to Quantum Mechanics*, and A. Messiah, *Quantum Mechanics*.

It may be shown quite generally that for motion in a central field of force where W depends only on r , that the solution of the Schrödinger equation must be of the form

$$\psi(r, \theta, \phi) = \mathcal{R}(r) Y(\theta, \phi)$$

$Y(\theta, \phi)$ being the eigenfunctions of σ_L^2 , σ_L being the orbital angular momentum (see textbook on quantum mechanics). Using the assumed form of $\psi(r, \theta, \phi)$, we may write the Schrödinger equation as

$$\frac{1}{\mathcal{R}} \frac{d}{dr} \left(r^2 \frac{d\mathcal{R}}{dr} \right) + \frac{2\mu}{\hbar^2} r^2 \left(E - \frac{C}{r} \right) = - \frac{1}{Y} \left[\frac{1}{\sin \theta} \frac{\partial}{\partial \theta} \left(\sin \theta \frac{\partial Y}{\partial \theta} \right) + \frac{1}{\sin^2 \theta} \frac{\partial^2 Y}{\partial \phi^2} \right]$$

Since the two sides of this equation depend on different variables, they can equal each other only if they are equal to a constant λ . The following two equations must be true simultaneously

$$\left\{ \begin{array}{l} \text{(a) } \frac{1}{r^2} \frac{d}{dr} \left(r^2 \frac{d\mathcal{R}}{dr} \right) + \left[\frac{2\mu}{\hbar^2} \left(E - \frac{C}{r} \right) - \frac{\lambda}{r^2} \right] \mathcal{R} = 0 \\ \text{(b) } \frac{1}{\sin \theta} \frac{\partial}{\partial \theta} \left(\sin \theta \frac{\partial Y}{\partial \theta} \right) + \frac{1}{\sin^2 \theta} \frac{\partial^2 Y}{\partial \phi^2} + \lambda Y = 0 \end{array} \right. \quad (1.2)$$

Only radial variables come into equation (a) and only angular variables into equation (b).

1.2.2 Study of the angular part

First it should be noted that equation (b) is separable by putting

$$Y(\theta, \phi) = \Theta(\theta) \Phi(\phi)$$

Θ and Φ satisfy the differential equations

$$\left\{ \begin{array}{l} \text{(a) } \frac{d^2 \Phi}{d\phi^2} \times \frac{1}{\Phi} = -k \\ \text{(b) } \frac{1}{\sin \theta} \frac{d}{d\theta} \left(\sin \theta \frac{d\Theta}{d\theta} \right) + \left(\lambda - \frac{k}{\sin^2 \theta} \right) \Theta = 0 \end{array} \right. \quad (1.3)$$

The general solution of equation (1.3a) may be written without difficulty

$$\Phi = A e^{i\sqrt{(k)} \phi} + B e^{-i\sqrt{(k)} \phi}$$

The existence of a physically acceptable solution requires that Φ should be a periodic function of the angle ϕ , so that

$$\Phi(\phi) = \Phi(\phi + 2\pi) \quad \text{or} \quad e^{i\sqrt{(k)}\phi} = e^{i\sqrt{(k)}(\phi+2\pi)}$$

$e^{i\sqrt{(k)}2\pi}$ must be equal to unity, which is possible only if $\sqrt{(k)}$ is an integer. The solution will be taken as

$$\Phi = A e^{im\phi} \quad (1.4)$$

by putting $k = m^2$, m being a positive or negative integer.

This value of k is substituted into equation (1.3b) which we rewrite by a change of variables $\omega = \cos\theta$, the function $\Theta(\theta)$ becoming $P(\omega)$

$$\frac{d}{d\omega} \left[(1 - \omega^2) \frac{dP}{d\omega} \right] + \left(\lambda - \frac{m^2}{1 - \omega^2} \right) P = 0 \quad (1.5)$$

Generally this second-order differential equation has two independent solutions that become infinite for $\omega = \pm 1$. However, we are studying the problem of the electron-nucleus bound state; consequently, whatever the values of the variables, the wavefunction must become zero at infinite distance. Therefore the general solution is not physically acceptable. Nevertheless, if

$$\lambda = l(l + 1) \quad \text{where } l \text{ is integral and } l \geq 0$$

one of the solutions can be finite for all values of ω :

for $m = 0$, $P(\omega)$ will be a Legendre polynomial;

for $m \neq 0$, a finite solution will be possible only if $|m| \leq l$.

In the latter case, the solution will be an associated Legendre polynomial $P_l^m(\omega)$ such that

$$P_l^{|m|}(\omega) = (1 - \omega^2)^{|m|/2} \frac{d^{|m|}}{d\omega^{|m|}} P_l(\omega) \quad (1.6)$$

The solution of the angular part of the Schrödinger equation will therefore be

$$Y_{lm}(\theta, \phi) = N_{lm} P_l^{|m|}(\cos\theta) \cdot e^{im\phi} \quad (1.7)$$

N_{lm} being a normalisation constant which we shall define later. Table 1.1 gives expressions for P_l^m for the commonest values of l .

$Y(\theta, \phi)$ are the eigenfunctions of the orbital angular momentum σ_L (see section 1.2.1); the quantum numbers l and m therefore allow the orbital angular momentum associated with the electron motion to be expressed

$$\begin{cases} \text{magnitude:} & |\sigma_L| = \sqrt{[l(l+1)]}\hbar \\ \text{component along Oz:} & (\sigma_L)_z = m\hbar \end{cases}$$

Table 1.1 Associated Legendre polynomials entering into the expression for the angular function $Y(\theta, \varphi)$ (see equation (1.7))

l	m	$P_l^m(\cos \theta)$
0	0	1
1	1	$\sin \theta$
1	0	$\cos \theta$
2	2	$3 \sin^2 \theta$
2	1	$3 \cos \theta \sin \theta$
2	0	$\frac{1}{2}(3 \cos^2 \theta - 1)$
3	3	$15 \sin^3 \theta$
3	2	$15 \cos \theta \sin^2 \theta$
3	1	$\frac{3}{2}(5 \cos^2 \theta - 1) \sin \theta$
3	0	$\frac{1}{2}(5 \cos^3 \theta - 3 \cos \theta)$

1.2.3 Study of the radial part

The results of the previous section require that λ has the value $l(l+1)$ in the radial equation (1.2a).

After rewriting the unknown function $\mathcal{R} = \chi(r)/r$, the radial equation becomes

$$\frac{d^2 \chi}{dr^2} + \left[\frac{2\mu}{\hbar^2} \left(E - \frac{C}{r} \right) - \frac{l(l+1)}{r^2} \right] \chi = 0 \quad (1.8)$$

This differential equation may be solved by using the reduced quantities

$$A = -2\mu E/\hbar^2, \quad B = -2\mu C/\hbar^2, \quad \lambda = l(l+1) \quad (1.9)$$

(We restrict ourselves to bound states of negative energy E .) The parameters A and B are positive, and the use of reduced quantities leads to

$$\frac{d^2 \chi}{dr^2} - \left(A - \frac{B}{r} + \frac{\lambda}{r^2} \right) \chi = 0 \quad (1.10)$$

The reader may find in quantum mechanics books a discussion leading to the solution of this reduced equation. Let us review the main steps.

(1) Finding the 'asymptotic' behaviour of $\chi(r)$ as r tends to infinity, the terms in $1/r$ and $1/r^2$ in equation (1.10) may be neglected, and the solution is then straightforward

$$\chi_{\text{asympt.}}(r) = e^{\pm\sqrt{A}r}$$

(2) Taking this asymptotic behaviour into account, $\chi(r)$ will be found to be of the form

$$\chi(r) = u(r) e^{-\sqrt{A}r}$$

$u(r)$ is a polynomial and the negative sign in front of the exponential is chosen so that the wavefunction does not become infinite for infinite r , which would be incompatible with the problem under consideration. $u(r)$ must satisfy the equation

$$\frac{d^2 u}{dr^2} - 2\sqrt{A} \frac{du}{dr} + \left(\frac{B}{r} - \frac{\lambda}{r^2} \right) u = 0 \tag{1.11}$$

(3) The solution of this differential equation will be obtained in the form of a series in increasing powers of r . However, in order to satisfy the physical conditions of the problem (see preceding section), this solution must remain finite for all values of r . This can be satisfied only if the series expansion has a limited number of terms. The recurrence relation giving an expression for the coefficients of the different terms of the series must therefore ‘cut off’ at a certain order p so that the coefficients of the terms for powers of r greater than p are zero. Calculation of these coefficients shows that this is possible only if the constant B is a multiple of $2\sqrt{A}$:

$$B = (l + p + 1)2\sqrt{A} = n \cdot 2\sqrt{A} \tag{1.12}$$

It may be shown that all the coefficients of the terms of power greater than $p = n - l - 1$ are zero. The integral number n must therefore satisfy the condition

$$n \geq l + 1$$

When this condition is satisfied, $u(r)$ is a finite polynomial, and by returning to the expression for $\mathcal{R}(r)$, one finds that

$$\mathcal{R} = K \left(\frac{2Zr}{na_1} \right)^l e^{-Zr/na_1} L_{n+l}^{2l+1} \left(\frac{2Zr}{na_1} \right) \tag{1.13}$$

$\left\{ \begin{array}{l} a_1 \text{ being the radius of the first Bohr orbit of the hydrogen atom (see} \\ \text{volume 1, chapter 6)} \\ \\ a_1 = \frac{2}{B} = - \frac{\hbar^2}{\mu C} = 4\pi\epsilon_0 \frac{\hbar^2}{\mu e^2} \\ \\ \text{and } K \text{ is a normalisation constant.} \end{array} \right.$

$L_{n+l}^{2l+1}(x)$ represents a polynomial derived from the Laguerre polynomials $L_k(x)$ by the relation

$$L_k^s(x) = \frac{d^s}{dx^s} L_k(x)$$

Table 1.2 gives the expression for L_{n+l}^{2l+1} for some values of n and l . Figure 1.1 shows the form of the radial function $\mathcal{R}(r)$.

Table 1.2 Polynomials $L_{n+l}^{2l+1}(x)$ entering into the radial functions (x is proportional to r) (see equation (1.13))

n	l	$L_{n+l}^{2l+1}(x)$
1	0	$-1!$
2	1	$-3!$
3	2	$-5!$
4	3	$-7!$
2	0	$2x - 4$
3	1	$24x - 96$
4	2	$720x - 5760$
3	0	$-3x^2 + 18x - 18$
4	1	$-60x^2 + 600x - 1200$
4	0	$4x^3 - 48x^2 + 144x - 96$

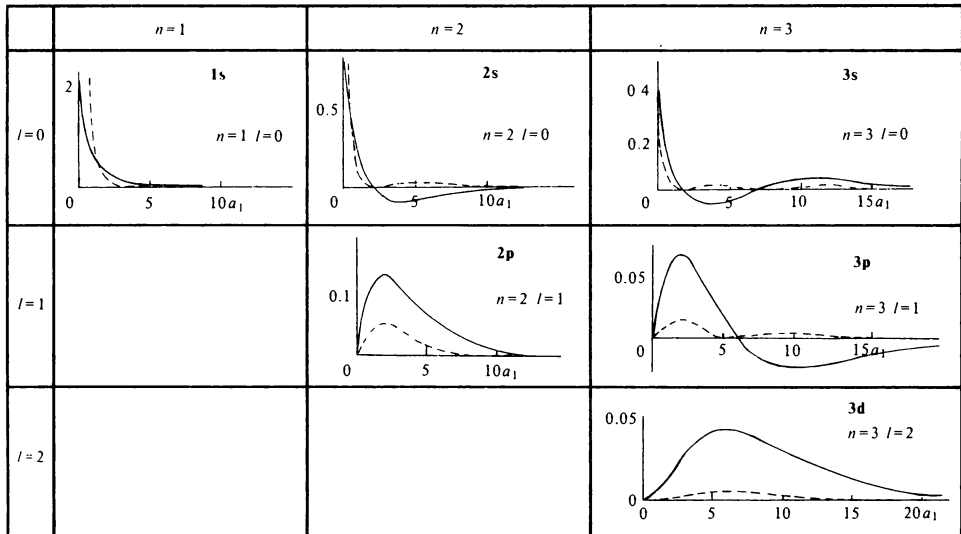


Figure 1.1 The radial part $\mathcal{R}(r)$ of the wave function of the hydrogen atom: the abscissa is the radius vector measured in units of a_1 , a_1 being the radius of the first Bohr orbit ($a_1 \approx 53$ pm); the ordinate is the dimensionless number $(a_1)^{3/2} \mathcal{R}(r)$; for comparison, the value of \mathcal{R}^* is in dotted lines

1.2.4 Main results

The solution of Schrödinger's equation (the stages of which were discussed above) with regard to the requirements of the physical problem propounded, has led to the definition of:

- (1) the magnetic quantum number m entering into the angular part in ϕ ; this quantum number m enables the observable values of the component σ_z of the orbital angular momentum to be obtained;
- (2) the quantum number l , which allows an acceptable solution for $\Theta(\theta)$ to be found, and moreover has to satisfy $l \geq |m|$ (this quantum number l characterises the magnitude of the orbital angular momentum);
- (3) the principal quantum number n , introduced into the solution of the radial equation, such that $n \geq l + 1$.

The eigenvalues E of the hamiltonian H , that is to say the possible values for the total energy of the electron-nucleus system, may be deduced from the condition (1.12), which we transform by using the expressions (1.9) for the reduced parameters A and B

$$\frac{4\mu^2 C^2}{\hbar^4} = -4n^2 \frac{2\mu E}{\hbar^2}$$

This requires that the possible values of energy depend only on n ; consequently they may be written

$$E_n = -\frac{\mu C^2}{2\hbar^2 n^2} = -\frac{Z^2}{n^2} Rhc \quad R \text{ is Rydberg's constant}$$

(see volume 1, chapter 6) (1.14)

Thus, without making any assumption other than Schrödinger's equation, we again derive the energy values deduced experimentally from the spectrum of the hydrogen atom. These energy values E depend only on the value of the quantum number n , they do not involve the values of l and m ; several distinct quantum states correspond to the same energy E . These energy levels are said to be degenerate, with a certain *order of degeneracy*, equal to the number of these distinct quantum states, in other words, to the number of possible combinations that can be formed with different values of l and m .

Bohr's theory of circular orbits did not introduce this concept of degeneracy; its introduction in this chapter should be particularly noted by the reader.

Notation. To characterise the various electronic states, frequent use is made of a pair of symbols, formed from a number, giving the value of n , and a letter, symbolising the value of l , according to the following code:

Value of the quantum number	0	1	2	3	4	etc.
Letter symbol		s	p	d	f	g etc.

the values for $l > 3$ following alphabetical order. The state 3p for example, is characterised by the values $n = 3$, $l = 1$. The symbols s, p, d . . . arise for historical reasons, and have no logical explanation.

1.3 Position Probability of the Electron in a Hydrogen-like Atom

Information about the locality of the electron (described by the wavefunction solution of the Schrödinger equation) will be obtained from the position probability. This problem will be treated in spherical co-ordinates and to avoid misunderstanding it is as well to recall that

$$\psi(r, \theta, \phi) \cdot \psi^*(r, \theta, \phi) d\mathcal{V}$$

(ψ^* being the complex conjugate function of ψ) represents the probability of finding an electron in an elementary volume $d\mathcal{V}$ defined in figure 1.2, this volume being

$$d\mathcal{V} = r^2 \sin \theta dr d\theta d\phi$$

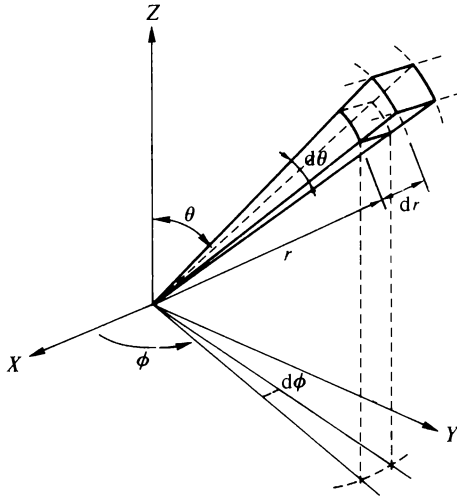


Figure 1.2 Differential elements in spherical co-ordinates

Normalising the wavefunction ψ will amount to equating to unity the integral over all space of this position probability; thus

$$\int \psi \psi^* r^2 dr \sin \theta d\theta d\phi = 1 \quad (1.15)$$

ψ may be expressed as the product $\psi = \mathcal{R}\Theta\Phi$, and the normalisation condition can be written in the form of three independent conditions for the variables r, θ, ϕ

$$\int \mathcal{R} \mathcal{R}^* r^2 dr = 1 \quad (1.16)$$

$$\int \Theta \Theta^* \sin \theta d\theta = 1 \quad (1.17)$$

$$\int \Phi \Phi^* d\phi = 1 \quad (1.18)$$

These three expressions allow calculation of the normalisation constants used previously. Using these constants, the wavefunction may be written

$$\psi(r, \theta, \phi) = \mathcal{R}(r) \Theta(\theta) \Phi(\phi) = \mathcal{R}(r) Y(\theta, \phi)$$

where

$$\mathcal{R}(r) = - \sqrt{\left\{ \left(\frac{2Z}{na_1} \right)^3 \frac{(n-l-1)!}{2n[(n+l)!]^3} \right\} \left(\frac{2Zr}{na_1} \right)^l e^{-Zr/na_1} L_{n+l}^{2l+1} \left(\frac{2Zr}{na_1} \right)}$$

$$Y(\theta, \phi) = \sqrt{\left[\frac{2l+1}{4\pi} \frac{(l-m)!}{(l+m)!} \right]} (-1)^m P_l^m(\cos \theta) e^{im\phi} \quad \text{for } m > 0$$

and for $m < 0$, one may use the relation

$$Y_l^{-m} = (-1)^m Y_l^{m*}$$

Comment Different authors use different conventions to represent $Y(\theta, \phi)$. We have followed that of A. Messiah, *Quantum mechanics*, and Condon and Shortley, *Theory of atomic spectra*. The reader should be wary of this in calculations involving wave functions.

1.3.1 Radial probabilities

The problem under consideration is treated in spherical co-ordinates; since \mathcal{R} depends only on the variable r , the expression

$$D(r) dr = \mathcal{R}\mathcal{R}^* r^2 dr \quad (1.19)$$

represents the probability of finding an electron situated between spheres of radius r and $r + dr$, that is to say whose distance from the nucleus is between r and $r + dr$. From the analytical expression for \mathcal{R} , diagrams of $D(r)$ as a function of r can be drawn. Figure 1.3 shows the probability function $D(r)$ for some hydrogen-like quantum states. It will be noted that the number of zeros of the function $D(r)$ is equal to the radial quantum number n_r , introduced by Sommerfeld: $n_r = n - k$ where k is identified as $l + 1$.

Position probability at the origin. The probability function $D(r)$ cannot be used to evaluate the position probability of the electron at the origin, where $r = 0$. It will be noted that the probability of finding an electron in a small volume $d\mathcal{V}$ at the origin is proportional to $\mathcal{R}\mathcal{R}^* d\mathcal{V}$. From the results given in figure 1.1, we see that $\mathcal{R}\mathcal{R}^*$ is zero for $r = 0$, *except for s electrons*. The latter therefore have a non-zero position probability at the nucleus. This result, specific to the quantum treatment, is very important. Its importance will be seen especially in chapter 6.

1.3.2 Angular probabilities

It may be seen immediately from the expressions (1.17) and (1.18) that

$$D(\phi) d\phi = \Phi_m \Phi_m^* d\phi$$

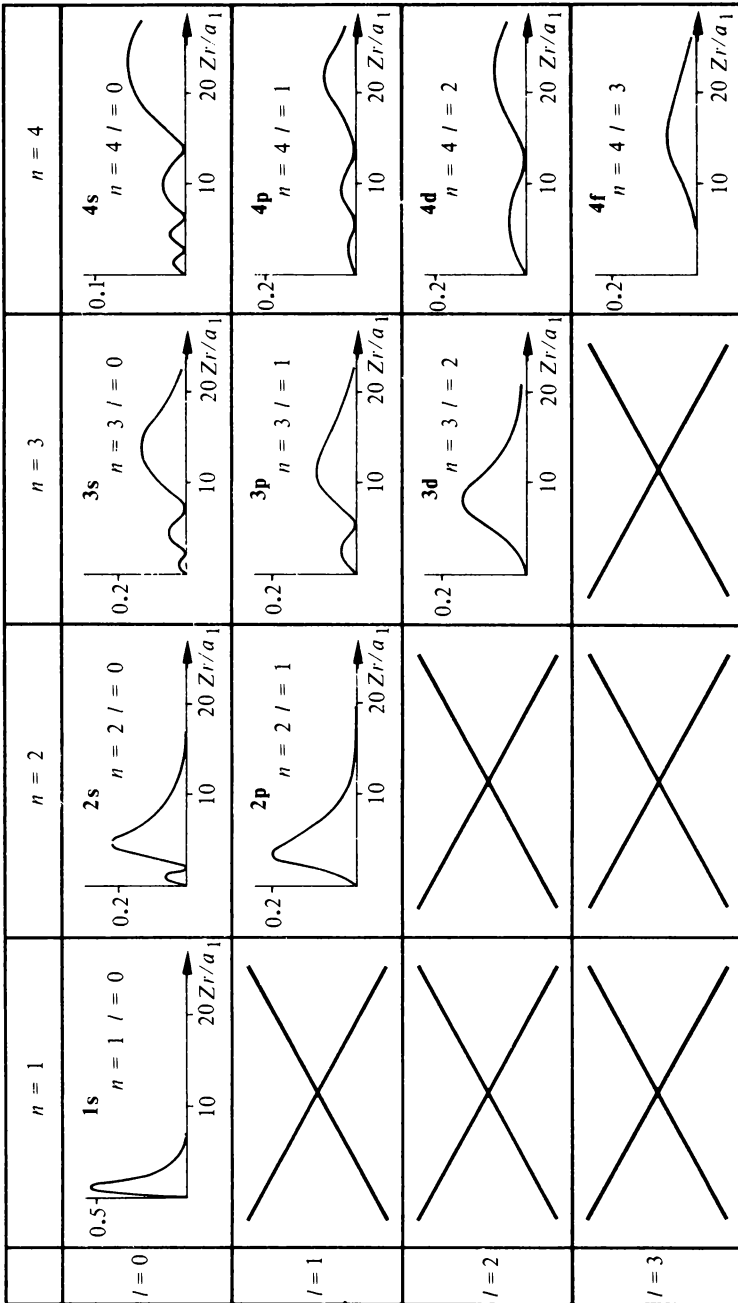


Figure 1.3 The radial probability density $D(r)$ for various values of n and l (the abscissa is the radius vector r expressed in units of a_1/Z ; this set of diagrams may be deduced from radial functions such as those presented in figure 1.1). In those representing 1s, 2p, 3d and 4f, the only maximum in $D(r)$ occurs at distances 1, 4, 9 and 16 respectively, equal to the radii of the circular orbits in Bohr's model

represents the probability of finding the electron within a region of space bounded by the two planes passing through the z axis and making angles ϕ and $\phi + d\phi$ with the x axis. A very simple calculation from the expression (1.4) shows that this probability is always equal to $d\phi/2\pi$. This indicates that the distribution of the electrons has a rotational symmetry around the Oz axis.

$\Theta\Theta^*\sin\theta d\theta$ represents the probability that the electron-nucleus radius vector makes an angle between θ and $\theta + d\theta$ with the Oz axis; but the solid angle $d\Omega$ corresponding to $d\theta$ (figure 1.2) is

$$d\Omega = 2\pi \sin\theta d\theta \quad \text{and} \quad \Theta\Theta^*\sin\theta d\theta = \Theta\Theta^* \frac{d\Omega}{4\pi}$$

Because of the rotational symmetry about the z axis, the probability of finding an electron within a fixed solid angle therefore will be proportional to $\Theta\Theta^*$.

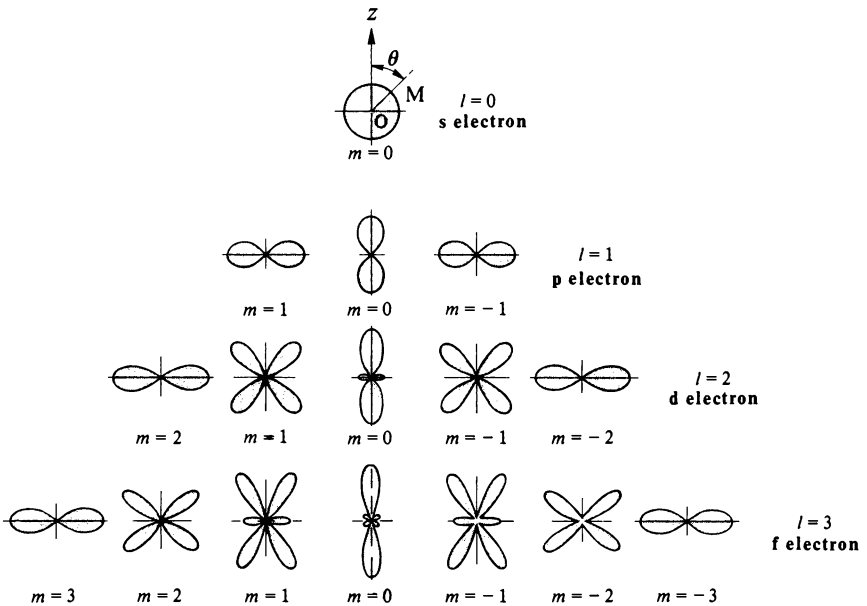


Figure 1.4 The angular probability density $D(\theta)$ in polar co-ordinates

The reader may verify without difficulty that a spherically symmetric distribution of particles has a constant probability per unit solid angle; this property justifies using $\Theta\Theta^*$ as a probability density.

The most important results arising from this discussion are given in figure 1.4, which, for different states, shows $D(\theta) = \Theta\Theta^*$ in polar co-ordinates, the length OM being proportional to $D(\theta)$. It may be seen immediately that for an s state, the probability function $D(\theta) = 1/4\pi$ is inde-

pendent of θ ; and since $D(\phi)$ is always independent of ϕ , an s state, corresponding to zero orbital angular momentum has spherical symmetry. This result is particularly satisfactory because in the Bohr model, although it was impossible to interpret the existence of zero orbital angular momentum for a classical orbit, this assumption was necessary nevertheless, in order to obtain agreement with experiment. To conclude, the notion of an electron orbit in a classical sense and as in Sommerfeld's theory has disappeared. It is replaced by a description in terms of the position probability of an electron. To simplify the language, and to generalise, the ensemble in this description is often called an 'orbit', and in the rest of this book, the reader will often find expressions such as '2s orbit', 'orbit of an electron in a central potential', and so on. He must therefore translate this into quantum language. In many books, especially in quantum chemistry, the term 'orbitals' is used to avoid any confusion.

1.4 Comparison with the Bohr–Sommerfeld Model

In volume 1, chapter 6, the reader may find results from the old Bohr–Sommerfeld semi-classical theory, in particular an expression for the energy E_{nk} involving the two quantum numbers n and k . Various other quantities such as the velocity of the electron, the axes of the elliptic trajectory, the mean radius vector between the electron and nucleus and so on, can be calculated. It is interesting to compare them with the results of section 1.2.

(1) *Energy.* The energy E_n given by the quantum model is identical to that found by Bohr's circular orbit hypothesis. This agreement is satisfactory since no relativistic assumptions were made in the discussion in section 1.2. The relativistic case will be discussed later.

(2) *The quantum number k .* In Sommerfeld's theory (volume 1, chapter 6), the quantum number k is related to the orbital angular momentum by

$$\sigma_L = k \frac{h}{2\pi} = k\hbar$$

Since σ_L represents the orbital momentum of the electron in an elliptic trajectory, it is impossible to imagine how σ_L could be zero, except in the unlikely case of a linear trajectory passing through the nucleus, the limiting case of an elliptic trajectory whose minor axis passes through the nucleus. Quantum theory showed the possibility of spherically symmetric states, corresponding to $l=0$. Correspondence can be contrived by identifying k with $l+1$, and it also ensures agreement between the possibility of $k=n$ in Sommerfeld's theory and the condition $n \geq l+1$ in quantum theory.

Comment By combining the results shown in figures 1.3 and 1.4, position probability functions may be obtained for hydrogen-like states. Some of these functions are illustrated in figure 1.5.

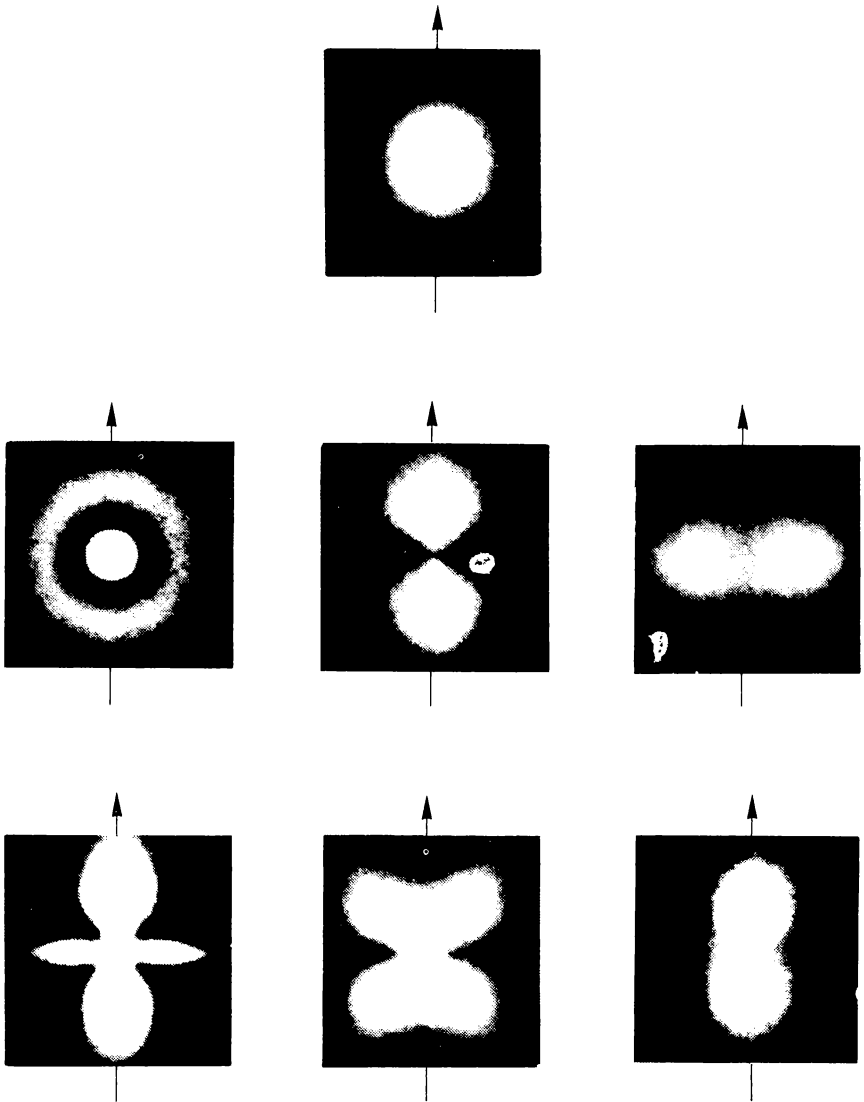


Figure 1.5 Electron clouds for several hydrogen-like states. An electron cloud may be imagined as a luminous material whose brilliance is proportional to the electron density. This material has rotational symmetry around the Oz axis (vertical in the figure). Each diagram represents a cross-section of this material, cut by a plane passing through the Oz axis. (From White, *Introduction to Atomic Spectra*, McGraw-Hill)

(3) *Mean radius.* From the expressions for the position probabilities, on the one hand, and from calculations involving the Bohr–Sommerfeld model on the other hand, the following table can be drawn up:

Mean value	Bohr–Sommerfeld model	Quantum model	Agreement if
$\langle r \rangle$	$\frac{a_1 n^2}{Z} \left[1 + \frac{1}{2} \left(1 - \frac{k^2}{n^2} \right) \right]$	$\frac{a_1 n^2}{Z} \left\{ 1 + \frac{1}{2} \left[1 - \frac{l(l+1)}{n^2} \right] \right\}$	$k = \sqrt{l(l+1)}$
$\langle r^2 \rangle$	$\frac{a_1^2 n^2}{Z^2} \left[1 + \frac{3}{2} \left(1 - \frac{k^2}{n^2} \right) \right]$	$\frac{a_1^2 n^2}{Z^2} \left\{ 1 + \frac{3}{2} \left[1 - \frac{l(l+1) - \frac{1}{3}}{n^2} \right] \right\}$	$k = \sqrt{[l(l+1) - \frac{1}{3}]}$
$\left\langle \frac{1}{r^3} \right\rangle$	$\frac{Z^3}{a_1^3 n^3 k^3}$	$\frac{Z^3}{a_1^3 n^3 l(l + \frac{1}{2})(l+1)}$	$k = \sqrt[3]{[l(l + \frac{1}{2})(l+1)]}$

(4) *Spatial quantisation.* The Bohr–Sommerfeld theory can be refined by taking into account the postulates of spatial quantisation; the normals to the orbits, parallel to the orbital angular momentum vector, can, depending on the value of l , make only a limited number of angles θ_N with the Oz direction, the axis of quantisation (figure 1.6). The orbits can only be in planes normal to these directions, defined by the possible values of the angle θ_N , but there is no physical parameter corresponding to a particular value of θ_N that allows a distinction to be made among the various possible different planes so as to localise the orbit. This classical model therefore suggests a certain delocalisation of the electrons.

Some similarity with the results of quantum model, shown graphically in figure 1.4, is therefore apparent. However, this can only be qualitative since in most instances the direction of the maximum probability does not coincide with the direction given by the Bohr–Sommerfeld model.

To summarise, we see that complete correspondence between the Bohr–Sommerfeld model and the quantum model cannot be found. The Bohr–Sommerfeld model can only be considered as a stage in the history of physics.

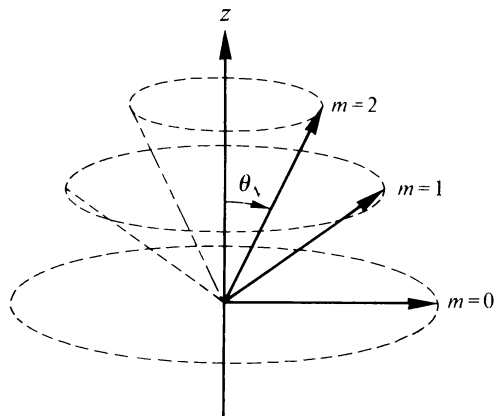


Figure 1.6 Spatial quantisation in the Bohr–Sommerfeld model

1.5 The Non-Coulomb Central Potential—Lifting the Degeneracy in l

At the same time as progress was being made in the study of the hydrogen atom, from the Bohr model to the use of quantum mechanics, models were developed in order to interpret the more complex spectra of atoms with several electrons. The various electrons are at a variety of mean distances from the nucleus; we shall define these in the following chapter, where the concept of successive 'electronic shells' will appear. In a certain class of atoms, an electron is situated at a mean distance from the nucleus far greater than that corresponding to the other electrons, and the assembly of the latter possesses an overall spherical symmetry; they are known as atoms with one outer electron. The different states usually observed for such atoms differ only in the trajectories of the outer electron, while the description of the other electrons remains the same.

A more complete description of atoms with one outer electron will be given later. In this section we shall study the motion of an outer electron interacting with the core of the atom, formed from the nucleus and the spherically symmetric assembly of the other electrons.

1.5.1 Penetrating and non-penetrating orbits

Let us first take a very simple example, inspired by the Bohr or Sommerfeld model, in which the orbits of the electrons have definite paths in the classical sense. Two possibilities exist.

(1) The first is the case when the outer electron has a *non-penetrating orbit*, shown in figure 1.7(a). If it is accepted that the mean symmetry of the cloud

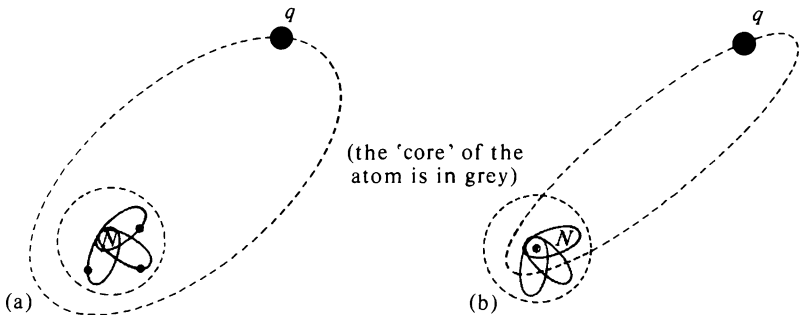


Figure 1.7 (a) Non-penetrating orbit, (b) penetrating orbit

formed by the $Z - 1$ inner electrons is spherical (this will be justified in a later chapter), the electron experiences the resultant electrostatic potential of the nuclear charge Ze and of the spherical distribution of charge $(Z - 1)q$. It will therefore be subjected to a potential identical to that created by a single charge e and the discussion presented for the hydrogen atom remains valid.

(2) On the other hand, if the orbit of the outer electron penetrates inside the 'core' of the atom (figure 1.7(b), *penetrating orbit*), the problem is much more complex. A fairly simple solution was given by Sommerfeld using the model shown in figure 1.8; the $Z - 1$ inner electrons are distributed within a

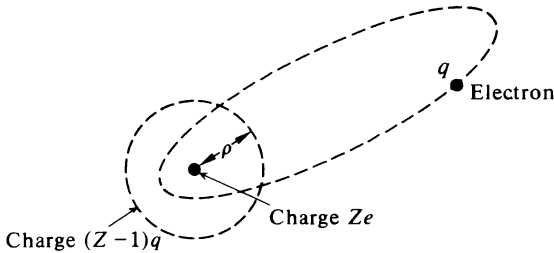


Figure 1.8 Sommerfeld's model of a penetrating orbit

sphere of radius ρ . Application of the elementary laws of electrostatics allows the evaluation of the electrostatic potentials $V_{\text{int.}}$ and $V_{\text{ext.}}$ interior and exterior to the sphere of radius ρ . Outside one has

$$V_{\text{ext.}} = \frac{1}{4\pi\epsilon_0} \frac{e}{r}$$

Inside the sphere of radius ρ , the potential will be

$$V_{\text{int.}} = \frac{1}{4\pi\epsilon_0} \frac{Ze}{r} + \text{constant}$$

the constant being determined from the continuity of the potential function at the surface of the sphere of radius ρ

$$V_{\text{int.}} = \frac{1}{4\pi\epsilon_0} \left(\frac{Ze}{r} + \frac{e}{\rho} - \frac{Ze}{\rho} \right)$$

1.5.2 A quantum model for atoms with one outer electron

During the study of the hydrogen-like quantum states, we saw that it was impossible to define the exact paths of the electrons and that only the concept of position probability had any meaning. The concepts of penetrating and non-penetrating orbits must therefore be modified. We retain only the fact that when the electron is close to the nucleus it experiences a potential energy

$$W(r) = -\frac{1}{4\pi\epsilon_0} \frac{Ze^2}{r} + \text{constant}$$

and that at a large distance it experiences a potential energy

$$W(r) = -\frac{1}{4\pi\epsilon_0} \frac{e^2}{r}$$

The solution of Schrödinger's equation can be attempted by determining a central potential whose analytic form is adjusted to give the best possible description of the atom in accordance with experimental results. In general, the solution can only be carried out numerically. Various methods have been used (Thomas–Fermi, Hartree); these are specialist problems and it is impossible for us to outline them here, even superficially. However, we shall present an abbreviated approach to the problem that will bring out the main result. We take as the potential energy

$$W(r) = -\frac{1}{4\pi\epsilon_0} \frac{e^2}{r} \left(1 + \frac{b}{r}\right) = \frac{C}{r} \left(1 + \frac{b}{r}\right) \quad \left(C = -\frac{e^2}{4\pi\epsilon_0}\right) \quad (1.20)$$

which at large distances behaves as $-e^2/r$ and which, by adjustment of the positive parameter b , may become $-Ze^2/r$ in the proximity of the nucleus. The main advantage of this potential is that it adapts to a simple analytical discussion. The solution of Schrödinger's equation will be carried out by following closely the analysis of section 1.2. Separation of the angular and radial variables is carried out in the same way, and the angular equation is the same. The radial equation may then be written

$$\frac{d^2\chi}{dr^2} + \left[\frac{2\mu}{\hbar^2} E - \frac{2\mu}{\hbar^2} \frac{C}{r} \left(1 + \frac{b}{r}\right) - \frac{l(l+1)}{r^2} \right] \chi = 0$$

so, by using the reduced quantities defined by equations (1.9)

$$\frac{d^2\chi}{dr^2} - \left[A - \frac{B}{r} + \frac{-Bb + l(l+1)}{r^2} \right] \chi = 0$$

If l^* is any number and we put

$$l^*(l^* + 1) = l(l+1) - Bb \quad (1.21)$$

the radial equation takes the same reduced form as in section 1.2 (equations (1.8) and (1.10)) the only difference being that l^* is not an integer. A solution is sought in the form

$$\chi(r) = e^{-\sqrt{(A)}r} u(r)$$

and will have physical meaning only if the polynomial $u(r)$ has a finite number of terms. So that the recurrence relations between the coefficients of the polynomial $u(r)$ may allow for this, p must be a positive integer or zero, and

$$B = 2(l^* + 1 + p)\sqrt{(A)}$$

A and B being reduced variables defined by equations (1.9). From the expression for these reduced variables, the only possible values of the energy are therefore

$$E = -\frac{Rhc}{(l^* + p + 1)^2} \quad (R \text{ is Rydberg's constant})$$

We see that not only the integer p but also l^* , related to the quantum number l , now appear in the expression for E .

We shall change the notation as follows

$$\left\{ \begin{array}{l} (1) \text{ The integer } n \text{ is called the principal quantum number } n, \text{ such that} \\ \qquad \qquad \qquad n = l + p + 1 \\ (2) \text{ The effective quantum number } n^* \text{ is defined as} \\ \qquad \qquad \qquad n^* = l^* + p + 1 = n - \Delta l, \quad \text{where } \Delta l = l - l^* \end{array} \right.$$

and we write

$$E = -\frac{Rhc}{n^{*2}} = -\frac{Rhc}{(n - \Delta l)^2}$$

If b is small so that $l \approx l^*$, it is easy to evaluate from equation (1.21)

$$\Delta l \approx \frac{Bb}{2l + 1} = \frac{1}{l + \frac{1}{2}} \frac{b}{a_1}$$

and the energy levels, a function of the integers n and l , will be characterised by the energy values

$$E_{nl} = \frac{-Rhc}{\left(n - \frac{b}{a_1} \frac{1}{l + \frac{1}{2}} \right)^2} \quad (1.22)$$

Our study of the particular potential

$$W(r) = \frac{C}{r} \left(1 + \frac{b}{r} \right)$$

allows us to see that *the degeneracy in l characteristic of the hydrogen-like orbits is lifted, and that an energy level is characterised by the two quantum numbers n and l . We shall assume that this result is independent of the central potential $W(r)$.* This can be described as the main conclusion of this section.

From the relationship (1.22), it is easy to see that for a given value of n , the algebraic value of the energy is an increasing function of l . In the following chapter we shall return to the order of the levels E_{nl} on the energy scale, a sequence depending only slightly on the shape of the potential $W(r)$. We shall see that this point is of great importance (see figure 2.1).

Comment *Application to the alkali atoms: some orders of magnitude.* In a later chapter, it will be seen that the alkali atoms (lithium, potassium, sodium, rubidium, caesium) come within the category of atoms having one outer electron. We now present some data.

The table below gives the values of the effective quantum number n^* for the sodium atom, calculated from the experimental values of the energy, for various values of n and l .

	$n = 3$	$n = 4$	$n = 5$	$n = 6$
$l = 0$	1.627	2.643	3.648	4.651
$l = 1$	2.177	3.133	4.138	5.441
$l = 2$	2.990	3.989	4.987	5.989
$l = 3$		4.000	5.001	6.008
$l = 4$			x	x
$l = 5$				x
$l = 6$				

We have not indicated in this table the values of n^* corresponding to $n = 5$, $l = 4$, and $n = 6$, $l = 4$ and $l = 5$. The corresponding spectral terms can be obtained only from low intensity infrared transitions, and there is too large a dispersion amongst the results to allow a meaningful determination of a value of n^* .

It will be noted from the table that when n and l have large values, n^* is found to be close to n . This corresponds to non-penetrating orbits. However, for $n = 4$, $l = 3$, and $n = 6$, $l = 3$, we see that n^* exceeds n , which is *a priori* contradictory to the relation (1.22). This may be attributed to the simplicity of the model used; a more precise theory must take into account the deformation of the spherical symmetry of the atomic core, a deformation produced by the electric field created by the outer electron (figure 1.9).

Various approximate solutions may be obtained for the wave functions corresponding to the orbits of an electron in a central potential. From the radial part of the wave function, it is possible, as for the hydrogen-like orbits, to draw curves giving the radial probability densities $D(r)$ as a function of the distance r from the nucleus. Figure 1.10 illustrates this for the sodium atom, where the curve drawn with a thick line represents the radial probability of finding one of the core electrons in a unit volume; curves (a), (b), (c) drawn with a thin line, represent respectively the radial probability densities for the outer electron according as it is in the 3s, 3p and 3d quantum states. The probability of finding a 3d electron in the 'core' is seen to be very small, and the 3d orbit may be considered as non-penetrating, in contrast to the 3s and 3p orbits.

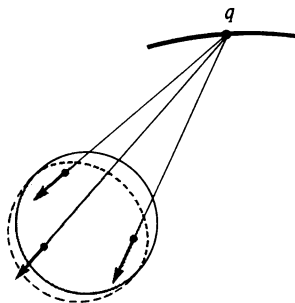


Figure 1.9 Core polarisation under the influence of the electric field due to the electron. The shaded part represents a non-spherically symmetric core

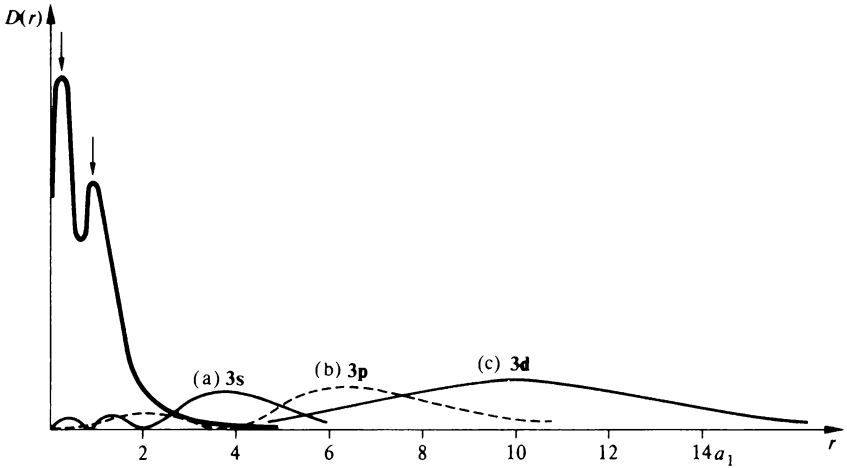


Figure 1.10 Radial probability densities for the sodium atom. The curves drawn in a thin line represent radial probability densities for the outer electron in various states. The curve drawn in a thick line represents the radial probability density for the assembly of core electrons. The two maxima marked with arrows should be noted; they substantiate the concept of an electronic shell, which will be introduced in the next chapter.

This figure is the quantum-mechanical description of the diagrams shown in figures 1.7(a) and 1.7(b)

To conclude this study of the motion of an electron in a central potential, we should remind ourselves of:

- (1) the introduction of the quantum numbers n , l and m imposed by the reality of the physical problem during the solution of the Schrödinger equation;
- (2) the description of the s orbits (corresponding to $l = 0$) in terms of the position probability and their spherical symmetry;
- (3) and, above all, the concept of degeneracy.

In the particular case of a Coulomb potential, the energy depends only on the quantum number n . In a more general central potential, this *degeneracy* is partially lifted, and consequently the energy levels of the electron in this potential $W(r)$ are described by the two quantum numbers n and l .

2

Independent Electron Approximation in a Central Potential. Electronic Configurations

2.1 The Various Interactions in a Complex Atom

In chapter 1 we considered two simple models, one being the hydrogen atom in which the electron moves in a coulomb potential, without spin being considered, the other enabling a simplified description of an alkali atom to be given, its outer electron again being considered without spin.

If we wish to study a given atom in detail, various interactions should be included when setting up the equation of the problem :

- (1) the electrostatic interaction of the electrons with an assumed infinitely heavy point nucleus;
- (2) the electrostatic interaction between the electrons;
- (3) the magnetic interaction of the electron spins with the orbital motion;
- (4) the interaction between the electron-spin magnetic moments.

The description of the nucleus of the atom is complex. Its existence requires the consideration of other terms :

- (5) the interaction of the orbital and spin magnetic moments of the electrons with the magnetic moment of the nucleus;
- (6) additionally, corrections should be made expressing the motion of the nucleus, its finite size, and the distribution of the nuclear charges when the latter is not spherically symmetric.

We see therefore that the study of an atom is an extremely complex problem. One approach to its solution is to neglect some of the interactions: terms (5) and (6), concerned with the influence of the nucleus, cause only very small changes in the energy levels and when they are neglected the resulting description of the atom is sufficient for many problems. We postpone their study to chapter 6 and until then we shall confine ourselves to studying the effect of the interactions (1), (2), (3) and (4).

Furthermore, for most atoms, the main ideas can be brought out by making the two following assumptions:

- (a) the non-relativistic Schrödinger equation may be used;
- (b) the spin-spin interaction (4) is much weaker than the spin-orbit interaction (5).

For atoms with very few electrons (hydrogen, helium, and so on) assumptions (a) and (b) are no longer valid. We shall discuss them again in chapter 4.

If we write the hamiltonian of the system, taking into account the three interactions (1), (2) and (3) together with the assumptions (a) and (b), we obtain a complicated Schrödinger equation which cannot be solved exactly. A solution involving successive approximations must be used. The most important terms of the hamiltonian correspond to the electrostatic interactions, so first we write the hamiltonian obtained by neglecting the magnetic interactions (3)

$$H = \sum_i \left(-\frac{\hbar^2}{2m} \Delta_i - \frac{1}{4\pi\epsilon_0} \frac{Ze^2}{r_i} + \sum_{j>i} \frac{1}{4\pi\epsilon_0} \frac{e^2}{r_{ij}} \right)$$

where the inequality $j > i$ is necessary to avoid counting a term in r_{ij} twice; Δ_i is the laplacian operator, defined with respect to co-ordinates $x_i y_i z_i$ of the i th electron, r_i is the distance between the nucleus and the electron i , and r_{ij} the distance between electron i and electron j . We still cannot accurately solve the Schrödinger equation involving this electrostatic hamiltonian. The difficulty of an accurate solution of the general problem of N interacting particles, where $N \geq 3$, is not unique to quantum mechanics. The same impossibility exists in classical mechanics. This is a very general result of the mathematical properties of systems of partial differential equations. Accordingly we try to simplify the problem further.

(i) *As a first approximation*, we assume that the electrons are independent of one another, and subjected to a central potential $W(r)$ (the word potential is often used for potential energy); thus the hamiltonian reduces to a relatively simple term H_0

$$H_0 = \sum_i \left(-\frac{\hbar^2}{2m} \Delta_i + W(r_i) \right)$$

It might seem that we could take for $W(r_i)$ just the term

$$-\frac{1}{4\pi\epsilon_0} \frac{Ze^2}{r_i}$$

of the hamiltonian H , but such an approximation would be very poor, because we should not have taken account of the electron–electron interactions. To improve this first approximation, one tries to represent the two terms

$$-\frac{1}{4\pi\epsilon_0} \frac{Ze^2}{r_i} \quad \text{and} \quad \sum_{j>i} \frac{1}{4\pi\epsilon_0} \frac{e^2}{r_{ij}}$$

as closely as possible by a central potential $W(r)$. We therefore generalise the problem of atoms with one outer electron, treated in the preceding chapter, where the interaction of this outer electron with the core electrons was expressed by a modification of the potential in $1/r$. Intuitively, we can imagine that as a result of the periodic motion of the electrons, the mean value of the electrostatic electron–electron interaction forces is a central force.

As we shall see in the next section, the problem described by the hamiltonian H_0 can be treated rigorously.

(ii) *As a second approximation*, it will be necessary to correct the results of the preceding approximation and also to add the magnetic terms previously neglected, that is to say we put

$$H = H_0 + T_1 + T_2$$

The term T_1 represents the error introduced by replacing the two electrostatic interaction terms by $W(r_i)$, so that

$$T_1 = \sum_i \left[-\frac{1}{4\pi\epsilon_0} \frac{Ze^2}{r_i} + \sum_{j>i} \frac{1}{4\pi\epsilon_0} \frac{e^2}{r_{ij}} - W(r_i) \right]$$

(the potential $W(r_i)$ is chosen such that T_1 is as small as possible); the term T_2 represents the magnetic spin–orbit interaction which for the moment we do not make explicit.

Here we must make an extremely important remark. In the explicit form of T_1 that we have given, only corrections due to the electrostatic electron–electron interactions appear. When the electrons are considered as particles having spin, the solutions of $H_0 + T_1$ resulting from the quantum treatment should include the description of the spin state of the electrons because of exchange effects. The corresponding energy terms are known as *exchange terms*. The reader should avoid confusing these effects with spin–spin interactions of magnetic origin which we have neglected (assumption (b)). In later chapters we shall often come across the importance of the exchange terms.

We should note also that only 'off-diagonal' interactions between electron i and electron j come into the term T_1 . After evaluating T_2 in the next chapter we shall see that T_2 , on the other hand, contains only 'diagonal' terms relative to the various electrons i . If we wish to take account of the magnetic spin-spin interactions, which are off-diagonal, they should be included in the term T_1 .

Study of the roles of T_1 and T_2 , taking account of their respective orders of magnitude, will be the subject of the next chapter.

2.2 The Energy Levels of a System of N Independent Electrons in a Central Potential. Configurations

2.2.1 The energy levels

The hamiltonian H_0 can be written in the form

$$H_0 = \sum_i h_i$$

where

$$h_i = -\frac{\hbar^2}{2m} \Delta_i + W(r_i)$$

The eigenvalues of H_0 can be calculated from those of each of the independent terms h_i . Each of the terms h_i represents the hamiltonian of an electron without spin subjected to a central potential $W(r_i)$, and finding these eigenvalues is a problem similar to one we have already treated.

In the study made in the preceding chapter of an electron without spin in a central potential, we obtained the energy levels as a function of two quantum numbers n and l of the electron. By studying the problem in more detail, it may be shown that *the respective positions of these energy levels depend very little on the exact value of the potential energy $W(r)$* ; their sequence in order of increasing energy is shown in figure 2.1, where each level is described by the number n and by a letter representing the number l (the convention concerning the use of these letters was described in section 1.2). Some states having different values of n and l may have nearly equal energies, and their relative position on an energy scale may then depend on the potential $W(r)$; in figure 2.1 we have shown them as coincident.

For a fixed value of n , the energy is always an increasing function of the quantum number l , conforming to the model in the preceding chapter (see also volume 1, chapter 7; the energy is higher for a circular orbit than for an elliptic orbit of the same major axis). For small values of the quantum number n , it behaves as a principal quantum number, in that it mainly determines the value of the energy: all the levels $n = 2$ lie above the level $n = 1$, and below all the levels $n = 3$. However, from $n = 4$, the situation is no longer so simple: the energy differences corresponding to variations of n or of l become of the same order of magnitude. Thus the 4s level is very close to the 3d level (and usually slightly lower); similarly, the 5s and 6s levels are very close to (and often

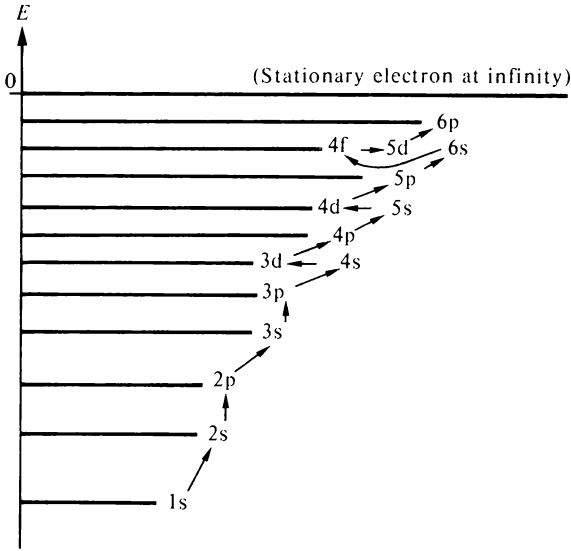


Figure 2.1 Order of the energy levels of a single electron in a central potential (each level is denoted by the principal quantum number n and a letter s, p, d or f, representing the values 0, 1, 2 or 3 of the quantum number l). The arrows indicate the normal order of filling (see section 2.4)

below) the 4d and 5d levels respectively. The most glaring, however, is observed with the 4f level, which is clearly higher than the two levels 5s and 5p and very close to the 5d level.

Knowing the energy levels E_i , eigenvalues of the hamiltonian h_i , we now seek the eigenvalues of H_0 . Since all the electrons are equivalent, we may apply the theory of identical particles in order to find the energy levels corresponding to the hamiltonian H_0 . We summarise the results of this theory, which are given in books on quantum mechanics, as follows.

- (1) The energy levels of a system of N identical particles may be obtained by summing the energies E_i that each particle can have when placed individually in the potential $W(r_i)$.
- (2) The wave function of the system of N electrons can be put in the form of a determinant (the Slater determinant) whose elements are obtained from the wave functions of the individual electrons. The form of this wave function forbids a state in which two or more electrons are described by the same set of quantum numbers (the Pauli principle). We shall discuss this latter point in section 2.3.

Property (1) allows the energy levels of the system to be determined immediately. We take a system of three electrons as an example; in figure 2.2, (a), (b) and (c), we have shown the energy levels of the three electrons separately, and (d) is the diagram corresponding to the total energy of the system.

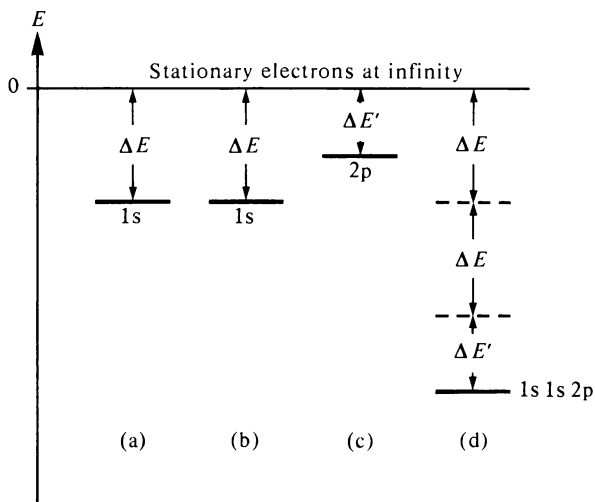


Figure 2.2 Determination of the energy of a system of three electrons

2.2.2 Description of the electronic states. Shells and sub-shells. Configurations

From property (2) summarised above, the total wave function of an atom formed from independent electrons is obtained from the wave functions of its individual electrons. Therefore, we describe the state of an atom corresponding to each of the above energy levels in terms of the state of each of its electrons. In particular we shall specify the quantum numbers n and l of each of the electrons.

The central potential approximation enables one to show that electrons having the same value of n are situated at a similar average distance from the centre of force. Consequently for these electrons, the potential $W(r_i)$ is of the same order of magnitude. This idea has already been expressed in the course of interpreting X-ray spectra (volume 1, chapter 7), the screening constant s having values differing considerably according to the value of the quantum number n . These electrons having the same value of n are said to be situated in the same *electronic shell*.

If electrons, situated within the same shell, also have the same quantum number l , they are said to be in the same *sub-shell*. A description of the state of an individual electron includes, *inter alia*, a specification of the sub-shell in which it appears. Following established convention, we shall symbolise each sub-shell by a number, equal to the principal quantum number n , followed by a letter representing the value of the quantum number l (see, for example, figure 2.2: two electrons are in the 1s sub-shell and one electron is in the 2p sub-shell).

We obtain a description of the overall state of the atom by indicating to which sub-shell each electron belongs. This overall description is said to

define a *configuration* of the atom. We denote a configuration by writing sequentially the symbols of the sub-shells to which the various electrons belong. When several electrons belong to the same sub-shell, we write the corresponding symbol only once, and indicate the number of electrons in this sub-shell by a superscript.

Examples The configuration corresponding to figure 2.2 is denoted $1s^22p$.

A configuration consisting of two $1s$ electrons, two $2s$ electrons, six $2p$ electrons, is denoted $1s^22s^22p^6$.

Among all the configurations of an atom, one of them possesses a minimum energy; it is described as forming the ground state corresponding to the most stable structure. All the others form excited states. It should be noted at this point that certain excited configurations are very unlikely since the states of several electrons would have to be changed simultaneously in order to excite them.

2.3 The Pauli Principle and Degeneracy of a Configuration

2.3.1 The four quantum numbers and the Pauli principle

In the preceding chapter, we studied the motion of an electron in a certain potential and characterised the electron by three quantum numbers: the principal quantum number n , the orbital quantum number l and the magnetic quantum number m . We recalled that the two quantum numbers l and m characterise the angular momentum due to the orbital motion of the electron. We must now introduce the spin angular momentum of the electron characterised by the quantum number m_s , which has values $\pm\frac{1}{2}$ (see volume 1, chapter 12) and the wavefunction of the electron must be modified to take this into account. To avoid confusion later, we shall no longer denote the magnetic quantum number, related to the orbital angular momentum, by m , but instead by m_l with the subscript l .

To summarise, the electron in the atom will therefore be characterised by the four quantum numbers:

- n , the principal quantum number;
- l , the quantum number defining the orbital angular momentum;
- m_l , defining the components of σ_l along the axis of quantisation;
- $m_s = \pm\frac{1}{2}$, defining the components of the electron spin.

The Pauli principle is a consequence of the indistinguishability of electrons and has been incorporated already in proposition (2) set out in the preceding section. It may be stated as follows: in an atom, the wave functions of the individual electrons must all be different from one another, and two electrons therefore cannot have identical values for the set of four quantum numbers n, l, m_l, m_s . This principle turns out to have fundamental consequences in the physics of the atom.

(1) It allows us to state the maximum number of electrons in an atom that can have the same energy. This concept is already familiar to the reader; the interpretation of X-ray emission spectra led us to conclude that some of the

energy levels that might be accepted by atomic electrons are normally *complete*: an X-ray emission line can be observed only if an electron from a complete level is first detached from the atom (see volume 1, chapter 7).

(2) It leads us to evaluate the order of degeneracy of a configuration. In the central potential model, a configuration specifies the quantum numbers n and l for each electron. Let us introduce, in addition, the quantum numbers m_l and m_s . (Note that, although we have not introduced the spin through the term T_2 in the hamiltonian, we take account of this parameter henceforth in order to classify the electronic states.) We see, therefore, that to each single configuration there will correspond a certain number of descriptions, differing in the values of m_l and m_s of each electron. A configuration will therefore have a certain *order of degeneracy*. In the next chapter, when we take account of the terms T_1 and T_2 , energy corrections will appear which more or less completely raise this degeneracy.

2.3.2 The maximum number of electrons belonging to the same shell or sub-shell

(1) *The case of a sub-shell.* We investigate the maximum number of electrons having simultaneously identical values of n and l . These electrons must differ either by the value of m_l (which can be one of the $(2l + 1)$ integral values between $-l$ and $+l$) or by m_s (which can take the two values $+\frac{1}{2}$ or $-\frac{1}{2}$).

There exist, therefore, $2(2l + 1)$ distinct quantum states corresponding to the same values of n and l , and therefore we can have $2(2l + 1)$ electrons in a sub-shell of quantum number l

$l = 0$ (s electrons)	maximum number = 2
$l = 1$ (p electrons)	maximum number = 6
$l = 2$ (d electrons)	maximum number = 10
$l = 3$ (f electrons)	maximum number = 14

A sub-shell containing $2(2l + 1)$ electrons is said to be complete.

(2) *The case of a shell.* Let us now determine the maximum number of electrons having the same n but different quantum numbers l, m_l, m_s . We know (see chapter 1) that the quantum number l can have all values such that

$$l \leq n - 1$$

Using the preceding results, we must add up the maximum number of electrons in each sub-shell

s electrons ($l = 0$)	p electrons ($l = 1$)	l anything	
maximum number	maximum number	maximum number	
2	+	6	+
			$\dots + 2(2l + 1)$
			electrons with $l = n - 1$ maximum number
			$+$ $\dots + 2(2n - 1)$

This series may be written as follows

$$\sum_{l=0}^{l=n-1} 2(2l+1) = 2n + 4 \sum_{l=0}^{l=n-1} l = 2n + 4 \frac{(n-1)n}{2} = 2n^2$$

using the well-known result for the sum of the first $(n-1)$ integers.

The maximum number of electrons of quantum number n is therefore $2n^2$. So in a configuration, there is a maximum of two electrons with $n=1$, eight electrons with $n=2$, 18 electrons with $n=3$, and so on. A shell containing the maximum number of electrons, $2n^2$, is called a *complete shell*.

2.3.3 Order of degeneracy of a configuration

We saw (in section 2.3.1) that a given configuration possesses a certain order of degeneracy. We shall now evaluate this order of degeneracy G .

First case: a single electron in each sub-shell. In the configuration considered, no electron is characterised by the same pair of quantum numbers n and l . An electron i may have Y_i states according to the values of m_l and m_s , Y_i representing the number of places in the sub-shell

$$Y_i = 2(2l_i + 1)$$

and thus there will be

$$G = \prod_i Y_i$$

different states corresponding to this configuration.

Example For a system with three electrons, we may readily find the following orders of degeneracy

$$\text{the configuration } 1s2s2p \rightarrow G = 2 \times 2 \times 6 = 24$$

$$2p3d4f \rightarrow G = 6 \times 10 \times 14 = 840$$

Second case: several electrons in the same sub-shell. Consider a configuration in which X electrons possess the same n and l quantum numbers. For this value of l , an electron can have $Y = 2(2l+1)$ different states characterised by different values of m_l and m_s .

To enumerate the number of possible states, we must take account of the Pauli principle and of the indistinguishability of the electrons. A simple procedure enables an easy solution of the problem: we must find the number of ways of arranging X non-distinguishable objects in Y places, each containing a maximum of one object.

We obtain these combinations by finding all the permutations of Y objects amongst themselves, this being $Y!$ permutations. However, among all these permutations there are a large number that do not give rise to distinct combinations: $X!$, arising from the permutation of two objects and $(Y-X)!$, corresponding to the permutations of the empty places, do not produce discernible changes. The actual number of distinct combinations is therefore

$$g = \frac{Y!}{X!(Y-X)!}$$

The number g also represents the number of different states corresponding to X electrons. (Note: in the special case of a complete sub-shell, only one combination exists, $X = Y \rightarrow g = 1$.) The total degeneracy of the configuration is obtained from the product of g and the degeneracy due to the electrons in other sub-shells.

Example 1 What is the degeneracy G of the ground state of carbon $1s^2 2s^2 2p^2$?

(a) for the set of two $1s$ electrons: $X = 2$ $Y = 2$ $g = 1$

(b) for the set of two $2s$ electrons: $X = 2$ $Y = 2$ $g = 1$

(c) for the set of two $2p$ electrons: $X = 2$ $Y = 6$ $g = 15$,

and from the product of the three, one obtains $G = 15$.

Example 2 What is the degeneracy G of an excited state of nitrogen of configuration $1s^2 2s^2 2p^2 3p^1$?

(a) $1s$ sub-shell: complete $\rightarrow g = 1$

(b) $2s$ sub-shell: complete $\rightarrow g = 1$

(c) $2p$ sub-shell: $X = 2$ $Y = 6 \rightarrow g = 15$

(d) $3p$ sub-shell: $X = 1$ $Y = 6 \rightarrow g = Y = 6$

$$G = 15 \times 6 = 90$$

2.4 The Periodic Classification of the Elements

2.4.1 The ground state configuration

The different atoms that exist in nature are characterised by a certain number of electrons, equal to the atomic number Z . The ground state of the structure is described by a configuration of these electrons such that the total energy is a minimum. For a description of this structure, it will be convenient to use the various properties set out in this chapter:

- (1) the total energy is the sum of the energies that would be possessed by each of the electrons alone in a potential $W(r)$;

Table 2.1

Number of electrons	Atom	Ground configuration
$Z = 1$	H	$1s$
$= 2$	He	Two electrons in the $1s$ state: configuration $1s^2$
$= 3$	Li	Since the maximum number of electrons in the $1s$ shell is two, the configuration of minimum energy is $1s^2 2s$
$= 4$	Be	The $2s$ sub-shell is complete and the ground configuration is $1s^2 2s^2$
$Z = 5$ to 9		The $1s$ and $2s$ sub-shells are complete; the $2p$ sub-shell progressively fills up
$= 10$	Ne	The $2p$ sub-shell is now complete and the configuration is $1s^2 2s^2 2p^6$
$Z = 11$ to 17		The three sub-shells $1s$, $2s$ and $2p$ are complete; the $3s$ and then $3p$ sub-shells fill up
$= 18$	A	The five sub-shells of lowest energy are complete: $1s^2 2s^2 2p^6 3s^2 3p^6$

Table 2.2 Electronic configuration of the elements

The number of electrons in a sub-shell is shown in each column. This number is printed on a grey background when the sub-shell is complete. (Line 1, line 2, and so on, refer to the Periodic table, table 2.3.)

Shell		K	L			M			N				O					P						Q	
Sub-shell		1s	2s	2p	3s	3p	3d	4s	4p	4d	4f	5s	5p	5d	5f	5g	6s	6p	6d	6f	6g	6h	7s		
Line 1	1 H 2 He	1 2																							
Line 2	3 Li 4 Be 5 B 6 C 7 N 8 O 9 F 10 Ne	2 2 2 2 2 2 2 2	1 2 2 2 2 2 2 2																						
Line 3	11 Na 12 Mg 13 Al 14 Si 15 P 16 S 17 Cl 18 A	2 2 2 2 2 2 2 2	2 2 2 2 2 2 2 2	6 6 6 6 6 6 6 6	1 2 2 2 2 2 2 2																				
	19 K 20 Ca	2 2	2 2	6 6	2 2	6 6		1 2																	
Line 4	21 Sc 22 Ti 23 V 24 Cr 25 Mn 26 Fe 27 Co 28 Ni 29 Cu 30 Zn	2 2 2 2 2 2 2 2 2 2	2 2 2 2 2 2 2 2 2 2	6 6 6 6 6 6 6 6 6 6	2 2 2 2 2 2 2 2 2 2	6 6 6 6 6 6 6 6 6 6	1 2 2 5 5 6 7 8	2 2 2 2 2 2 2 2 10 10																	
	31 Ga 32 Ge 33 As 34 Se 35 Br 36 Kr	2 2 2 2 2 2	2 2 2 2 2 2	6 6 6 6 6 6	2 2 2 2 2 2	6 6 6 6 6 6	10 10 10 10 10 10	2 2 2 2 2 2	1 2 3 4 5 6																
	37 Rb 38 Sr	2 2	2 2	6 6	2 2	6 6	10 10	2 2	6 6								1 2								
Line 5	39 Y 40 Zr 41 Nb 42 Mo 43 Tc 44 Ru 45 Rh 46 Pd 47 Ag 48 Cd	2 2 2 2 2 2 2 2 2 2	2 2 2 2 2 2 2 2 2 2	6 6 6 6 6 6 6 6 6 6	2 2 2 2 2 2 2 2 2 2	6 6 6 6 6 6 6 6 6 6	10 10 10 10 10 10 10 10 10 10	2 2 2 2 2 2 2 2 2 2	6 6 6 6 6 6 6 6 6 6	1 2 4 5 5 7 8 10 10															
	49 In 50 Sn 51 Sb 52 Te 53 I 54 Xe	2 2 2 2 2 2	2 2 2 2 2 2	6 6 6 6 6 6	2 2 2 2 2 2	6 6 6 6 6 6	10 10 10 10 10 10	2 2 2 2 2 2	6 6 6 6 6 6	10 10 10 10 10 10															

Transition elements (1st series)

Transition elements (2nd series)

Table 2.2—continued

Shell Sub-shell	K 1s	L			M			N				O			P				Q 7s			
		2s	2p	3s	3p	3d	4s	4p	4d	4f	5s	5p	5d	5f	5g	6s	6p	6d		6f	6g	6h
55 Cs	2	2	6	2	6	10	2	6	10		2	6				1						
56 Ba	2	2	6	2	6	10	2	6	10		2	6			2							
57 La	2	2	6	2	6	10	2	6	10		2	6	1		2							
58 Ce	2	2	6	2	6	10	2	6	10		2	6	2		2							
59 Pr	2	2	6	2	6	10	2	6	10	3	2	6			2							
60 Nd	2	2	6	2	6	10	2	6	10	4	2	6			2							
61 Pm	2	2	6	2	6	10	2	6	10	5	2	6			2							
62 Sm	2	2	6	2	6	10	2	6	10	6	2	6			2							
63 Eu	2	2	6	2	6	10	2	6	10	7	2	6			2							
64 Gd	2	2	6	2	6	10	2	6	10	7	2	6	1		2							
65 Tb	2	2	6	2	6	10	2	6	10	9	2	6			2							
66 Dy	2	2	6	2	6	10	2	6	10	10	2	6			2							
67 Ho	2	2	6	2	6	10	2	6	10	11	2	6			2							
68 Er	2	2	6	2	6	10	2	6	10	12	2	6			2							
69 Tm	2	2	6	2	6	10	2	6	10	13	2	6			2							
70 Yb	2	2	6	2	6	10	2	6	10	14	2	6			2							
71 Lu	2	2	6	2	6	10	2	6	10	14	2	6	1		2							
72 Hf	2	2	6	2	6	10	2	6	10	14	2	6	2		2							
73 Ta	2	2	6	2	6	10	2	6	10	14	2	6	3		2							
74 W	2	2	6	2	6	10	2	6	10	14	2	6	4		2							
75 Re	2	2	6	2	6	10	2	6	10	14	2	6	5		2							
76 Os	2	2	6	2	6	10	2	6	10	14	2	6	6		2							
77 Ir	2	2	6	2	6	10	2	6	10	14	2	6	7		2							
78 Pt	2	2	6	2	6	10	2	6	10	14	2	6	9		1							
79 Au	2	2	6	2	6	10	2	6	10	14	2	6	10		1							
80 Hg	2	2	6	2	6	10	2	6	10	14	2	6	10		2							
81 Tl	2	2	6	2	6	10	2	6	10	14	2	6	10		2	1						
82 Pb	2	2	6	2	6	10	2	6	10	14	2	6	10		2	2						
83 Bi	2	2	6	2	6	10	2	6	10	14	2	6	10		2	3						
84 Po	2	2	6	2	6	10	2	6	10	14	2	6	10		2	4						
85 At	2	2	6	2	6	10	2	6	10	14	2	6	10		2	5						
86 Rn	2	2	6	2	6	10	2	6	10	14	2	6	10		2	6						
87 Fr	2	2	6	2	6	10	2	6	10	14	2	6	10		2	6					1	
88 Ra	2	2	6	2	6	10	2	6	10	14	2	6	10		2	6					2	
89 Ac	2	2	6	2	6	10	2	6	10	14	2	6	10		2	6	1				2	
90 Th	2	2	6	2	6	10	2	6	10	14	2	6	10		2	6	2				2	
91 Pa	2	2	6	2	6	10	2	6	10	14	2	6	10		2	6	1				2	
92 U	2	2	6	2	6	10	2	6	10	14	2	6	10	3	2	6	1				2	
93 Np	2	2	6	2	6	10	2	6	10	14	2	6	10	4	2	6	1				2	
94 Pu	2	2	6	2	6	10	2	6	10	14	2	6	10	5	2	6	1				2	
95 Am	2	2	6	2	6	10	2	6	10	14	2	6	10	6	2	6	1				2	
96 Cm	2	2	6	2	6	10	2	6	10	14	2	6	10	7	2	6	1				2	
97 Bk	2	2	6	2	6	10	2	6	10	14	2	6	10	8	2	6	1				2	
98 Cf	2	2	6	2	6	10	2	6	10	14	2	6	10	10	2	6					2	
99 E	2	2	6	2	6	10	2	6	10	14	2	6	10	11	2	6					2	
100 Fm	2	2	6	2	6	10	2	6	10	14	2	6	10	12	2	6					2	
101 Md	2	2	6	2	6	10	2	6	10	14	2	6	10	13	2	6					2	
102 No	2	2	6	2	6	10	2	6	10	14	2	6	10	14	2	6					2	
103 Lw	2	2	6	2	6	10	2	6	10	14	2	6	10	14	2	6	1				2	

← Rare earths

← Transition elements (3rd series)

← Actinides

- (2) the increasing sequence of energies for electrons belonging to the various sub-shells depends only slightly on the exact value of this potential $W(r)$ and is as indicated in figure 2.1: 1s, 2s, 2p, 3s, 3p, and so on;
- (3) as a result of the indistinguishability of the electrons and Pauli's principle, there is a maximum number of electrons that may belong to each sub-shell.

These three properties enable the ground configuration of an atom to be determined once the total number Z of its electrons is known (see table 2.1).

For atoms having more than 18 electrons, it is difficult to state the ground configuration at once. As we have already indicated (see section 2.2 and figure 2.1), a certain number of electronic states such as 4s and 3d, 5s and 4d, have nearly equal energies, and the form of the central potential used for the best description of the atom will determine which one is the greater. Therefore it is not always obvious which configuration corresponds to a minimum energy. Table 2.2 gives the ground configurations of different atoms (see page 32). Examination of this table prompts the following remarks.

(a) The order of filling of the sub-shells, with a few exceptions, is given in figure 2.1 (the direction of the arrows). When several electronic states have nearly the same energy, under the assumption of a central potential, those with the smallest l (s state, $l = 0$) fill up first. It may be asserted that the order of filling corresponds to a regular increase of the quantity $n + l$.

(b) This order of filling means that certain sub-shells start to fill, even though a sub-shell of smaller principal quantum number n may be completely empty. The ground configurations of many atoms demonstrate this anomaly.

Examples Potassium, calcium ($n = 3$, $l = 2$); rubidium, strontium ($n = 4$, $l = 2$ and $l = 3$); elements 39–57 ($n = 4$, $l = 3$) and so on.

(c) The so-called *transition elements* are groups of ten elements that correspond to the progressive filling of an $(n - 1)d$ sub-shell even though the ns sub-shell is already occupied. Three series of transition elements exist:

filling of the 3d sub-shell from $Z = 21$ to $Z = 30$,

filling of the 4d sub-shell from $Z = 39$ to $Z = 48$,

filling of the 5d sub-shell from $Z = 71$ to $Z = 80$.

(d) The so-called *rare-earth elements* are the 14 elements corresponding to the progressive filling of the 4f sub-shell, even though the 6s sub-shell is already complete (from $Z = 57$ to $Z = 70$).

(e) Irregularities exist in the order of filling: compare, for example, the adjacent elements 23 and 24; 40 and 41; 57 and 58; 77 and 78, and so on.

2.4.2 The ground configuration and the properties of an atom

(1) *Ionisation potential*. Experiments such as Lenard's permit investigation of the binding energy of the electrons that are least strongly bound to the rest of the atom, and allow ionisation potentials to be defined (see volume 1, chapter 1). Figure 2.3 shows the ionisation potentials for atoms of atomic number up to 40. Simple considerations enable these results to be understood.

Let us first consider a very elementary picture of a spherically symmetric distribution of electrons in successive shells. Let r be the number of electrons in the outermost shell, that is those with the largest value of the quantum number n . An elementary electrostatic model (such as that discussed in the course of the study of Moseley's law in volume 1, chapter 7) shows us that each of the external electrons sees a field corresponding to the attraction by r protons only. A single outer electron ($r = 1$) will therefore be much more weakly

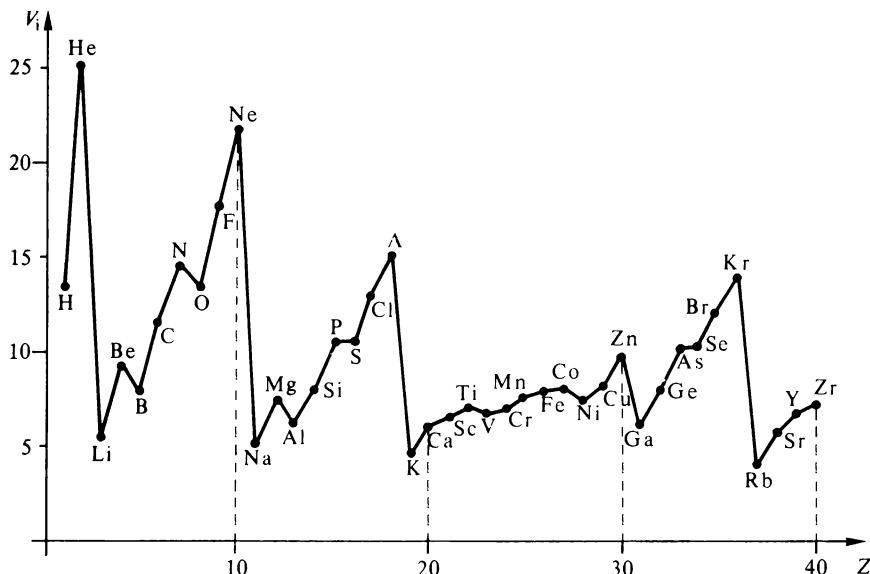


Figure 2.3 Ionisation potential V_i of elements whose atomic number Z is between 1 and 40

bound than an electron belonging to an outer shell for which the number r is large. The ionisation potential V_i will therefore be an increasing function of r , which is particularly noticeable in figure 2.3: V_i is a minimum for the alkali atoms (Li, Na, K, Rb, Cs) which have only one outer electron. On the other hand V_i is a maximum for the rare gases (He, Ne, Ar, Kr, Xe) whose outer s and p sub-shells are complete and contain a total of $r = 8$ electrons.

The preceding outline is far from perfect because the picture of shells of successive charges of spherical symmetry is not realistic. It should be noted in particular that potassium and copper, each having one outer s electron, have very different ionisation potentials. The efficiency of screening from the nuclear charge depends on the exact nature of the interior sub-shells. Let us refer back to the curves giving the position probability density of an electron in a central potential (figure 1.10). We may verify that the position probability of a $3d$ electron extends to much greater distances from the nucleus than those of a $3p$ electron. Hence the inner shells $1s^2 2s^2 2p^6 3s^2 3p^6$ of potassium form a more efficient screen between the outer $4s$ electron and the nuclear charge than that formed by the inner shells $1s^2 2s^2 2p^6 3s^2 3p^6 3d^{10}$ of copper.

(2) *Chemical properties.* The chemical properties of an atom are related to the bonding possibilities of that atom with others. This problem is extremely complex—it may involve a wide variety of interaction processes: electrostatic forces, exchange forces of quantum origin (see section 4.3.5). We shall confine ourselves to a few very elementary remarks that concern in particular the relation between the configuration of the atom and its chemical properties.

(a) We saw previously that electrons of a slightly filled outer shell were characterised by a small ionisation potential. The corresponding atoms can easily lose the electrons of this outer shell, called valence electrons; the atoms then form a positive ion, providing the origin of very strong electrostatic bonding.

(b) Now let us consider an atom such as chlorine, bromine or iodine. The number of electrons in the outer shell is $r = 7$. It requires one more for the p shell to be complete. This outer shell, therefore, is not spherically symmetric and so provides only imperfect screening between a charge external to the atom and the charges of the inner shells and nucleus. In particular, an additional electron is often captured and a negative ion is thereby formed. These atoms are also very reactive.

(c) Interactions between atoms can result also from an electrostatic bonding involving the absence of spherical symmetry of the charge distribution (see appendix 3). The noble gases (helium, neon, argon, krypton, xenon, radon), with all their sub-shells complete, have a spherically symmetric distribution of charges, enabling their great chemical inactivity to be understood.

(d) In table 2.2, we remarked that a certain number of elements have an incompletely filled inner sub-shell, and we called them 'transition elements'. Electrons in an incomplete sub-shell may have a binding energy only slightly different from that of the outer electrons. Several types of positive ions may be formed and the element is characterised by several valencies (for example mono- or divalent copper, bi- or trivalent iron, chromium, manganese and so on).

These elements are also characterised by noteworthy magnetic properties: the magnetic moment of the atom or ion resulting from the combination of orbital and spin angular momenta of incomplete sub-shells usually has a large value.

(3) *The periodic classification of the elements.* In the last century, Mendeléev proposed a classification of the elements by their chemical properties, in the form of a table in which elements of the same vertical column possess comparable chemical properties, elements in the same horizontal line forming a period. The atomic number Z of each element was obtained by numbering the positions in this table.

Chemists have come to perfect this table by dividing each of the vertical columns into a column A and a column B, displayed separately by extending the layout as in table 2.3. The correspondence between this extended table, the manner of filling the sub-shells, and the value of the ionisation potentials is remarkable, and in agreement with the discussion in the preceding section.

Table 2.3 is a relatively simple presentation of this periodic classification, showing the correlations between properties of the elements and their electronic configuration; the parts of the table corresponding to the elements classified by columns are shown in thick lines. Information concerning the electronic configuration is shown in thin lines and thin characters. At the centre are the groups of transition elements. The position of the elements traditionally called 'rare-earths' is marked by a cross. The latter differ from

Table 2.3 Periodic table
Column numbers are those of the early periodic tables

1s	2s	3s	4s	5s	6s	7s	IA	IIA											IIIB	IVB	VB	VIB	VII B	VIII B																																																																																						
1	2						H	He																																																																																																						
3	4						Li	Be											5	6	7	8	9																																																																																							
11	12						Na	Mg											13	14	15	16	17	18																																																																																						
19	20						K	Ca											31	32	33	34	35	36																																																																																						
37	38						Rb	Sr											49	50	51	52	53	54																																																																																						
55	56						Cs	Ba											81	82	83	84	85	86																																																																																						
87	88						Fr	Ra											81	82	83	84	85	86																																																																																						
1	2											1	2	3	4	5	6	7	8	9	10																																																																																									
									3d	21	22	23	24	25	26	27	28	29	30																																																																																											
									4d	39	40	41	42	43	44	45	46	47	48																																																																																											
									5d	71	72	73	74	75	76	77	78	79	80																																																																																											
									6d	89	90	91	92																																																																																																	
									1	2	3	4	5	6	7	8	9	10																																																																																												
																			Number of electrons in the last sub-shell forming the ground state (except those elements encircled)																																																																																											
									4f	57	58	59	60	61	62	63	64	65	66	67	68	69	70	71	72	73	74	75	76	77	78	79	80	81	82	83	84	85	86	87	88	89	90	91	92																																																																	
									1	2	3	4	5	6	7	8	9	10	11	12	13	14	15	16	17	18	19	20	21	22	23	24	25	26	27	28	29	30	31	32	33	34	35	36	37	38	39	40	41	42	43	44	45	46	47	48	49	50	51	52	53	54	55	56	57	58	59	60	61	62	63	64	65	66	67	68	69	70	71	72	73	74	75	76	77	78	79	80	81	82	83	84	85	86	87	88	89	90	91	92										

Symbol refers to the last sub-shell

Note. To simplify this table, the transuranium elements (unstable) are not shown.

one another (see table 2.2) essentially by the filling of the 4f sub-shell. Their chemical properties are very similar. We have displayed on a grey background the elements whose chemical properties correspond to an affinity for external electrons (see paragraph 2(b) of this section). They are called metalloids in some traditional chemistry books.

3

Angular Momenta and Enumeration of the Energy Levels

A possible state of an atom is characterised not only by its energy, but also by its total angular momentum. This total angular momentum is obtained by the addition of the various angular momenta involved in the atom. In this chapter, we shall assume that the nucleus of the atom possesses no angular momentum; we shall take account only of the angular momenta of the electrons. Accordingly, the conclusions that are reached are valid only for atoms without nuclear angular momentum. The complete problem will be dealt with in chapter 6.

The determination of the total angular momentum of an atomic state is important for the following two reasons.

(1) It is closely related to the total magnetic moment, a property which can be inferred from the angular momentum and which can be measured by various types of experiment (see volume 1, chapters 9–11). However, we defer until chapter 5 the determination of the total magnetic moment of an atom, and the exact theoretical interpretation of these experiments.

(2) It presupposes a detailed study of the different elementary angular momenta which add together within the atom, and the way in which they orient themselves in relation to each other. Each of the possible orientations has a different energy value, and because of this, the degeneracy of each configuration is partially lifted. In general, it is impossible to calculate these

energies, but on the other hand it is easy to predict the number of these distinct energy values, and thus to label the separate energy levels that can be observed. This chapter is devoted to the second of these tasks.

3.1 Composition of Angular Momenta

3.1.1 Results of the quantum mechanical theory of angular momentum

An angular momentum σ can be characterised by two observable quantities: its magnitude $|\sigma|$ and its component σ_z . These two observables are characterised by the two quantum numbers j and m , which may be either integral or half-integral, and which enable the eigenvalues to be expressed

$$\begin{cases} \sigma_z = m\hbar & \text{(see volume 1, section 10.2 and figure 10.4)} \\ |\sigma| = \sqrt{[j(j+1)]}\hbar & \text{where } -j \leq m \leq j \end{cases}$$

If we consider only the orbital angular momentum of a particular electron, the quantum number j is integral and is identical to the quantum number l introduced in chapter 1 in the solution of Schrödinger's equation for a central potential.

The rules for combining angular momenta are established in textbooks on quantum mechanics: consider two angular momenta σ_1 and σ_2 with quantum numbers j_1, m_1 and j_2, m_2 respectively. The resultant angular momentum

$$\sigma = \sigma_1 + \sigma_2$$

will be characterised by the quantum numbers j and m such that

$$-j \leq m \leq +j$$

and

$$|j_1 - j_2| \leq j \leq j_1 + j_2$$

j can vary only by integer values between these two limits.

If j_1 and j_2 are both integral or both half-integral, the resultant quantum number j is necessarily integral. On the other hand, if one of them is integral and the other half-integral, then j is necessarily half-integral.

From the equation above we see that the number of possible values of j is equal to the smaller of the two numbers $2j_1 + 1$ and $2j_2 + 1$.

Comment To derive the preceding results, use is often made of the 'vector model'. Nowadays, the formalism of quantum mechanics is familiar to many students, and the vector model is becoming obsolete. In certain instances, however, it may be a useful 'model'; we shall discuss it later (chapter 4).

3.1.2 Notation

In studying the atom, a certain number of angular momenta of various origins have to be defined. We shall use the following conventions.

- (1) The quantum numbers are represented by the following letters:
- l = the quantum number associated with the orbital motion of an electron;
 - s = the spin quantum number of an electron, which always has the value $\frac{1}{2}$;
 - j = the quantum number associated with the total angular momentum of an electron;
 - L = the quantum number associated with the sum of the orbital angular momenta of the electrons of an atom;
 - S = the quantum number associated with the sum of the spin angular momenta of the electrons of an atom;
 - J = the quantum number associated with the total angular momentum of an atom.
- $m_l, m_s, m_j, m_L, m_S, m_J$ designate the magnetic quantum numbers associated with the projection of the preceding angular momenta on the axis of quantisation.
- (2) The angular momentum vector will be represented by the vector σ , with a subscript letter corresponding to the quantum number.

Example

$$\sigma_j = J\hbar$$

To summarise: in the case, for example, of the orbital motion of an electron, we write

$$\left\{ \begin{array}{l} \text{the vector operator:} \quad \sigma_l = l\hbar \\ \text{the eigenvalue of the modulus:} \quad |\sigma_l| = \sqrt{[l(l+1)]}\hbar \\ \text{the eigenvalue of the } O_z \text{ component: } (\sigma_l)_z = \sigma_{lz} = m_l\hbar \end{array} \right.$$

With this notation, we may define the resultant vectors

$$\left\{ \begin{array}{l} \sigma_j = \sigma_l + \sigma_s \\ \sigma_L = \sum_i \sigma_{l_i} \\ \sigma_S = \sum_i \sigma_{s_i} \\ \sigma_J = \sigma_L + \sigma_S = \sum_i \sigma_{j_i} = \sum_i \sigma_{l_i} + \sum_i \sigma_{s_i} \end{array} \right.$$

or, in units of \hbar ,

$$\left\{ \begin{array}{l} j = l + s \\ L = \sum_i l_i \\ S = \sum_i s_i \\ J = L + S = \sum_i j_i = \sum_i l_i + \sum_i s_i \end{array} \right.$$

the sum \sum being extended over all the electrons of the atom, denoted by the subscript i .

By projecting the dimensionless vector equations on to an Oz axis, we obtain the relations between the magnetic quantum numbers

$$m_j = m_l + m_s \quad m_L = \sum_i m_{l_i} \quad m_S = \sum_i m_{s_i}$$

$$m_J = m_L + m_S = \sum_i m_{j_i} = \sum_i m_{l_i} + \sum_i m_{s_i}$$

This notation, relating to the quantum numbers and the associated *dimensionless* vectors, has been adopted internationally by spectroscopists. Care should be taken because some quantum mechanics books adopt a slightly different notation.

3.1.3 Total angular momentum of a complete sub-shell

The resultant angular momentum of an assembly of electrons forming a complete sub-shell is zero. The quantum number m_l , defining the orientation with respect to an axis of quantisation, takes all values between $-l$ and $+l$, and an equal number of electrons have the values $m_s = +\frac{1}{2}$ and $m_s = -\frac{1}{2}$. Whatever the Oz axis on which we project the angular momentum vector, we will therefore have for the assembly of electrons

$$\sigma_z = \hbar \sum m_l + \hbar \sum m_s = 0$$

Thus an assembly of electrons forming a complete sub-shell will have spherical symmetry. This property allows us to simplify the problem of finding the total angular momentum of an atom: it will result from the combination of the angular momenta of the electrons in incomplete sub-shells. The study will be especially simple in the most common situation where only the outermost sub-shell is incomplete. The transition elements will present more complications since one of the inner sub-shells is also incomplete.

3.1.4 Angular momentum of the ground state: some examples

In the preceding chapter, we presented a table of the ground state configurations. For certain atoms, it is easy to go further and indicate the angular momentum of the ground state. Some examples may be given as follows.

(1) Sodium has the configuration $1s^2 2s^2 2p^6 3s$. The single $3s$ electron, with orbital angular momentum zero, gives the atom an angular momentum equal to $\frac{1}{2}\hbar$ by virtue of its spin. This accounts for the historical importance of the Stern and Gerlach experiment; by verifying the existence of a magnetic moment in the ground state and by demonstrating that the atom should be associated with an angular momentum of quantum number $J = \frac{1}{2}$, this experiment confirmed a theory incorporating the electron's own magnetic moment.

(2) Mercury is formed from complete sub-shells; the total angular momentum will therefore be zero.

(3) Carbon also has some complete sub-shells and two outer electrons which are p electrons. Thus the resultant angular momentum can have different values, depending upon the way in which the orbital and spin angular

momenta are combined. A more refined investigation that we shall carry out in the following sections will show that the degeneracy of the ground state (here equal to 15; see section 2.3) is lifted and that several energy levels corresponding to this configuration, but characterised by other parameters, may be defined. One of these, of minimum energy, is the ground state with its related angular momentum. Its magnitude can be determined only by a far more detailed study (see section 3.4).

(4) Gadolinium is a very complex atom, the 4f sub-shell containing seven electrons. The total angular momentum will result from the combination of these seven electrons with the angular momentum of the electron in the 5d sub-shell, which is also incomplete. The degeneracy of the ground configuration will be found to be equal to 34 320, and the statements concerning carbon are equally applicable.

3.2 Spin-Orbit Interaction

To explain the term T_2 , which was introduced in the preceding chapter to account for the interactions between the spin and orbital magnetic moments of the electrons, we shall consider the case of an electron subjected to a central potential $W(r)$. The electron of velocity v , spin s , describes an orbit with an orbital angular momentum $\sigma_l = r \times mv = \hbar l$. The calculation is carried out in two stages as follows.

3.2.1 The magnetic field \mathbf{B}' in a frame bound to the electron

The electron of charge $q = -e$ moves in the electrostatic potential

$$V(r) = W(r)/q = -W(r)/e$$

Thus in the laboratory frame, there exists a coulomb electric field $\mathbf{E} = -\text{grad } V$. However, in the frame R' bound to the electron there also exists, as a result of its motion and the laws of relativistic electromagnetism, a magnetic field \mathbf{B}' which can be calculated from v and \mathbf{E} . Let us consider the two galilean reference frames (R) $Oxyz$ and (R') $O'x'y'z'$, the reference frame (R') being in uniform translational motion in the Ox direction with velocity v with respect to (R). The usual formulae for the electric and magnetic fields under a change of reference frame may be written (using the conventional constant κ that depends on the units, and is defined in the introduction or in appendix 1)

$$\left\{ \begin{array}{l} E_x' = E_x \\ E_y' = \frac{E_y - \frac{v}{\kappa} B_z}{\sqrt{(1 - v^2/c^2)}} \\ E_z' = \frac{E_z + \frac{v}{\kappa} B_y}{\sqrt{(1 - v^2/c^2)}} \end{array} \right. \quad \left\{ \begin{array}{l} B_x' = B_x \\ B_y' = \frac{B_y + \frac{\epsilon_0 \mu_0}{\kappa} v E_z}{\sqrt{(1 - v^2/c^2)}} \\ B_z' = \frac{B_z - \frac{\epsilon_0 \mu_0}{\kappa} v E_y}{\sqrt{(1 - v^2/c^2)}} \end{array} \right.$$

Our problem is more complex because of the non-rectilinear motion of the electron.

We consider a particular instant t , and we choose as a moving frame (R'), the galilean frame tangential to the motion of the electron at this instant: its origin O' is coincident with the electron at this instant, and its velocity v coincides with that of the electron at the same instant t ; the axis $O'x'$ is therefore parallel to the tangent to the orbit. We may also choose a laboratory frame (R) whose axes have an origin O coincident with the position of the electron at the instant t (see figure 3.1). Between these two frames (R) and (R'), we apply the field transformation formulae set out above.

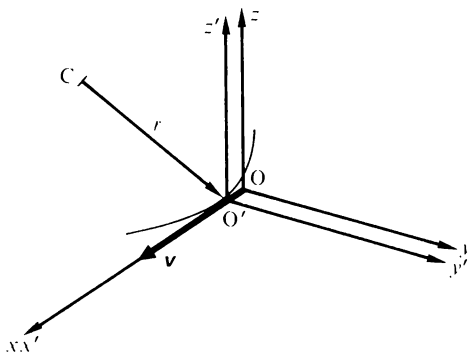


Figure 3.1 Diagram showing axes $Oxyz$ in the laboratory and axes $O'x'y'z'$ at an instant of time in a frame tangential to the motion of an electron

In addition we assume that (1) $v \ll c$, and thus the square root is nearly equal to unity; (2) the magnetic field is zero in the laboratory reference frame

$$B_x = B_y = B_z = 0$$

In the frame (R') we deduce that

$$\left\{ \begin{array}{l} B_x' = 0 \\ B_y' = \frac{\epsilon_0 \mu_0}{\kappa} v E_z = \frac{\kappa}{c^2} v E_z \quad (\text{using the relation } \epsilon_0 \mu_0 c^2 = \kappa^2) \\ B_z' = -\frac{\epsilon_0 \mu_0}{\kappa} v E_y = -\frac{\kappa}{c^2} v E_y \end{array} \right.$$

or, in vector form, independent of the particular axes used in the calculation

$$\mathbf{B}' = \frac{\kappa}{c^2} (\mathbf{E} \times \mathbf{v})$$

3.2.2 Interaction of the spin magnetic moment with the magnetic field \mathbf{B}'

The spin-orbit interaction energy, which we shall call ΔE , results from the interaction between the magnetic field \mathbf{B}' and the spin magnetic moment

$$\mathcal{M}_s = \frac{1}{\kappa} \frac{q}{m} \sigma_s = \frac{1}{\kappa} \frac{q}{m} \hbar s = -2\beta s$$

(q is negative, but the Bohr magneton β is positive).

We may make use of the results of classical electromagnetism by writing

$$\Delta E = \mathcal{M}_s \cdot \mathbf{B}'$$

However, it must be noted that \mathbf{B}' has a direction in a particular instantaneous reference frame (R') and that the electron is continually 'jumping' from one frame (R') to another tangential reference frame (R''). Evaluation of the coupling energy ΔE was carried out for this case by Thomas (in 1926). By expressing the energy in the laboratory frame (R), he obtained

$$\Delta E = -\frac{1}{2} \mathcal{M}_s \cdot \mathbf{B}'$$

We shall use this expression in the following calculation.

The remainder of the calculation of ΔE does not present difficulties. The electrostatic field \mathbf{E} may be deduced from $W(r)$

$$\mathbf{E} = -\text{grad } V = -\text{grad } \frac{-W(r)}{e} = \frac{1}{e} \frac{dW}{dr} \frac{\mathbf{r}}{r}$$

(\mathbf{r} is the radius vector directed from the centre of force C towards the electron at O').

If we write

$$\mathbf{B}' = \frac{\kappa}{c^2 m} \mathbf{E} \times m\mathbf{v} = \frac{\kappa}{c^2 m e} \frac{1}{r} \frac{dW}{dr} \mathbf{r} \times m\mathbf{v}$$

and since

$$\boldsymbol{\sigma}_l = \mathbf{r} \times m\mathbf{v}$$

we have

$$\mathbf{B}' = \frac{\kappa}{c^2 m e r} \frac{dW}{dr} \boldsymbol{\sigma}_l = \frac{\kappa}{m e c^2 r} \frac{dW}{dr} \hbar \mathbf{l}$$

The interaction energy between the magnetic moment \mathcal{M}_s and the field is therefore

$$\Delta E = -\frac{1}{2} \mathcal{M}_s \cdot \mathbf{B}' = -\frac{1}{2} \left(-\frac{1}{\kappa} \frac{e}{m} \hbar s \right) \cdot \mathbf{B}'$$

whence

$$\Delta E = \frac{\hbar^2}{2m^2 c^2 r} \frac{dW}{dr} \mathbf{l} \cdot \mathbf{s}$$

Important comment We note that dV/dr is negative and consequently dW/dr is positive. The quantity that precedes the scalar product $\mathbf{l} \cdot \mathbf{s}$ is positive.

The preceding calculation may be generalised to the case where the potential is not central, simply by replacing dW/dr with the partial derivative of W with respect to r . Thus we may finally write the spin-orbit interaction energy

$$\Delta E = \frac{\hbar^2}{2m^2 c^2 r} \frac{\partial W}{\partial r} l \cdot s \quad (3.1)$$

We note that this result involves only mechanical quantities. The formula is therefore the same in MKSA or CGS units. This ceases to be so if we transform the previous expressions by using the Bohr magneton

$$\beta = \frac{1}{\kappa} \frac{e\hbar}{2m}$$

We then obtain

$$B' = -2\varepsilon_0 \mu_0 \frac{\beta}{e} \frac{1}{r} \frac{\partial V}{\partial r} l \quad \text{and} \quad \Delta E = -2\varepsilon_0 \mu_0 \frac{\beta^2}{e} \frac{1}{r} \frac{\partial V}{\partial r} l \cdot s$$

Comment A simpler and more intuitive but less general argument also allows the preceding results to be derived. Suppose that the electron describes a circular path. In its rest frame, it sees the nucleus orbiting with a velocity $-v$. By using the elementary laws of electricity, the reader may easily show that the electron will see, as a result of this motion of the nucleus, a magnetic field

$$B' = \frac{\mu_0}{4\pi\kappa} Ze(-v) \times \frac{r}{r^3} = \frac{\mu_0}{4\pi\kappa} \frac{Ze}{r^3} r \times v$$

the radius vector r being directed from the nucleus C towards the electron. B' may be transformed straightforwardly

$$B' = \frac{\mu_0}{4\pi\kappa} \frac{Ze}{r^3} \frac{\sigma_1}{m} = \frac{\kappa}{c^2 4\pi\varepsilon_0} \frac{Ze}{r^3} \frac{\sigma_1}{m} = \frac{\kappa}{c^2 mer} \frac{dW}{dr} \sigma_1$$

$W(r)$ is the potential energy corresponding to the coulomb attraction of the nucleus. Thus we again arrive at the same expression for B' and the calculation may be completed as before.

Evaluation of the assembly of spin-orbit couplings in an atom. The expression for ΔE obtained above during the study of an electron moving in a potential $W(r)$, will allow us to evaluate the term T_2 of the hamiltonian H of the atom (see section 2.1). We note that in the calculation of ΔE , the appearance of the orbital angular momentum $\hbar l$ expresses only the interaction of the spin with the potential $W(r)$ in which the electron moves. For an atom with N electrons, we must sum over N terms, each term corresponding to an electron labelled i and involving the product $l_i \cdot s_i$. The reader should satisfy himself that an expression containing a product such as $l_j \cdot s_i$, involving the orbital angular momentum of the electron j and the spin of the electron i , is meaningless. (This is strictly true only when assumptions (a) and (b) mentioned in section 2.1 are valid. A spin i -spin j interaction may lead to a spin i -orbit j coupling

by means of a spin j -orbit j coupling.) The term T_2 of the hamiltonian may then be written

$$T_2 = \sum_i \frac{\hbar^2}{2m^2 c^2 r_i} \frac{\partial W_i}{\partial r_i} l_i \cdot s_i$$

where $W_i(r)$ is the potential in which the electron i moves. Since T_2 enters only as a correction term, the non-central part in $W_i(r)$ can be neglected; $W_i(r)$ will then be the potential involved in H_0 .

3.3 Principles of the Calculation of Energy Levels in Atoms with Many Electrons

We now wish to show how the first approximation of a central potential discussed in chapter 2 can be refined by taking account of the terms T_1 and T_2 . The degeneracy of a given configuration will then be partially lifted and several energy levels corresponding to the same configuration will be obtained, which gives a more realistic situation. Two successive parts of the problem must be distinguished as follows.

- (1) From general considerations, related above all to the symmetries of the problem, it is possible to show, from the hamiltonian

$$H = H_0 + T_1 + T_2 \quad (\text{see section 2.1})$$

how the degeneracy is lifted and which are the parameters (in particular, the angular momenta) that allow characterisation of the energy levels thus distinguished.

- (2) A later stage—that we cannot treat in depth—consists of using approximation methods and then numerical calculations, in order to find the position of the energy levels. Chapter 4 will provide an introduction to this problem in the simple case of atoms with one or two electrons.

3.3.1 The possible approximations to the hamiltonian

The hamiltonian H describes an atom isolated in space, and the angular momentum \mathbf{J} must therefore be a constant of the motion. This is manifested quantum mechanically by the fact that H commutes with the vector operator \mathbf{J} , and every determined state of the atom is described by a value of the total angular momentum quantum number J .

As it is impossible to solve the problem described by the hamiltonian H exactly, the discussion will proceed in successive stages of approximation.

(1) The *first stage* (stage (1)) is already familiar to us: it consists of considering only the part H_0 ; this is the approximation of independent electrons in a central potential. Its solutions are the electronic configurations studied in the preceding chapter.

The next stages depend on the respective orders of magnitude of the two terms T_1 and T_2 .

(2) The *second stage* (stage (2)) associates either T_1 or T_2 with H_0 , so as to obtain either

$$\begin{aligned} H_1 &= H_0 + T_1 && \text{if } T_1 \gg T_2 \\ H_2 &= H_0 + T_2 && \text{if } T_1 \ll T_2 \end{aligned}$$

(3) Having obtained the descriptions of the energy levels corresponding to H_1 or H_2 , the *third stage* (stage (3)) consists of studying the small corrections that must be applied to these results in order to express the influence of the term that has been neglected:

either the influence of T_2 on the description corresponding to H_1 —this is described as *L-S coupling* ($T_1 \gg T_2$);
or the influence of T_1 on the description corresponding to H_2 —this is described as *j-j coupling* ($T_2 \ll T_1$).

The more general case, in which the two terms T_1 and T_2 are of the same order of magnitude, presents far greater difficulties; this intermediate coupling will not be considered in this book.

3.3.2 L-S coupling

We consider the case where $T_1 \gg T_2$ and study in broad outline stages (2) and (3) above, in order to understand how the degeneracy of a configuration such as calculated in the preceding chapter can be at least partially lifted.

Stage (2). Let us consider the hamiltonian $H_1 = H_0 + T_1$; it describes an isolated system and consequently commutes, like H , with the total angular momentum \mathbf{J} . By using the general properties of invariance demonstrated in texts on quantum mechanics, we establish that:

- (1) H_1 commutes with \mathbf{S} , where \mathbf{S} represents the angular momentum vector obtained by combining the individual spins \mathbf{s}_i of each electron (we remind the reader that although electron spins do not enter into T_1 explicitly, exchange effects require that the existence of electron spin be taken into account; see section 2.1);
- (2) H_1 commutes also with \mathbf{L} , where \mathbf{L} represents the angular momentum vector obtained by combining the orbital momenta \mathbf{l}_i of each electron.

Hence the following points may be deduced.

(a) The preceding commutation properties require that the different eigenstates of the system described by H_1 should be characterised by a pair of possible values of the quantum numbers L and S . The electrostatic interaction energy between the electrons depends on the relative positions of the electronic orbits, and therefore also on the relative orientations of the vectors \mathbf{l}_i . It is

these orientations that determine the vector \mathbf{L} ; consequently it may be understood why the energy is different for each value of the quantum number L . Exchange effects also require that the energy depends on S for a given value of L . Thus the degeneracy of the configuration obtained in stage (1) is found to be at least partially lifted.

(b) H_1 does not contain any term expressing the relative orientations of the pairs of vectors $\mathbf{l}_i, \mathbf{s}_i$. All states having given values of L and of S , whatever the value of J , have the same energy; they remain degenerate.

(c) To a possible value of L , there correspond $2L + 1$ orientations of this momentum with respect to the axis of quantisation; similarly, for a given value of S there correspond $2S + 1$ possible orientations of this momentum. Therefore an energy level characterised by the pair of numbers LS will still be $(2L + 1)(2S + 1)$ times degenerate.

We obtain distinct energy levels arising from the same configuration by seeking the different pairs of quantum numbers L, S compatible with this configuration. Since the orbital momenta and the spin momenta resultants of a complete sub-shell are zero, it is sufficient to consider only the electrons of incomplete sub-shells in order to obtain the vectors \mathbf{L} and \mathbf{S} . When we combine on the one hand the vectors \mathbf{l}_i and on the other hand the vectors \mathbf{s}_i , in order to obtain \mathbf{L} and \mathbf{S} , the possible mathematical solutions are not all necessarily compatible with the Pauli principle and the principle of indistinguishability of the electrons. This will be considered in more detail in the examples in section 3.3.4.

Stage (3). We now seek the predictable results of the perturbation calculation that takes into account the term T_2 . The hamiltonian $H = H_0 + T_1 + T_2$ no longer commutes with \mathbf{L} and \mathbf{S} but only with \mathbf{J} . The eigenstates will be characterised by the single quantum number J and the degeneracy in J , mentioned in paragraph (b), will be lifted.

The spin-orbit interaction energy T_2 depends on the relative orientations of the pairs of vectors $\mathbf{l}_i, \mathbf{s}_i$ and consequently on the relative orientation of the resultant vectors \mathbf{L} and \mathbf{S} . This relative orientation determines the vector $\mathbf{J} = \mathbf{L} + \mathbf{S}$; thus it may be understood why each value of the quantum number J corresponds to a different value of the energy. These energy differences between levels of the same S and the same L but different J , resulting from the influence of the term T_2 , are usually called fine structures. Each energy level characterised by the quantum number J is still $2J + 1$ times degenerate.

We obtain all the distinct energy levels arising from the same level (L, S) of stage (2), by finding all the values of J compatible with the quantum numbers L and S . From the rules for combining angular momenta, reviewed in section 3.1, the number of possible values of J is equal to the smaller of the two numbers $2S + 1$ and $2L + 1$. In most cases, S is smaller than or equal to L , and the number of distinct energy levels arising from the same level (L, S) is then equal to $2S + 1$. This number $2S + 1$ is often called *the multiplicity* of the level (L, S) of stage (2); this terminology is retained even if L is less than S .

The distinct levels J obtained in this way are fairly close, since the term T_2

is small in relation to the other terms of the hamiltonian. They are described as forming a multiplet:

- a singlet if $2S + 1 = 1$ that is to say $S = 0$
- a doublet if $2S + 1 = 2$ that is to say $S = \frac{1}{2}$
- a triplet if $2S + 1 = 3$ that is to say $S = 1$
- a quartet if $2S + 1 = 4$ that is to say $S = \frac{3}{2}$, and so on.

Figure 3.2 summarises these ideas by showing successively the influence of the terms T_1 and T_2 , for the case of a p-p configuration (the atoms of carbon or silicon for example). In this diagram we give details of the different levels corresponding to stages (2) and (3) of successive approximation. In the enumeration of the possible levels, we have taken into account the influence

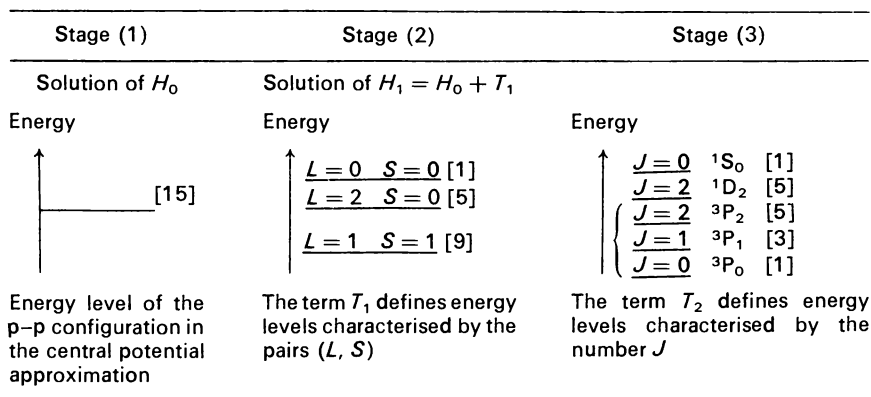


Figure 3.2 Fine structure of the energy levels of the p-p configuration in L - S coupling (the orders of degeneracy are in square brackets)

of Pauli's principle and of the indistinguishability of the electrons. The reader should note particularly that in stage (2) not all possible combinations of the values of L and S are present. In drawing up figure 3.2 we have anticipated the results of section 3.4.

Spectroscopic notation. In L - S coupling, it is usual to designate an energy level (or spectral term) by a set of symbols defining the values of L , S and J .

- (1) A letter characterises the value of L according to a notation convention introduced by early spectroscopists. It is merely the transposition in capital letters of the convention already described at the end of section 1.2 for the quantum number l of an electron:

Letter symbol:	S P D F G H
Corresponding value of L :	0 1 2 3 4 5 etc.

- (2) A superscript in front of the letter gives the value of the multiplicity $2S + 1$ (and not the value of S). This may seem at first sight to be a little irrational but in practice it proves to be useful.

(3) A subscript after the letter gives the value of J .

To summarise, this notation may be represented thus

$${}^{2S+1}[\text{letter symbolising value of } L]_J$$

Examples

$${}^2F_{5/2} \rightarrow S = \frac{1}{2} \quad L = 3 \quad J = \frac{5}{2}$$

$${}^3D_2 \rightarrow S = 1 \quad L = 2 \quad J = 2$$

Often, the configuration of which the level considered forms part can be designated without ambiguity by indicating the quantum number n of an electron that has been excited. For example, the ground configuration of an atom of mercury is

$$(i) (\text{---}) 6s^2$$

and some of the excited configurations are

$$(ii) (\text{---}) 6s 6p \quad (iii) (\text{---}) 6s 7p \quad (iv) (\text{---}) 6s 6d, \text{ etc.}$$

The different levels of the configurations (i), (ii) and (iv) are defined by putting the number 6 in front of the symbol defined previously

$$6 {}^1S_0, 6 {}^3P_1, 6 {}^3D_2$$

and so on, and the levels of configuration (iii) by putting the number 7:

$$7 {}^3P_1$$

3.3.3 j - j coupling

In *stage* (2) we study the hamiltonian $H_2 = H_0 + T_2$, where H_0 is a hamiltonian describing a central potential, as is T_2 , in accordance with the approximation that we stated at the end of section 3.2; H_2 can then be written

$$H_2 = \sum_i \left[-\frac{\hbar^2}{2m} \Delta_i + W(r_i) + l_i \cdot s_i \frac{\hbar^2}{2m^2 c^2} \frac{1}{r_i} \frac{dW(r_i)}{dr_i} \right]$$

This is the hamiltonian of identical independent particles in a central potential.

Each of the electrons, assumed isolated in this central potential, will have energy levels characterised by j_i , the quantum number corresponding to the total angular momentum of the electron, and by the values l_i and s_i . The problem is the same as that treated in section 1.5 and continued in section 2.2, but as a result of spin-orbit interaction, the eigenstates of the electron will be characterised not only by n_i and l_i but also by j_i . It should be noted that, for a given configuration, j_i can take only two values, $l_i - \frac{1}{2}$ and $l_i + \frac{1}{2}$.

The energy levels of the hamiltonian H_2 may be found without difficulty, the energy being the sum of the individual energies of the electrons, and a particular level will be characterised by the set of quantum numbers n_i , l_i and j_i of the individual electrons. Figure 3.3 shows the energy levels for two p electrons of given quantum number n , characterised by j values equal to $\frac{1}{2}$ and $\frac{3}{2}$. The centre column defines the energy levels of the hamiltonian H_2 . We note that as a result of the indistinguishability of the electrons, the two states $j_1 = \frac{1}{2}, j_2 = \frac{3}{2}$ and $j_1 = \frac{3}{2}, j_2 = \frac{1}{2}$ have the same energy.

In *stage* (3), we now investigate the influence of the term T_1 considered as a correction to the preceding results. The energy levels that we obtained as eigenvalues

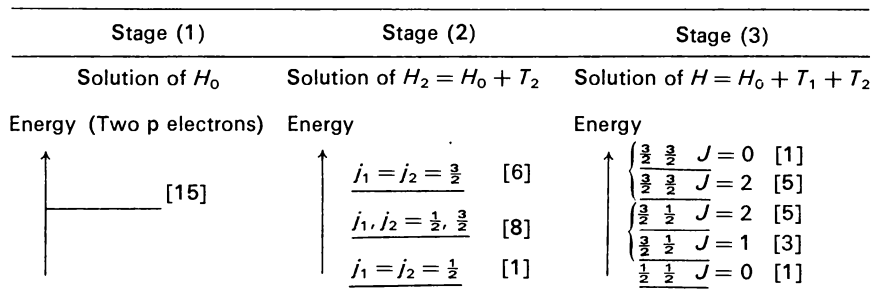
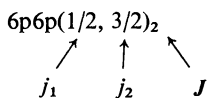


Figure 3.3 Fine structure of the energy levels of the p-p configuration in $j-j$ coupling (as for the ground state of lead (Xe) $6s^2 6p^2$). *Note*: The positions of the levels (the orders of degeneracy are in square brackets) as shown in figures 3.2 and 3.3 are entirely arbitrary. Only the principle is illustrated

of H_2 are characterised by the different j_i and can thus correspond to various values of the angular momentum J ; these energy levels are therefore degenerate in J . On the other hand $H = H_2 + T_1$ has eigenvalues characterised by J . The degeneracy in J will be lifted and the energy levels will now be defined by the j_i and a particular value of J . The third column in figure 3.3 gives the result for an atom with two p electrons. We suggest that the reader confirms, after studying section 3.4, the number of levels arising from stages (2) and (3) as consequences of the indistinguishability of the electrons and of Pauli's principle.

Notation. It is obvious that neither the resultant L of the orbital momenta nor the resultant S of the spins are involved in any way. The notation for the spectral terms must state the quantum numbers n_i, l_i, j_i and the total angular momentum J for each electron. The values of j_i are usually written within brackets, followed by a subscript denoting the value of J and preceded by the characteristic set of n_i and l_i for the electrons contributing to the angular momentum.

Example One of the levels of the ground configuration of lead (corresponding to figure 3.3) may be denoted as



Comments The two cases treated in sections 3.3.2 and 3.3.3 are extreme cases permitting a fairly precise theoretical study of a certain number of elements; but many actual cases are only imperfectly described by one or other of these models. Consider for example the elements that possess complete internal sub-shells and two p electrons in their ground state: carbon, silicon, germanium, tin, lead (Group IV B of the periodic table). Carbon is adequately described by $L-S$ coupling, lead by $j-j$ coupling, but silicon, germanium and tin must be studied under conditions of intermediate coupling.

Now H commutes with J ; also, the number of possible states derived from the assembly of electrons, characterised individually by s_i and l_i , is always the same, whatever the type of coupling. The reader should be able to deduce that the number of levels having the same value of J is independent of the type of coupling (compare figures 3.2 and 3.3).

Different models have been proposed to study intermediate coupling, especially for atoms involving more than two electrons (the excited states of the rare gases in particular). Even a schematic study of them is beyond the scope of this book.

3.4 Determination of the Angular Momenta and Enumeration of the Different Energy Levels of a Configuration



In the previous section we presented general outlines of the methods of calculation of energy levels by means of stages (1), (2) and (3) of successive approximation. The study can now be taken a little further. By taking account on the one hand of the indistinguishability of electrons and of the Pauli principle, and on the other hand of the rules for combining angular momenta, we will show in this section how the exact number of distinct energy levels corresponding to the same configuration may be counted, and how to attribute an angular momentum to each of them. In this section we shall consider only the case of L - S coupling. The reader could—and this would be an excellent exercise—carry out an analogous study for the case of j - j coupling.

As remarked in the preceding section, in order to determine the values of L , S and J , it is sufficient to combine the angular momenta of electrons not belonging to complete sub-shells. For the various elements, these electrons appear on a white background in table 2.2. Two cases should be considered as follows.

3.4.1 Electrons belonging to different sub-shells



None of the electrons belonging to incomplete sub-shells has both quantum numbers n and l simultaneously equal to those of another electron. (These are called non-equivalent electrons.) All combinations of the vectors l_i and s_i are possible, none being forbidden by Pauli's principle. The quantum numbers L , S and J are determined by seeking all possible combinations, first of s_i and l_i , then of S and L . To each different value of J obtained (from the different

Table 3.1

Stage (1)	Stage (2)		Stage (3)			
Configuration	S	L	Order of degeneracy ($2S + 1$) ($2L + 1$)	J	Spectral term	Order of degeneracy $2J + 1$
$ns-np$	0	1	3	1	1P_1	3
$l_1 = 0 \quad l_2 = 1$				0	3P_0	1
Order of degeneracy ($4l_1 + 2$) ($4l_2 + 2$) = 12	1	1	9	1	3P_1	3
				2	3P_2	5
						
	Two distinct levels			Four distinct levels		

values of L or S) there corresponds a distinct energy level. Tables 3.1 and 3.2 provide two examples, and the agreement between the degeneracies obtained may be confirmed.

Table 3.2

Stage (1)	Stage (2)		Stage (3)				
Configuration	S	L	Order of degeneracy ($2S + 1$)	($2L + 1$)	J	Spectral term	Order of degeneracy $2J + 1$
	0	0	1		0	1S_0	1
	0	1	3		1	1P_1	3
	0	2	5		2	1D_2	5
$np\text{-}mp$ $l_1 = 1 \quad l_2 = 1$ Order of degeneracy $(4l_1 + 2)(4l_2 + 2) = 36$	1	0	3		1	3S_1	3
					0	3P_0	1
	1	1	9		1	3P_1	3
					2	3P_2	5
					1	3D_1	3
	1	2	15		2	3D_2	5
					3	3D_3	7
							

3.4.2 Equivalent electrons (belonging to the same sub-shell)

Apart from complete sub-shells, an atom may possess equivalent electrons, that is to say, belonging to the same sub-shell and having the same quantum numbers n and l . We confine ourselves to considering the case of two equivalent electrons. More complex cases can be treated by means of a similar technique.

An elegant method provides an immediate solution to the problem: it is sufficient to use the symmetries of the wave function and we refer the reader who is sufficiently familiar with quantum mechanics to specialised books (see Messiah, page 600). Here we use the more elementary method of deducing the different states satisfying Pauli's principle and of seeking the spectral terms that can be formed with these states.

We explain the method by taking the example of two equivalent p electrons. The order of degeneracy of a p-p configuration is $G = 15$ (see chapter 2). Let us set up a table (table 3.3) allowing all the possible states to be classified. To do this, we set out the magnetic quantum numbers m_l ($-1, 0, +1$) and m_s ($-\frac{1}{2}$ and $+\frac{1}{2}$) of electron 1 in a horizontal line and the same quantities for electron 2 in a vertical line.

Thus we form 36 squares, but we note:

- (1) that the squares placed on the principal diagonal of the table correspond to states having two electrons with the same quantum numbers m_l and m_s —Pauli's principle requires that they be eliminated:

(2) that since the electrons are equivalent, it is impossible to distinguish states represented by two symmetric positions with respect to the principal diagonal—a straightforward analysis shows that only 15 states are realisable, which is consistent with the value of G already calculated.

In each square, we indicate the values of the magnetic quantum numbers m_L and m_S corresponding to the total angular momenta. From the principle of composition of angular momenta, they are equal to

$$m_L = m_{l_1} + m_{l_2}$$

$$m_S = m_{s_1} + m_{s_2}$$

respectively.

Without Pauli's principle and indistinguishability we would obtain from stage (2) of approximation the six distinct levels (L, S) obtained in table 3.2.

Table 3.3

1	1	0	0	-1	-1	m_{l_1}
$\frac{1}{2}$	$-\frac{1}{2}$	$\frac{1}{2}$	$-\frac{1}{2}$	$\frac{1}{2}$	$-\frac{1}{2}$	m_{s_1}

1	$\frac{1}{2}$								
1	$-\frac{1}{2}$	2	0						
0	$\frac{1}{2}$	1	1	1	0				
0	$-\frac{1}{2}$	1	0	1	-1	0	0		
-1	$\frac{1}{2}$	0	1	0	0	-1	1	-1	0
-1	$-\frac{1}{2}$	0	0	0	-1	-1	0	-1	-1
m_{l_2}	m_{s_2}								

In each square

$m_L m_S$

(e) (d) (c) (b) (a)

1S_0 3P 1D_2

We now show for the case with which we are concerned that the values indicated for m_L and m_S are compatible only with a restricted number of levels.

(a) We note that in table 3.3, the particular value $m_S = 1$ and $m_L = 2$ does not exist. A 3D set of levels (the multiplet $S = 1, L = 2$) therefore cannot exist since some of the states required for this multiplet are missing.

(b) We find the values $m_S = 0, m_L = 2$ and $m_S = 0, m_L = -2$. A multiplet with $L = 2$ therefore must exist, and as we have eliminated the multiplet 3D , it can only have $S = 0$, that is to say the multiplet 1D consisting of the single level 1D_2 . The set of values situated on the line (a) allows this 1D_2 term to be constructed.

(c) In the remaining squares, we note especially the states $m_L = 1, m_S = 1$ and $m_L = 1, m_S = -1$. The multiplet $S = 1, L = 1$ therefore should exist; the corresponding levels ${}^3P_2, {}^3P_1, {}^3P_0$ can therefore be constructed from the set of values situated on lines (b), (c) and (d).

(d) The last remaining square, on line (e), corresponds to the term 1S_0 .

To summarise, the p-p configuration will contain five levels as shown in table 3.4 below. This is the assumption made in setting up figure 3.2 and which is now vindicated.

Table 3.4

Stage (1)	Stage (2)			Stage (3)		
Configuration	S	L	Order of degeneracy ($2S + 1$) ($2L + 1$)	J	Spectral term	Order of degeneracy $2J + 1$
	0	0	1	0	1S_0	1
$np-np$	0	2	5	2	1D_2	5
$l_1 = 1 \quad l_2 = 1$				0	3P_0	1
Order of degeneracy	1	1	9	1	3P_1	3
$G = 15$				2	3P_2	5
	⏟			⏟		
	Three distinct levels			Five distinct levels		

3.4.3 Hund's rule

The analysis carried out in sections 3.4.1 and 3.4.2 has led to an enumeration of the energy levels corresponding to a particular configuration, but we have no information, even qualitative, as to the position of these levels. Hund's rule partially fulfils this requirement by providing information about the structure of the level whose energy is the lowest within a configuration. It states that:

the lowest energy level of a given configuration has the largest possible value of S , and for this value of S , the greatest possible value of L .

The proof of this rule is not strictly rigorous and is beyond the scope of this book. Hund's rule is valuable for a ground configuration; it allows the values of S and L of the ground configuration to be determined, an important application, especially in the study of magnetism.

3.5 Summary

The central potential approximation involves only *the electrostatic* interactions within the atom. As shown in chapter 2, it gives rise to the notion of a *configuration* that characterises the atom by a description of the individual electrons distributed in shells and sub-shells.

The next stage, developed in this chapter, was to complete the model of the atom by introducing, in particular, *magnetic interactions* and seeking the values of the total angular momentum. Thus we defined the possible energy levels that correspond to a given configuration. The complexity of the problem did not permit us to go beyond the stage of enumerating energy levels, but the results obtained are fundamental: they are preliminary to all more detailed studies, such as those of the following chapter, and are introductory to the discussion of atomic magnetism in chapter 5.

4

The Spectroscopy of Systems with One and Two Electrons

The main purpose of the discussion in the preceding chapters was to explain and characterise the various energy levels of the atom. We met the concept of a configuration (chapter 2), and then the characterisation of the levels as a function of the various angular momenta involved (chapter 3). However, we only established qualitative results and there is little possibility of obtaining more detailed information about the position of these levels on an energy scale. There are two main reasons for this:

- (1) as we indicated at the beginning of chapter 2, the formulation of the complete equation proves to be very complex: it is necessary to take account of many interactions that, depending on the atoms considered, can have a wide range of relative magnitudes;
- (2) no rigorous solution is possible and a quantitative study requires, in a majority of cases, the use of numerical methods.

The object of this chapter, in contrast to that of chapter 3, is to present a more detailed study of some particular cases for which we may either establish some simple results for the position of the levels, or provide interesting information from a historical point of view or in terms of the ideas that emerge from such information.

The influence of the nucleus (interactions (5) and (6) described in section 2.1)

should also be studied. These interactions will be considered as the final stage of our study and will be the subject-matter of a special chapter. Thus the results obtained in this chapter will be valid—apart from small corrections—only for atoms whose nuclear spin is zero.

Atomic spectroscopy is concerned with the study of the characteristic frequencies of the radiation emitted by atoms. Since many properties of an atom derive from the spectra observed, this discipline has considerable importance. In this chapter we shall make use of the relationship between the energy levels and the radiative transitions that are observed. As a result of the Ritz combination principle, the wave numbers $1/\lambda$ of the observed transitions may be obtained from the difference of two spectral terms

$$\frac{1}{\lambda} = T_p - T_q$$

the spectral term T being equal to

$$T = -\frac{1}{hc}E$$

where E is the energy of a level. However, not all combinations of spectral terms are possible; only a limited number of them can be observed, and *selection rules* allow these to be determined. In some simple cases the selection rules can be established from a semi-classical theory of radiation. In each case studied in this chapter, we confine ourselves to stating the selection rules and describing their use by means of examples. Nevertheless, in section 4.1, we indicate the stages in the quantum treatment that allow the selection rules to be derived. Some of the points raised will become familiar to the reader only after studying chapter 5 and appendixes 3 and 5. Therefore we suggest that the study of this next section could be postponed.

4.1 Selection Rules

The quantitative study of transition probabilities between two levels 1 and 2 requires knowledge of the values of the coefficients A_{21} , B_{21} , B_{12} (see volume 1, chapter 3). Direct study of the spontaneous emission coefficient A_{21} , which is the main concern of this chapter, proves to be more difficult in quantum formalism than that of the coefficients B_{21} and B_{12} ; however, we note that the relation

$$A_{21} = \frac{8\pi h}{\lambda^3} B_{21}$$

allows us to reduce the problem to the study of the absorption and induced emission coefficients B_{12} and B_{21} .

These two coefficients express the interaction of an atom with an external electromagnetic field. In the presence of such a field, the hamiltonian of an atom may be obtained by adding the terms defined by relation (5.12) to the hamiltonian of the free atom. Some of the terms of the hamiltonian are rearranged into a term $H^{(1)}$ dependent on time. The study of the hamiltonian may therefore be carried out by using time-dependent perturbation theory and from this we learn that the transition

probability, induced by the perturbation between the states 1 and 2 of the atom, is proportional to the square of the matrix element

$$\langle 1 | H^{(1)} | 2 \rangle$$

connecting the description of state 1 to that of state 2.

In general, it is impossible to evaluate transition probabilities rigorously, and so an expansion of $H^{(1)}$ in terms of successive multipole orders is used (see appendix 3). These terms express successively:

- (1) the coupling of the electric field $\mathbf{E}(t)$, assumed uniform over the volume of the atom, with the electric dipole moment \mathbf{p} of the atom;
- (2) the coupling of the magnetic field $\mathbf{B}(t)$, assumed uniform, with the magnetic dipole moment \mathcal{M} of the atom;
- (3) the coupling of the electric field and of the magnetic field with the electric quadrupole moments; and so on.

We restrict ourselves to a brief analysis of the case of *electric dipole emission* corresponding to the first term, disregarding the rest. $H^{(1)}$ may then be written

$$H^{(1)} = -\mathbf{p} \cdot \mathbf{E}$$

Since \mathbf{E} is assumed uniform over the volume of the atom, the transition probability is proportional to the square of the matrix element

$$\langle 1 | \mathbf{p} | 2 \rangle$$

\mathbf{p} being a vector operator. Let us assume that state 1 is characterised by the quantum numbers J and m_J , and state 2 by the quantum numbers J' and m_J' . As a direct result of the Wigner–Eckart theorem (see appendix 5) we may state a general selection rule as follows.

From the general form of the Wigner–Eckart theorem given in appendix 5.3, it follows from the properties of the Clebsch–Gordan coefficients that the matrix element

$$\langle \tau J m_J | T_q^k | \tau' J' m_J' \rangle$$

of the component q of the tensor operator T^k must be zero unless

$$m_J - m_J' = q$$

$$|J - J'| \leq k \leq J + J'$$

In the particular case of a vector operator, $k = 1$, $q = 0, \pm 1$. Therefore, the only matrix elements $\langle 1 | \mathbf{p} | 2 \rangle$ different from zero are those such that

$m_J - m_J' = 0, \pm 1$ $J - J' = 0, \pm 1$ excluding $J = J' = 0$
--

Comment The selection rule for the quantum number m_J is the one that we obtained from the conservation of angular momentum of radiation, and confirmed by means of the Zeeman effect (volume 1, chapter 11).

Thus we find selection rules for electric dipole emission, valid whatever the type

of coupling. Other selection rules involve either L and S in LS coupling or j_1 and j_2 in j - j coupling. They arise from a more complex analysis that we shall not attempt here. We shall merely point out that a relatively simple calculation for the case of a hydrogen-like atom allows one to show, from expressions for the wave functions and by using a recurrence relation for the associated Legendre polynomials, that the only non-zero electric dipole matrix elements are those connecting two states l and l' such that

$$l = l' \pm 1$$

A numerical calculation shows that the electric dipole transition probabilities are much greater than magnetic dipole transition probabilities. Therefore evidence of magnetic dipole transition phenomena can be obtained only in certain circumstances where the selection rules forbid electric dipole transitions. Such is the case for magnetic resonance transitions between Zeeman sublevels of a level J ; we shall meet other examples in chapter 7.

4.2 An Atom with One Outer Electron, Taking into Account Electron Spin

We studied previously (section 1.5) the energy levels of a system formed by one electron without spin, moving in a non-coulomb central potential; each of the energy levels of this system is characterised by one value of the orbital quantum number. For the elements of Group IA (the alkalis), all the states observed correspond to the following scheme: an outer electron, and a core formed from the nucleus and the other electrons. However, to obtain results in agreement with observation, it is necessary to take account of the spin of the electron. In a more detailed study, therefore, we should introduce the total angular momentum and study the energy corrections resulting from spin-orbit coupling.

Comment Silver, in column IB, may be similarly described; in the case of copper, excited states of a more complex configuration are observed in addition.

4.2.1 The total angular momentum

If the core has a total orbital angular momentum and spin angular momentum of zero, L reduces to l , S to s and J to j , where l , s and j are respectively the orbital, spin and total angular momenta of the outer electron. In order to obtain the total angular momentum of an atom we shall add to l the angular momentum s by applying the coupling rules for angular momenta. For a given value of l different from zero, we therefore have two values of the angular momentum j . To each value of j there will correspond an energy level that we shall denote with the aid of the spectroscopic notation defined in the preceding chapter. It should be noted that all the levels of the simplified model of the alkali atom without spin will now be found to be doublets except the s levels ($l = 0$) (see figure 4.1).

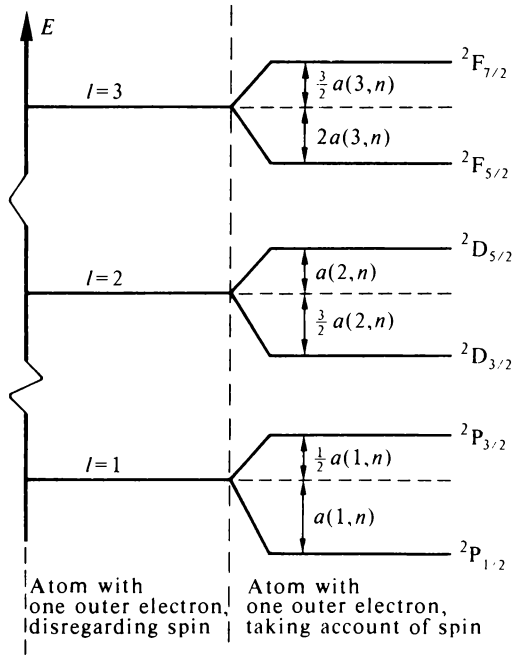


Figure 4.1 Influence of spin-orbit coupling on the energy levels of an atom with one outer electron

4.2.2 Spin-orbit coupling

To the values of energy obtained solely from the coulomb interaction between electrons (as obtained in section 1.5), we shall add the spin-orbit coupling energy (section 3.2)

$$\Delta E = \frac{\hbar^2}{2m^2 c^2 r} \frac{dW}{dr} l \cdot s = a l \cdot s$$

We saw previously that for a given value of l , there are two values of j , that is to say, two different values of the scalar product $l \cdot s$. The scalar product may be evaluated easily by squaring the sum of the operators

$$\mathbf{j} = \mathbf{l} + \mathbf{s}$$

so

$$\mathbf{j}^2 = \mathbf{l}^2 + \mathbf{s}^2 + 2\mathbf{l} \cdot \mathbf{s}$$

whence

$$l \cdot s = \frac{\mathbf{j}^2 - \mathbf{l}^2 - \mathbf{s}^2}{2}$$

By means of the expressions for the eigenvalues of the operators representing squares of the angular momenta, we obtain

$$l \cdot s = \frac{j(j+1) - l(l+1) - s(s+1)}{2}$$

and so we may write the spin-orbit coupling energy

$$\Delta E = a(l, n) \frac{j(j+1) - l(l+1) - s(s+1)}{2}$$

where

$$a(l, n) = \frac{\hbar^2}{2m^2 c^2 r} \frac{dW}{dr}$$

$a(l, n)$ depends on the quantum numbers n and l through the mean value of r , and can be written explicitly in terms of expressions for the mean radius r and the potential energy $W(r)$.

For given values of l and n ($l \neq 0$), there are two values of j and thus two values of ΔE . Let us take as an example the case where the orbital momentum l of the electron is equal to one. We have

$$\begin{aligned} l = 1, \quad j = \frac{3}{2} \rightarrow \Delta E_2 &= a(1, n) \frac{(\frac{3}{2} \times \frac{5}{2}) - (1 \times 2) - (\frac{1}{2} \times \frac{3}{2})}{2} \\ &= \frac{a(1, n)}{2} \end{aligned} \quad (1)$$

$$\begin{aligned} l = 1, \quad j = \frac{1}{2} \rightarrow \Delta E_1 &= a(1, n) \frac{(\frac{1}{2} \times \frac{3}{2}) - (1 \times 2) - (\frac{1}{2} \times \frac{3}{2})}{2} \\ &= -a(1, n) \end{aligned} \quad (2)$$

Comment The reader may confirm that the difference $\Delta E_2 - \Delta E_1$ is equal to $a \cdot j_{\max}$, whatever the value of l , j_{\max} being the larger j value for the pair of levels.

By letting E_0 be the energy obtained from the theory involving only the coulomb interaction (E_0 is an eigenvalue of H_0 , stage (1) of chapter 2; we note that there is no stage (2) in this example), the two corresponding levels have energies

$$\begin{aligned} E_1 &= E_0 + \Delta E_1 \\ E_2 &= E_0 + \Delta E_2 \end{aligned}$$

Figure 4.1 shows the results obtained for different values of l , and figure 4.2 shows the principal energy levels of sodium obtained experimentally. In this diagram, the energy levels have been labelled in accordance with the spectroscopic notation defined in chapter 3, and for the sake of clarity, the levels corresponding to the different values of l have been set out in a direction perpendicular to the energy axis. It should be remarked that the existence of doublet levels was of considerable historical importance: they demonstrated experimentally the existence of spin.

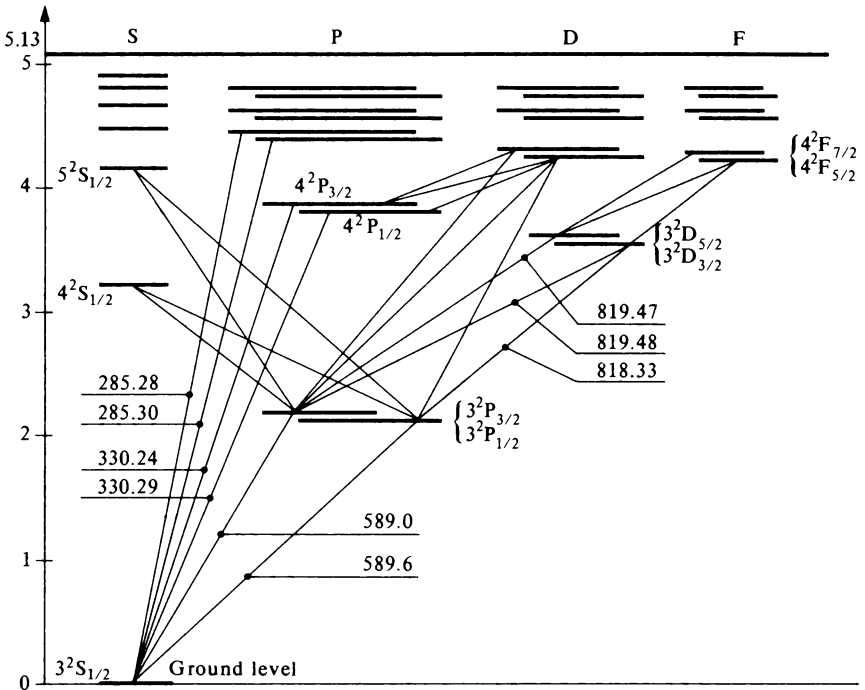


Figure 4.2 Energy levels and spectrum of sodium. Only a few transitions are shown in this diagram (the numbers indicate the wavelengths measured in nanometres). The ordinate is the energy measured in electron-volts, the energy of the ground level being taken as zero. *Note:* The separations between doublet levels have been strongly exaggerated

4.2.3 The observed spectra

The following selection rules are used.

The allowed transitions are those corresponding to a transition between an energy level described by the quantum numbers n_1, l_1, j_1 and a level described by n_2, l_2, j_2 , such that

$$\begin{aligned} \Delta n &= n_2 - n_1 = \text{any value} \\ \Delta l &= l_2 - l_1 = \pm 1 \\ \Delta j &= j_2 - j_1 = 0, \pm 1 \end{aligned}$$

We should note that in figure 4.2, the lines connected to an S state are doublets whereas the lines not connected to an S state are triplets. Since the two lines

$$3^2P_{\frac{3}{2}} \rightarrow 3^2S_{\frac{1}{2}} \quad \text{and} \quad 3^2P_{\frac{1}{2}} \rightarrow 3^2S_{\frac{1}{2}}$$

are by far the most intense of the spectrum, they are often incorrectly described as ‘the sodium doublet’—such a generalisation should not be made.

4.3 Atoms with Two Electrons

Under this heading come atoms formed from complete sub-shells with two additional electrons. Apart from the helium atom, there are atoms having complete internal shells and two valence electrons such as the alkaline earths (magnesium, calcium, barium, strontium), zinc, cadmium and mercury. There are other atomic systems in this category, for instance the ions Li^+ , C^{2+} , N^{3+} and so on. The calcium atom may be taken as an example. Its ground configuration is

$$[1s^2 2s^2 2p^6 3s^2 3p^6] 4s^2 = [—] 4s^2$$

Many types of excited states can occur, the most probable being those where only one electron is excited

$$[—] 4s ns \quad [—] 4s np \quad [—] 4s nd \quad [—] 4s nf$$

In addition, the states

$$[—] 3d 4s \quad [—] 3d 4p \quad [—] 3d 3d \quad [—] 4p 4p$$

may be observed.

4.3.1 Method of approach

It is possible to obtain some quite simple results for atoms with two electrons by generalising the method used for the alkali atoms. We saw (section 4.2) that the only correction to be made to the energy E_0 of an electron without spin in a central potential is related to the existence of electron spin and its coupling with the orbital angular momentum. Let E_0 be the energy associated with the configuration of an atom with two electrons in the central potential approximation. The angular momenta involved are:

- (1) the spins s_1 and s_2 and the orbital angular momenta l_1 and l_2 of the two electrons;
- (2) the resultants

$$\text{in } L\text{-}S \text{ coupling: } \mathbf{L} = \mathbf{l}_1 + \mathbf{l}_2 \quad \text{and} \quad \mathbf{S} = \mathbf{s}_1 + \mathbf{s}_2$$

$$\text{in } j\text{-}j \text{ coupling: } \mathbf{j}_1 = \mathbf{l}_1 + \mathbf{s}_1 \quad \text{and} \quad \mathbf{j}_2 = \mathbf{l}_2 + \mathbf{s}_2;$$

- (3) the total angular momentum $\mathbf{J} = \mathbf{L} + \mathbf{S} = \mathbf{j}_1 + \mathbf{j}_2$.

We assume that the energies E of the different levels of an electronic configuration, characterised by a particular set of angular momenta, are obtained from the relations

$$\text{in } L\text{-}S \text{ coupling: } E = E_0 + \underbrace{a_1 s_1 \cdot s_2 + a_2 l_1 \cdot l_2}_{T_1} + \underbrace{A \mathbf{L} \cdot \mathbf{S}}_{T_2} \quad (4.1)$$

$$\text{in } j\text{-}j \text{ coupling: } E = E_0 + \underbrace{a_3 l_1 \cdot s_1 + a_4 l_2 \cdot s_2}_{T_2} + \underbrace{A' \mathbf{j}_1 \cdot \mathbf{j}_2}_{T_1} \quad (4.2)$$

a_1, a_2, a_3 and a_4 have fixed values within a configuration. A and A' are functions, within a configuration, of L and S or of j_1 and j_2 respectively.

4.3.2 Coupling between angular momenta and the vector model

Let us try to justify the relations (4.1) and (4.2) that we wrote above. According to chapters 2 and 3, we should add to H_0 , describing the central potential approximation, terms expressing the electron-electron coulomb interactions and the interactions involving the spins of the electrons explicitly. We assume here that the energy-level solutions of the hamiltonian can be written

$$E = E_0 + a_1 s_1 \cdot s_2 + a_2 \mathbf{l}_1 \cdot \mathbf{l}_2 + a_3 \mathbf{l}_1 \cdot \mathbf{s}_1 + a_4 \mathbf{l}_2 \cdot \mathbf{s}_2$$

or

$$E = E_0 + \underbrace{\quad}_{T_1} + \underbrace{\quad}_{T_2}$$

the term $a_2 \mathbf{l}_1 \cdot \mathbf{l}_2$ expressing the electrostatic interaction and the term $a_1 s_1 \cdot s_2$, the exchange effects (see section 2.1). T_2 represents the spin-orbit coupling. We have not included the terms $\mathbf{l}_1 \cdot \mathbf{s}_2$ and $\mathbf{l}_2 \cdot \mathbf{s}_1$ because we are neglecting magnetic spin-spin interactions (see section 3.2.2).

The coefficients a_i cannot in general be expressed analytically; but we can state how the coefficients a_i depend upon the type of coupling in an atom.

(1) *L-S coupling.* We saw that the angular momenta L and S , obtained by coupling the orbital angular momenta \mathbf{l}_1 and \mathbf{l}_2 and the spin angular momenta \mathbf{s}_1 and \mathbf{s}_2 respectively, were characteristics of the levels together with the total angular momentum J . For a given level, the existence of L and S imply strong coupling between \mathbf{l}_1 and \mathbf{l}_2 , and \mathbf{s}_1 and \mathbf{s}_2 , that is to say constant values for the scalar products $\mathbf{s}_1 \cdot \mathbf{s}_2$ and $\mathbf{l}_1 \cdot \mathbf{l}_2$. On the other hand, j_1 and j_2 are not characteristics of the levels, the scalar products $\mathbf{l}_1 \cdot \mathbf{s}_1$ and $\mathbf{l}_2 \cdot \mathbf{s}_2$ having values that vary with time.

The existence of L and S necessitates a greater coupling energy between \mathbf{l}_1 and \mathbf{l}_2 and \mathbf{s}_1 and \mathbf{s}_2 than between \mathbf{l}_1 and \mathbf{s}_1 and \mathbf{l}_2 and \mathbf{s}_2 and numerically the coefficients a_1 and a_2 therefore have greater values than a_3 and a_4 .

(2) *j-j coupling.* If one argues by analogy, then the existence of the angular momenta \mathbf{j}_1 and \mathbf{j}_2 implies that:

- (a) the scalar products $\mathbf{l}_1 \cdot \mathbf{s}_1$ and $\mathbf{l}_2 \cdot \mathbf{s}_2$ are fixed;
- (b) the scalar products $\mathbf{l}_1 \cdot \mathbf{l}_2$ and $\mathbf{s}_1 \cdot \mathbf{s}_2$ have values that vary with time.

The first two scalar products of expressions (4.1) and (4.2) are self-evident. This is not true of the third products. We shall show that they can be readily interpreted by means of the 'vector model'.

The vector model. This is often used in atomic physics and many books describe and use it. Nevertheless, the reader should regard it only as a tool for treating certain parts of a problem which could otherwise be carried out rigorously by means of quantum mechanics. In this model the angular momentum operators are represented by vectors, an angular momentum σ_j being associated with a vector of length $\sqrt{[j(j+1)]}\hbar$.

The angle between two vectors will be such that the expression for the scalar product will be the same as that obtained by a quantum mechanical calculation. The angle α between the vectors \mathbf{s} and \mathbf{l} , whose resultant is \mathbf{j} , will be given by

$$2\mathbf{l} \cdot \mathbf{s} = 2|\mathbf{l}| |\mathbf{s}| \cos \alpha$$

so that

$$\cos \alpha = \frac{j(j+1) - l(l+1) - s(s+1)}{2\sqrt{l(l+1)}\sqrt{s(s+1)}}$$

If the vector \mathbf{j} is a characteristic of the atomic state, no favoured plane defined by l and s can exist, and l and s may be pictured as precessing around their resultant \mathbf{j} (figure 4.3). We shall have an opportunity in chapter 5 of showing that the vector model illustrates one of the general properties of vector operators.

This model allows a number of simple calculations to be made. The diagram for a system of two electrons in L - S coupling is shown in figure 4.4: l_1 and l_2 precess

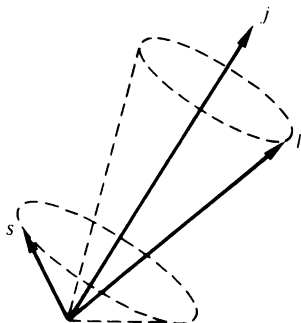


Figure 4.3 The vector model: coupling between l and s

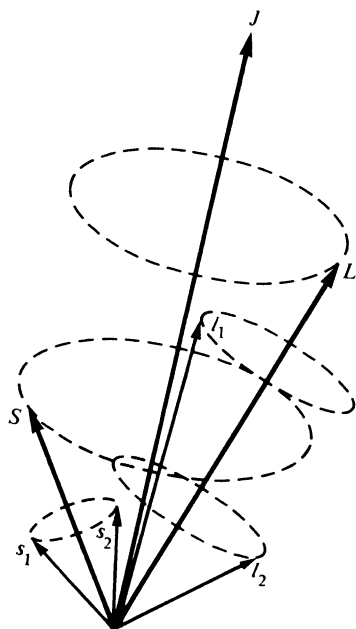


Figure 4.4 The vector model: L - S coupling

around their resultant L , s_1 and s_2 around their resultant S , and S and L around J . The spin-orbit coupling energy T_2 can be written

$$T_2 = a_3 |I_1| |s_1| \cos(I_1, s_1) + a_4 |I_2| |s_2| \cos(I_2, s_2)$$

However, the angles (I_1, s_1) and (I_2, s_2) are not constants. The mean values of their cosines may be written as equal to

$$\overline{\cos(I_1, s_1)} = \cos(I_1, L) \cos(L, S) \cos(S, s_1)$$

$$\overline{\cos(I_2, s_2)} = \cos(I_2, L) \cos(L, S) \cos(S, s_2)$$

respectively. These relations may be confirmed readily by taking the mean value of

$$I_1 \cdot s_1 = (\text{vector projection of } I_1 \text{ on } L) \cdot (\text{vector projection of } s_1 \text{ on } S)$$

and so

$$I_1 \cdot s_1 = [|I_1| \cos(I_1, L)] [|s_1| \cos(s_1, S)] \cos(L, S)$$

and similarly for $I_2 \cdot s_2$.

We may write, therefore

$$T_2 = \cos(L, S) [a_3 |I_1| |s_1| \cos(I_1, L) \cos(S, s_1) + a_4 |I_2| |s_2| \cos(I_2, L) \cos(S, s_2)]$$

which may be written after using the cosine rule

$$T_2 = A |L| |S| \cos(L, S) = AL \cdot S$$

where

$$A = a_3 \left(\frac{|s_1|^2 - |s_2|^2 + |S|^2}{2|S|^2} \right) \left(\frac{|I_1|^2 - |I_2|^2 + |L|^2}{2|L|^2} \right) \\ + a_4 \left(\frac{|s_2|^2 - |s_1|^2 + |S|^2}{2|S|^2} \right) \left(\frac{|I_2|^2 - |I_1|^2 + |L|^2}{2|L|^2} \right)$$

When $s_1 = s_2$, the preceding expression may be considerably simplified. We note that, for given values of S and L , the term A has a fixed value.

A similar calculation may be carried out to evaluate $\Delta E_1 + \Delta E_2$ for the case of $j-j$ coupling, and gives the third scalar product in expression (4.2).

4.3.3 $L-S$ coupling

(1) *Position of the energy levels.* By expanding the scalar products in expression (4.1) we obtain

$$\Delta E = a_1 s_1 \cdot s_2 + a_2 I_1 \cdot I_2 + AL \cdot S$$

$$\Delta E = \frac{a_1}{2} [S(S+1) - s_1(s_1+1) - s_2(s_2+1)] \\ + \frac{a_2}{2} [L(L+1) - I_1(I_1+1) - I_2(I_2+1)] \\ + \frac{A}{2} [J(J+1) - L(L+1) - S(S+1)] \quad (4.3)$$

which allows us to determine the relative positions of the different levels. The coefficients a and A can have positive or negative values, according to the

case considered; this explains one feature of the diagrams given in figures 4.5 and 4.6, which correspond to the two examples we shall now study.

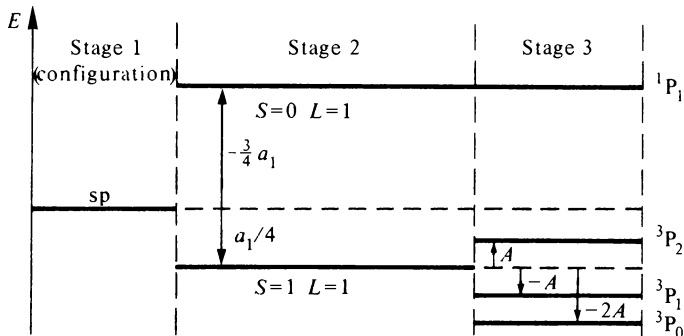


Figure 4.5 Relative positions of the energy levels of an sp configuration in L - S coupling. *Note:* In figures 4.5 and 4.6, and in figures 4.8 and 4.9, the energy differences $a_1, s_1, s_2, a_2, l_1, l_2$, etc. are given their algebraic values and symbolised by a line with an arrow in the direction of the energy shift. In other figures (figures 4.1, 4.10 and 4.13) absolute values of the energy differences are given and are symbolised by a line with two arrows

Let us consider first the simple case of an atom having one s electron and one p electron as outer electrons. The four energy levels corresponding to such a configuration were specified in table 3.1. In table 4.1 we recall their quantum numbers, and indicate the corresponding energy corrections. The values given may be verified without difficulty by the use of equation (4.3). The relative positions of the energy levels are shown in figure 4.5.

The more complicated case of a p electron and a d electron may be treated in the same way. Table 4.2 gives the values of the correction energies ΔE and figure 4.6 shows the arrangement of the energy levels.

(2) *The Landé interval rule.* Let us consider three levels having the same values of S and L , but different J . They are said to form a triplet. Let $J_0, J_0 + 1, J_0 + 2$ be the respective values of J for these three levels. The energy correction T_1 (stage (2)) is the same for each; from equation (4.3) the values of T_2 are

$$\text{for the level } J_0: \frac{1}{2}A[J_0(J_0 + 1) - L(L + 1) - S(S + 1)]$$

$$\text{for the level } J_0 + 1: \frac{1}{2}A[(J_0 + 1)(J_0 + 2) - L(L + 1) - S(S + 1)]$$

$$\text{for the level } J_0 + 2: \frac{1}{2}A[(J_0 + 2)(J_0 + 3) - L(L + 1) - S(S + 1)]$$

The energy difference between the levels J_0 and $J_0 + 1$ is $A(J_0 + 1)$. The energy difference between the levels $J_0 + 1$ and $J_0 + 2$ is $A(J_0 + 2)$. Hence we can state the Landé interval rule:

‘The separations between pairs of consecutive levels in a triplet are proportional to the larger of the J values characterising the pair of levels.’

The reader may confirm this rule for the triplet levels of the pd configuration given in table 4.2 and figure 4.6.

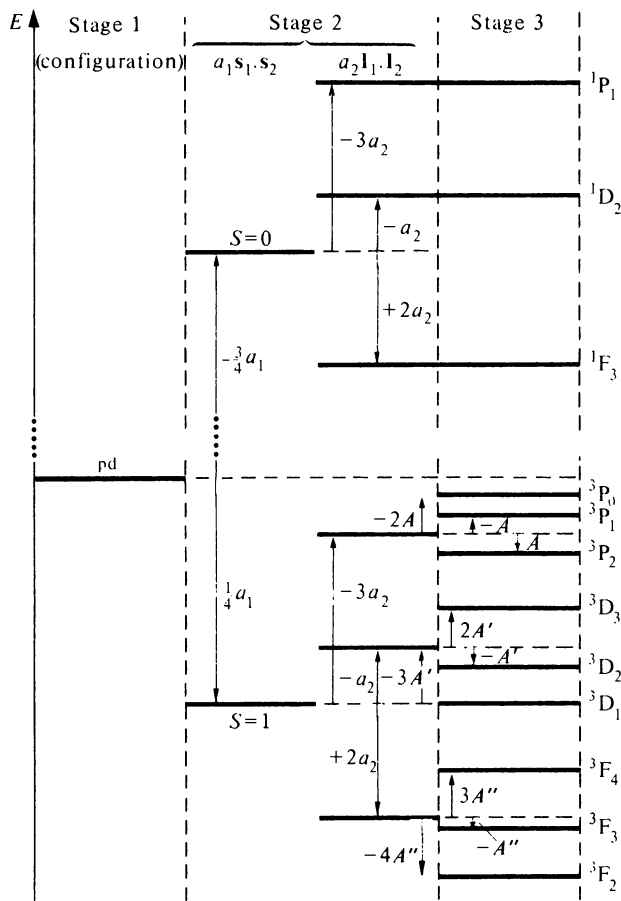


Figure 4.6 Relative positions of the energy levels of a pd configuration in $L-S$ coupling

Table 4.1

Spectral term	S	L	J	Stage 2 (T_1)		Stage 3 (T_2) $AL \cdot S$
				$a_1 s_1 \cdot s_2$	$a_2 l_1 \cdot l_2$	
1P_1	0	1	1	$-\frac{3}{4}a_1$	0	0
3P_0	1	1	0	$\frac{1}{4}$	0	$-2A$
3P_1	1	1	1			$-A$
3P_2	1	1	2			$+A$

Table 4.2

Spectral term	S	L	J	Stage 2 (T_1)		Stage 3 (T_2) $T_2 = AL \cdot S$
				$a_1 s_1 \cdot s_2$	$a_2 l_1 \cdot l_2$	
$1P_1$	0	1	1	$-\frac{3}{2}a_1$	$-3a_2$	0
$1D_2$	0	2	2		$-a_2$	
$1F_3$	0	3	3		$2a_2$	
$3P_0$	1	1	0	$\frac{1}{2}a_1$	$-3a_2$	$-2A$
$3P_1$	1	1	1			$-A$
$3P_2$	1	1	2			A
$3D_1$	1	2	1		$-a_2$	$-3A'$
$3D_2$	1	2	2			$-A'$
$3D_3$	1	2	3			$2A'$
$3F_2$	1	3	2		$2a_2$	$-4A''$
$3F_3$	1	3	3			$-A''$
$3F_4$	1	3	4			$3A''$

Note In this table, as in figure 4.6, A , A' and A'' represent different numerical values of the constant A . They should not be confused with the constant A' used elsewhere, especially in the discussion of $j-j$ coupling.

(3) *The optical spectrum of an atom with two valence electrons.* The lines that are observed during transitions from excited states towards the ground state are determined from the following selection rules, valid only if $L-S$ coupling applies:

- no transition is possible between a singlet state $S=0$ and a triplet state $S=1$;
- the only permitted transitions are those satisfying

$$\Delta L = \pm 1$$

$$\Delta J = 0, \pm 1$$

the transition $J=0 \rightarrow J=0$ being forbidden.

Figure 4.7 shows the most intense transitions observed from a discharge in mercury vapour. The reader will notice the existence of the 'resonance' line $6^3P_1 \rightarrow 6^1S_0$; this is an 'intercombination' line between a singlet level and a triplet, which violates condition (a) but which can be particularly intense in certain discharge conditions (the light emitted by fluorescent tubes commonly used for illumination comes from the fluorescence of a coating, excited by

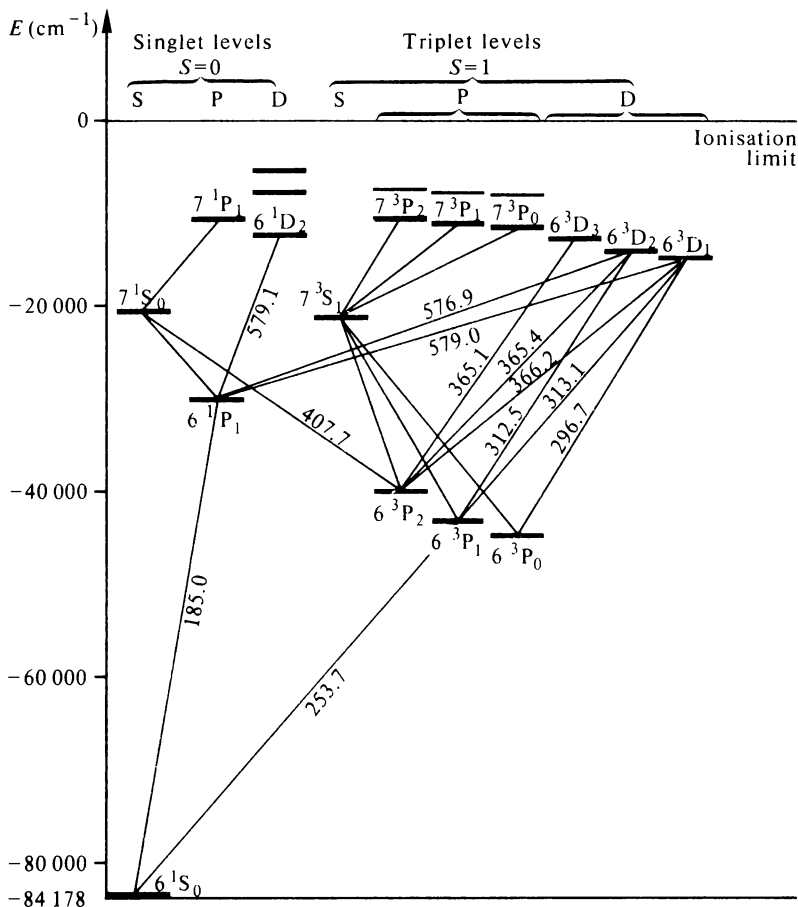


Figure 4.7 Principal energy levels of the mercury atom. The numbers indicate the wavelengths measured in nm. Note the various intercombination lines. (Comment: because of the selection rule $\Delta S = 0$, the 3S_1 level is classified as a triplet although it is single.)

this ultraviolet transition). This arises from the fact that the coupling in the mercury atom is not represented perfectly by L - S coupling.

Atoms of Group IIA (see chapter 2) and Group IIB are in general described quite well by L - S coupling. Nevertheless, this representation is often inadequate, and this is revealed in particular:

(a) by appreciable departures from the Landé interval rule—mercury is a typical example:

Triplet 6^3D_3 - 6^3D_2 - 6^3D_1 . Experimental value of the difference $6^3D_3 - 6^3D_2$ is 35 cm^{-1} , and of the difference $6^3D_2 - 6^3D_1$ is 60 cm^{-1} .

Ratio of the intervals is 0.58, whereas the theoretical value is 1.5;

(b) by the appearance of spectral lines forbidden for perfect L - S coupling.

Comment In figure 4.7, we also notice levels, such as 6^3P_0 and 6^3P_2 , from which there is no spontaneous transition. They are described as metastable levels; an atom in this state cannot return to the ground state by the emission of electric dipole radiation. However, various processes (collisions, complex radiative processes and so on) allow such a transition, although with a small probability, which give these metastable levels a longer lifetime—of the order of 10^{-3} seconds—than the other excited states, whose lifetimes are of the order of 10^{-8} seconds.

4.3.4 j - j coupling

The problem can be treated in a way similar to that of L - S coupling. Equation (4.2) of section 4.3.1 leads to

$$\begin{aligned} \Delta E = & \frac{a_3}{2} [j_1(j_1 + 1) - l_1(l_1 + 1) - s_1(s_1 + 1)] \\ & + \frac{a_4}{2} [j_2(j_2 + 1) - l_2(l_2 + 1) - s_2(s_2 + 1)] \\ & + \frac{A'}{2} [J(J + 1) - j_1(j_1 + 1) - j_2(j_2 + 1)] \end{aligned}$$

Figure 4.8 shows the relative energy differences in j - j coupling, corresponding to an sp configuration. As an exercise, the reader should check the values indicated.

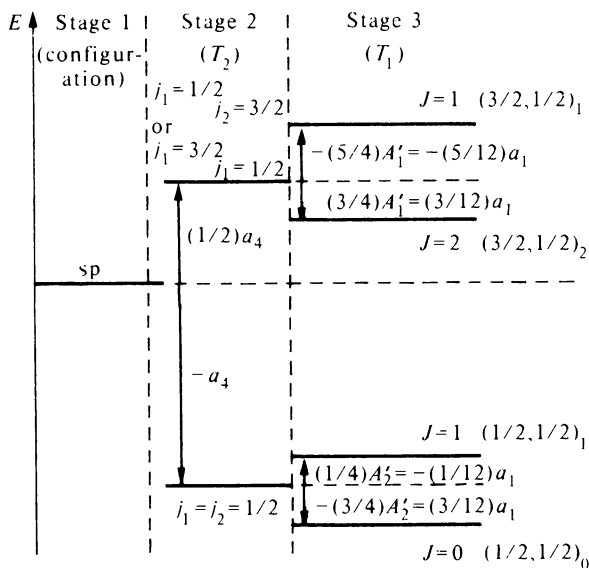


Figure 4.8 Relative positions of the energy levels of an sp configuration in j - j coupling. (As an exercise, the reader should confirm that the coefficients A' can, in this particular configuration, be expressed solely as a function of a_1 : $A_1' = -A_2' = a_1/3$.)

The following selection rules must be used in j - j coupling

- (1) $\Delta J = 0, \pm 1$, the transition $J = 0 \rightarrow J = 0$ being excluded
- (2) $\left\{ \begin{array}{l} \Delta j_1 = 0 \text{ and } \Delta j_2 = 0 \pm 1 \\ \text{or} \\ \Delta j_2 = 0 \text{ and } \Delta j_1 = 0 \pm 1 \end{array} \right.$

The examples corresponding to j - j coupling are less numerous than those corresponding to L - S coupling. The elements of Group IVB (carbon, silicon, germanium, tin and lead) have the following configuration: complete sub-shells, and four outer electrons—two s electrons and two p electrons. Some excited states arise from placing one of the p electrons into a different state. Since the two s electrons form a complete sub-shell, the study of these excited states reduces to that of a system of two electrons. Carbon may be described by L - S coupling, and lead may be described by j - j coupling. The other elements correspond to intermediate coupling.

4.3.5 Light atoms

The light atoms represent rather special cases; relativistic effects become especially important, and the magnetic spin-spin interactions, together with the exchange term, cannot be expressed entirely by a term of the form $a_1 s_1 \cdot s_2$. The Landé interval rule then fits very poorly and in the case of helium, one can even observe an inversion in the sequence of term energies.

For helium, a three-body system, several methods of approximation can be used to solve the hamiltonian of the problem. The elementary steps may be found in the usual quantum mechanics textbooks (see, for example, Messiah, pages 690 and 771). They allow a physical interpretation to be given which is far more satisfactory than the phenomenological treatment we have applied in this section. In particular, if we return to the case of the $1s2s$ configuration, we find

$$a_1 s_1 \cdot s_2 = \frac{a_1}{4} (S = 1) \quad \text{and} \quad a_1 s_1 \cdot s_2 = -\frac{3a_1}{4} (S = 0)$$

$$a_2 l_1 \cdot l_2 = a_3 l_1 \cdot s_1 = a_4 l_2 \cdot s_2 = 0$$

The interpretation of the perturbation calculation amounts to identifying the energy difference between the states $S = 0$ and $S = 1$, equal to a_1 (figure 4.9), as twice the

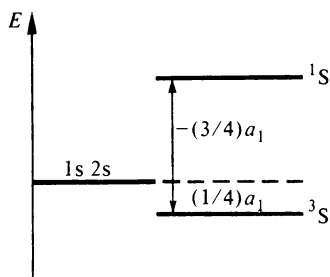


Figure 4.9 Splitting of a term due to exchange interaction

exchange integral. The main source of this energy separation is therefore related to the quantum phenomenon of exchange.

4.4 Energy Levels of the Hydrogen Atom: Fine Structure of the Lines

In the preceding section, we emphasised the fact that some of the approximations used were not valid for light atoms. The study of the hydrogen atom is a particularly good example. The quantum model presented in chapter 1 should be regarded only as an elementary stage in the argument. Spectroscopic observation with apparatus of sufficient resolution shows that different lines, such as H_α ($n = 3 \rightarrow n = 2$) for example, actually consist of several closely spaced wavelength components. A fine structure of the energy levels must be sought. Theoretical studies are difficult and in this book we can present only an overall view, outlined in a series of steps reflecting historical progress. Our aim is to present the fundamental ideas.

4.4.1 First step: Bohr's circular orbits model

This was explained in volume 1, chapter 6 and leads to the following expression for the spectral term T

$$T = -E/hc = R/n^2$$

where R is the Rydberg constant. This formula exhibits degeneracy in l . Using the non-relativistic Schrödinger equation (chapter 1), the quantum treatment results in the same expression for the spectral term T .

4.4.2 Second step: the Bohr–Sommerfeld relativistic model

By using the methods of theoretical mechanics and by supplementing Bohr's quantisation postulates with the postulates of relativistic mechanics, Sommerfeld in 1916 developed a model in which he took account of the relativistic corrections due to the variation of mass with velocity. This rather complicated calculation leads to the following expression for the spectral term as a function of the quantum numbers n and k ($k \leq n$)

$$T = -\frac{E}{hc} = \frac{\mu c}{h} \left[1 + \frac{\alpha^2}{(n-k + \sqrt{(k^2 - \alpha^2)})^2} \right]^{-\frac{1}{2}} + \frac{\mu c}{h}$$

μ being the reduced mass of the electron and α the fine structure constant (see volume 1, chapter 6):

$$\alpha = \frac{e^2}{\hbar c} = \frac{e^2}{4\pi\epsilon_0 \hbar c}$$

in CGS in SI

T can be put in the form of a convergent expansion in powers of α

$$T = \frac{R}{n^2} + \frac{R\alpha^2}{n^4} \left(\frac{n}{k} - \frac{3}{4} \right) + \frac{R\alpha^4}{n^6} (\dots) + \dots$$

where $R = \mu c \alpha^2 / 2h$. We note that the first term (R being the Rydberg constant) corresponds to the result of Bohr's theory; the other terms result in corrections whose values depend not only on n but also on k . The degeneracy of each level n is therefore lifted.

Column II of figure 4.10 shows the energy levels obtained from the preceding expression for the spectral term T for different values of k . There is excellent agreement with experimental results from optical spectra.

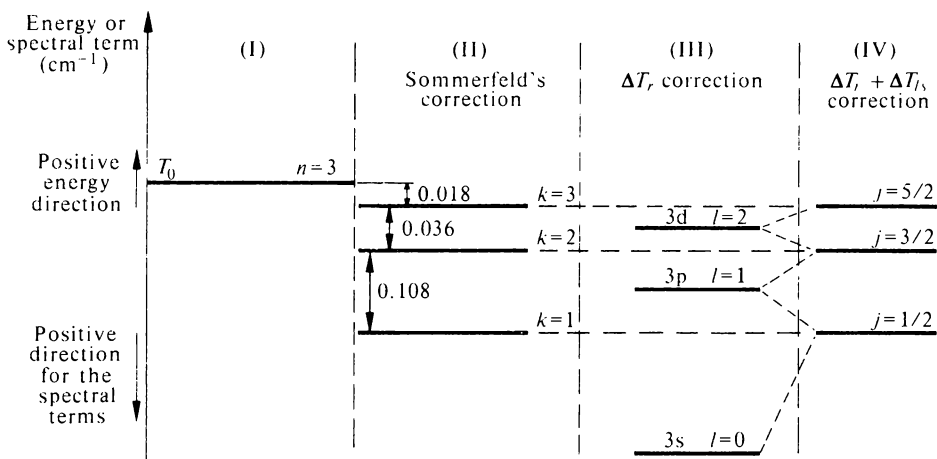


Figure 4.10 The $n = 3$ level of the hydrogen atom (upper level of the first Balmer line, see volume 1, figure 1.3). T_0 represents the spectral term deduced from Bohr's theory

4.4.3 Third step: relativistic correction to the quantum model

By using the relativistic Schrödinger equation, Heisenberg and Jordan (1926) found the following expression for the spectral term

$$T = \frac{R}{n^2} + \frac{R\alpha^2}{n^4} \left(\frac{n}{l + \frac{1}{2}} - \frac{3}{4} \right) = \frac{R}{n^2} + \Delta T_r \quad (4.4)$$

The corresponding energy levels are shown for different values of l in column III of figure 4.10. The optical lines that can be deduced from this are not in agreement with experiment.

4.4.4 Fourth step: spin-orbit coupling

Let us modify the results of the third step by taking account of the spin of the electron: a correction designed to take account of spin-orbit coupling is

added to the spectral term defined previously. The calculation may be carried out as for an alkali atom by writing the spin-orbit coupling energy as

$$\Delta E_{ls} = \frac{\hbar^2}{2m^2 c^2 r} \frac{dW}{dr} \frac{|j|^2 - |l|^2 - |s|^2}{2}$$

but the potential W is

$$W = \frac{C}{r} = -\frac{e^2}{4\pi\epsilon_0} \frac{1}{r}$$

and from the mean value of $1/r^3$ given by a quantum mechanical calculation

$$\left\langle \frac{1}{r^3} \right\rangle = \frac{1}{a_1^3 n^3 l(l + \frac{1}{2})(l + 1)}$$

(a_1 is the radius of the first Bohr orbit) we may write

$$\Delta E_{ls} = \frac{e^2 \hbar^2}{2m^2 c^2 4\pi\epsilon_0} \frac{1}{a_1^3 n^3 l(l + \frac{1}{2})(l + 1)} \frac{|j|^2 - |l|^2 - |s|^2}{2}$$

The correction to be applied to the spectral term ΔT_{ls} may be written by introducing the Rydberg constant R and the fine structure constant α

$$\Delta T_{ls} = -\frac{\Delta E_{ls}}{hc} = -\frac{R\alpha^2}{n^3 l(l + \frac{1}{2})(l + 1)} \frac{|j|^2 - |l|^2 - |s|^2}{2}$$

Since j can take only the values $j = l - \frac{1}{2}$ and $j = l + \frac{1}{2}$, the previous expression may be simplified after substitution and leads to

$$\left. \begin{aligned} \Delta T_{ls} &= -\frac{R\alpha^2}{n^3 2(l + \frac{1}{2})(l + 1)} && \text{for } j = l + \frac{1}{2} \\ \Delta T_{ls} &= +\frac{R\alpha^2}{n^3 2l(l + \frac{1}{2})} && \text{for } j = l - \frac{1}{2} \end{aligned} \right\} \quad (4.5)$$

The levels predicted in the third step are now split and figure 4.11(a) illustrates this prediction by taking as an example $n = 3$, $l = 2, 1, 0$. The exact position

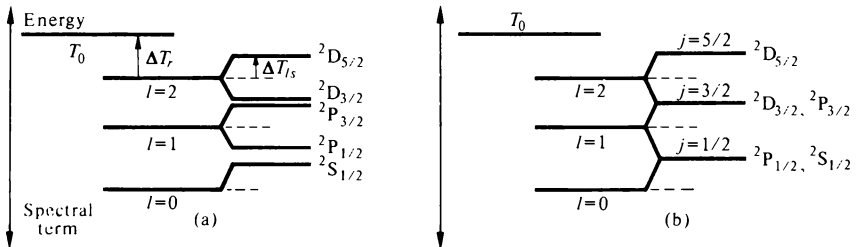


Figure 4.11 Fine structure of the $n = 3$ level of hydrogen, excluding radiative corrections but including relativistic and spin-orbit corrections

of the different levels indicated in figure 4.11(a) may be obtained by adding the corrections ΔT_r and ΔT_{ls} to the spectral term T .

For a given value of l , we have, from expressions (4.4) and (4.5)

$$\Delta T = \Delta T_r + \Delta T_{ls} = \frac{R\alpha^2}{n^3} \left(\frac{1}{l+1} - \frac{3}{4n} \right) \quad \text{for } j = l + \frac{1}{2} \quad (4.5a)$$

$$\Delta T = \Delta T_r + \Delta T_{ls} = \frac{R\alpha^2}{n^3} \left(\frac{1}{l} - \frac{3}{4n} \right) \quad \text{for } j = l - \frac{1}{2} \quad (4.5b)$$

Let us now consider two levels of the same j , but corresponding to two successive values of l (for example $D_{\frac{3}{2}}$ and $P_{\frac{3}{2}}$); the correction ΔT is obtained by replacing l in (4.5a) by $j - \frac{1}{2}$ and in (4.5b) by $j + \frac{1}{2}$. The two values of ΔT are therefore equal to

$$\Delta T = \frac{R\alpha^2}{n^3} \left(\frac{1}{j + \frac{1}{2}} - \frac{3}{4n} \right) \quad (4.6)$$

Levels of the same j are therefore coincident and the energy level diagram is that shown in figure 4.11(b), and displayed in column IV of figure 4.10.

We note that by identifying k with $j + \frac{1}{2}$ we obtain a result similar to Sommerfeld's. Figure 4.10 thus summarises the first four steps of this account of the hydrogen atom, with certain numerical values being defined.

In 1928, Dirac developed a relativistic quantum theory in which the concept of spin was inherent, resulting from the underlying postulates. The theory of the hydrogen atom can be worked out in this formalism and leads to:

- (1) an expression for the spectral term identical to that obtained by adding the relativistic and spin-orbit corrections (4.6);
- (2) the wavefunctions, allowing the position probabilities of the electron to be obtained as in chapter 1.

The results are clearly different from those given in chapter 1, where the electron spin was not taken into account and, as a result, the values of the total angular momentum were integer multiples of \hbar . Figure 4.12 illustrates the hydrogen atom as represented by the results of the Dirac theory. It shows the variation of certain angular probability densities $D(\theta)$. On the other hand, the radial probability densities $D(r)$ are hardly affected by the introduction of spin: they correspond very closely to those obtained from the solution of the non-relativistic Schrödinger equation. This point is very significant; it justifies the use of the simple non-relativistic model in many situations.

The excellent agreement (except for the corrections defined in the next step of the discussion) between the experimental results and the results of the Dirac theory must be considered as one of the great historical achievements of physics, showing the importance of the relativistic theories and firmly establishing the concept of electron spin.

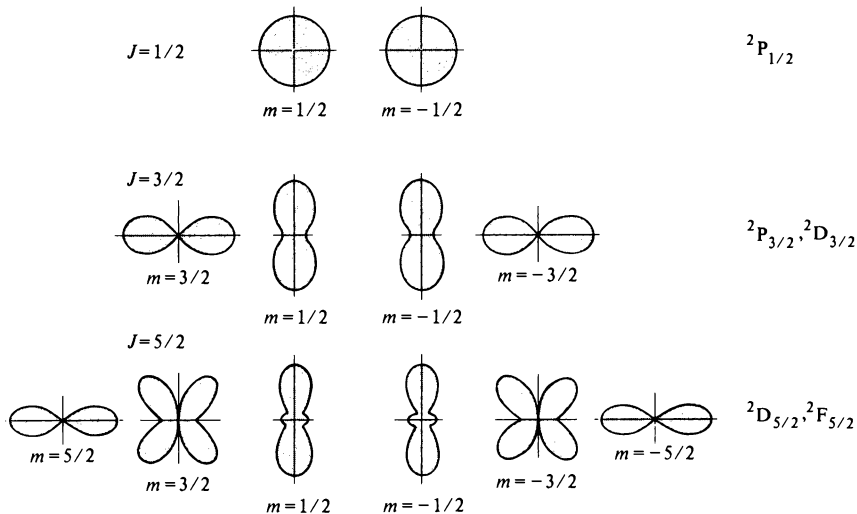


Figure 4.12 Angular probability density $D(\theta)$ for the hydrogen atom obtained from Dirac's theory (compare with figure 1.4). The radial probability densities $D(r)$ are very similar to those obtained by solution of the Schrödinger equation for the same values of n and l (figure 1.3)

4.4.5 Fifth step : radiative corrections

The correct description of phenomena concerned with the interaction of an electromagnetic wave and an atom is possible only within the framework of a theory involving quantisation of the electromagnetic fields. In this theory, a single electron in a vacuum should be considered as surrounded or 'dressed' by an electromagnetic field. As a result of the interaction between the electron and this electromagnetic field, the electron has an additional electromagnetic mass. In the case of a bound electron forming part of a system of particles, this interaction with the electromagnetic field of the 'vacuum' will also lead to a change of the effective potential energy of this electron. The calculation of this 'radiative correction' gives rise to a series expansion in $Z\alpha$, α being the fine structure constant, the first term being in $(Z\alpha)^4$:

$$\Delta E \propto \frac{\alpha(Z\alpha)^4 mc^2}{2\pi n^3}$$

The constant of proportionality is a function of the quantum number l .

This correction removes the coincidence between the levels of the same j , such as $S_{\frac{1}{2}}$, $P_{\frac{1}{2}}$, for example, and the actual energy level diagram will therefore appear as in figure 4.11(a). The energy separations between the levels $S_{\frac{1}{2}} - P_{\frac{1}{2}}$ and $P_{\frac{3}{2}} - D_{\frac{3}{2}}$ are nevertheless very small, of the order of a fraction of a cm^{-1} in wave numbers and smaller than the separations between levels of different j . An order of magnitude determination of these separations was carried out in 1938 by optical interferometric measurements on the transitions

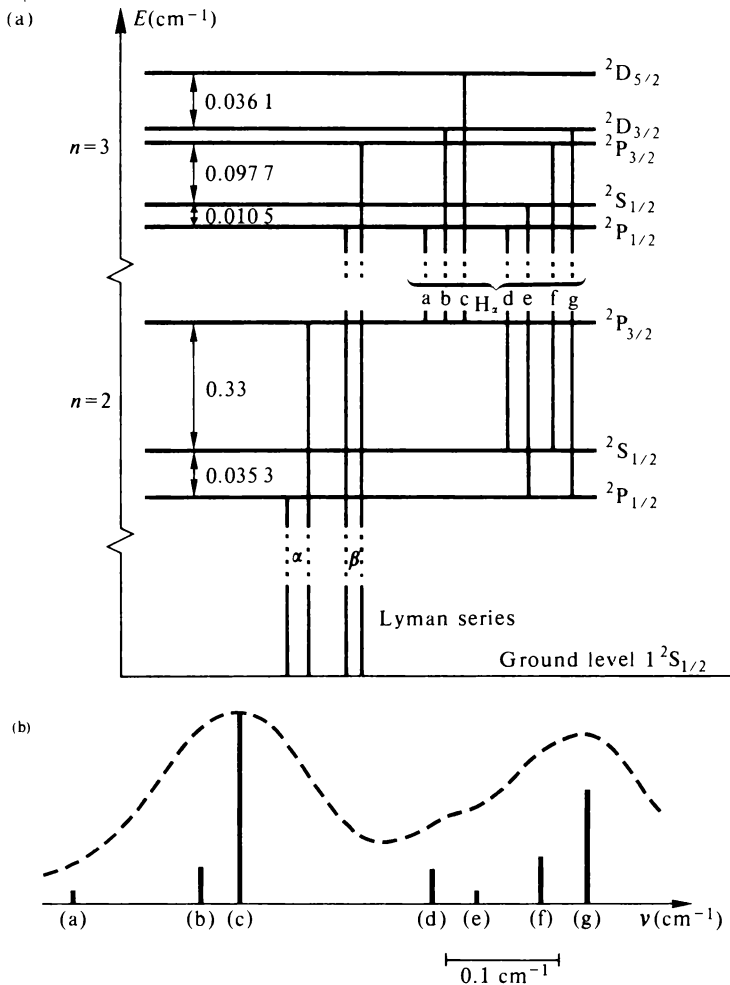


Figure 4.13 (a) Structure of the $n=2$ and $n=3$ levels of the hydrogen atom. (b) Structure of the H_α transition. The letters refer to the various transitions of figure 4.13(a). The curve in dotted lines shows the appearance of the spectrum obtained with a Fabry-Perot etalon

$n=3 \rightarrow n=2$. Lamb and Retherford devised a method involving radio-frequency spectroscopy (see chapter 7) that allowed the difference $2S_{\frac{1}{2}} - 2P_{\frac{3}{2}}$ to be determined with remarkable precision. The value found from their measurements, sometimes called δS , was

$$\delta S = 1057.3 \text{ MHz}$$

and is in excellent agreement with theoretical determinations based on quantum electrodynamics. Several differences of the same origin—usually called the ‘Lamb shift’—have been determined in recent years.

The optical lines of the hydrogen spectrum may be obtained without difficulty from the energy levels, by applying the selection rules already stated in section 4.2 for the alkali atoms. In respect of the levels $n = 1$, $n = 2$ and $n = 3$ alone, figure 4.13(a) shows the transitions that may be observed. In particular, the H_α transition ($n = 3 \rightarrow n = 2$) has a complex structure, known as the fine structure of the H_α line and which is shown on a wave number scale in figure 4.13(b). We should note, however, that as a result of the width of the optical lines, related mainly to the Doppler effect (see volume 1, chapter 1), observation of the H_α line provides evidence for only two components, each corresponding to the sum of several transitions. (*Translator's note*: a recent experiment by Hänsch, Shahin and Schawlow, *Nature*, **235**, 56 (1972) has permitted resolution of the components (d), (e) and (f) in figure 4.13(b) by means of a new technique involving the use of tunable lasers (see section 7.1).)

The hydrogen atom has a particularly simple structure that allows detailed study; comparison between theoretical and experimental results is therefore crucial. Considerable interest was aroused between 1947 and 1953 when measurements of the Lamb shift confirmed very clearly the hypotheses of quantum electrodynamics. The reader should not forget, however, that hydrogen is a *very special case*: the degeneracy in l is lifted only through the influence of spin-orbit coupling and by application of the laws of relativistic mechanics, whereas in other atoms it is also lifted by electrostatic interactions between electrons.

4.5 X-Ray Spectra

With the information that the reader has acquired in the preceding sections, we can complete the study of X-rays started in volume 1, chapter 7. We confine ourselves mainly to studying a very simple case that will allow the principal ideas to emerge: we shall consider an atom in its ground state that has all its inner sub-shells complete, and a ground state whose total angular momentum is zero. Atoms of cadmium or of zinc can be taken as an example.

4.5.1 The angular momenta attributed to the different levels

Let us reconsider the diagram in volume 1, figure 7.8(b). We recall that the different energy levels labelled K, L_I , L_{II} , L_{III} and so on, can be interpreted as those of an atom that has lost one of its electrons. We can characterise each of these levels (figure 4.14):

- (1) by its electronic configuration: this is denoted in column I; for simplicity, we indicate in column II the characteristic letter of the missing electron followed by the number -1 as a superscript;
- (2) by the total angular momentum of the ion formed in this level.

Since the ground state has zero angular momentum, and since an electron is removed from a complete shell of total angular momentum zero, the angular momentum of the ion has the opposite direction and same magnitude as that of the extracted electron. Let us examine the various shells.

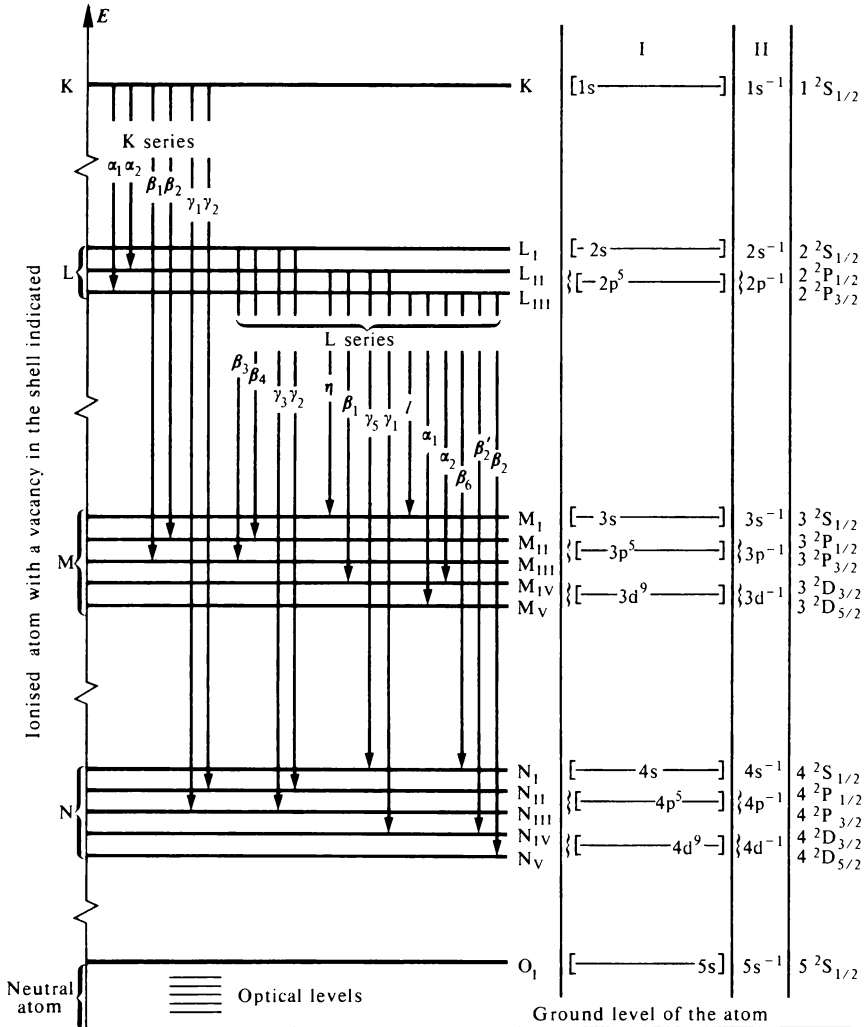


Figure 4.14 X-ray spectrum of the cadmium atom. In this figure we have used the convention of volume 1, figure 7.8(b). Any alteration with respect to the ground configuration $[1s^2 2s^2 2p^6 3s^2 3p^6 3d^{10} 4s^2 4p^6 4d^{10} 5s^2]$ is shown in column I. In this figure, we have shown only the transitions of the K and L series mentioned in the table in volume 1, chapter 7. By applying the selection rules, the reader may determine other allowed transitions

(1) *The K shell.* If an electron is removed from the K shell, where $n = 1$, it can have only zero orbital angular momentum and a spin angular momentum characterised by the quantum number $s = \frac{1}{2}$. Thus the level of the corresponding ion will be characterised by

$$l = 0, \quad s = \frac{1}{2} \quad \text{and} \quad j = \frac{1}{2}$$

This is described, therefore, as a $2S_{\frac{1}{2}}$ level.

(2) *The L shell.* Either an s electron or a p electron may be removed. Since these electrons have a spin quantum number $s = \frac{1}{2}$, three combinations of angular momenta are possible:

		Corresponding level
for an s electron,	$l = 0$	$j = \frac{1}{2}$ $^2S_{\frac{1}{2}}$ L_I
for a p electron,	$l = 1$	$j = \frac{1}{2}$ $^2P_{\frac{1}{2}}$ L_{II}
		$j = \frac{3}{2}$ $^2P_{\frac{3}{2}}$ L_{III}

By anticipating somewhat, these three states will have different energies and consequently the ion formed by the detachment of an electron from the L shell may have three energy levels which will be characterised by the symbols $^2S_{\frac{1}{2}}$, $^2P_{\frac{1}{2}}$, $^2P_{\frac{3}{2}}$ or in X-ray level notation L_I , L_{II} , L_{III} .

(3) *The five M levels.* In the same way the existence of the five M levels can be explained by the detachment

		Corresponding level
either of an s electron,	$l = 0$	$j = \frac{1}{2}$ $^2S_{\frac{1}{2}}$ M_I
or of a p electron,	$l = 1$	$j = \frac{1}{2}$ $^2P_{\frac{1}{2}}$ M_{II}
		$j = \frac{3}{2}$ $^2P_{\frac{3}{2}}$ M_{III}
or of a d electron,	$l = 2$	$j = \frac{3}{2}$ $^2D_{\frac{3}{2}}$ M_{IV}
		$j = \frac{5}{2}$ $^2D_{\frac{5}{2}}$ M_V

4.5.2 Spectral terms and energy

In volume I, chapter 7, we wrote the value of the binding energy of the detached electron, using the convention corresponding to figure 7.8(a)

$$E_n = -Rhc \frac{(Z - s_n)^2}{n^2}$$

and the fact that the screening constant s_n depends on l explains in part the fine structure. In addition, phenomena related to ls coupling must be taken into account. These latter corrections cannot, however, be studied in the disjointed way in which we treated the alkalis: the K and L levels involve electrons in close proximity to the nucleus for which relativistic corrections are important and of the same order—as we saw in the case of the hydrogen atom—as those due to spin-orbit coupling.

The position of the energy levels will be obtained, therefore, from a relativistic theory similar to that used for the hydrogen atom (see section 4.4). The result may be written in the form

$$E_{n, l, j} = - \frac{Rhc(Z - s_n)^2}{n^2} + \frac{Rhc\alpha^2(Z - s_n)^4}{n^3} \left(\frac{3}{4n} - \frac{1}{j + \frac{1}{2}} \right)$$

α being the fine structure constant. We note that the screening constant that must be used in the term in α^2 does not have the same value as that in the first term.

In X-ray language, a separation such as $L_I - L_{II}$ is called 'the screening separation', and such as $L_{II} - L_{III}$ 'the spin-relativity separation'. (The levels L_I and L_{II} have the same j but different l ; the levels L_{II} and L_{III} have the same l but different j .)

4.5.3 The observed spectra

The lines which are observed in an X-ray emission spectrum are determined by using the following selection rules, the same as those for optical spectra:

$$\left\{ \begin{array}{l} \Delta n: \text{ any value} \\ \Delta l: \pm 1 \\ \Delta j: \pm 1, 0 \end{array} \right.$$

On the left-hand side of figure 4.14, transitions that can be observed have been indicated with an arrow. Certain features not explained in volume 1, chapter 7, are thus clarified.

The X-ray emission spectrum of certain elements such as the rare earths is far more complex than that shown in figure 4.14. This is due to the fact that some inner shells are not complete and as a result possess a non-zero angular momentum. The angular momentum of the ion formed when an atom with this incomplete shell is excited will now result from the combination of two angular momenta, and several values can be obtained. Therefore the problem becomes equivalent to the one in the case of optical spectra, of an atom with several valence electrons. Some of the lines observed will have complex structures, called multiplets.

5

Atomic Magnetism. The Zeeman and Paschen–Back Effects

The fundamentals of the Zeeman effect were established in volume 1, chapters 10 and 11. A level corresponding to an atomic state of angular momentum σ_J and magnetic moment $\gamma\sigma_J$ (γ being the gyromagnetic ratio), splits into $2J + 1$ Zeeman sublevels whose separation is proportional to the field B . The energy difference between two consecutive sublevels is

$$E = g\beta B$$

where the Bohr magneton $\beta = e\hbar/2m\kappa$.

The polarisation state of the emitted light was also studied. After studying this chapter, the reader will understand the origin of the Landé factor, g , and will appreciate that the previous account relates to a special situation. In general, the action of the magnetic field is complex: the total angular momentum J results from the combination of the various angular momenta of the atom, which interact with the magnetic field not only together but also individually. The various interactions compete and only a detailed study will permit a valid description of the action of the magnetic field on the energy levels.

We shall give a quantum mechanical description of the atom under the influence of a magnetic field. First we shall establish an expression for the hamiltonian of an atom in the presence of a magnetic field, a fundamental

expression which is the starting point of many theories. Then, after stating the main approximations used, we shall present the stages in the solution of the hamiltonian of the atom in the presence of a constant magnetic field, so as to bring out the main features: the Zeeman effect in a weak magnetic field and the Paschen–Back effect in a strong magnetic field.

As in the preceding chapters, our study will be limited to atoms whose nuclei do not have a nuclear magnetic moment. The general case will be discussed at the end of chapter 6.

This chapter may seem difficult to some readers. They should note that they can acquire the main ideas from a partial study: section 5.1 can be omitted, and on a first reading sections 5.3.5, 5.4.3 and 5.5.1 will suffice. We deal with certain aspects of the Zeeman effect and Paschen–Back effect by use of the vector model. There are two reasons for this: the reader who has some difficulty with quantum formalism should be able to understand the fundamental points more easily; the others will notice that the quantum models provide a justification for the vector model which is then no longer simply a tool for calculation, but instead a very useful representation.

5.1 The Hamiltonian of a Charged Particle in the Presence of an Electromagnetic Field

5.1.1 The lagrangian and the equation of motion of the particle

The theory of electromagnetism rests on certain assumptions, the justification of which may be found in the agreement between their consequences and experimental facts. Depending on the approach used, the propositions taken as assumptions can differ widely. If we take Maxwell's equations and the force acting on a particle of charge q situated in an electromagnetic field

$$\mathbf{f} = q\mathbf{E} + \frac{q}{\kappa} \mathbf{v} \times \mathbf{B} \quad (5.1)$$

as postulates, we cannot deduce by means of logical steps the lagrangian required to write the hamiltonian of a charged particle in the presence of an electromagnetic field. On the other hand, we shall show that equation (5.1) may be obtained if, in addition to Maxwell's equations, we take as a postulate, the lagrangian

$$\mathcal{L} = mc^2\sqrt{1 - v^2/c^2} + \frac{q}{\kappa} \mathbf{A} \cdot \mathbf{v} - qV \quad (5.2)$$

where \mathbf{A} is a vector potential and V is a scalar potential. This result is obtained within the framework of relativistic mechanics (m designates the rest mass of the electron).

The lagrangian (5.2) differs from the lagrangian of a free particle in the second and third terms, which are zero in the absence of an electromagnetic field. They should not seem arbitrary if it is noted that $-(q/\kappa) \mathbf{A} \cdot \mathbf{v}$ represents the magnetic energy of a particle, a form that reduces easily to the general expression for the magnetic energy: the integral, over the distribution of current \mathbf{j} , of $-(1/\kappa)\mathbf{j} \cdot \mathbf{A}$.

For a free particle, the momentum vector \mathbf{p} may be calculated

$$\mathbf{p} = \frac{\partial \mathcal{L}}{\partial \mathbf{v}} = \frac{m\mathbf{v}}{\sqrt{(1-v^2/c^2)}}$$

The notation $\mathbf{p} = \partial \mathcal{L} / \partial \mathbf{v}$ signifies that the components of the vector \mathbf{p} have the values

$$p_x = \frac{\partial \mathcal{L}}{\partial v_x} \quad p_y = \frac{\partial \mathcal{L}}{\partial v_y} \quad p_z = \frac{\partial \mathcal{L}}{\partial v_z}$$

In the same way, for a particle in the presence of an electromagnetic field, we define a generalised momentum from equation (5.2)

$$\mathcal{P} = \frac{\partial \mathcal{L}}{\partial \mathbf{v}} = \frac{m\mathbf{v}}{\sqrt{(1-v^2/c^2)}} + \frac{q}{\kappa} \mathbf{A} = \mathbf{p} + \frac{q}{\kappa} \mathbf{A} \quad (5.3)$$

The lagrange equations may be written in a contracted form by using the notation defined previously

$$\frac{d}{dt} \left(\frac{\partial \mathcal{L}}{\partial \mathbf{v}} \right) = \frac{\partial \mathcal{L}}{\partial \mathbf{r}} \quad (5.4)$$

We may write

$$\frac{\partial \mathcal{L}}{\partial \mathbf{r}} = \frac{q}{\kappa} \text{grad}(\mathbf{A} \cdot \mathbf{v}) - q \text{grad} V$$

A well-known formula of vector calculus gives us

$$\text{grad}(\mathbf{A} \cdot \mathbf{v}) = (\mathbf{A} \cdot \text{grad})\mathbf{v} + (\mathbf{v} \cdot \text{grad})\mathbf{A} + \mathbf{A} \times \text{curl} \mathbf{v} + \mathbf{v} \times \text{curl} \mathbf{A}$$

In order to evaluate this partial derivative, it must be assumed that \mathbf{v} is constant and the terms in

$$(\mathbf{A} \cdot \text{grad})\mathbf{v} \quad \text{and} \quad \text{curl} \mathbf{v}$$

may then be equated to zero. Thus we have

$$\frac{\partial \mathcal{L}}{\partial \mathbf{r}} = \frac{q}{\kappa} (\mathbf{v} \cdot \text{grad})\mathbf{A} + \frac{q}{\kappa} \mathbf{v} \times \text{curl} \mathbf{A} - q \text{grad} V$$

Taking account of equation (5.3) the lagrange equation (5.4) may be written

$$\frac{d}{dt} \left(\mathbf{p} + \frac{q}{\kappa} \mathbf{A} \right) = \frac{q}{\kappa} (\mathbf{v} \cdot \text{grad})\mathbf{A} + \frac{q}{\kappa} \mathbf{v} \times \text{curl} \mathbf{A} - q \text{grad} V \quad (5.5)$$

We transform this equation by noting (since \mathbf{A} is a function of time and position) that

$$\frac{d\mathbf{A}}{dt} = \frac{\partial \mathbf{A}}{\partial t} + \left(\frac{d\mathbf{r}}{dt} \cdot \text{grad} \right) \mathbf{A} = \frac{\partial \mathbf{A}}{\partial t} + (\mathbf{v} \cdot \text{grad}) \mathbf{A}$$

Equation (5.5) may then be written

$$\frac{d\mathbf{p}}{dt} = -\frac{q}{\kappa} \frac{\partial \mathbf{A}}{\partial t} - q \text{grad } V + \frac{q}{\kappa} \mathbf{v} \times \text{curl } \mathbf{A} \quad (5.6)$$

Equation (5.6) can be recognised as the dynamical equation

$$\frac{d\mathbf{p}}{dt} = \mathbf{f}$$

The right-hand side of equation (5.6) is therefore equal to the force \mathbf{f} acting on the particle

$$\mathbf{f} = -q \text{grad } V - \frac{q}{\kappa} \frac{\partial \mathbf{A}}{\partial t} + \frac{q}{\kappa} \mathbf{v} \times \text{curl } \mathbf{A}$$

or alternatively

$$\mathbf{f} = q\mathbf{E} + \frac{q}{\kappa} \mathbf{v} \times \mathbf{B}$$

where

$$\mathbf{E} = -\text{grad } V - \frac{1}{\kappa} \frac{\partial \mathbf{A}}{\partial t} \quad \text{and} \quad \mathbf{B} = \text{curl } \mathbf{A}$$

5.1.2 The hamiltonian

The hamiltonian may be obtained by writing

$$\mathcal{H} = \mathbf{v} \cdot \frac{\partial \mathcal{L}}{\partial \mathbf{v}} - \mathcal{L} = \mathbf{v} \cdot \mathcal{P} - \mathcal{L} \quad (5.7)$$

and so, from equations (5.2) and (5.3)

$$\mathcal{H} = \mathbf{v} \cdot \left(\mathbf{p} + \frac{q}{\kappa} \mathbf{A} \right) + mc^2 \sqrt{(1 - v^2/c^2)} - \frac{q}{\kappa} \mathbf{A} \cdot \mathbf{v} + qV$$

which, after evaluating the scalar product $\mathbf{v} \cdot \mathbf{p}$

$$\mathbf{v} \cdot \mathbf{p} = \frac{mv^2}{\sqrt{(1 - v^2/c^2)}}$$

reduces to

$$\mathcal{H} = \frac{mc^2}{\sqrt{(1 - v^2/c^2)}} + qV = T + qV \quad (5.8)$$

T denotes the energy of the particle, and is the sum of the rest energy and the kinetic energy.

The latter expression for \mathcal{H} could have been written directly by noting that the potential energy of the particle is qV , since the magnetic forces, always perpendicular to the trajectory, do no work.

Let us express \mathcal{H} solely as a function of the generalised momentum \mathcal{P} . In order to eliminate the velocity \mathbf{v} , we use equation (5.3), written in the form

$$\mathcal{P} - \frac{q}{\kappa} \mathbf{A} = \frac{m\mathbf{v}}{\sqrt{(1 - v^2/c^2)}} = \mathbf{p}$$

in addition to the relation

$$T = \sqrt{(m^2 c^4 + p^2 c^2)}$$

From equation (5.8) we obtain an expression for \mathcal{H}

$$\mathcal{H} = \sqrt{\left(m^2 c^4 + c^2 \left| \mathcal{P} - \frac{q}{\kappa} \mathbf{A} \right|^2 \right)} + qV \quad (5.9)$$

If the velocity of the particle is small compared with the velocity of light, we can use the *non-relativistic approximation*. From the lagrangian, which may then be written (dropping the constant mc^2)

$$\mathcal{L} = \frac{mv^2}{2} + \frac{q}{\kappa} \mathbf{A} \cdot \mathbf{v} - qV$$

and from the relationship $T = p^2/2m$, we obtain by a similar argument

$$\mathcal{H} = \frac{1}{2m} \left(\mathcal{P} - \frac{q}{\kappa} \mathbf{A} \right)^2 + qV \quad (5.10)$$

Comment The hamiltonian written in the form

$$\mathcal{H} = \frac{p^2}{2m} + qV$$

is clearly simpler; but subsequently we shall see that it cannot be used in this form.

5.1.3 The hamiltonian operator

From the basic assumptions of quantum mechanics, the hamiltonian operator may be obtained by replacing the *generalised momentum* \mathcal{P} by the operator

$$-i\hbar \text{grad} \quad \text{or} \quad -i\hbar \nabla$$

By confining ourselves to the non-relativistic approximation, we write the hamiltonian operator by using equation (5.10)

$$H = \frac{1}{2m} \left(-i\hbar \nabla - \frac{q}{\kappa} \mathbf{A} \right)^2 + qV \quad (5.11)$$

and by expanding the square

$$H = \frac{1}{2m} \left(-\hbar^2 \nabla^2 + i\hbar \frac{q}{\kappa} \nabla \cdot \mathbf{A} + i\hbar \mathbf{A} \cdot \nabla + \frac{q^2}{\kappa^2} A^2 \right) + qV$$

When the operator H is applied to wave function ψ , we must pay attention to the operator $\nabla \cdot \mathbf{A}$ which gives two terms

$$\nabla \cdot \mathbf{A}\psi = (\nabla \cdot \mathbf{A})\psi + \mathbf{A} \cdot (\nabla\psi) = (\text{div } \mathbf{A})\psi + (\mathbf{A} \cdot \text{grad})\psi$$

(∇ and \mathbf{A} do not commute), and we find

$$H\psi = \frac{1}{2m} \left[-\hbar^2 \nabla^2 \psi + i\hbar \frac{q}{\kappa} (\nabla \cdot \mathbf{A})\psi + 2i\hbar \frac{q}{\kappa} \mathbf{A} \cdot \nabla\psi + \frac{q^2}{\kappa^2} A^2 \psi \right] + qV\psi$$

By returning to the usual notation for the laplacian, the divergence and the gradient, we write the hamiltonian operator

$$H = \frac{1}{2m} \left(-\hbar^2 \Delta + i\hbar \frac{q}{\kappa} \text{div } \mathbf{A} + 2i\hbar \frac{q}{\kappa} \mathbf{A} \cdot \text{grad} + \frac{q^2}{\kappa^2} A^2 \right) + qV \quad (5.12)$$

5.2 The Hamiltonian in the Presence of a Constant, Uniform Magnetic Field

5.2.1 The case of one electron

The expression (5.12) obtained above is valid for the most usual electromagnetic field, a function of space and time. The hamiltonian (5.12) is, in particular, the starting point of the theory of radiation describing the interactions between an electromagnetic wave and an atom. In this chapter we are concerned with the Zeeman effect, involving the interaction between an atom and a constant, uniform magnetic field, whose direction is assumed to be parallel to the z axis. The potential V is zero and, moreover, in a spherical co-ordinate system at a point defined by the radius vector \mathbf{r} , it may be shown without difficulty that the vector potential from which a uniform magnetic field \mathbf{B} is derived can be written

$$\mathbf{A} = \frac{1}{2}(\mathbf{B} \times \mathbf{r}), \quad \text{and so} \quad \begin{cases} A_x = -\frac{1}{2}B \cdot y \\ A_y = \frac{1}{2}B \cdot x \\ A_z = 0 \end{cases}$$

The hamiltonian (5.12) may be simplified thus

$$\text{div } \mathbf{A} = 0$$

and the operator $\mathbf{A} \cdot \text{grad}$ may be evaluated easily

$$\mathbf{A} \cdot \text{grad} \equiv -\frac{1}{2}B \left(y \frac{\partial}{\partial x} - x \frac{\partial}{\partial y} \right)$$

The operator l_z , the Oz component of the orbital angular momentum

measured in units of \hbar in accordance with our convention (see section 3.1), is equal to

$$l_z = i \left(y \frac{\partial}{\partial x} - x \frac{\partial}{\partial y} \right)$$

Therefore we may write

$$2i\hbar \frac{q}{\kappa} \mathbf{A} \cdot \text{grad} = -\frac{q\hbar}{\kappa} B l_z$$

The last term in the brackets of (5.12) may be written

$$\frac{q^2}{\kappa^2} A^2 = \frac{q^2}{4\kappa^2} (\mathbf{B} \times \mathbf{r}) \cdot (\mathbf{B} \times \mathbf{r}) = \frac{q^2}{4\kappa^2} B^2 r^2 \sin^2 \theta$$

θ being the angle between the radius vector and the Oz direction.

The hamiltonian therefore reduces to

$$H = \frac{1}{2m} \left(-\hbar^2 \Delta - \frac{q\hbar}{\kappa} B l_z + \frac{q^2}{4\kappa^2} B^2 r^2 \sin^2 \theta \right) \quad (5.13)$$

which can also be written by introducing the Bohr magneton β (see volume 1, section 5.2), remembering that q is negative and β positive

$$H = -\frac{\hbar^2}{2m} \Delta + \beta B l_z + \frac{q^2}{8m\kappa^2} B^2 r^2 \sin^2 \theta \quad (5.14)$$

Comment If for the moment we disregard the term in B^2 whose order of magnitude will be discussed later, $\beta B l_z$ can be identified as $-\mathcal{M}_z B$ which justifies the quantum mechanical expression for the orbital magnetic moment

$$\mathcal{M} = -\beta l = -\frac{1}{\kappa} \frac{q}{2m} \hbar l$$

The term in B^2 gives rise to diamagnetic effects.

5.2.2 The case of an atom

In chapter 2, we studied the hamiltonian of an atom, written in the form

$$H = H_0 + T_1 + T_2$$

In the presence of a static magnetic field \mathbf{B} , the interaction between the orbital motion of an atomic electron designated by the subscript i , and the field \mathbf{B} , may be expressed by an additional term in the hamiltonian, as previously established

$$\beta \mathbf{B} \cdot \mathbf{l}_i + \frac{q^2}{8m\kappa^2} B^2 r_i^2 \sin^2 \theta_i$$

However, we must also take account of the interaction between the field \mathbf{B} and the spin magnetic moment \mathcal{M}_{s_i} of this electron; this is done by adding the interaction potential energy

$$-\mathcal{M}_{s_i} \cdot \mathbf{B} = -\frac{q}{m\kappa} \sigma_{s_i} \cdot \mathbf{B} = -\frac{q\hbar}{m\kappa} s_i \cdot \mathbf{B} = 2\beta s_i \cdot \mathbf{B}$$

We may now write the hamiltonian of the atom, taking into account the contributions of all the electrons

$$H = H_0 + T_1 + T_2 + W \quad (5.15)$$

where

$$W = \sum_i \beta \mathbf{B} \cdot (\mathbf{l}_i + 2\mathbf{s}_i) + \sum_i \frac{q^2}{8m\kappa^2} B^2 r_i^2 \sin^2 \theta_i$$

Let us evaluate the order of magnitude of the two terms in the equation for W for an electron of quantum number $l = 1$ and for a magnetic field \mathbf{B} of 1 tesla

$$\beta B = \frac{e\hbar}{2m} B \approx 10^{-23} \text{ joule}$$

By taking $r_i \sin \theta_i \approx 100 \text{ pm} = 10^{-10} \text{ m}$, we have

$$\frac{q^2}{8m\kappa^2} B^2 r_i^2 \sin^2 \theta_i \approx 10^{-28} \text{ joule}$$

Therefore the term in B^2 , for normal magnetic fields, can be neglected and, after putting (in the conventional manner—see section 3.1)

$$\mathbf{S} = \sum_i \mathbf{s}_i \quad \mathbf{L} = \sum_i \mathbf{l}_i$$

we may write

$$W = \beta \mathbf{B} \cdot (\mathbf{L} + 2\mathbf{S}) = \beta B (L_z + 2S_z) \quad (5.16)$$

the z axis being in the direction of the magnetic field.

Comment The quantity $(q\hbar/2m\kappa)\mathbf{L}$ can be identified as \mathcal{M}_L and can be interpreted as the resultant of the orbital magnetic moments. Similarly $(q\hbar/2m\kappa)2\mathbf{S}$ can be identified as \mathcal{M}_S the resultant of the spin magnetic moments, the Landé factor in this case being equal to two. If \mathcal{M} is the resultant magnetic moment of the atom, the term W may be written

$$W = -(\mathcal{M}_L + \mathcal{M}_S) \cdot \mathbf{B} = -\mathcal{M} \cdot \mathbf{B}$$

Thus in a briefer study we could have written the expression for the term W directly.

The hamiltonian H describing the atom in the presence of a field cannot be studied rigorously. The solution may be undertaken by approximation methods; the procedure used will depend on the relative size of the terms T_1 , T_2 and W . In the following two sections, we shall consider only the case of L - S coupling. The main ideas apply equally to the case of j - j coupling.

5.3 The Zeeman Effect in a Weak Magnetic Field in the Case of L - S Coupling

The field conditions are said to be weak when the term W is small compared with T_1 and T_2 ; W may then be considered as a perturbation on the system described by the hamiltonian $H_0 + T_1 + T_2$. The term T_2 describes the spin-orbit coupling and is manifest in the fine structure differences of the energy levels (see chapter 3). A field will therefore be weak when its influence on a level gives rise to energy differences much smaller than the fine structure.

We shall consider an atomic level defined by a description of its electronic configuration and by the values of S , L and J . This $2J + 1$ times degenerate level will be characterised by its energy E_J^0 in the absence of a field. The influence of W will be studied by using perturbation theory. Accordingly we shall assume that the reader has already studied this technique in a quantum mechanics book.

5.3.1 The application of perturbation theory

In our discussions concerning the energy levels of an atom, we have recognised the existence of perturbation theory but have not until now used the technique in calculations. Let us review the notation and the results that we shall use for a first-order perturbation calculation, applied to a degenerate level (they are given, for example, in Messiah, page 698):

- (1) to an unperturbed level, denoted by E_i^0 , characterised by the parameter i and having an order of degeneracy G_i , the perturbation $H^{(1)}$ is applied;
- (2) k is an index which takes G_i values;
- (3) the first-order corrections $E_{ik}^{(1)}$ to be added to the unperturbed value of the energy E_i^0 are equal to the matrix elements of the diagonalised matrix $H^{(1)}$

$$\langle i, k | H^{(1)} | i, k' \rangle = E_{ik}^{(1)} \delta_{kk'} \quad (5.17)$$

In the problem with which we are concerned we apply a perturbation to an atomic level E_J^0 characterised by a given value of the angular momentum J and of degeneracy $2J + 1$. We shall use the $\{J^2, J_z\}$ representation in the subspace characterised by the energy E_J^0 . The basis states will be denoted by $|E_J^0 J m_J\rangle$. In order to use the results that we have described, we must identify i with J , G_i with $2J + 1$ and $H^{(1)}$ with W . The first-order correction, written as

$$\Delta E = E^{(1)} = E_{J m_J}^{(1)}$$

will be found by diagonalising the matrix $W_{m_J m_J'}$

$$W_{m_J m_J'} = \langle E_J^0 J, m_J | W | E_J^0 J, m_J' \rangle$$

The conditions for application of perturbation theory require that

$$\frac{W_{m_J m_J'}}{E_J^0 - E_{J'}^0} \ll 1$$

$E_j^{\prime 0}$ being a value of energy corresponding to any state of the atom other than that of energy E_j^0 . The influence of the magnetic field, described by W , must therefore give rise to a change of energy far smaller than any separation between the levels existing in zero field. This conforms with the assertion made at the beginning of section 5.3.

The operator W is given by equation (5.16)

$$W = \beta(L_z + 2S_z)B$$

In the next section we shall see that the operator W commutes with J_z . Consequently, the matrix $W_{m_j m_j'}$ is diagonal in the representation $|E_j^0 J m_j\rangle$. Our problem reduces to finding the elements of this matrix.

5.3.2 The Wigner–Eckart theorem and the introduction of the Landé g factor

In order to evaluate the matrix elements $W_{m_j m_j'}$ we shall use the following two properties.

(1) In the $\{J^2, J_z\}$ representation, in a subspace corresponding to the energy E_j^0 of the atom and to a given J value (in which the basis vectors are represented by $|E_j^0 J m_j\rangle$), the matrix elements of the components of vector operators are proportional to one another. The coefficient of proportionality is the same for each component.

If A and B are any two vector operators and if we introduce the standard components A_q , the index q taking the values $-1, 0, +1$

$$A_0 = A_z \quad A_{-1} = \frac{1}{\sqrt{2}}(A_x - iA_y) \quad A_{+1} = \frac{1}{\sqrt{2}}(A_x + iA_y)$$

we may then write

$$\langle E_j^0 J m_j | A_q | E_j^0 J m_j' \rangle = a \langle E_j^0 J m_j | B_q | E_j^0 J m_j' \rangle \quad (5.18)$$

a being the coefficient of proportionality, independent of m_j, m_j' and q .

This can be written more concisely

In the subspace E_j^0 and in the representation $\{J^2, J_z\}$

$$A = aB$$

(2) Within the subspace E_j^0 , the matrix elements of the component A_q are related to those of the component J_q of the angular momentum by the relation

$$\langle E_j^0 J m_j | A_q | E_j^0 J m_j' \rangle = \frac{\langle E_j^0 J m_j | J \cdot A | E_j^0 J m_j \rangle}{J(J+1)} \langle E_j^0 J m_j | J_q | E_j^0 J m_j' \rangle \quad (5.19)$$

Since in the given representation, $\langle E_j^0 J m_j | J \cdot A | E_j^0 J m_j \rangle$ is equal to the mean value of the scalar operator $J \cdot A$, which we denote by $\langle J \cdot A \rangle$, equation (5.19) may be written

$$\langle E_j^0 J m_j | A_q | E_j^0 J m_j' \rangle = \frac{\langle J \cdot A \rangle}{J(J+1)} \langle E_j^0 J m_j | J_q | E_j^0 J m_j' \rangle$$

This second property provides us with an expression for the coefficient of

proportionality a in equation (5.18), for the special case where one of the vector operators is the angular momentum operator J .

Properties (1) and (2) stated above are the consequences of a more general principle which forms the *Wigner-Eckart theorem*. The reader wishing for more information on this subject is referred either to a book on quantum mechanics (see, for example, A. Messiah, *Quantum Mechanics* (Wiley), chapter XIII; E. Merzbacher, *Quantum Mechanics* (Wiley), chapter 16) or to appendix 5, where proofs of properties (1) and (2) are presented and where a general statement of the Wigner-Eckart theorem is given.

Property (1) allows us to say that in the $|E_J^0 J m_J\rangle$ representation, the matrix elements of $L_z + 2S_z$ and of J_z are proportional. Since the matrix of J_z is diagonal, the matrix of $L_z + 2S_z$ will be as well. (This property also results, more directly, from the commutation relation $[A_z, J_z] = 0$ proved in the appendix.) The proportionality relationship may be written

$$\langle E_J^0 J m_J | L_z + 2S_z | E_J^0 J m_J' \rangle = g \langle E_J^0 J m_J | J_z | E_J^0 J m_J' \rangle = g m_J \delta_{m_J m_J'} \quad (5.20a)$$

The coefficient of proportionality g is called the Landé factor.

Comment I Property (1) can be accepted more readily by means of the following intuitive argument: consider an atom, the vector operator J and another operator A ; the only conservative vector in the atomic system is the vector J . For reasons of symmetry the only observable component of the operator A is its projection on the vector J . Therefore we write its average value $\langle A \rangle$ as proportional to J

$$\langle A \rangle = \text{constant} \times J$$

The same reasoning can be used for the operator B and as a result we may write

$$A = a \langle B \rangle$$

Comment II Properties (1) and (2) provide the theoretical justification of the vector model (see section 4.3). Let us take the simplest example of an operator A and an operator J , as in the preceding comment. Only the projection of A on the vector J has any physical meaning and so the vector A can be represented as having any position within a certain cone whose axis is defined by the vector J . Property (2) is a justification of the various calculations carried out by means of the rules of the vector model.

5.3.3 Calculation of the Landé factor

The discussion in the preceding section may be summarised by the vector equation

$$L + 2S = gJ \quad (5.20b)$$

provided that it is applied only within the representation $\{J^2, J_z\}$.

In order to evaluate the Landé g factor, let us consider the operator

$$J \cdot (L + 2S) = J \cdot (J + S) = J^2 + J \cdot S$$

By squaring $L = (J - S)$, we can write

$$L^2 = J^2 + S^2 - 2J \cdot S$$

and so

$$\mathbf{J} \cdot \mathbf{S} = \frac{\mathbf{J}^2 + \mathbf{S}^2 - \mathbf{L}^2}{2}$$

allowing us to write

$$\mathbf{J} \cdot (\mathbf{L} + 2\mathbf{S}) = \mathbf{J}^2 + \frac{\mathbf{J}^2 + \mathbf{S}^2 - \mathbf{L}^2}{2} \quad (5.21)$$

In the representation in which the basis vectors are $|L, S, J, m\rangle$ the average value of $\mathbf{J} \cdot (\mathbf{L} + 2\mathbf{S})$ is, from (5.21), equal to

$$\langle \mathbf{J} \cdot (\mathbf{L} + 2\mathbf{S}) \rangle = J(J+1) + \frac{J(J+1) + S(S+1) - L(L+1)}{2} \quad (5.22)$$

However, in this same representation we can evaluate the mean value of the operator $\mathbf{J} \cdot (\mathbf{L} + 2\mathbf{S})$, directly from property (2) of the preceding section. Equation (5.19) may be written

$$\langle E_J^0 J m_J | L_z + 2S_z | E_J^0 J m_J' \rangle = \frac{\langle \mathbf{J} \cdot (\mathbf{L} + 2\mathbf{S}) \rangle}{J(J+1)} \langle E_J^0 J m_J | J_z | E_J^0 J m_J' \rangle$$

and from (5.20a) this becomes

$$g \langle E_J^0 J m_J | J_z | E_J^0 J m_J' \rangle = \frac{\langle \mathbf{J} \cdot (\mathbf{L} + 2\mathbf{S}) \rangle}{J(J+1)} \langle E_J^0 J m_J | J_z | E_J^0 J m_J' \rangle$$

which, after simplification, leads to

$$\langle \mathbf{J} \cdot (\mathbf{L} + 2\mathbf{S}) \rangle = gJ(J+1) \quad (5.23)$$

Thus property (2) shows us that in order to calculate the mean value of the scalar product $\mathbf{J} \cdot (\mathbf{L} + 2\mathbf{S})$, it is permissible to replace the vector $(\mathbf{L} + 2\mathbf{S})$ by $g\mathbf{J}$.

By combining (5.22) and (5.23), we obtain

$$g = 1 + \frac{J(J+1) + S(S+1) - L(L+1)}{2J(J+1)} \quad (5.24)$$

or

$$g = \frac{3}{2} + \frac{S(S+1) - L(L+1)}{2J(J+1)}$$

The latter form is easier to remember; it is simple to verify the special cases

$$S = 0 \rightarrow J = L \rightarrow g = 1 \quad (\text{pure orbital momentum})$$

$$L = 0 \rightarrow J = S \rightarrow g = 2 \quad (\text{pure spin momentum})$$

From this formula, it is seen that g values may sometimes be negative.

5.3.4 The Zeeman diagram in a weak field

Returning to the expression (5.16) for the operator W , and using equation (5.20), we may write the matrix element $W_{m_J m_J'}$

$$W_{m_J m_J'} = g\beta B m_J \delta_{m_J m_J'} \quad (5.25)$$

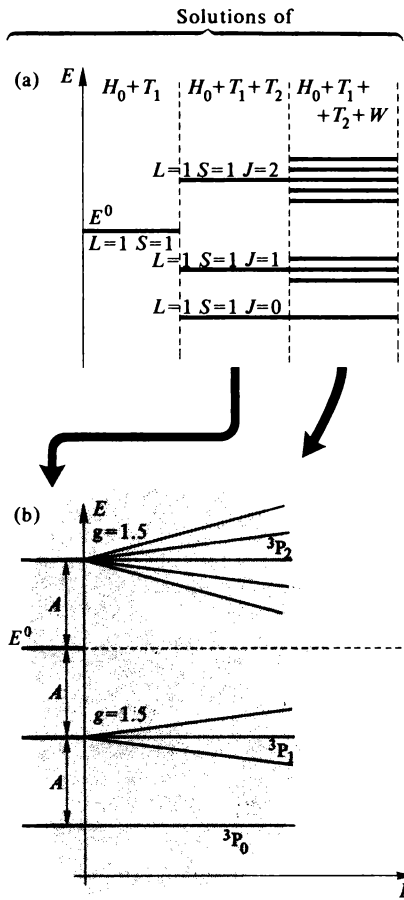
The first-order correction may be written immediately

$$E^{(1)} = \Delta E = g\beta B m_J \tag{5.26}$$

The quantum number m_J can take $2J + 1$ values

$$m_J = -J, \quad m_J = -J + 1, \dots, m_J = J$$

Thus, in the weak-field approximation, we derive the results given in volume 1, section 10.3: the presence of the magnetic field lifts the degeneracy and a given magnetic field gives rise to $2J + 1$ equidistant Zeeman sublevels, the distance between two consecutive sublevels being $g\beta B$.



Note: For weak fields, the energy scale is expanded

Figure 5.1 Weak-field case (Zeeman effect): (a) for a given value of B ; (b) as a function of B

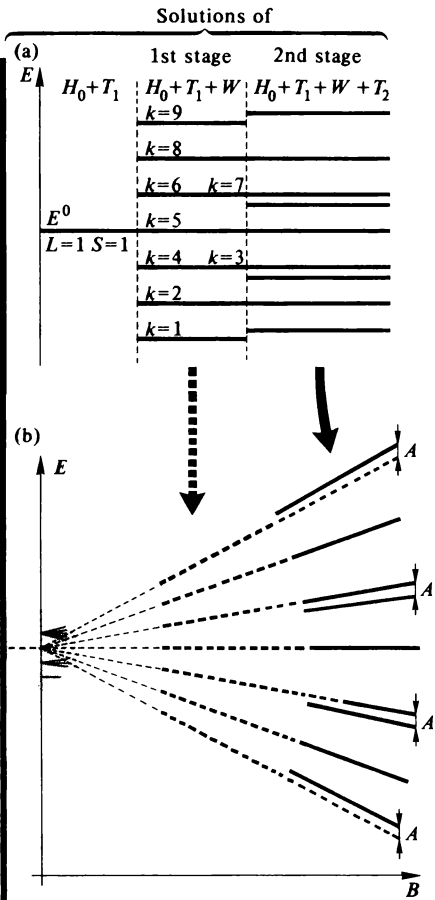


Figure 5.2 Strong-field case (Paschen-Back effect): (a) for a given value of B ; (b) as a function of B

The results of our study in a weak field are summarised in figures 5.1(a) and 5.1(b). Figure 5.1(a) summarises the successive stages of approximation in the absence of a field (see figure 3.2, but we have limited ourselves to the values $L = 1$ and $S = 1$) and the result of lifting the degeneracy for one value of B is shown. Figure 5.1(b) shows the result obtained as a function of B for the same levels as those considered in figure 5.1(a). Figure 5.1(b) thus represents the 'Zeeman diagram' of the three fine-structure levels 3P_0 , 3P_1 , 3P_2 ; the 3P_0 level has no electronic magnetic moment and is clearly unaffected by an external magnetic field. A calculation using equation (5.24) leads to numerical values of g for the 3P_1 and 3P_2 levels that may be shown to be equal.

Comment In order to position the levels of figure 5.1(b) correctly, we have started from the results in figure 4.5.

5.3.5 The Zeeman effect described by means of the vector model

In some books, the Zeeman effect is studied by using the vector model. Although this may result in a repetition of our preceding study, we shall review the principal features.

We saw (section 4.3.2) how, in the absence of a magnetic field, the vector L representing the orbital momentum and the vector S representing the spin momentum of the electron precess together around their resultant J . When a magnetic field B is applied, the coupling of L with B and the coupling of S with B become evident. In the absence of coupling between L and S , the latter precess independently around B , but in general the motion will be complicated as a result of this coupling. In the first instance, we shall study the case where *the magnetic field is weak*. Here the coupling energy between the orbital momentum and the spin momentum is much greater than that due to the coupling between these momenta and the field. This means that:

- (1) the presence of the magnetic field does not perturb the coupling between L and S —the diagram formed by the vectors J , L and S is unaltered;
- (2) the interaction with the magnetic field is represented by the precession of the aforementioned diagram—with respect to the vector J , for example—around the magnetic field B (see figure 5.3).

Let us examine the situation with respect to the magnetic moments:

(a) the orbital magnetic moment is a vector colinear with the angular momentum L :

$$\mathcal{M}_L = -\beta L$$

(b) the spin magnetic moment is a vector colinear with the angular momentum S

$$\mathcal{M}_S = -2\beta S$$

but because of the different gyromagnetic ratios, the triangle with sides \mathcal{M}_L and \mathcal{M}_S is not similar to the triangle with sides L and S . *The resultant angular magnetic moment \mathcal{M} is not colinear with the resultant momentum J .*

\mathcal{M} therefore precesses around \mathbf{J} with the angular velocity of the precession of \mathbf{L} and \mathbf{S} around \mathbf{J} , a velocity that we have assumed to be much greater than that of the precession of \mathbf{J} around \mathbf{B} . The angle between \mathcal{M} and \mathbf{B} varies continually, but its average value is equal to the angle (\mathbf{J}, \mathbf{B}) . We may therefore write the interaction energy between \mathcal{M} and \mathbf{B} as equal to

$$\Delta E = -\langle \mathcal{M}_J \rangle \cdot \mathbf{B} \quad (5.27)$$

$\langle \mathcal{M}_J \rangle$ denotes the vector projection of \mathcal{M} on the direction of the vector \mathbf{J} ; if \mathbf{u} is a unit vector parallel to \mathbf{J} , we may evaluate $\langle \mathcal{M}_J \rangle$ by writing

$$\begin{aligned} \langle \mathcal{M}_J \rangle &= (\text{projection of } \mathcal{M}_L \text{ on } \mathbf{J} + \text{projection of } \mathcal{M}_S \text{ on } \mathbf{J}) \mathbf{u} \\ &= - \left(\beta \frac{1}{|\mathbf{J}|} \mathbf{L} \cdot \mathbf{J} + 2\beta \frac{1}{|\mathbf{J}|} \mathbf{S} \cdot \mathbf{J} \right) \mathbf{u} = -\beta \frac{\mathbf{J}}{J^2} (\mathbf{L} \cdot \mathbf{J} + 2\mathbf{S} \cdot \mathbf{J}) \end{aligned}$$

which, after evaluation of the scalar products $\mathbf{L} \cdot \mathbf{J}$ and $\mathbf{S} \cdot \mathbf{J}$ in the usual way (squaring $\mathbf{S} = \mathbf{J} - \mathbf{L}$ and $\mathbf{L} = \mathbf{J} - \mathbf{S}$), leads to

$$\langle \mathcal{M}_J \rangle = -\beta \mathbf{J} \left(\frac{3J^2 + S^2 - L^2}{2J^2} \right)$$

Since $\langle \mathcal{M}_J \rangle$ is colinear with \mathbf{J} , equation (5.27) gives us, after replacing J^2 with $J(J+1)$ and so on

$$\Delta E = -(-\beta g \mathbf{J}) \cdot \mathbf{B} = +g\beta \mathbf{J} \cdot \mathbf{B} = g\beta m_J B$$

where

$$g = 1 + \frac{J(J+1) + S(S+1) - L(L+1)}{2J(J+1)}$$

This is in agreement with the results of the quantum mechanical calculation of sections 5.3.1, 5.3.2, 5.3.3 and 5.3.4.

5.4 The Paschen-Back Effect in a Strong Field. The Case of Intermediate Fields

As in the preceding sections, we confine our study to the case of L - S coupling. Strong-field conditions are said to exist when the separations between sub-levels produced by the magnetic field become much greater than the energy separations due to spin-orbit coupling. Thus the various terms of the hamiltonian H describing the atom in the presence of the magnetic field are such that

$$T_1 > W > T_2$$

The conditions for application of perturbation theory, used in the preceding section, are no longer valid. We shall carry out the calculation in two successive stages which are illustrated in Figures 5.2(a) and 5.2(b)

5.4.1 First stage, neglecting spin-orbit coupling

If we neglect spin-orbit coupling, we may apply the perturbation W to the hamiltonian $H = H_0 + T_1$, which excludes spin-orbit coupling. This means that in this first stage, in the absence of a field, the level E^0 corresponding to particular values of the angular momenta L and S is $(2S+1)(2L+1)$ times degenerate. We shall therefore use as a basis representation the basis defined by the vectors L and S , and denoted by $|E^0 L S m_L m_S\rangle$. The use of the notation of section 5.3.1 results in the matrix elements of the perturbation W being denoted by $W_{kk'}$, the subscript k being able to take $(2S+1)(2L+1)$ values.

We note immediately that L_z and S_z are diagonal in the $|E^0 L S m_L m_S\rangle$ representation, since the matrix elements may be written

$$\begin{aligned}\langle E^0 L S m_L m_S | L_z | E^0 L S m_L' m_S' \rangle &= m_L \delta_{m_L m_L'} \\ \langle E^0 L S m_L m_S | S_z | E^0 L S m_L' m_S' \rangle &= m_S \delta_{m_S m_S'}\end{aligned}$$

and thus

$$\begin{aligned}W_{kk'} &= \langle E^0 L S m_L m_S | \beta(L_z + 2S_z) | E^0 L S m_L' m_S' \rangle \\ &= \beta(m_L + 2m_S) \delta_{kk'}\end{aligned}\quad (5.28)$$

The matrix $W_{kk'}$ is diagonal, and to clarify its interpretation we have drawn up a table (table 5.1) giving the value of $m_L + 2m_S$ as a function of the subscript k . This table has been drawn up for the case $S = 1, L = 1$. In order to define k we have chosen a sequence such that an increase in the value of k corresponds to an increase of $m_L + 2m_S$ (but this is completely arbitrary).

The first-order energy corrections $E^{(1)}$ will be equal to the diagonal elements W_{kk}

$$E^{(1)} = \Delta E = W_{kk} = \beta B(m_L + 2m_S)$$

Table 5.1 Table of values of $k, m_S m_L$ and $2m_S + m_L$ for $S = 1, L = 1$
(Note the arbitrary order of numbering k)

k	m_S	m_L	$2m_S + m_L$	$A m_L m_S$	$m_L + m_S$
1	-1	-1	-3	A	-2
2	-1	0	-2	0	-1
3	-1	+1	-1	$-A$	0
4	0	-1	-1	0	-1
5	0	0	0	0	0
6	0	+1	+1	0	+1
7	+1	-1	+1	$-A$	0
8	+1	0	+2	0	+1
9	+1	+1	+3	A	+2

relates to section 5.4.2

Comment I In examining table 5.1, we note that some energy levels remain degenerate after application of the perturbation W ($m_L + 2m_S = +1$ or -1 in the example given).

Comment II Since $m_L + 2m_S$ can take only integer values, the separation between the levels that is obtained is given by the classical equation for the Zeeman effect with a Landé factor equal to unity.

The results of this first stage, for a given value of B , are shown in the middle part of figure 5.2(a) (still limited to the particular case $S = 1, L = 1$). The levels obtained as a function of the field B have been drawn in dotted lines in figure 5.2(b); in the weak-field region, these levels are clearly without physical meaning.

5.4.2 Second stage

We now apply to the energy levels defined above, the perturbation expressed by the term T_2 , which may be written as a result of the discussion in section 3.2.2

$$T_2 = \sum_i a_i l_i \cdot s_i$$

In the case of L - S coupling, it may be shown by application of the Wigner-Eckart theorem (A. Messiah, *Quantum Mechanics*, page 705) that T_2 can be put in the form

$$T_2 = AL \cdot S$$

(This result was proved in section 4.3.2 in the case of a system of two electrons, by means of the vector model.)

Let us consider the simplest case, where the levels to which we shall apply T_2 are not degenerate. Using the results of perturbation theory, the energy correction $E^{(1)}$ is equal to the mean value of T_2 evaluated for the unperturbed state. If we write

$$T_2 = A(L_x S_x + L_y S_y + L_z S_z)$$

the mean value of the first two terms in the bracket is zero. In addition, since a state is characterised by given values of m_L and m_S , the mean value of $L_z S_z$ is equal to $m_L m_S$, and so

$$\langle T_2 \rangle = A m_L m_S$$

By using the various methods of evaluating mean values, the reader can establish this result rigorously, and generalise it to the case where the perturbation T_2 is applied to a still degenerate level ($k = 3$ and 4 or $k = 6$ and 7 in the example shown in figure 5.2).

Thus, finally, we may write the energy separation ΔE between the various sublevels in a strong field

$$\Delta E = \beta B(m_L + 2m_S) + A m_L m_S$$

The results obtained in this second stage, after application of the perturbation T_2 , are shown in figure 5.2 for the particular case just studied:

- (1) for a given value B , in the last column of figure 5.2(a);
- (2) as a function of B , by the thick lines in figure 5.2(b).

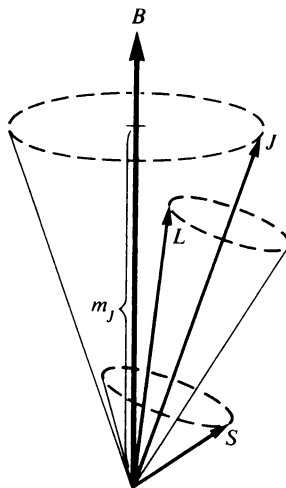


Figure 5.3 Vector model of the weak-field Zeeman effect: L and S remain coupled

Comment The reader may establish, by drawing up a table similar to table 5.1 for other cases ($S = 1, L = 2$; $S = \frac{1}{2}, L = 1$ and so on), that the perturbation $AL \cdot S$ does not always completely lift the degeneracy of all the levels that are solutions of $H_0 + T_1 + W$. In a strong field some of the levels obtained from first-order perturbation theory can remain degenerate.

5.4.3 Use of the vector model

Let us re-derive the preceding results by using the vector model. Under the assumption of a *strong field*, the coupling energy between the magnetic moments and the applied field B is much greater than the coupling energy between the magnetic moments. Accordingly, the following scheme is adopted (figure 5.4):

- (1) the vector L , coupled only to the magnetic field B , precesses around the direction of this field with an angular velocity ω_L ;
- (2) the vector S , also coupled only to the magnetic field B , precesses around the direction of this field with an angular velocity ω_S .

Since $\omega_S \neq \omega_L$, the resultant J has a length and direction that are continually varying with time, and it becomes impossible to define the quantum numbers J and m_J . We cannot therefore use J , which has become meaningless. The vectors S and L retain their meaning and we shall use as the quantisation condition:

- (a) the projection of L on B , which takes an integer value m_L such that

$$-L \leq m_L \leq L$$

- (b) the projection of S on B , which takes an integer or half-integer value m_S such that

$$-S \leq m_S \leq S$$

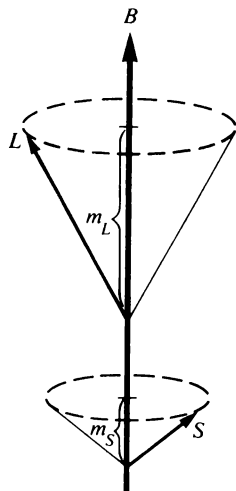


Figure 5.4 Vector model of the strong-field Zeeman effect: L and S no longer coupled

Let us evaluate the energy of an atom in a strong field. We must add to the energy E^0 in the absence of a field the coupling energy ΔE_{LB} of L with the field B , the coupling energy ΔE_{SB} of S with the field B , and the spin-orbit coupling energy ΔE_{LS} which we have assumed to be a very small term compared with ΔE_{LB} and ΔE_{SB} . The first two of these terms may be evaluated without difficulty

$$\Delta E_{LB} = -\frac{q}{2m\kappa} \hbar L \cdot B = B\beta m_L$$

$$\Delta E_{SB} = -\frac{q}{m\kappa} \hbar S \cdot B = 2B\beta m_S$$

The coupling energy between L and S may be written by using the notation of chapter 4

$$\Delta E_{LS} = A L \cdot S$$

but since L and S precess independently around B , the angle (L, S) varies continually. By means of spherical trigonometry, we can evaluate the mean value of this angle

$$\overline{\cos(L, S)} = \cos(L, B) \cos(S, B)$$

If u is a unit vector parallel to the field B , we may write

$$\Delta E_{LS} = A(L \cdot u) \cdot (S \cdot u) = A m_L m_S$$

The energy of the Zeeman sublevels may then be obtained by adding to the energy E^0 in the absence of a field, the quantity

$$\Delta E = \Delta E_{LB} + \Delta E_{SB} + \Delta E_{LS} = (m_L + 2m_S)\beta B + A m_L m_S$$

This is identical to equation (5.29) on page 101.

5.4.4 Intermediate fields

This is the situation where the perturbations are of the same order of magnitude, and consequently we must apply the total perturbation

$$W = \beta(L + 2S) \cdot B + AL \cdot S$$

directly to the solution of $H_0 + T_1$.

It is therefore necessary to find the matrix elements of the operator $AL \cdot S$ in the representation $|LSm_L m_S\rangle$. The energy correction resulting from perturbation theory should be expressed as a function of a physical parameter that retains its meaning for all values of the magnetic field; this is not so for m_L and m_S . The only conservative vector is the vector J . Therefore $m_J = m_L + m_S$ is taken as a parameter as it will retain a physical meaning in the perturbed states. The calculation of the matrix elements should be carried out in such a way as to express them as a function of m_J . The calculation is generally complicated, although the particular case where $S = \frac{1}{2}$ may be treated without difficulty.

The qualitative features of the energy diagram are often sufficient for discussion of an experiment. The physicist may then merely join in freehand style the weak-field and strong-field diagrams. The fact that $m_J = m_S + m_L$ must be conserved for a given level usually removes much of the uncertainty in the joining. In addition, it can be shown that two levels with the same m_J do not cross one another. Figure 5.5

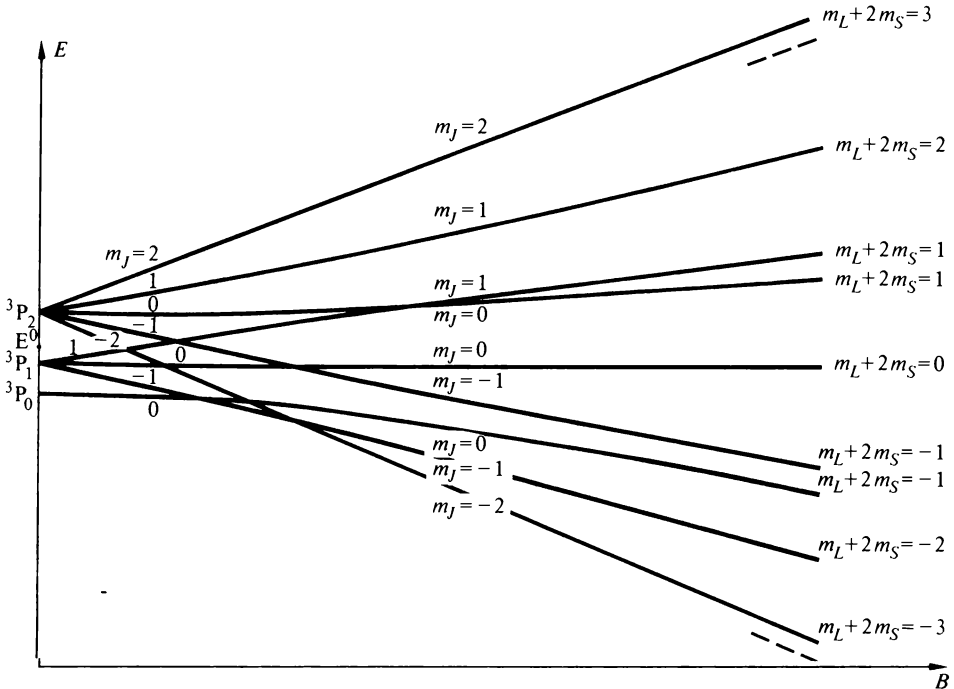


Figure 5.5 Complete energy diagram obtained by joining up figures 5.1 (b) and 5.2 (b). It should be noted that the two levels $m_J = +2$ and $m_J = -2$ are represented by straight lines. It should also be noted that the two dotted lines, and the asymptotes of certain levels, converge towards the value of the unperturbed level E^0 in zero field

shows the energy diagram covering the regions of weak, intermediate and strong fields for the case of 3P levels. This figure was obtained by joining figures 5.1(b) and 5.2(b).

The reader will note that a certain number of 'level-crossings' exist. Spectral transitions taking place in the presence of a magnetic field and corresponding to a level-crossing may show certain unusual effects. The use of this feature in spectroscopy will be discussed in chapter 7.

Comment Suppose an atomic system is placed in a very strong magnetic field such that

$$W > T_1 > T_2$$

We must then reconsider the various stages of the perturbation calculation and start by applying the perturbation W to the level E^0 corresponding to the approximation of independent electrons in a central potential. The procedure is not difficult and we limit ourselves in the following section to pointing out the results obtained in the particular case of an atom with two electrons.

We should also note that these conditions of very strong fields (total Paschen-Back effect) are rarely achieved with the magnetic fields that are commonly obtainable in the laboratory.

5.5 The Zeeman Effect and the Paschen-Back Effect of Atoms with One or Two Electrons

Chapter 4 was devoted to a detailed study of systems with one or two electrons. In this section we collect together additional information concerning the atomic magnetism of these simple systems.

5.5.1 Atoms with one outer electron

The theory developed in sections 5.3 and 5.4 may be applied straightforwardly, the operators L and S representing in this case the orbital angular momentum operator l and the spin angular momentum operator s of the outer electron.

To illustrate the theory, we give some calculated Landé factors in table 5.2.

Table 5.2

l	0	1	1	2	2	3	3
s	$\frac{1}{2}$	$\frac{1}{2}$	$\frac{1}{2}$	$\frac{1}{2}$	$\frac{1}{2}$	$\frac{1}{2}$	$\frac{1}{2}$
j	$\frac{1}{2}$	$\frac{1}{2}$	$\frac{3}{2}$	$\frac{3}{2}$	$\frac{5}{2}$	$\frac{5}{2}$	$\frac{7}{2}$
Spectral term	$^2S_{\frac{1}{2}}$	$^2P_{\frac{1}{2}}$	$^2P_{\frac{3}{2}}$	$^2D_{\frac{3}{2}}$	$^2D_{\frac{5}{2}}$	$^2F_{\frac{5}{2}}$	$^2F_{\frac{7}{2}}$
g	2	$\frac{2}{3}$	$\frac{4}{3}$	$\frac{4}{5}$	$\frac{6}{5}$	$\frac{6}{7}$	$\frac{8}{7}$

In figures 5.6 to 5.9 we shall illustrate the study of the Zeeman and Paschen-Back effects for the two resonance transitions of the alkali atoms, usually called D_1 and D_2 :

$$\begin{cases} D_1: n^2P_{\frac{1}{2}} \rightarrow n^2S_{\frac{1}{2}} \\ D_2: n^2P_{\frac{3}{2}} \rightarrow n^2S_{\frac{1}{2}} \end{cases}$$

Before discussing the spectral transitions themselves, the effect of the magnetic field on the levels concerned must be studied. The upper levels form a doublet corresponding to the quantum numbers $s = \frac{1}{2}$ and $l = 1$; for these quantum numbers we can follow the example studied in the preceding section where we chose $S = 1, L = 1$.

In this new case, figures 5.6, 5.7 and 5.8 replace figures 5.1, 5.2 and 5.5 respectively in the previous example. Figure 5.6 represents the weak-field problem: figure 5.6(a) for a given value of B , and figure 5.6(b) as a function of the variable field B . Figure 5.7 represents the strong-field problem with parts (a) and (b) having the same significance. The upper part of figure 5.8 presents the complete energy diagram obtained by joining figures 5.6(b) and 5.7(b).

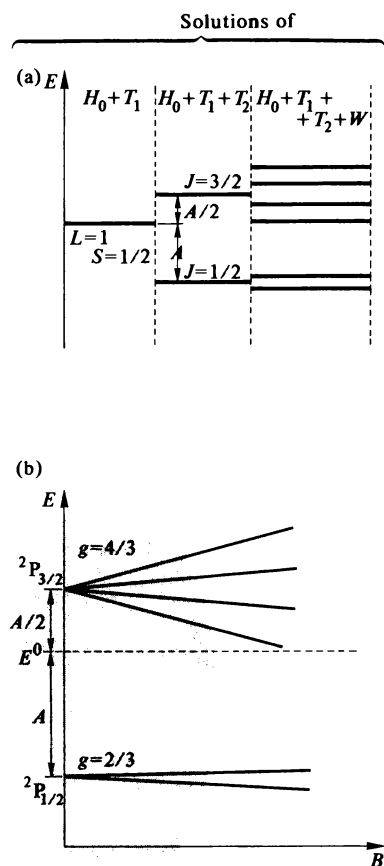


Figure 5.6 Weak-field case (Zeeman effect): (a) for a given value of B ; (b) as a function of B

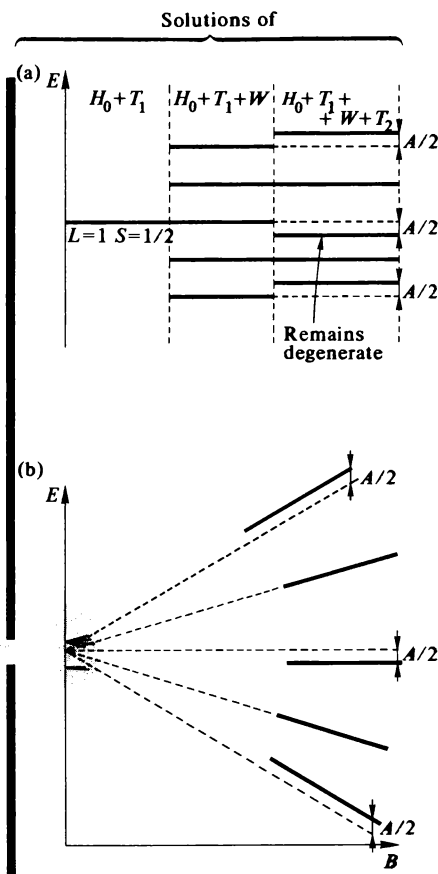


Figure 5.7 Strong-field case (Paschen-Back effect): (a) for a given value of B ; (b) as a function of B

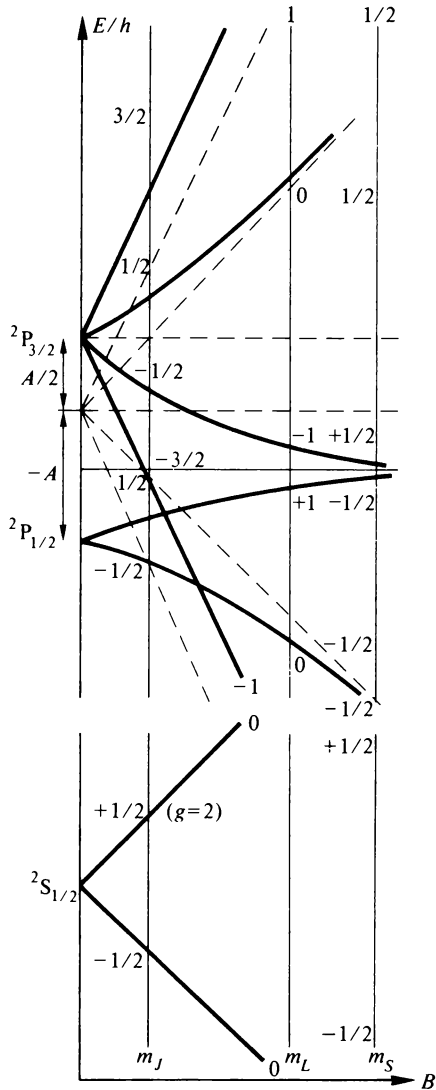


Figure 5.8 Zeeman and Paschen-Back effects of the $2S_{1/2}$, $2P_{3/2}$ and $2P_{1/2}$ levels of an alkali atom

The diagram of the Zeeman splitting of the $2S_{1/2}$ ground state of an alkali atom has been added in the lower part of figure 5.8. The latter diagram presents no difficulty because the ground state is one of zero orbital momentum and there is no spin-orbit coupling.

The experimentally observed spectral transitions take place between the sublevels shown in the two parts of figure 5.8. By using the selection rules

stated in volume 1, chapter 11 and in section 4.1, the reader may confirm that the frequencies of the various transitions, as well as their polarisation states, are correctly represented by figure 5.9. Figure 5.9(a) shows the observed

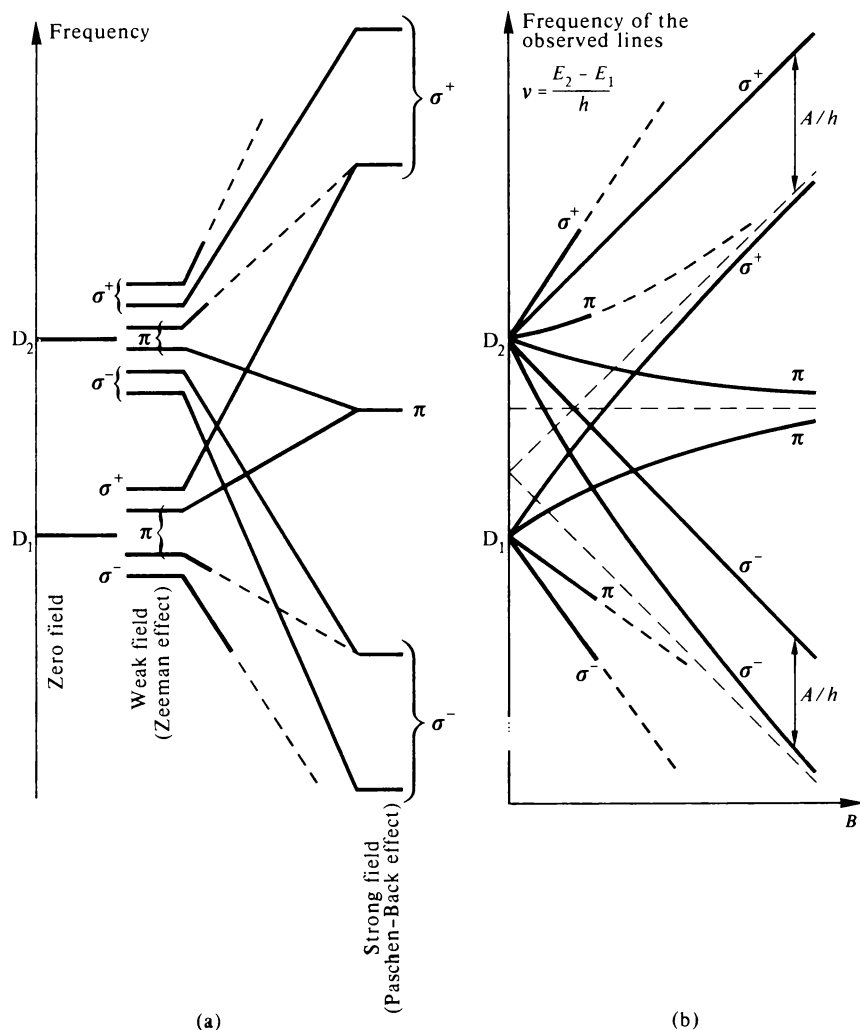


Figure 5.9 Zeeman effect of the $2P_{\frac{1}{2}} \rightarrow 2S_{\frac{1}{2}}$ and $2P_{\frac{3}{2}} \rightarrow 2S_{\frac{1}{2}}$ transitions of an alkali atom. (a) Polarisation state of the observed spectral lines for particular values of B . (b) Frequency of the observed spectral lines as a function of B . *Note:* Figure 5.9(b) is drawn with ordinate and abscissa having the same scales as in figure 5.8.

lines for two given values of B : in a weak field, four Zeeman components of the D_1 line are observed separately, and six components of the D_2 line; in a strong field the Paschen-Back effect, common to both the D_1 and D_2 lines, is observed. In figure 5.9(b) we show the variation of the observed frequencies

as the field B is changed, by joining up the two limiting cases. As an exercise, the reader may put numerical orders of magnitude for the various alkalis on to the different axes (field and frequency) with the help of the values given in table 5.3.

Table 5.3

	n	λ measured in nm		The spin-orbit coupling constant A (cm $^{-1}$)
		D_1 transition	D_2 transition	
Lithium	2	670·785		0·22339
Sodium	3	589·592	588·996	11·45
Potassium	4	769·898	766·491	38·5
Rubidium	5	794·764	780·023	158·4
Caesium	6	894·346	852·112	369·4

5.5.2 Atoms with two electrons in j - j coupling

The theory presented in section 5.3 and 5.4 relates to the case of L - S coupling; this is a rather special case, but the method can be adapted without much difficulty. As an example, we shall show how the Zeeman and Paschen-Back effects can be described for two electrons in j - j coupling.

(1) *The weak-field case.* We could apply the Wigner-Eckart theorem, as in L - S coupling, and write

$$\langle E_j^0 J m_j | L_z + 2S_z | E_j^0 J m_j' \rangle = g m_j \delta_{m_j m_j'} \quad (5.30)$$

but the stages that follow cannot be used because the angular momenta S and J are not physical characteristics of the levels in j - j coupling. Therefore we write the operator W in such a way as to emphasise the operators \mathbf{j}_1 and \mathbf{j}_2

$$W = \beta(\mathbf{j}_1 + \mathbf{j}_2 + \mathbf{s}_1 + \mathbf{s}_2) \cdot \mathbf{B}$$

The Wigner-Eckart theorem must now be applied several times consecutively; for brevity, we confine ourselves to applying it without giving a complete account of the various steps in the calculation. The form of the argument may be understood if it is appreciated that it is analogous with the evaluation of g in L - S coupling.

(a) Let us apply the Wigner-Eckart theorem to the matrix elements of the operator j_{1z}

$$\langle J m_j | j_{1z} | J m_j' \rangle = a \langle J m_j | J_z | J m_j' \rangle$$

After squaring $\mathbf{j}_2 = \mathbf{J} - \mathbf{j}_1$, the operator $\mathbf{j}_1 \cdot \mathbf{J}$ may be written

$$\mathbf{j}_1 \cdot \mathbf{J} = \frac{J^2 + \mathbf{j}_1^2 - \mathbf{j}_2^2}{2}$$

and hence the mean value of $\mathbf{j}_1 \cdot \mathbf{J}$ is

$$\langle \mathbf{j}_1 \cdot \mathbf{J} \rangle = \frac{J(J+1) + j_1(j_1+1) - j_2(j_2+1)}{2}$$

We can also calculate $\langle \mathbf{j}_1 \cdot \mathbf{J} \rangle$ directly from property (2) stated in section 5.3, equation (5.19), and we readily obtain

$$\langle \mathbf{j}_1 \cdot \mathbf{J} \rangle = aJ(J+1)$$

Hence

$$a = \frac{J(J+1) + j_1(j_1+1) - j_2(j_2+1)}{2J(J+1)}$$

(b) The matrix elements of the operator \mathbf{j}_{2z} may be found by a similar process. We write

$$\langle \mathbf{J}m_J | j_{2z} | \mathbf{J}m_J' \rangle = b \langle \mathbf{J}m_J | J_z | \mathbf{J}m_J' \rangle$$

and deduce that

$$b = \frac{J(J+1) + j_2(j_2+1) - j_1(j_1+1)}{2J(J+1)}$$

(c) If we consider the matrix elements of the operator $j_{1z} + s_{1z}$, the Wigner–Eckart theorem allows us to write

$$\langle \mathbf{J}m_J | j_{1z} + s_{1z} | \mathbf{J}m_J' \rangle = g_1 \langle \mathbf{J}m_J | J_z | \mathbf{J}m_J' \rangle$$

The evaluation of g_1 is carried out in the same way as the evaluation of g in L - S coupling; after evaluating the mean value of $\mathbf{j}_1 \cdot (\mathbf{j}_1 + \mathbf{s}_1)$ in both ways one obtains

$$g_1 = 1 + \frac{j_1(j_1+1) + s_1(s_1+1) - l_1(l_1+1)}{2j_1(j_1+1)}$$

(d) Similarly, after writing

$$\langle \mathbf{J}m_J | j_{2z} + s_{2z} | \mathbf{J}m_J' \rangle = g_2 \langle \mathbf{J}m_J | J_z | \mathbf{J}m_J' \rangle$$

we obtain

$$g_2 = 1 + \frac{j_2(j_2+1) + s_2(s_2+1) - l_2(l_2+1)}{2j_2(j_2+1)}$$

From these four steps, we can write

$$\langle \mathbf{J}m_J | L_z + 2S_z | \mathbf{J}m_J' \rangle = (ag_1 + bg_2) \langle \mathbf{J}m_J | J_z | \mathbf{J}m_J' \rangle$$

from which we obtain the Landé factor

$$g = ag_1 + bg_2$$

The study may then proceed as for L - S coupling.

(2) *The strong-field case.* First we apply the perturbation W to the solutions of the hamiltonian $H_0 + T_2$ which form levels each characterised by particular values of the angular momenta \mathbf{j}_1 and \mathbf{j}_2 . These levels are $(2j_1+1)(2j_2+1)$ times degenerate; the perturbation W will partially lift this degeneracy. Next we apply the perturbation T_1 , in the form $A'\mathbf{j}_1 \cdot \mathbf{j}_2$ (see chapter 4). As an exercise we leave the reader to show that the energy differences with respect to the E^0 solution of the hamiltonian $H_0 + T_2$, are given by

$$\Delta E = (g_1 m_{j_1} + g_2 m_{j_2})B + A' m_{j_1} m_{j_2}$$

(3) *The total Paschen-Back effect for an atom with two electrons.* The energy levels in this case can be defined without further difficulty. We confine ourselves to illustrating the physical phenomena by means of the vector model diagram (figure 5.10): the coupling energies between each magnetic moment and the applied field B become much greater than the coupling energies between the various orbital or spin magnetic moments. The four vectors l_1 , l_2 , s_1 and s_2 then precess independently around B .

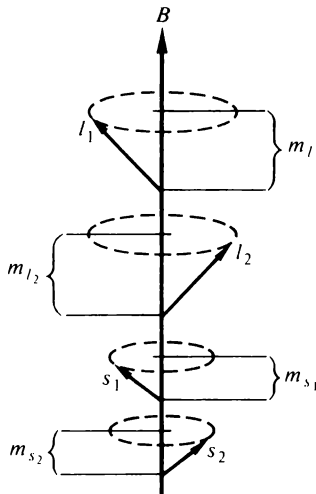


Figure 5.10 Total Paschen-Back (strong field) effect for a two-electron atom in j - j coupling

6

The Nucleus and the Physics of the Atom

In the preceding chapters, the nucleus of the atom was considered as a point charge, providing a very simple $1/r$ electrostatic potential. This assumption proved to be very useful for a preliminary discussion of the properties of the atom, but it is insufficient to explain many experimental results. In particular, the lines of an atomic spectrum, when observed with a high-resolution spectrograph, often show a 'hyperfine structure' which cannot be explained within the framework of the atomic model as developed until now.

Some of the earliest observations of 'hyperfine structure' of spectral lines were made by Michelson (1891), Fabry and Perot (1897) and Janicki (1909). In the interpretation by Pauli (1924) and Russel (1927) the assumption was made that the nucleus possessed its own angular momentum and its own magnetic moment. By analogy with the electron, the angular momentum of the nucleus itself is called the nuclear spin.

The existence of this nuclear magnetic moment complicates the study of atomic magnetism; so we shall refine the study of the Zeeman effect and show in particular that the deflections of an atomic beam in a magnetic field (the Stern and Gerlach experiment) can be correctly described only by taking account of the nuclear magnetic moment.

A detailed account of the atom should also take account of the finite size of the nucleus in the evaluation of the electrostatic interactions between the

nucleus and the electrons. This problem presents great difficulties and many atomic spectroscopy groups devote their attention to it. In this chapter we shall often have to be satisfied with a qualitative account and confine ourselves to particularly simple cases.

6.1 The Nucleus: Magnetic Moment and Angular Momentum

6.1.1 The magnetic moment of the proton

The reader has seen how the hypothesis of electron spin was confirmed by the interpretation of the Stern and Gerlach experiment (see section 3.1.4). Some years later, Esterman, Frisch and Stern (1932) provided evidence of the angular momentum and magnetic moment of the proton.

The hydrogen molecule is formed from two hydrogen atoms, that is, two electrons and two protons. The magnetic moment of this molecule results from the composition of the orbital and spin magnetic moments of the electrons, and of the magnetic moments of the protons. The hydrogen molecule can exist in two forms: orthohydrogen, in which the nuclear moments of the protons are parallel, and parahydrogen, in which the nuclear moments of the protons are anti-parallel. Methods based on the properties of the thermodynamic equilibrium between these two forms enable them to be separated. Esterman, Frisch and Stern performed a Stern and Gerlach experiment with orthohydrogen and parahydrogen in succession. The difference between the results obtained was then related to angular and magnetic moments of the protons and the following two hypotheses allowed a coherent interpretation of the experiments:

- (1) the proton possesses an angular momentum σ_p described by the spin quantum number $\frac{1}{2}$; this angular momentum obeys the general rules of quantisation

$$\left\{ \begin{array}{l} \text{component along the Oz axis: } (\sigma_p)_z = \pm \frac{1}{2} \hbar \\ \text{magnitude: } |\sigma_p| = \sqrt{[\frac{1}{2}(\frac{1}{2} + 1)]} \hbar \end{array} \right.$$

- (2) the proton possesses a magnetic moment \mathcal{M}_p parallel to and *in the same sense* as its angular momentum σ_p ; the gyromagnetic ratio is therefore positive, in contrast with that of the electron.

The term 'magnetic moment of the proton' is used to indicate, not the vector \mathcal{M}_p but the magnitude of its component along an axis; expressed as a function of the positive charge e and of the mass M of the proton, it is numerically equal to

$$\mathcal{M}_p = |(\mathcal{M}_p)_z| = 2.79 \frac{e\hbar}{2M\kappa} = 2.79 \beta_N$$

introducing the 'nuclear magneton' β_N derived from the Bohr magneton by replacing the mass m of the electron by the mass M of the proton

$$\beta_N = \frac{e\hbar}{2M\kappa} = \beta \frac{m}{M} \approx \beta \frac{1}{1836}$$

(The value 2.79 was found from more accurate measurements obtained by the same method in 1937.†) We should emphasise that the numerical factor of 2.79 has no direct relationship with the spin magnetic moment of the electron. The introduction of β_N might therefore seem to be rather artificial.

Evidence of the precession of the proton's magnetic moment can easily be obtained by means of magnetic resonance (see volume 1, chapter 9). Frequency measurements allow a very accurate value to be obtained for the magnetic moment of the proton. The presently accepted value is

$$\mathcal{M}_p = |(\mathcal{M}_p)_z| = 2.792775 \beta_N$$

6.1.2 The magnetic moment of the neutron

The picture of a charged particle, of a certain size, rotating around an axis, allows the existence of a magnetic moment to be explained qualitatively by means of a classical argument. In such a classical picture, we can understand the existence of a magnetic moment for the neutron only if we accept that the zero charge of the neutron arises through the balancing of a distribution of positive and negative charges. It may be concluded from the interpretation of the results of certain nuclear reactions that the neutron possesses an angular momentum σ_n described by the quantum number $\frac{1}{2}$.

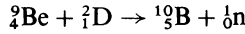
It is very difficult to carry out an experiment similar to Stern and Gerlach's in order to determine the nuclear magnetic moment of the neutron. This type of experiment requires a very well collimated beam of particles, which is incompatible with a sufficiently high neutron density. The methods used involve Larmor precession.

The basic idea (F. Bloch, 1936) is related to the possibility of obtaining a partially polarised beam of neutrons by using scattering from a magnetised medium. The neutron scattering process involves an interaction between the magnetic moment \mathcal{M}_n of the neutrons and the magnetic moment \mathcal{M}_A of the atoms of the scattering material. If this is a magnetically saturated ferromagnetic substance, all the moments \mathcal{M}_A are in the same direction, and the number of scattered neutrons will depend on the angle between the moment \mathcal{M}_n of the incident neutrons and the direction of magnetisation. The moments \mathcal{M}_n of the transmitted neutrons that have not been scattered, thus have a non-isotropic distribution. The beam is said to be partially polarised (figure 6.1). It will be noted that the method used to polarise neutrons is quite similar to that used for polarising electrons (see volume 1, section 12.2).

We shall now describe the experiment illustrated in figure 6.2. A beam of

† Esterman, I., Simpson, O. C., and Stern, O. (1937) *Phys. Rev.*, **52**, 535.

neutrons is obtained by bombarding a target of deuterium, according to the reaction



It is partially polarised by a magnetically saturated piece of steel, number I, acting as a 'polariser'. It then passes into a region where there is a magnetic

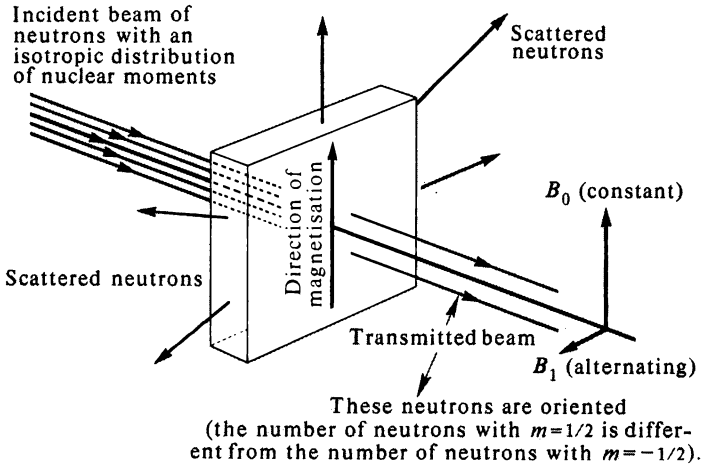


Figure 6.1 Illustrating the method of obtaining a partially polarised beam of neutrons

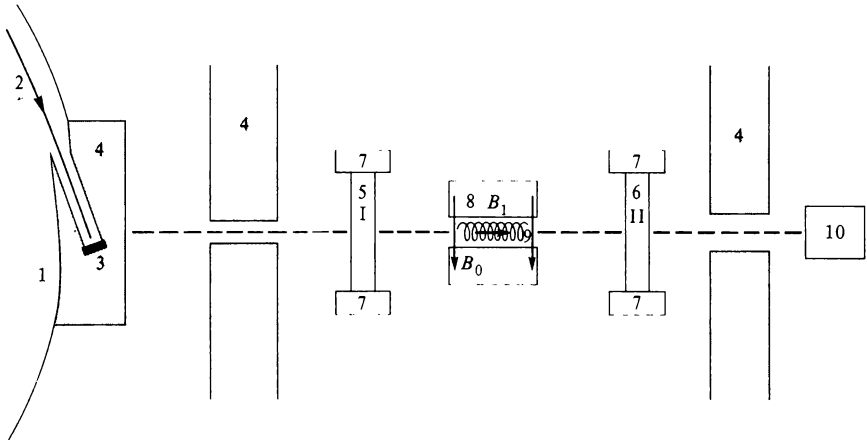


Figure 6.2 Diagram of the Bloch and Alvarez experiment: (1) cyclotron, (2) cyclotron beam, (3) target, (4) hydrogen-containing material (paraffin) serving to slow down and collimate the neutrons, (5) steel block No. I serving as a polariser, (6) steel block No. II serving as an analyser, (7) pole pieces of the electromagnets (not shown) magnetising the pieces of steel to saturation, (8) pole pieces of the electromagnets creating the static field B_0 , (9) coil creating the radio frequency field B_1 , (10) a BF_3 neutron detector

field B_0 in the same direction as the polarisation direction of the neutrons. This means that in this region of space the number of neutrons of magnetic quantum number $m = +\frac{1}{2}$ is different from the number of neutrons of quantum number $m = -\frac{1}{2}$. If an oscillating magnetic field B_1 of frequency ω_0 produces magnetic resonance in this field B_0 , the number of neutrons in the states $m = +\frac{1}{2}$ and $m = -\frac{1}{2}$ are equalised (see volume 1, chapter 10) and the beam will then be depolarised.

The piece of steel, number II, acts as an analyser: the number of neutrons scattered, and hence the number of neutrons transmitted, will depend on the polarisation state of the incident beam. Magnetic resonance, producing a change of polarisation of the beam, will therefore be detected by a change of the beam intensity reaching the detector. The magnetic moment \mathcal{M}_n will be found easily from the resonance frequency ω_0 (see volume 1, chapter 9). In practice, the apparatus is designed so as to produce nuclear magnetic resonance of protons at a frequency ω_0' in the same field B_0 . The measurement of ω_0 and ω_0' allows the determination of the ratio of the magnetic moments (their components in the direction of the field B_0)

$$\mathcal{M}_n/\mathcal{M}_p = \omega_0/\omega_0'$$

The magnetic resonance technique has other refinements which permit the orientation of the magnetic moment in relation to the angular momentum to be determined, that is to say the sign of the gyromagnetic ratio. This sign is often indicated by describing the sign of the magnetic moment. The magnetic moment of the neutron is found to be in the opposite direction to that of its angular momentum; by convention it is given a negative value.

The first experiments† date from 1940. When repeated with a much more intense beam of slow neutrons originating from a reactor, they led to the adoption of the following value‡

$$\mathcal{M}_n = -(1.913148 \pm 0.000066)\beta_N$$

6.1.3 Angular momenta and magnetic moments of some nuclei

It seems reasonable that a nucleus can possess an angular momentum and a magnetic moment in view of the fact that its constituents possess them. However, it is difficult to go much beyond this assertion, as the example of deuterium demonstrates. The nucleus of deuterium, or the deuteron, consists of a proton and a neutron, possesses a spin quantum number equal to one, and a magnetic moment

$$\mathcal{M}_d = 0.857406 \beta_N$$

which, even within experimental error, cannot be considered as the sum of the magnetic moments of the proton and neutron

$$\mathcal{M}_n + \mathcal{M}_p = (2.79277 - 1.91314) \beta_N = 0.87963 \beta_N$$

† Bloch, F., and Alvarez, L. W. (1940). *Phys. Rev.*, **57**, 111.

‡ Cohen, V. W., Corngold, N. R., and Ramsey, N. F. (1956). *Phys. Rev.*, **104**, 283.

The structure of the nucleus is very complex: the inter-nucleon forces are non-central forces involving the angles between the magnetic moments and the radius vector joining the nucleons. Furthermore, within the nucleus, the nucleons possess an orbital angular momentum. Therefore, all we can say is that each nucleus is described by a magnetic moment and an angular momentum—which can be zero for certain nuclei—an assumption in good agreement with experimental results. The nuclear angular momentum σ_N will be characterised by the integral or half-integral quantum number I

$$|\sigma_N| = \sqrt{I(I+1)}\hbar; \quad (\sigma_N)_z = m_I \hbar, \quad \text{where } -I \leq m_I \leq I$$

and we shall use the dimensionless vector I such that $\sigma_N = \hbar I$.

The nuclear magnetic moment vector is usually characterised by indicating the maximum value of its component along an axis, when $m_I = I$. It is this value which is called the nuclear magnetic moment \mathcal{M}_N in tables of constants. It is measured in units defined either by the Bohr magneton β , or by the nuclear magneton β_N (see section 6.1.2). The values measured experimentally by various methods, some of which are cited in chapter 7, are usually of the order of the nuclear magneton (see table 6.1).

Table 6.1 Values of I , \mathcal{M}_N , g_I and Q for several nuclei

Atom	I	Nuclear magnetic moment \mathcal{M}_N		Landé factor		Q , in barns (10^{-24} cm 2)
		in nuclear magnetons	in Bohr magnetons	g_I'	g_I	
^1_1H	$\frac{1}{2}$	+2.79278	0.00152112	5.5883	0.00304226	
^2_1D	1	+0.85742	0.00046700	0.85742	0.0004670	0.0028
^3_2He	$\frac{1}{2}$	-2.1276	-0.0011588	-4.255	-0.002317	
$^{39}_{19}\text{K}$	$\frac{3}{2}$	+0.3914	0.0002132	0.2609	0.00014212	0.09
$^{67}_{30}\text{Zn}$	$\frac{5}{2}$	+0.8757	0.0004769	0.35028	0.00019076	0.17
$^{85}_{37}\text{Rb}$	$\frac{5}{2}$	+1.3527	0.0007367	0.54108	0.00029470	0.28
$^{129}_{54}\text{Xe}$	$\frac{1}{2}$	-0.7768	-0.0004231	-1.5536	-0.00084622	
$^{133}_{55}\text{Cs}$	$\frac{7}{2}$	+2.579	0.0014097	0.7369	0.00040133	-0.003
$^{199}_{80}\text{Hg}$	$\frac{1}{2}$	+0.5027	0.0002738	1.0054	0.0005477	
$^{201}_{80}\text{Hg}$	$\frac{3}{2}$	-0.5567	-0.00030321	-0.37113	-0.00020214	+0.45

Likewise we define a *nuclear Landé factor*. However, the reader should be very careful because the conventions used vary according to the authors or tables consulted. We shall put

$$\mathcal{M}_N = g_I \beta I$$

and

$$\mathcal{M}_N = g_I' \beta_N I \quad \text{so} \quad g_I \approx \frac{1}{1836.1} g_I'$$

g_I or g_I' is called the nuclear Landé factor. (According as the numerical value of the nuclear magnetic moment is expressed in Bohr magnetons or in nuclear magnetons, it has the value $\mathcal{M}_N = g_I$ or $\mathcal{M}_N = g_I' I$.)

The above formulae are based on the following generally adopted sign convention: the Landé factor is considered as positive when the nuclear magnetic moment and the angular momentum are in the same direction, and as negative when in the opposite direction. Similarly a nuclear magnetic moment is represented by a positive or negative number according as it is in the same direction as the nuclear angular momentum or in the opposite direction (see figure 6.3). We should note that this convention is opposite to that used for electronic moments: the Landé factors g_J are considered as positive when the magnetic moments (orbital and spin) are in opposite directions to the corresponding angular momenta (figure 6.3).

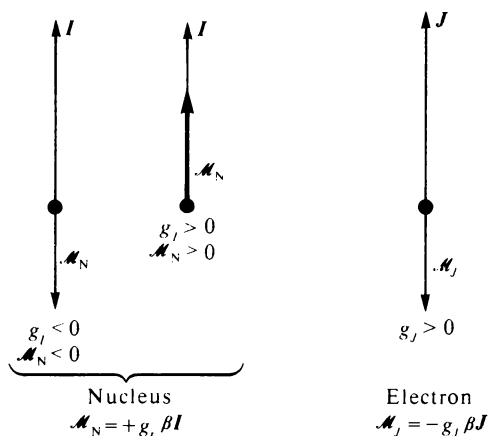


Figure 6.3 Sign convention.

By consulting a complete table of nuclear moments, we may state that:

- (1) all isotopes having an even mass number A and an even atomic number Z have zero nuclear spin and zero nuclear magnetic moment.

Example ${}^4_2\text{He}$, ${}^{16}_8\text{O}$, and ${}^{20}_{10}\text{Ne}$; all even isotopes of mercury ($Z = 80$ with $A = 196, 198, 200, 202, 204$), and so on.

- (2) all isotopes having an even mass number A and an odd atomic number Z have an integral nuclear spin.

Example ${}^2_1\text{D}$, $I = 1$; ${}^6_3\text{Li}$, $I = 1$; ${}^{10}_5\text{B}$, $I = 3$; etc.

- (3) all isotopes having an odd mass number A have a half-integral nuclear spin (see tables 6.1 and 6.3).

6.2 The Magnetic Hyperfine Structure of the Energy Levels

Back and Goudsmit interpreted the hyperfine structure of spectral lines by making two hypotheses that we state below in sections 6.2.1 and 6.2.2. The

reader should note the similarity with the previous account of an atom without nuclear spin, where a level is characterised by the total angular momentum J and where a coupling energy exists between different angular momenta.

6.2.1 Composition of the angular momenta

An energy level of an atom will be characterised by the quantum number F describing the total angular momentum of an atom, the sum of the angular momenta of the nucleus and the assembly of electrons

$$\sigma_F = \sigma_J + \sigma_I$$

or in units of \hbar

$$F = I + J \tag{6.1}$$

For given values of I and J , the operator F will be obtained by using the rules for combining angular momenta, already stated in chapter 3; as a result, several levels having different values of F will correspond to one value of J (figure 6.4).

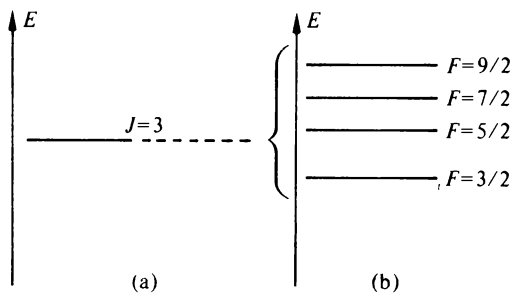


Figure 6.4 Hyperfine splitting of a level arising from the interaction between the electronic and nuclear magnetic moments. Hyperfine levels are characterised by different values of the quantum number F . (a) Ignoring the existence of nuclear spin; level characterised by $J = 3$. (b) Taking account of a nuclear spin $I = 3/2$

6.2.2 The interaction energy

A correction to the energy E_0 of a level J will be introduced as a consequence of the interactions between the nuclear magnetic moment and the electrons. It will take the form

$$\Delta E_0 = A' I \cdot J \tag{6.2}$$

A' being a constant, characteristic of the level J .

This hypothesis, which will be discussed in more detail in the next section, reduces to the assumption that the nuclear moment

$$\mathcal{M}_N = g_I \beta I$$

interacts with a magnetic field B_0 which is parallel to J . The field at the nucleus is the resultant of the magnetic field created by the orbital motion of the

electrons and of the magnetic field created by the magnetic dipole moment due to the spin of the electrons. The interaction energy may then be written

$$\Delta E_0 = -\mathcal{M}_N \cdot \mathbf{B}_0$$

The two hypotheses above facilitate a simple study of the relative positions of energy levels of the same J and different F . The energy change of a level characterised by F (with respect to E_0 , a solution in the absence of a nuclear moment) may be found by expanding the scalar product $\mathbf{I} \cdot \mathbf{J}$. To do this, we square the identity $\mathbf{F} = \mathbf{I} + \mathbf{J}$:

$$\mathbf{F}^2 = \mathbf{I}^2 + \mathbf{J}^2 + 2\mathbf{I} \cdot \mathbf{J}$$

from which we obtain

$$\mathbf{I} \cdot \mathbf{J} = \frac{\mathbf{F}^2 - \mathbf{I}^2 - \mathbf{J}^2}{2}$$

and after substituting the eigenvalues, we have

$$\Delta E_0(F) = \frac{A'}{2} [F(F+1) - I(I+1) - J(J+1)] \quad (6.3)$$

Figures 6.5(a) and 6.5(b) show, for two particular cases, the values of the energy differences ΔE_0 calculated as a function of the quantum number F and of the parameter A' (which is independent of F). It should be remarked that

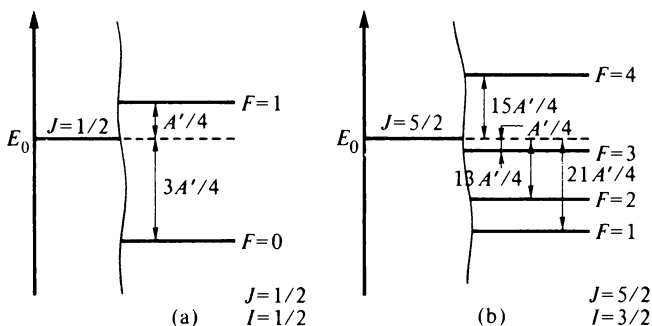


Figure 6.5 Hyperfine structures

experimentally, one does not measure the energy correction $\Delta E_0(F)$ corresponding to a level characterised by F , but instead the energy separation between two levels of different F , and generally between two consecutive values F and $F+1$. A typical separation

$$\Delta E_0(F+1) - \Delta E_0(F)$$

is called the 'hyperfine splitting' or 'hyperfine structure'.

In table 6.2 values for several levels are given. It will be noticed that some measurements can be made to a high degree of precision; indeed, certain

Table 6.2 Values of hyperfine separations for several atomic levels

Atom	I	Configuration of level	J	$F'' \rightarrow F'$ transition	Measured hyperfine structure (MHz)
^1_1H	$\frac{1}{2}$	$\uparrow 1s$	$\frac{1}{2}$	$1 \rightarrow 0$	1420.4057518 †
^3_2He	$\frac{1}{2}$	$1s 2s$	1	$\frac{3}{2} \rightarrow \frac{1}{2}$	6739.7013
$^{39}_{19}\text{K}$	$\frac{3}{2}$	$\uparrow [—] 4s$	$\frac{1}{2}$	$2 \rightarrow 1$	461.71971
$^{67}_{30}\text{Zn}$	$\frac{5}{2}$	$[—] 4s 4p$	2	$\frac{9}{2} \rightarrow \frac{7}{2}$	2418.111
				$\frac{7}{2} \rightarrow \frac{5}{2}$	1855.690
				$\frac{5}{2} \rightarrow \frac{3}{2}$	1312.065
				$\frac{3}{2} \rightarrow \frac{1}{2}$	781.865
$^{133}_{55}\text{Cs}$	$\frac{7}{2}$	$\uparrow [—] 6s$	$\frac{1}{2}$	$4 \rightarrow 3$	9192.63177 †

† The levels marked with a dagger correspond to ground levels.

‡ Transitions used as frequency standards.

hyperfine splittings serve as frequency standards and hence as time standards. The General Conference of Weights and Measures held in 1964 recommended, alongside the definition of the second based on astronomical observations, the use of the 'atomic second' defined from 'the transition between the hyperfine energy levels $F = 4, m_F = 0$ and $F = 3, m_F = 0$ of the $6^2S_{\frac{1}{2}}$ ground state of caesium 133, unperturbed by the external magnetic fields, the frequency assigned to this transition being 9 192 631 770 Hz'. The thirtieth General Conference of Weights and Measures in 1969 adopted this definition of the second as the fundamental unit of the 'Système International' (SI). In some countries it has not yet become the legal unit.

Note In the following few lines and in the next section (6.3.1) we denote the orbital momentum vector of an electron by the symbol L , contrary to our usual practice. This is to avoid confusion between the two symbols I (commonly used for the orbital momentum of an electron) and I (the nuclear angular momentum).

Comment I Depending on the level J considered, the coefficient A' can be positive or negative:

- (1) the nuclear magnetic moment can be in the same direction or in the opposite direction to the vector I ;
- (2) the field B_0 can be oriented parallel to J or in the opposite direction.

The field B_{0L} created at the nucleus by the orbital motion of an electron is in the opposite direction to the vector L (figure 6.6) due to the negative charge of the electron, whereas the field B_{0s} created at the nucleus by the spin magnetic moment \mathcal{M}_s is parallel to s . For the assembly of atomic electrons, depending on the respective values of S and L in L - S coupling or the different j_i in j - j coupling, the projection of the resultant of these fields on J , representing the mean value B_0 of the field at the nucleus, can be either parallel to J or in the opposite direction.

Comment II From the equation giving $\Delta E_0(F)$ the reader could easily derive a Landé interval rule similar to that found in section 4.3.3: 'for a given value of J , the

separations between consecutive hyperfine sublevels are proportional to the greater of the F numbers of these two sublevels'.

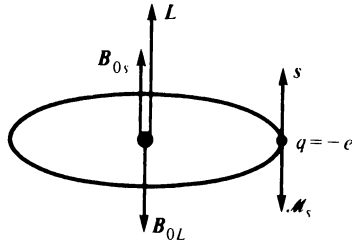


Figure 6.6 Illustrating the magnetic fields created at the nucleus by the orbital motion of an electron and by its spin angular momentum

6.3 Magnetic Interactions Between the Nucleus and the Electrons: Calculation of the Hyperfine Structure Constant

The results of section 6.2 were obtained from the hypothesis of a field B_0 created at the nucleus by the atomic electrons. A quantitative study justifies this hypothesis, and permits a more detailed approach, allowing the parameter A' to be related to the various fundamental constants. The calculations are very complex and require specialised techniques. We limit ourselves to a general discussion. The evaluation of the parameter A' requires that the various contributions to the energy correction ΔE , expressing different physical effects, are studied successively.

6.3.1 The interaction between the nuclear magnetic moment and the orbital magnetic moment of an electron

The nuclear magnetic moment \mathcal{M}_N creates at a point r anywhere in space, a vector potential

$$A = \frac{\mu_0}{4\pi\kappa} \frac{1}{r^3} (\mathcal{M}_N \times r)$$

In the first step the interaction energy w_1 with the electron cloud will be expressed by introducing a volume current density \mathbf{j} at each point in space. Using classical electromagnetism we may calculate w_1 by means of a volume integral

$$w_1 = - \iiint_{\text{space}} A \cdot \mathbf{j} d\mathcal{V} = - \frac{\mu_0}{4\pi\kappa} \iiint_{\text{space}} \frac{\mathcal{M}_N \times r}{r^3} \cdot \mathbf{j} d\mathcal{V}$$

By introducing the charge dq placed at the point M at the extremity of the vector r and moving with a velocity v , we have

$$w_1 = - \frac{\mu_0}{4\pi\kappa} \iiint_{\text{space}} \frac{\mathcal{M}_N \cdot (r \times \mathbf{j})}{r^3} d\mathcal{V} = - \frac{\mu_0}{4\pi\kappa} \mathcal{M}_N \cdot \iiint_{\text{space}} \frac{r \times v}{r^3} dq$$

Since the orbital angular momentum $\sigma_L = m(\mathbf{r} \times \mathbf{v})$ is a constant of the motion it can be taken out of the integral. By introducing the Bohr magneton and the orbital momentum measured in units of \hbar we can write

$$w_1 = + \frac{\mu_0}{4\pi} 2\beta L \cdot \mathcal{M}_N \langle r^{-3} \rangle$$

where

$$\langle r^{-3} \rangle = \frac{1}{q} \iiint_{\text{space}} \frac{dq}{r^3}$$

(the minus sign disappears when q is replaced by $-e$ in order to introduce the Bohr magneton β).

Finally, after introducing the nuclear spin I , we obtain

$$w_1 = + \frac{\mu_0}{4\pi} 2g_I \beta^2 L \cdot I \langle r^{-3} \rangle \quad (6.4)$$

Comment The preceding result can be obtained more simply by imagining a point charge $q = -e$ describing a classical orbit with velocity \mathbf{v} . At a given instant, the field it creates at the nucleus is

$$\mathbf{B} = \frac{\mu_0}{4\pi\kappa} q \mathbf{v} \times \frac{-\mathbf{r}}{r^3} = \frac{\mu_0}{4\pi m\kappa} \frac{q}{r^3} m\mathbf{r} \times \mathbf{v} = \frac{\mu_0 q}{4\pi m\kappa} \frac{\sigma_L}{r^3}$$

(\mathbf{r} is still directed from the nucleus towards the charge q); hence the average field is

$$\mathbf{B}_{0L} = \frac{\mu_0 q \hbar}{4\pi m\kappa} \left\langle \frac{1}{r^3} \right\rangle \mathbf{L} = - \frac{\mu_0}{4\pi} 2\beta \left\langle \frac{1}{r^3} \right\rangle \mathbf{L}$$

and it only remains to write the interaction energy $w_1 = -\mathcal{M}_N \cdot \mathbf{B}_{0L}$.

6.3.2 The interaction between the nuclear magnetic moment and the spin of an electron describing a non-penetrating orbit

The nuclear magnetic moment \mathcal{M}_N and the electronic spin magnetic moment \mathcal{M}_S are considered as magnetic dipoles, localised at a separation r . By using an entirely classical equation from electromagnetism (see appendix 3), the interaction energy may be written

$$w_2 = \frac{\mu_0}{4\pi} \left[\frac{\mathcal{M}_N \cdot \mathcal{M}_S}{r^3} - \frac{3(\mathcal{M}_N \cdot \mathbf{r})(\mathcal{M}_S \cdot \mathbf{r})}{r^5} \right] \quad (6.5)$$

\mathbf{r} being the radius vector separating the two moments. We note that the expression for w_2 , equation (6.5), cannot easily be simplified.

6.3.3 The case of a penetrating electronic orbit

Here the electron has a finite probability of being within a sphere whose radius is equal to that of the nucleus. The electron-nucleus separation r considered in the previous calculations can reduce to zero, and the method used is then meaningless. The coupling energy between the part of the electron close to the nucleus and the

nuclear magnetic moment may be evaluated by means of Fermi's 'contact term'. The case of *s* orbits is particularly important. In chapter 1 we saw that in this case the position probability at $r = 0$ is finite; however, since the orbital momentum is zero, the term w_1 is zero. The contribution made by the contact term is then the most important. The calculation of the interaction between the nuclear magnetic moment and the electronic spin for a hydrogen-like *s* orbit is quite simple: its starting point is the classical expression giving the energy of a magnetic moment placed at the centre of a spherically symmetric magnetised medium; the magnetisation of this medium is taken as the magnetic moment per unit volume resulting from the non-localisation of the electron spin.

It should be noted that the numerical value of the contact term has great importance; it represents the main contribution to the hyperfine splittings in the case of *s* orbits.

6.3.4 Various corrections

In addition to the fundamental interactions that we have just described, the discussion of the theoretical results and their comparison with the experimentally obtained values of hyperfine structures leads to the introduction of several further corrections as follows.

Polarisation of the inner shells. For atoms with many electrons, the resultant of the electron spins in the completed inner subshells cannot be regarded as exactly zero, due to electronic exchange phenomena; statistically each spin has a slight tendency to align parallel to the spins of the valence electrons. In evaluating the field B_0 , it is therefore necessary to take account of this magnetisation of the inner shells. The correction to ΔE can be large, as in the case of the lithium atom where it is 30 per cent.

Relativistic effects. These become important for atoms of high atomic number Z . As a result of the high electrostatic charge of the nucleus, the velocity of the electrons is high in the neighbourhood of the nucleus and relativistic corrections are necessary. These corrections can modify the results found for heavy atoms, for levels with a small value of J , by a factor of the order of two.†

Volume effects. Since the size of the proton is of the order of $1/40\,000$ of the radius of the first Bohr orbit of the hydrogen atom, the dimensions of the nucleus of a heavy atom can be about $1/5000$ of the mean radius of the trajectories of its valence electrons. In more accurate calculations the approximation of a point nucleus cannot be preserved.

When the different contributions that we have listed are combined for the various atomic electrons, it is possible to factorise the scalar product $\mathbf{I} \cdot \mathbf{J}$, the rest of the expression having a mean value which depends only on the description of the level E_0 , and which may thus be identified with the parameter A' .

Comment *The case of a hydrogen-like orbit, other than an s orbit.* In this particularly simple case, the hyperfine energy correction $\Delta E(F)$ may be obtained directly from the contributions w_1 and w_2

† This should be contrasted with relativistic effects in fine structure which are important only in the lighter atoms, as discussed in sections 2.1 and 4.4.

$$\Delta E(F) = \omega_1 + \omega_2$$

The vector model allows ΔE to be evaluated from expressions (6.4) and (6.5) by a calculation similar to those carried out in section 4.3. Its application here is of little use because the results obtained are inaccurate. The study of the problem within the framework of quantum theory leads to a particularly simple result

$$A' = \frac{\mu_0}{4\pi} 2g_1 \beta^2 \frac{Z^3}{a_1^3 n^3 (l + \frac{1}{2}) j(j+1)}$$

6.4 Corrections due to the Electrostatic Interaction Between the Electrons and the Nucleus

The hyperfine splitting expressed in frequency units between levels of the same J is usually of the order of 10^9 Hz. Compared with the energy difference between the ground level and the excited levels ($\approx 10^{14}$ Hz), the effects of hyperfine structure therefore appear as very small energy corrections, with a relative magnitude of the order of 10^{-5} . For these corrections to be meaningful, it is necessary to study the atom in sufficient detail; in particular it is necessary to take account of the fact that the nucleus is not a point, the ratio of its dimensions to those of the electronic orbits being of the order of 10^{-3} or 10^{-4} . We shall discuss two aspects of this. First we shall see that a quadrupole coupling term can lead to corrections that depend on the value of F ; the interpretation of the hyperfine splittings must therefore take account of this effect. Then we shall study isotope effects; they are manifested by a shift of the level E_0 , and therefore do not influence the separations between hyperfine levels.

6.4.1 Electric quadrupole effects

Often, the distribution of the charge q_N within the nucleus is not spherically symmetric, and the electron–nucleus electrostatic interaction term

$$\sum_i \frac{q_N q_i}{r_i}$$

must be refined so as to take account of the departure from spherical symmetry, by the inclusion of higher-order terms of the multipole expansion (see appendix 3).

In classical theory, if the origin is taken as the centre of gravity of the electric charges within the nucleus, the corresponding electric dipole moment is zero; there then remains the problem as to the relative positions of the centre of gravity of the electric charges and of the centre of gravity of the masses within the nucleus. In quantum theory, symmetry rules result in zero electric dipole moment for the nucleus, and there is no experimental evidence for an appreciable nuclear electric dipole moment (see chapter 7). The first term that must be considered in the multipole moment expansion therefore corresponds to the interaction of the electric quadrupole moment with the electric field gradient created by the electrons in the region of the nucleus.

Let us assume that the nucleus has a cylindrical charge distribution around the OZ axis, defined by the direction of the nuclear angular momentum I . The electron cloud has cylindrical symmetry about Oz, Oz being the direction of the electronic angular momentum J . The electric field gradient (see appendix 3) may then be defined by a single component $\phi_{zz} = -\partial E_z / \partial z = \partial^2 U / \partial z^2$. By using the parameter Q , the quadrupole moment of the nucleus, the additional energy ΔE_Q resulting from quadrupole coupling will be

$$\Delta E_Q = \frac{eQ\phi_{zz}}{4} \left(\frac{3}{2} \cos^2 \theta - \frac{1}{2} \right)$$

θ being the angle between the Oz and OZ axes, that is to say between the vectors I and J . ϕ_{zz} depends on the level considered, corresponding to a given configuration and a given value of J , for which we shall define the 'quadrupole coupling constant'

$$B = eQ\phi_{zz}$$

To a hyperfine sublevel with given quantum numbers J and I , it is therefore necessary to apply the energy correction

$$\Delta E_Q = \frac{B}{4} \left[\frac{3}{2} \cos^2 \theta - \frac{1}{2} \right]$$

However, the expression obtained by replacing $\cos \theta$ by its value from the vector model

$$\cos \theta = \frac{F(F+1) - I(I+1) - J(J+1)}{2\sqrt{[I(I+1)J(J+1)]}}$$

proves to be inaccurate. The correct result obtained by Casimir using quantum mechanics is

$$\Delta E_Q = \frac{B \frac{3}{2} C(C+1) - 2I(I+1)J(J+1)}{4 I(2I-1)J(2J-1)}$$

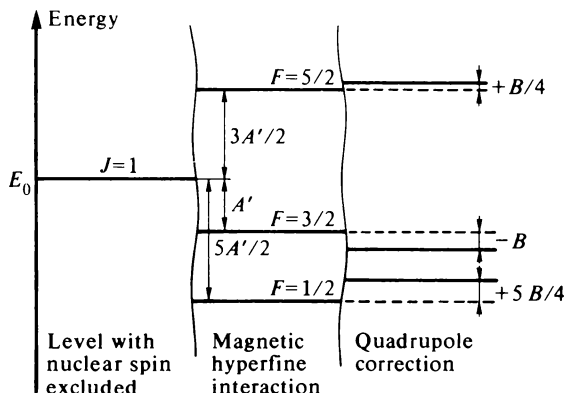


Figure 6.7 Magnetic hyperfine structure and quadrupole correction (for $J = 1$ and $I = \frac{3}{2}$)

where

$$C = F(F + 1) - I(I + 1) - J(J + 1)$$

Table 6.1 gives the order of magnitude of Q measured in barns (10^{-24} cm²) for several nuclei. Figure 6.7 shows the corrections that must be applied to the position of the energy levels having $J = 1$, $I = \frac{3}{2}$. It should be remembered that nuclei without nuclear spin or with a nuclear spin of $\frac{1}{2}$ have spherical symmetry and their quadrupole moment is zero (see table 6.1).

6.4.2 Mass and volume isotope effects

When the spectra emitted by isotopes of the same element are observed, it is found that a complete interpretation can be given only if, apart from the corrections ΔE due to hyperfine and quadrupole effects, it is assumed that the position E_0 of the level J depends on the isotope under consideration. These differences of the energy levels between *different atoms* having the same number of electrons but different mass numbers are called isotope shifts. They are of a similar order of magnitude to hyperfine differences.

Isotope shifts arise from two independent effects as follows.

(1) *The mass effect or motion of the nucleus.* The reduced mass of the electron

$$\mu = \frac{m}{1 + m/M_N}$$

entering into the Schrödinger equation depends on the mass M_N of the nucleus and varies therefore with the isotope considered. It is easy to show for a hydrogen-like atom that the energy difference δE between two equivalent levels E_0 of two different isotopes is such that (see volume 1, chapter 6, comparison between the hydrogen atom and the He⁺ ion)

$$\frac{\delta E}{E_0} = +\delta \left(\frac{1}{1 + m/M_N} \right) = -\delta \left(\frac{m}{M_N} \right) = + \frac{m}{M_N} \frac{\delta M_N}{M_N}$$

(Since the energy E_0 is negative, δE has the opposite sign to δM_N .)

For an atom with many electrons, the simple reasoning above is only qualitative. The evaluation of the reduced mass of a given electron must involve the various electron orbits of the atom and a complete calculation is complex.

It should be noted that the motion of the nucleus leads to appreciable relative energy shifts only for elements of low atomic number, where there is a large relative variation of the nuclear mass between different isotopes. The effect is therefore considerable between hydrogen and deuterium. In this case, a very simple calculation shows that the isotope shift in a level of quantum number n is expressed in terms of frequency by the formula

$$E_H - E_D = \frac{894\,000}{n^2} \text{ MHz}$$

(2) *Volume effects.* For the heavy elements, the observed isotope shift is much greater than that caused by the motion of the nucleus, and, moreover, the energy shift is in the opposite sense. In addition, it depends on the configuration of the levels. Pauli and Peierls provided the first interpretation, based on the variation of the volume of the nucleus and of the charge distribution within the nucleus between one isotope and another.

The electrostatic potential function $V(r)$ varies from one isotope to another. The largest relative change of $V(r)$ occurs near the origin, and therefore volume effects have the greatest influence for s orbits. For a given atom, isotope shifts therefore depend on the configuration of the level under consideration.

Comment When an electron is found within a spherically symmetric nucleus, it is attracted towards the centre by only a fraction of the nuclear charge (this is a classical electrostatics problem, see volume 1, section 5.2.3). Compared with a point nucleus, its binding energy therefore has a smaller absolute value, and a greater algebraic value. It may thus be understood why a nucleus of larger volume (the heavier isotope) results in higher energy values: δE has the same sign as δM_N , in contrast with the mass effect.

6.5 The Hyperfine Structure of Spectral Lines

The effects of hyperfine structure and of quadrupole shifts become apparent experimentally through electromagnetic transitions between levels; similarly,

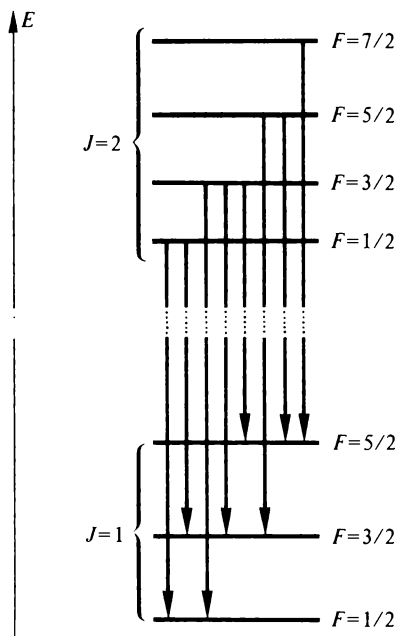


Figure 6.8 Examples of allowed hyperfine transitions: $J = 2 \rightarrow J = 1$, with $l = \frac{3}{2}$

the comparison of spectra originating from two different isotopes leads to the determination of isotope shifts. In previous chapters, we saw that only transitions satisfying certain selection rules could be observed. Having improved the description of the atom, we must also refine the selection rules. Radiation theory shows that the selection rules expressed in various parts of chapter 4 for electric dipole transitions remain valid and all that is necessary is to include a selection rule for the quantum number F

$$\Delta F = 0, \pm 1$$

a transition $F = 0 \rightarrow F = 0$ being forbidden.

By applying these rules, it is easy to determine the set of hyperfine components that can be observed spectroscopically. Some examples are given in figures 6.8 and 6.9.

When a light source emitting an atomic spectrum is constructed, one

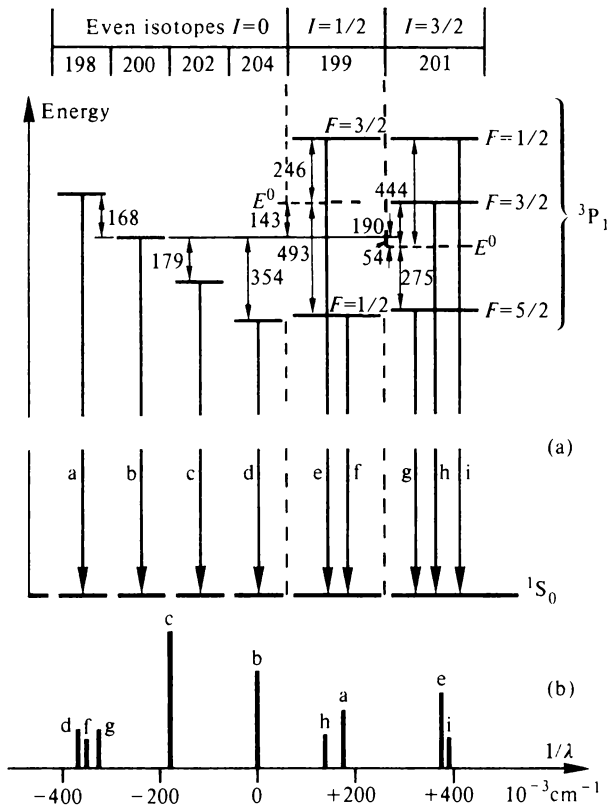


Figure 6.9 6^3P_1 transitions in the mercury atom for various isotopes. (a) Energy differences with respect to the 6^3P_1 state of the even isotope 200. Their values are given in 10^{-3} cm^{-1} . Note the inverted order of the hyperfine sublevels corresponding to the isotopes 199 and 201. The mean wavelength of the transitions is 253.7 nm . (b) Position of the spectral lines on a wavenumber scale

normally uses a natural element, formed from a mixture of isotopes which can have different nuclear spins. The observed spectrum will therefore be complex: first, the hyperfine and quadrupole effects differ according to the isotope and secondly, the effects of isotope shifts are involved. Spectroscopists often have to make light sources from pure isotopes, obtained by costly separation in a mass spectrometer; fortunately, several fractions of a milligram are usually enough to make a sufficiently intense light source.

Figure 6.9 shows the structure of the $6^3P_1-6^1S_0$ transition observed with a natural mercury lamp. The latter contains many isotopes (see table 6.3); the levels of the two odd isotopes exhibit hyperfine structure (complicated by quadrupole shifts for the 201 isotope); the levels of the four even isotopes do not have hyperfine structure but do not overlap due to isotope effects.

Table 6.3 Isotopic composition of a few natural elements

Element	A	I	Percentage
B	10	3	18.83
	11	$\frac{3}{2}$	81.17
Br	79	$\frac{1}{2}$	50.53
	81	$\frac{3}{2}$	49.47
Kr	78	0	0.354
	80	0	2.266
	82	0	11.56
	83	$\frac{9}{2}$	11.55
	84	0	56.9
Hg	86	0	17.4
	196	0	0.15
	198	0	10.12
	199	$\frac{1}{2}$	17.04
	200	0	23.25
	201	$\frac{3}{2}$	13.18
	202	0	29.54

Figure 6.9(a) shows the energy-level diagrams corresponding to each isotope; in each case, the energy of that isotope in the 6^1S_0 ground state has been taken as a reference energy. (This simplifies the diagram, but bears no relation to the energy values of the ground state with respect to the usual reference energy, an electron at infinity.) Figure 6.9(b) shows the observed spectrum on a wave number scale; it should be noted that the Doppler width, about $50 \times 10^{-3} \text{ cm}^{-1}$, is of the same order of magnitude as the differences between the indicated spectral components; some of them are almost coincident.

For a level of given quantum number J , transitions between hyperfine sub-levels are allowed, but they fall in the microwave region and their spontaneous emission probabilities are extremely small (see volume 1, chapter 3); their observation in spontaneous emission is almost impossible under laboratory conditions. However, we should point out that radioastronomers observe the transition between hyperfine sublevels of the ground state of hydrogen

$(1^2S_{\frac{1}{2}}, F=1) \rightarrow (1^2S_{\frac{1}{2}}, F=0)$ at a frequency of 1420 MHz in the radio-frequency spectrum emitted by interstellar space. Observation in induced emission is technically much easier; it requires the existence of a population difference between the sublevels under consideration, obtained either by the method of optical pumping or by a mode of excitation which preferentially populates some of the sublevels, or by atomic beam deflection methods (see volume 1, section 4.3.3). We shall return to this in chapter 7.

The general aims of research in physics will be discussed in chapter 7. Here we emphasise the importance of hyperfine structure measurements of atomic lines: they provide values of the hyperfine constant A' related to the nuclear magnetic moment, of the hyperfine constant B' related to the quadrupole moment, and of isotope shifts related to the volume of the nucleus; from them, considerable experimental evidence supporting the theories of nuclear structure is obtained. They provide a link between nuclear and atomic physics.

6.6 The Magnetism of an Atom Possessing Nuclear Spin. The Zeeman and Back-Goudsmit Effects

In the preceding sections we saw how each energy level of an atom possessing a nuclear magnetic moment is characterised by the total angular momentum F , and consequently has an order of degeneracy $2F + 1$.

The study of raising the degeneracy by a magnetic field is more complicated than in the case where the nuclear magnetic moment is zero (see chapter 5), but the main ideas in the solution of the problem remain the same. The hamiltonian of an atom in the absence of a field will now contain, in addition to the terms T_1 and T_2 , a term T_3 expressing the interaction between the electrons and the nucleus. In this section our discussion of the term T_3 will be limited to the hyperfine magnetic interaction $A'I \cdot J$ and will disregard the terms expressing isotope effects and quadrupole shifts; the latter produce shifts on the Zeeman diagram independent of the magnetic field.

6.6.1 The field-dependent perturbation W

W is given by equation (5.16) to which we add the term $-\mathcal{M}_N \cdot \mathbf{B}$ expressing the coupling between the nuclear magnetic moment and the magnetic field. We write

$$W = \beta(\mathbf{L} + 2\mathbf{S}) \cdot \mathbf{B} - \mathcal{M}_N \cdot \mathbf{B}$$

But

$$\mathcal{M}_N = g_I \beta \mathbf{I}$$

so that

$$W = \beta(\mathbf{L} + 2\mathbf{S} - g_I \mathbf{I}) \cdot \mathbf{B} = \beta(L_z + 2S_z - g_I I_z) B \quad (6.6)$$

(In passing, we note the minus sign in front of g_I resulting from the convention described in section 6.1.3.)

The discussion is based on the conditions of L - S coupling ($T_1 > T_2$); the

term T_3 produces energy shifts much smaller than T_2 . We must distinguish the following cases according to the strength of the applied magnetic field.

- (1) $T_1 > T_2 > T_3 > W$. W may then be considered as a perturbation which is applied to the solutions of the hamiltonian $H = H_0 + T_1 + T_2 + T_3$. This is described as the weak-field region.
- (2) $T_1 > T_2 > W > T_3$. The perturbation W is applied first to the hamiltonian $H_0 + T_1 + T_2$ describing the atom in the absence of a nuclear magnetic moment; then the perturbation T_3 is applied to the solution obtained. This condition is described as I - J decoupling or the Back-Goudsmit effect.
- (3) $T_1 > W > T_2 > T_3$. The treatment of the Paschen-Back effect (section 5.4) must be refined by corrections expressed by T_3 .

6.6.2 The case of weak fields—the Zeeman effect

We shall apply the perturbation W to the $(2F + 1)$ times degenerate level E_F^0 , eigenvalues of the hamiltonian $H_0 + T_1 + T_2 + T_3$. By using the results of perturbation theory (see section 5.3), the energy corrections to E_F^0 will be given by the elements of the diagonalised matrix W which commutes with F_z , the component of the total angular momentum of the atom along Oz :

$$\langle E_F^0, F, m_F | W | E_F^0, F, m_F' \rangle$$

m_F being the quantum number describing the projection of the angular momentum F on the Oz direction.

Application of the Wigner-Eckart theorem allows us to write, as in section 5.3.2

$$\begin{aligned} \langle E_F^0, F, m_F | L_z + 2S_z - g_I J_z | E_F^0, F, m_F' \rangle &= g \langle E_F^0, F, m_F | F_z | E_F^0, F, m_F' \rangle \\ &= g m_F \delta_{m_F m_F'} \end{aligned} \quad (6.7)$$

g may be evaluated in several successive steps; these steps are very like those presented in section 5.5.2 for the case of two electrons in j - j coupling. We shall only outline them.

(1) We may write

$$\langle E_F^0, F, m_F | L_z + 2S_z | E_F^0, F, m_F' \rangle = g_J \langle E_F^0, F, m_F | J_z | E_F^0, F, m_F' \rangle$$

From a calculation identical to that for the weak-field case in the absence of a nuclear moment, we obtain

$$g_J = 1 + \frac{J(J+1) + S(S+1) - L(L+1)}{2J(J+1)}$$

(2) We can also write

$$\langle E_F^0, F, m_F | J_z | E_F^0, F, m_F' \rangle = a \langle E_F^0, F, m_F | F_z | E_F^0, F, m_F' \rangle$$

and the calculation of the mean value of the operator $J \cdot F$ leads to

$$a = \frac{F(F+1) + J(J+1) - I(I+1)}{2F(F+1)}$$

(3) Similarly, by using the mean value of the operator $I \cdot F$

$$\langle E_F^0, F, m_F | I_z | E_F^0, F, m_F \rangle = b \langle E_F^0, F, m_F | F_z | E_F^0, F, m_F \rangle$$

where

$$b = \frac{F(F+1) + I(I+1) - J(J+1)}{2F(F+1)} = 1 - a$$

From these three steps, we may write

$$\langle E_F^0, F, m_F | L_z + 2S_z - g_I I_z | E_F^0, F, m_F \rangle = (ag_J - bg_I) \langle E_F^0, F, m_F | F_z | E_F^0, F, m_F \rangle$$

and from equation (6.7)

$$g = g_J \frac{F(F+1) + J(J+1) - I(I+1)}{2F(F+1)} - g_I \frac{F(F+1) + I(I+1) - J(J+1)}{2F(F+1)} \quad (6.8)$$

where g_J has the value calculated in the absence of nuclear spin in the preceding chapter.

The energy correction to first order may then be written

$$E = gm_F \beta B$$

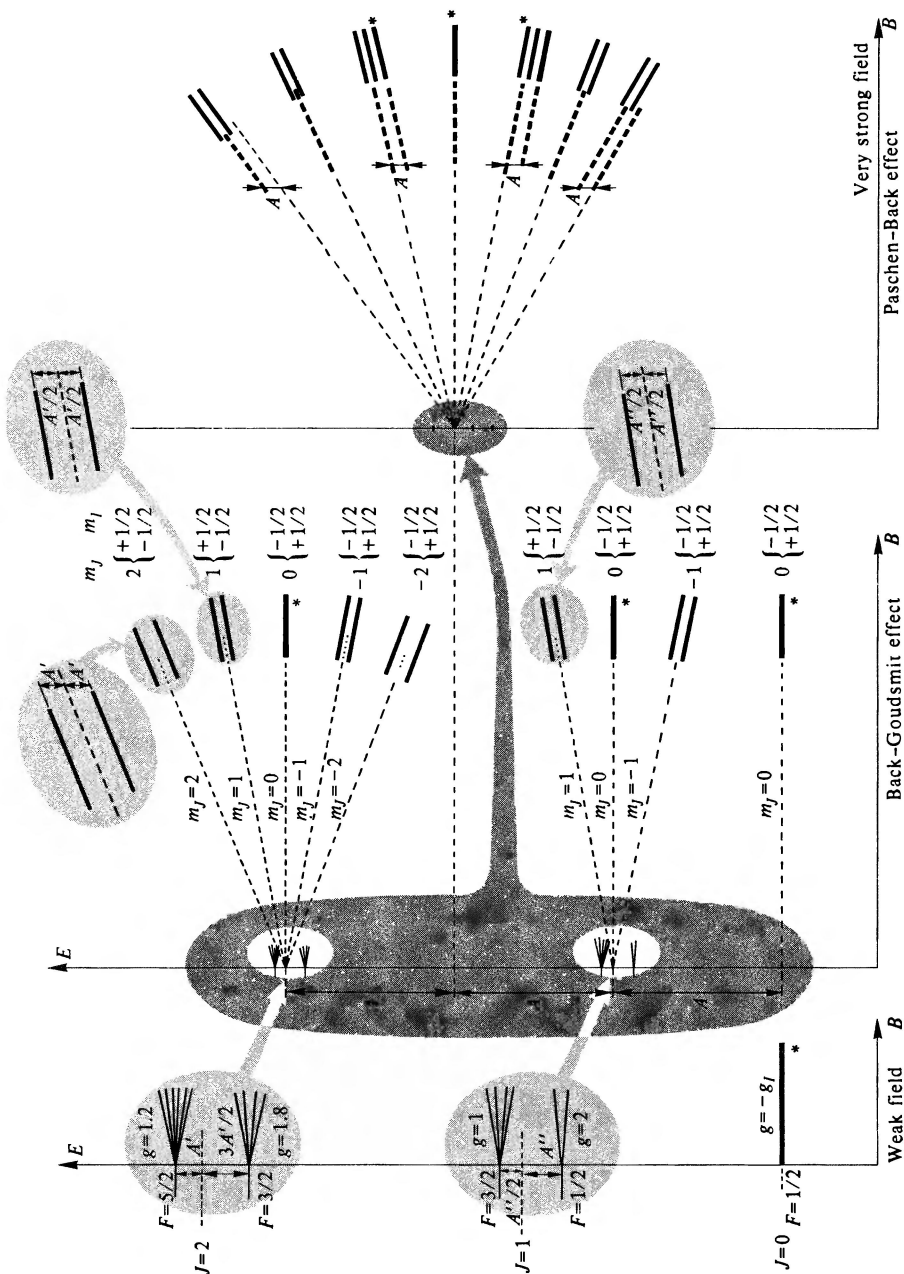
The sublevels for a given field are equidistant. The left-hand side of figure 6.10 gives the Zeeman splitting of the various hyperfine levels corresponding to the spectral terms 3P_2 , 3P_1 , 3P_0 for $I = \frac{1}{2}$. In this figure we have taken the same electronic levels as those used in figure 5.1. The reader may thus compare the effect of the magnetic field with and without a nuclear magnetic moment.

Comment I g_I is of the order of 10^{-3} (see table 6.1). In most cases it is therefore justifiable to neglect the second term of equation (6.8) and write g as

$$g \approx \frac{F(F+1) + J(J+1) - I(I+1)}{2F(F+1)} g_J$$

Comment II g can be positive or negative according to the respective numerical values of F , I and J . With the conventions used for atomic magnetic moments, a negative value of g would correspond to the case where the total angular momentum σ_F and the magnetic moment \mathcal{M}_F are in the same direction. The existence of negative Landé g factors in connection with nuclear moments explains the discussions in volume 1, section 11.2 concerning magnetic resonance experiments.

Comment III A level with quantum number $J = 0$ has a resultant electronic magnetic moment $\mathcal{M}_S + \mathcal{M}_L$ of zero. Without nuclear spin, the magnetic field therefore has no influence. The existence of a nuclear spin then gives this level a *purely nuclear magnetism*. Because $g_J = 0$, the Landé g factor equals g_I . (Since different sign conventions are chosen for the nuclear Landé factor g_I and the total Landé factor g , one strictly obtains $g = -g_I$.) For a given field the separation between the Zeeman sublevels is much smaller than in the case of electronic magnetism. An example of this is the 6^1S_0 ground state of the 199 and 201 isotopes of mercury ($I = \frac{1}{2}$ and $I = \frac{3}{2}$).



6.6.3 The Back–Goudsmit effect in a strong field

Let us now consider the case $W > T_3$. First we apply the perturbation W to the solution of the hamiltonian $H_0 + T_1 + T_2$. Although it does not enter explicitly, we must take account of the nuclear spin in the description of the state; so each level is characterised by the values of I and J , and as no coupling energy between I and J is involved, the order of degeneracy is $(2J + 1)(2I + 1)$. The problem is studied in the E_J, J, m_J, I, m_I representation and is entirely analogous to that of the Paschen–Back effect (section 5.4). By transposition, it may then be easily shown that the energy correction is

$$\Delta E = (m_J g_J - m_I g_I) \beta B$$

The levels thus obtained are drawn in dotted lines in the middle section of figure 6.10. If we disregard $m_I g_I$ in comparison with $m_J g_J$ which is much larger, the diagram is identical to that obtained in a weak field for the same atom without nuclear spin (compare with figure 5.1(b)). However, it should not be forgotten that each of the dotted lines in fact represents $(2I + 1)$ close but distinct lines, corresponding to the various values of m_I .

We now apply the perturbation

$$T_3 = A' I \cdot J$$

to the levels obtained above. It is applied to non-degenerate levels and produces an energy shift equal to the mean value of $A' I \cdot J$ for the level considered. In a way similar to the study of the Paschen–Back effect, this mean value is found to be $A' m_I m_J$.

The various levels, represented by thick lines in the middle section of figure 6.10, therefore correspond to a shift

$$\Delta E = (m_J g_J - m_I g_I) \beta B + A' m_I m_J$$

with respect to the energy E_J^0 .

6.6.4 The case of very strong fields

This is where $T_1 > W > T_2 > T_3$, that is to say the Paschen–Back effect conditions for an atom without nuclear spin. Experimentally, the problem is of little interest and we shall merely give a qualitative picture of the energy diagram on the right-hand side of figure 6.10: the dotted lines represent the energy levels in the absence of nuclear spin (Paschen–Back effect, see figure 5.2(b)); the continuous lines represent the levels taking account of the hyperfine interaction T_3 .

6.7 Energy Diagrams in the Intermediate Field Region. Effective Magnetic Moments

In the preceding section, our study was limited to certain special cases: weak field and strong field. However, in many atoms with nuclear spin, hyperfine structures are very small, of an order of magnitude between several megahertz

and about 10 000 MHz. With a Landé factor $g = 1$, the energy difference between two consecutive Zeeman sublevels, in frequency units, is about 14 GHz per tesla, and it is very probable that in the magnetic field conditions of an experiment, one of the preceding approximations will not hold; many experiments are carried out—particularly in radiofrequency spectroscopy—in conditions of intermediate field. Therefore it is often necessary to solve the problem where the total perturbation $W + T_3$ must be applied to the solutions of $H_0 + T_1 + T_2$. As we remarked in section 5.4, the solutions should be expressed as functions of $m_F = m_J + m_I$ since the only conservative quantity, whatever the field, is the projected total angular momentum F_z .

In general, an analytical solution is impossible, and numerical methods of solution must be used. However, in the special case where either J or I is equal to $\frac{1}{2}$, an analytical solution can be found; it is known as the Breit–Rabi formula. For example, let us state this formula for a level with $J = \frac{1}{2}$ and any value of I . Let $E(F, m_F)$ be the energy in the field B of an atom of total angular momentum F , and characterised by the quantum number

$$m_F = m_I + m_J$$

E_0 is the energy calculated without taking account of hyperfine structure. Finally, let us introduce the reduced parameter x in place of the magnetic field B

$$x = \frac{2(g_J + g_I)\beta B}{(2I + 1)A'} = (g_J + g_I) \frac{\beta B}{\delta W}$$

(where $\delta W = [(2I + 1)/2]A'$ is the energy difference between the two levels $F = I \pm \frac{1}{2}$ in zero field). The Breit–Rabi formula may then be written

$$E(F, m_F) - E_0 = -\frac{A'}{4} - g_I m_F \beta B \pm \frac{(2I + 1)A'}{4} \sqrt{\left(1 + \frac{4m_F}{2I + 1} x + x^2\right)}$$

The plus sign is taken for levels $F = I + \frac{1}{2}$ and the minus sign for $F = I - \frac{1}{2}$ when the field is weak ($x < 1$); on the other hand, when the field is strong ($x > 1$), the sign chosen is that of the quantum number m_J . These relations permit Zeeman diagrams to be constructed by simple numerical calculation, and figure 6.11 gives some examples. The reader should show that the Breit–Rabi formula, in the limiting cases ($x \rightarrow 0$, $x \rightarrow \infty$), reduces to the relations established for strong and weak fields in the preceding sections.

In this book, we have frequently used an expression giving the coupling energy between a magnetic moment \mathcal{M} and a magnetic field \mathbf{B}

$$\Delta E = -\mathcal{M} \cdot \mathbf{B} = -\mathcal{M}_z B$$

The variation of ΔE with the magnetic field B is then linear and the component \mathcal{M}_z of the magnetic moment \mathcal{M} represents the slope of the line $\Delta E = f(B)$. For intermediate fields, the relation $\Delta E = f(B)$ is no longer linear. We shall generalise the concept of magnetic moment as follows: let us consider a given magnetic field \mathbf{B} and let us vary \mathbf{B} by $\delta\mathbf{B}$; the energy varies by δE and we put

$$\delta E = -\mathcal{M}_{\text{eff}} \delta B$$

We shall let \mathcal{M}_{eff} be the effective magnetic moment of the atom in the Zeeman sublevel under consideration, for the field B_0 . \mathcal{M}_{eff} is therefore a function of B ; physically this corresponds to the fact that the total effect of the various interactions undergone by the elementary magnetic moments is a function of the magnetic field. The curves representing \mathcal{M}_{eff} as a function of the field B may be obtained by differentiating the curves $\Delta E = f(B)$. Figure 6.12 shows

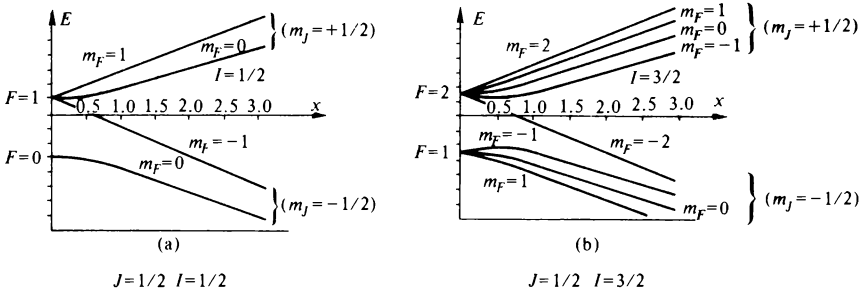


Figure 6.11 Splitting of a $J = \frac{1}{2}$ level in the presence of a magnetic field, in (a) with $I = \frac{1}{2}$ and in (b) with $I = \frac{3}{2}$. The abscissae are proportional to the magnetic field and measured in terms of the parameter x defined in the text

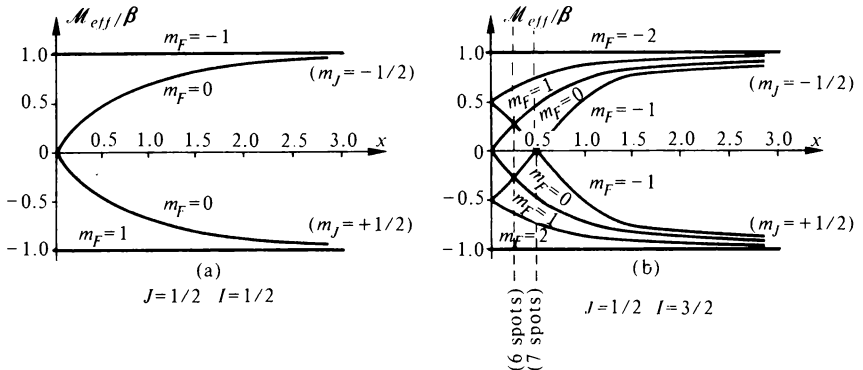


Figure 6.12 Effective magnetic moment \mathcal{M}_{eff} as a function of magnetic field measured in terms of the parameter x proportional to the magnetic field

the variation of \mathcal{M}_{eff} (measured in terms of the Bohr magneton β) as a function of the magnetic field, for the levels corresponding to the Zeeman diagrams in figure 6.11.

The concept of an effective magnetic moment allows in particular the Stern and Gerlach experiments to be described in all field conditions: an atom in the apparatus having a quantum number m will follow a trajectory corresponding to the effective magnetic moment \mathcal{M}_{eff} that it possesses in a field B , where B is the average field in the apparatus.

For example, suppose that we carry out a Stern and Gerlach experiment

with the natural isotope ^{23}Na of sodium. The ground level is a $^2\text{S}_{\frac{1}{2}}$ level, but since the nucleus has a nuclear spin $I = \frac{3}{2}$, the level splits into two hyperfine sublevels $F = 1$, and $F = 2$. The Zeeman diagram corresponds to that of figure 6.11(b), the hyperfine separation in zero field being 1773 MHz. For a given field in the apparatus there will be as many spots observed on the screen as there are values of the effective magnetic moment. The number and the position of the spots may be predicted from the curve $\mathcal{M}_{\text{eff}} = f(B)$ (figure 6.12(b)). Eight spots are generally observed except for the two particular values indicated in figure 6.12(b), where only six or seven spots respectively are observed. For the value of B corresponding to $x = 0.5$ ($B \approx 30$ millitesla in the case of sodium) an undeflected spot is observed. This property has been used experimentally by certain authors in order to investigate hyperfine structures.

7

Experimental Methods in Atomic Physics

The scope of this chapter is necessarily limited. We cannot describe fully all the work that has been done in the field of atomic physics; therefore we shall present only a survey, supported in some sections by experimental details, so that the reader will be able to appreciate some of the problems studied in research laboratories. Some additional, rather specialised, concepts will also be introduced. We confine our study to free atoms, disregarding problems such as magnetic resonance phenomena in solids which involve the collective interactions of atoms described by macroscopic quantities.

The various sections of this chapter are, for the most part, independent. They may be regarded as illustrations of the fundamental ideas which have been presented in this book so far. Many references are therefore made to volume 1 and chapters 1–6 of this volume, often to material in small print because these sections were not regarded as essential to the general understanding of the subject.

7.1 Introduction

7.1.1 The aims of research

There are several thousand physicists engaged in carrying out and utilising experiments in the sphere of atomic physics. The main aim of research is the

increase of knowledge, and the field of atomic physics has received considerable attention. Although practical applications have sometimes been a direct result of these studies (frequency standards, magnetometers, methods of analysis) it should be said that, in general, discussion of the aim of a piece of research is often difficult. However, the following points can be made.

The relationship between atomic physics and theoretical physics is very important; a certain number of problems in atomic physics, especially those concerned with the hydrogen atom, can be studied in depth theoretically. Consequently, there has always been a close connection between these two disciplines; an experiment might suggest or require extension of a theory, or a theory might be tested by means of an experiment in the field of atomic physics. Several times in this chapter we shall describe experiments whose results have confirmed fundamental theories to a high degree of precision.

Most experiments provide a considerable amount of data which, apart from their intrinsic interest, give physicists the necessary information to construct models, used in a majority of problems where rigorous study, in the mathematical sense of the term, is impossible. For example, the results of the study of isotope shifts and quadrupole effects have an important bearing on the concept of a nuclear model.

Finally, numerous parameters related to the description of the atom are required in other fields of physics: the description of the ground state of an atom is required by the solid-state physicist and by the physical chemist; astrophysicists and plasma physicists need values of excitation cross-sections and the lifetimes of excited states.

7.1.2 The interpretation of an experimental signal

The techniques used in experimental atomic physics are extremely varied, but it will be noticed that quite similar problems arise when it comes to interpretation of the signal provided directly by the apparatus so as to extract the information sought. Two rather different aspects of interpretation should be noted in particular.

(1) In some cases, the result sought is expressed by a quantity requiring either a set of measurements on the phenomenon studied (for example the width at half height of a resonance curve), or the knowledge of various experimental parameters. (The interpretation of the experiment described in volume 1, section 12.2.2, leading to the magnetic moment of the electron, requires the knowledge of the velocity of the electrons. The determination of the Landé factor by a Stern and Gerlach experiment requires the value of the field gradient in the airgap of the electromagnet.) Discussion of the accuracy of a measurement may therefore involve several parameters.

(2) In other cases, the signal is presented as a graph plotted as a function of an abscissa which can be measured very accurately (the current creating a magnetic field, the frequency of an electromagnetic wave and so on). The plot will enable the parameter to be measured directly. Measurements of gyromagnetic ratios by magnetic resonance methods, of hyperfine structure

by radiofrequency spectroscopy, and measurements in optical spectroscopy are examples of this.

The accuracy obtained in a measurement involves two phenomena in particular.

(a) *The width of a line.* When the result of an experiment is expressed as a line which must be plotted or analysed, this line possesses a certain width which will affect the expected precision of the measurements. In many experiments the phenomenon studied is an electromagnetic transition and the width of the experimental curve is equal to (or maybe proportional to) the frequency width of an electromagnetic transition emitted or absorbed by an atom. This problem has been considered several times in this book and we shall recall the various aspects that may be involved:

- (i) the natural width related to the lifetime of the atom in the state under consideration (volume 1, section 4.2.3);
- (ii) the Doppler width resulting from the motion of the atom (see volume 1, section 1.3.3);
- (iii) other causes, such as the Stark effect, which can be minimised by careful choice of the experimental conditions (see volume 1, section 1.3.3).

The study of the width of a line, therefore, may be reduced in a first approximation to the comparison between the natural width and the Doppler width. This matter is often of prime importance and we take care to discuss it in the experiments that we shall describe.

(b) *The noise.* An experimental signal recorded as a function of a variable parameter never appears as an infinitely thin line, even if all experimental imperfections (instabilities, vibrations, and so on) are eliminated (figure 7.1).

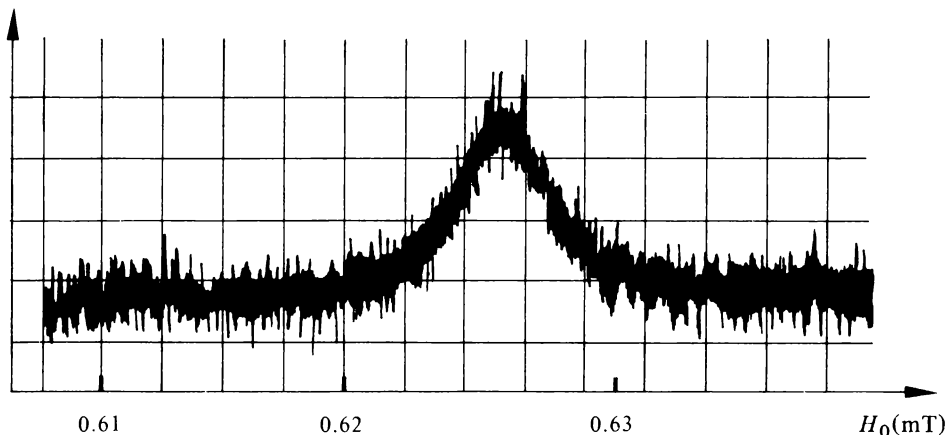


Figure 7.1 Signal and noise. Magnetic resonance on the 5^3P_1 level of cadmium, detected optically, the frequency of the field H_1 being very low (14 MHz). The field H_0 is the abscissa and the degree of polarisation of the $5^3P_1 \rightarrow 5^1S_0$ transition is the ordinate (see section 7.4)

The signal is subjected to random fluctuations, related to the discontinuous nature of the quantities involved in the experiment: an electric current results from the flow of a finite number of electrons; the measurement of the intensity of a beam of light by a photoelectric detector reduces to counting photons. In a given experiment these fluctuations are characterised by a certain 'signal-to-noise ratio'. It is not possible for us to analyse these phenomena in this book so we confine ourselves to asserting intuitively that for a given experiment, the longer the measurement time, the better the signal-to-noise ratio. Figure 7.2 is an illustration of this: a particular magnetic resonance phenomenon on an excited atomic state (see section 7.3) is observed, in figure 7.2(a) after sweeping a field for 30 minutes, and in figure 7.2(b) after an

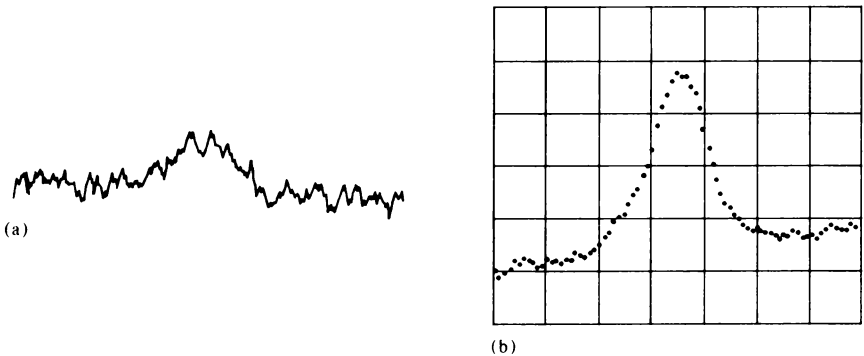


Figure 7.2 The same magnetic resonance curve (an excited level of argon, optical detection): (a) recording time of 30 minutes; (b) total duration of experiment, 48 hours

experiment lasting for a total of 48 hours, by averaging over a large number of measurements by means of a data accumulation apparatus. The theory of measurement shows that the improvement in the signal-to-noise ratio is proportional to the square root of the ratio of the measurement times, which can be confirmed by figure 7.2.

7.2 Optical Spectroscopy

In this section, we bring together experiments which enable excited atomic levels to be studied by analysis of the radiation emitted in the visible or near visible region. We shall distinguish mainly: interference spectroscopy which consists of analysing the wavelengths of the emitted radiation (we shall not discuss methods utilising a prism spectrograph which in practice are hardly ever used in atomic spectroscopy), and level-crossing spectroscopy, where the intensity of radiation emitted as a function of magnetic field is studied. The latter technique has been considerably improved in recent years.

7.2.1 Interference spectroscopy

Interference spectroscopy has emerged as the most general method of studying atomic levels. It has provided a considerable amount of information; consultation of energy-level tables shows the wealth of results that have been obtained. As an example, a partial reproduction of the spectroscopic results obtained on the excited levels of platinum is shown in figure 7.3. In the case of complex atomic spectra (the rare earths, actinides, and so on) where the light

	α		β		γ
	Term		$\Delta\nu$	195 A'	194-196
a ₀	5d ⁹ 6s	³ D ₃	+696	+199	+82
a ₁	—	³ D ₂	-203	-81	+117
a ₂	5d ⁸ 6s ²	³ F ₄	+140	+31	+203
a ₃	5d ¹⁰	¹ S ₀	—	—	—
a ₄	5d ⁸ 6s ²	³ P ₂	+197	+89	+160
a ₅	—	³ F ₃	+192	+55	+202
a ₆	5d ⁹ 6s	³ D ₁	-252	-168	≈+90
a ₇	—	¹ D ₂	+481	+192	+120
a ₈	5d ⁸ 6s ²	³ F ₂	+189	+76	+200
b	—	¹ G ₄	+403	+90	+93
c	5d ⁸ 6s 6p	⁵ D ₄ ⁰	+626?	+139?	+110?
d	5d ⁹ 6p	³ P ₂ ⁰	+169	+67	+36
e	5d ⁸ 6s 6p	⁵ G ₅ ⁰	+725	+132	+108
f	5d ⁹ 6p	³ F ₃ ⁰	+389	+111	+56
g	5d ⁸ 6s 6p	⁵ D ₃ ⁰	+75	+21	+85
h	—	⁵ G ₆	+1006	+155	+107
i	—	5 ₁ ⁰	≈-55	≈-22	+84
j	—	6 ₂ ⁰	+204	+82	+49
k	5d ⁹ 6p	³ F ₄ ⁰	+253	+56	≈+30
l	5d ⁸ 6s 6p	8 ₈ ⁰	+252	+72	≈+40
m	—	³ F ₅ ⁰	+606	+110	+112
n	—	5 _{F₄} ⁰	+174	+39	+107
o	—	⁵ D ₂ ⁰	+308	+123	≈+50

Figure 7.3 Extract from the Landolt-Börnstein tables (1952). Column α gives the spectral term and the configuration. Column β is relative to the 195 isotope. It gives the hyperfine structure $\Delta\nu$ in thousandths of cm^{-1} , as well as the coefficient A' defined in chapter 6 and related directly to $\Delta\nu$. Column γ shows, in thousandths of cm^{-1} , the relative isotope shift of the levels between the isotopes 194 and 196

intensity is dispersed among many lines, modern methods of high resolution spectroscopy involving subtle techniques of exploiting the signal have made very detailed experimental analysis possible. Comparison of results from optical spectroscopy with the various theories describing the interactions within the atom has proved to be very useful. In fact optical spectroscopy laboratories always include groups of atomic theoreticians; progress in this field results from continual competition between theoreticians and experimentalists.

The general features of an optical spectroscopy experiment may always be reduced to those of figure 7.4. An interference device (grating, Fabry-Perot,

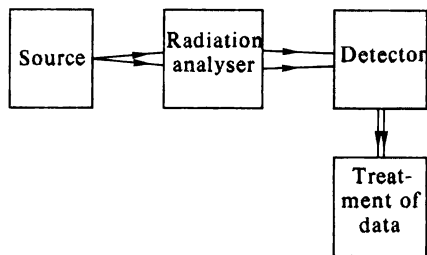


Figure 7.4 Principal features of an experiment in optical spectroscopy

or other interferometer) is used to analyse the radiation. The detector is usually a photoelectric detector used under optimum conditions of signal-to-noise ratio. This detector is very often connected to devices for treating the signal so as to exploit to the maximum the experimental results. For instance, when a Michelson interferometer is used, the detector records an interferogram from which the spectrum $I = f(\nu)$ must be extracted by calculation. (Descriptions of the various techniques of instrumental spectroscopy may be found in specialised books.)

The width of a line. In an optical spectroscopy experiment the width of a line results mainly from the Doppler effect. The phenomena studied are either in the visible or in the near ultraviolet region and, referring back to volume 1, section 1.3.3, we see that Doppler widths are of the order of 1000 MHz, whereas natural widths, depending on the lifetimes of the excited states involved, are between 1 and 100 MHz. However, this short discussion should only be considered as very approximate. The theoretical profile of a line broadened only by the Doppler effect and the theoretical profile resulting from the natural width have different mathematical expressions; for, from the centre of the line, it is generally the effect related to the natural width that becomes predominant (see figure 7.5).

In order to obtain the greatest possible accuracy, the experimenter must

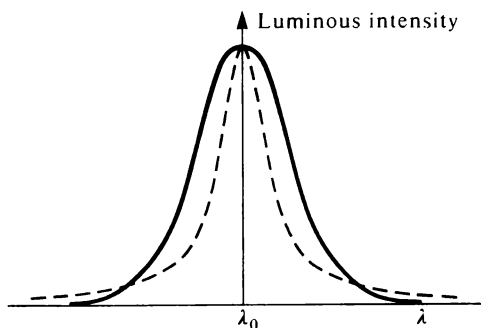


Figure 7.5 Solid line : shape of a Doppler broadened line. Dotted line : natural lineshape

therefore construct a source having the smallest possible Doppler broadening. A method often used consists of employing a 'hollow cathode', illustrated in figure 7.6. The light used is that emitted in the region of the cathode, which is cooled to a very low temperature. The discharge is established in a gas such as argon. The atoms are extracted from the cathode containing the element under study and are excited by the discharge; as a result of the low temperature of the cathode, the thermal velocity of these atoms is small. In addition, the magnitude of the discharge current is small, so that Stark broadening does not become predominant. An ordinary spectral light source has a line width of several thousand megahertz. For lines in the visible spectrum, a cooled

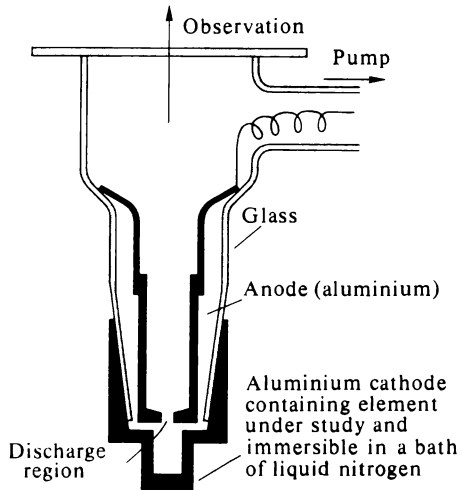


Figure 7.6 Hollow cathode (schematic)

hollow cathode allows line widths of several hundred megahertz to be obtained.

An atomic beam excited by a beam of electrons (figure 7.7) in which all atoms move in the same direction, has also been used. Doppler broadening for transverse observation is theoretically zero. However, this type of source always provides a low light intensity and is not often used. It should be noted that to obtain an atomic beam, it is necessary to heat the atoms to a high temperature; their speed is therefore large, and to ensure that the Doppler width of the emitted light is small, observation must be as close to transverse as possible. If α is the angle of divergence of the beam and β the angular aperture of the light beam, $\sin(\alpha + \beta)$ must always be much smaller than unity.

The treatment of a spectrum consists usually of analysing the line profile and enables components that are closer together than the line width to be studied. An example may be found by referring to chapter 4; a detailed analysis of the profile of the $H\alpha$ lines obtained by interferometric methods allowed an approximate evaluation of the Lamb shift. By means of a careful study of a

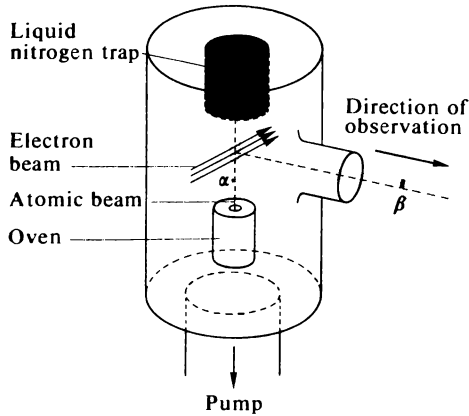


Figure 7.7 Diagram of an atomic beam lamp

line profile, the ultimate resolution that one can hope to attain in optical spectroscopy is a few tens of megahertz.

It should be noticed that in atomic spectroscopy, most transitions are in the near ultraviolet, visible and near infrared regions (0.2 to $2\ \mu\text{m}$). The more specialised techniques of infrared spectroscopy are used mainly in molecular spectroscopy.

Use of the laser. Compilation tables show that quite a large number of atomic transitions can be observed in stimulated emission. Analysis of their spectra shows that they can have frequency widths as small as a few hertz. At first sight, it might seem that there are sources available with much narrower line widths than conventional sources, and that considerable improvement could be obtained in ultimate resolution. However, one should bear in mind the laser mechanism: a vapour excited by a discharge is placed within a resonant Fabry–Perot cavity. This cavity possesses a large number of modes. For a cavity $1\ \text{m}$ long, the frequency separation of the modes is $150\ \text{MHz}$. The laser oscillations may be ‘locked’ on to one of the modes contained within the Doppler width of the transition under consideration (see volume 1, figure 4.11). Various techniques allow the mode to be selected and the oscillation to be stabilised. However, the frequency of the oscillation can have an arbitrary value within the Doppler profile: to within the precision corresponding to the stability obtained, it does not represent any parameter related to the excited level of the emitter.

In general, no spectacular gain in resolution can be obtained at the moment by using a laser, but the laser is used as a source in some spectroscopic experiments—some rather weak transitions in spontaneous emission in a conventional source can be intense in a laser. The gain obtained in signal amplitude is then of considerable interest to the experimenter, and allows resolution to be gained by improvement of the signal-to-noise ratio. We should note, however, that in special cases accurate measurements of isotope shifts have

been carried out by taking advantage of the resolution gained as a result of the line width of laser emission.

It is possible that in a short time, the use of the laser will bring about spectacular progress in spectroscopy. Techniques are being studied for controlling the cavity in such a way that the Fabry-Perot mode remains exactly at the centre of the Doppler line; in addition, research has been undertaken in order to develop super-radiant sources from which emission is observed without a resonant cavity (see volume 1, section 4.3.4).†

7.2.2 Level-crossing spectroscopy

(1) *The principle.* Let us consider a set of excited atomic states \mathcal{A} in the presence of a magnetic field of such a value that the energy diagram describes a situation of intermediate field (see section 5.4.4); a certain number of level crossings exist. This set of atomic states can be either a set of multiplets exhibiting a fine structure in zero field, or a set of hyperfine states with the same value of J (see chapter 6). Various transitions may be observed, such as those indicated by the arrows ① and ② in figure 7.8, corresponding to the de-excitation from two of the states of the group \mathcal{A} towards another common level.

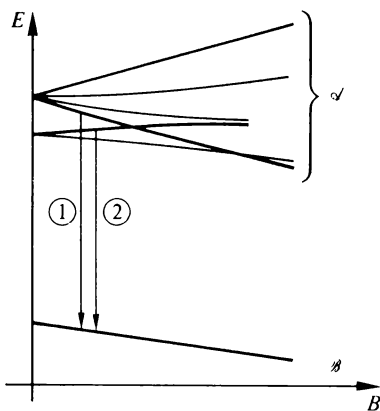


Figure 7.8 Level-crossings

We shall assume for the moment—we return in paragraph (3) to the actual situation—that the radiations corresponding to the transitions ① and ② observed in a given direction, are plane electromagnetic waves of amplitudes

† *Translator's note:* Since this book was written, developments have taken place enabling narrow (≈ 1 MHz), stabilised, and *continuously tunable* radiation throughout the visible region to be obtained from lasers in which the active medium is a solution of an organic dye. These dye lasers are now being widely used in high resolution optical spectroscopy (see, for example, Hänsch, T. W. (1972). *Proc. 3rd int. Conf. Atomic Physics, Boulder, Colorado*), and considerable progress has already been made.

$a_1 \cos \omega_1 t$ and $a_2 \cos \omega_2 t$ respectively. Let us observe with the aid of a photodetector the light corresponding to the sum of the transitions ① and ②.

- (a) For a magnetic field not corresponding to a level crossing, the transitions ① and ② have different wavelengths and the mean signal observed will have an intensity proportional to $a_1^2 + a_2^2$. (The photomultiplier is followed by an amplifier whose band width is a few Hz or kHz and therefore cannot detect higher frequency beats.)
- (b) Let us now suppose that the value of the magnetic field corresponds to a level crossing. Both transitions ① and ② have the same wavelength, and the two electromagnetic waves will interfere at the photocathode. We have assumed that these two waves are in phase; the observed intensity will then be proportional to $(a_1 + a_2)^2$.

When the magnetic field is swept, the output current from the photomultiplier will therefore change as the field passes through a value corresponding to a level crossing. The experiment thus allows us to investigate the magnetic-field values at which the various level crossings occur, and by using the results from a theoretical study of the diagram of the levels \mathcal{A} in intermediate fields, it is possible to obtain fine structure values (the parameter A of chapters 4 and 5) or hyperfine structures (the parameter A' of chapter 6).

(2) *Selection rules.* The lower level is the same for both the observed transitions ① and ②. If we apply the selection rule for an electric dipole transition, $\delta m = 0, \pm 1$, the two upper levels must be levels with quantum numbers m_1 and m_2 such that $|m_1 - m_2|$ equals 0, 1 or 2.

However, as we indicated when studying intermediate field diagrams, levels of the same m_j do not cross; therefore $|m_1 - m_2| = 0$ must be excluded. Hence, the study of intensity variations of light emitted in the presence of a magnetic field can only provide evidence of level crossings such that $|m_1 - m_2| = 1$ or 2. Depending on the state of polarisation of the light received by the photodetector, either both types of crossing $|m_1 - m_2| = 2$ and $|m_1 - m_2| = 1$ may be observed, or only one type. In addition, the curves giving the intensity I as a function of B (the shape of the line) can have different shapes according to the state of polarisation.

(3) *Coherence of the excitation.* The description of the level-crossing phenomenon given above used a representation of the emitted light in terms of a plane wave. As a result, it left out one of the subtle features of the effect. Classically, the emission of light by an atom takes place in the form of a succession of damped wave trains unrelated in phase. During an observation on a human time scale, all the phase fluctuations are averaged out and consequently no interference effects between light produced by different atoms can be observed. However, in a quantum representation, if the excited atom is described by a wave function which is a coherent superposition of the wave functions of two states of different m , the emitted radiation at each instant will possess properties allowing the observation of the interference effects described in paragraph (1). The method of exciting the state \mathcal{A} that

one wishes to study must be carefully chosen; as we have just mentioned, it must allow a coherent superposition to be achieved. Figure 7.9 gives an example of one type of excitation.

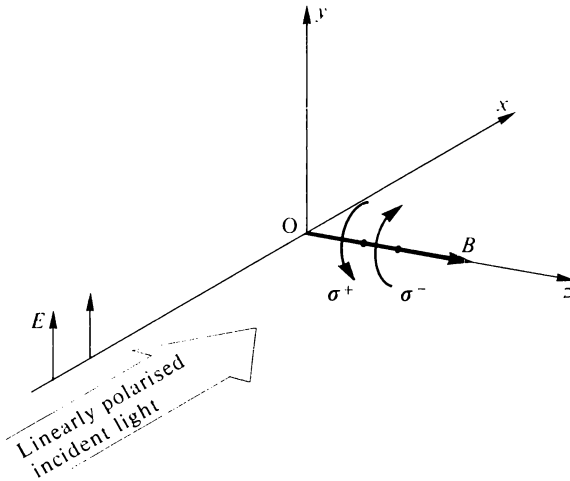


Figure 7.9

The atoms, at O , are subjected to a magnetic field directed along Oz . A beam of resonance light, linearly polarised parallel to Oy and propagating along Ox , excites atoms in the ground state to an excited state \mathcal{A} . The atoms situated at O experience a linearly oscillating electric field, which can be resolved into two circular vibrations σ^+ and σ^- rotating around B in opposite directions. The Zeeman effect selection rules then require that the excitation from the ground level to the excited levels satisfies $\delta m = 1$ and $\delta m = -1$. In an experiment where the Doppler width of the source allows the energy conditions to be satisfied, the state obtained by such a mode of optical excitation will be a coherent superposition of the states $m = -1$ and $m = +1$. This is called 'coherent excitation'. We should also point out (see section 7.3.4) that a beam of electrons with an energy of several tens of electron-volts and a well-defined direction perpendicular to the magnetic field, can produce a partially coherent excitation, also allowing level crossings to be detected.

(4) *The line width.* The curves observed express the variation of the light intensity at the photodetector in passing through a level crossing. This effect is produced by the interference of waves coming from the *same atom*, as described in the preceding paragraph. Consequently, any frequency difference between the waves that interfere cannot result from the Doppler effect. Only the frequency spread related to the uncertainty principle will be involved; *the width of the lines is therefore related to the natural width of the levels.* Here we come across a fundamental difference, accounting for the superior resolution which may be obtained experimentally in comparison with interference

spectroscopy. The fact that the width of a line is closely related to the natural width has led some authors to analyse level-crossing experiments within the framework of radiofrequency spectroscopy where one comes across the same property.

Comment The width of the level-crossing curves is also a function of the Landé factors of the levels; the width of the effect involves the slope of the levels, a fact easily understood from figure 7.10.

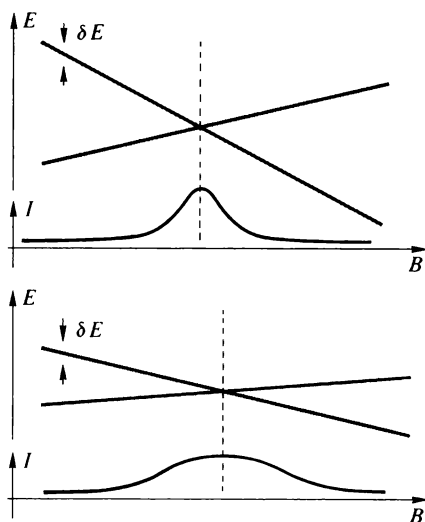


Figure 7.10 Diagrams illustrating that for levels of the same lifetime, and therefore the same energy uncertainty δE , the width of the level crossing curves depends on the Landé factor

(5) *Level crossings at zero field: the Hanle effect.* All Zeeman sublevels cross at zero field. If the conditions for observing level crossings are realised, a variation of the observed light intensity must also occur when the applied field passes through zero. The width of the observed phenomenon in terms of field will be a function of the Landé factor and the lifetime of the level under consideration. This zero field effect was discovered by Hanle in 1925, much earlier than the discovery of level-crossing effects (Franken, 1959). Its interpretation was first given from a classical viewpoint of the radiation.

Let us briefly present this classical argument by modernising it somewhat. The atoms are subjected to a magnetic field B in the Oz direction. Let us consider excitation conditions corresponding to those described in figure 7.11 and assume that the exciting light, linearly polarised parallel to Oy , is the superposition of two circularly polarised beams, one right circular and one left circular. By using results from the study of the angular momentum of radiation (volume 1, chapter 11), we see that the atoms excited by the left-circularly polarised light acquire a magnetic moment in the positive Ox direction, whereas those excited by right-circularly polarised light acquire a magnetic moment in the negative Ox direction. Thus we express the con-

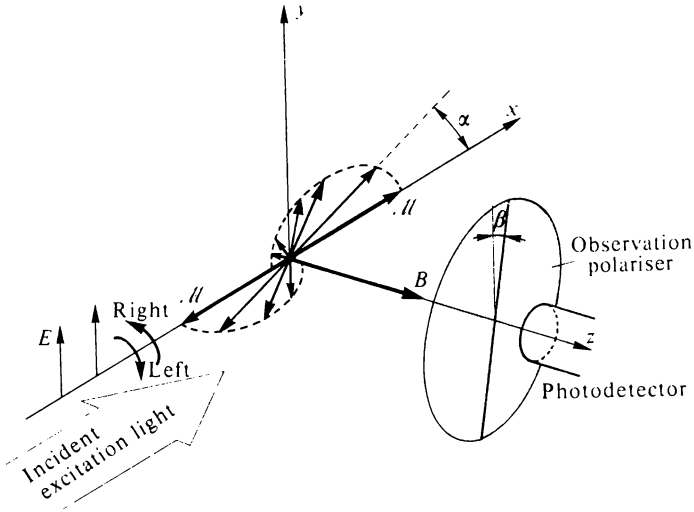


Figure 7.11 Diagram of a Hanle experiment. The lengths of the arrows from the origin O are proportional to $N(\alpha)$

cept of coherent excitation in classical language, by saying that if dN atoms are excited in a time interval dt , $dN/2$ atomic angular momenta are aligned in the positive Ox direction, and $dN/2$ in the negative Ox direction.

As a result of Larmor precession around Oz (see volume 1, chapter 9), the magnetic moments aligned along Ox will precess with an angular velocity

$$\omega = -\gamma B = g \frac{e}{2m\kappa} B$$

and they will make an angle α with the Ox direction after a time $t = \alpha/\omega$.

However, due to spontaneous emission with lifetime τ , the number of excited atoms decreases progressively with the rotation of the magnetic moments. Under steady-state conditions we can write that the number of atoms $N(\alpha)d\alpha$ whose magnetic moments are between the angles α and $\alpha + d\alpha$ is

$$N(\alpha) d\alpha = A e^{-t/\tau} d\alpha = A e^{-\alpha/\omega\tau} d\alpha$$

where

$$\int_0^\infty N(\alpha) d\alpha = N_0$$

which gives

$$A = N_0/\omega\tau$$

(The atomic magnetic moments are represented in figure 7.11 by vectors of angle α and with a length proportional to $N(\alpha)$.)

Let us assume that the radiation emitted in the Oz direction by an atomic state whose angular momentum is directed parallel to Ox possesses an electric field along Oy (see classical study of the Zeeman effect, volume 1, section 8.4) and let us place in front of the detector a polariser whose direction of polarisation makes an angle β with the Oy direction (figure 7.11).

Consider atoms whose magnetic moment vector makes an angle between α and $\alpha + d\alpha$ with the Ox direction, that is to say whose electric field radiated in the Oz direction makes an angle between α and $\alpha + d\alpha$ with the Oy direction; the intensity $I(\alpha)d\alpha$ transmitted through the polariser is proportional to $N(\alpha)d\alpha$ and to $\cos^2(\beta - \alpha)$.

The total intensity received by the detector is therefore

$$I = \frac{\text{constant}}{\omega\tau} \int_0^\infty e^{-\alpha/\omega\tau} \cos^2(\beta - \alpha) d\alpha$$

This integral may easily be evaluated for particular values of β . By letting I_0 be the intensity received by the photodetector in zero field for $\beta = 0$, we obtain

$$\left. \begin{aligned} \text{for } \beta = 0: \quad I &= \frac{I_0}{2} \left(1 + \frac{1}{1 + 4\omega^2 \tau^2} \right) \\ \text{for } \beta = \pi/4: \quad I &= \frac{I_0}{2} \left(1 + \frac{\omega\tau}{1 + 4\omega^2 \tau^2} \right) \end{aligned} \right\} \omega = g \frac{e}{2m\kappa} B$$

Figure 7.12 shows the curves obtained. They have the same shape as magnetic resonance curves (see volume 1, chapter 9) and as the absorption and dispersion curves studied in appendix 2. From the preceding expressions, the reader may show that for the frequency $\omega_0 = \frac{1}{2}\tau$, corresponding to a field

$$B_0 = \frac{m\kappa}{e g \tau}$$

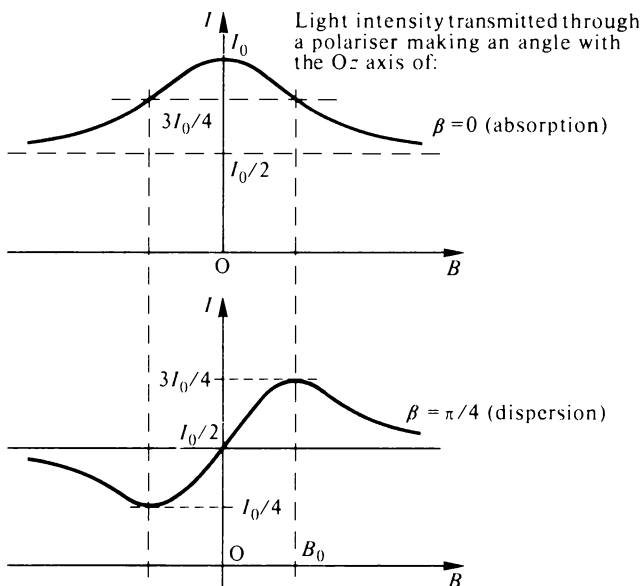
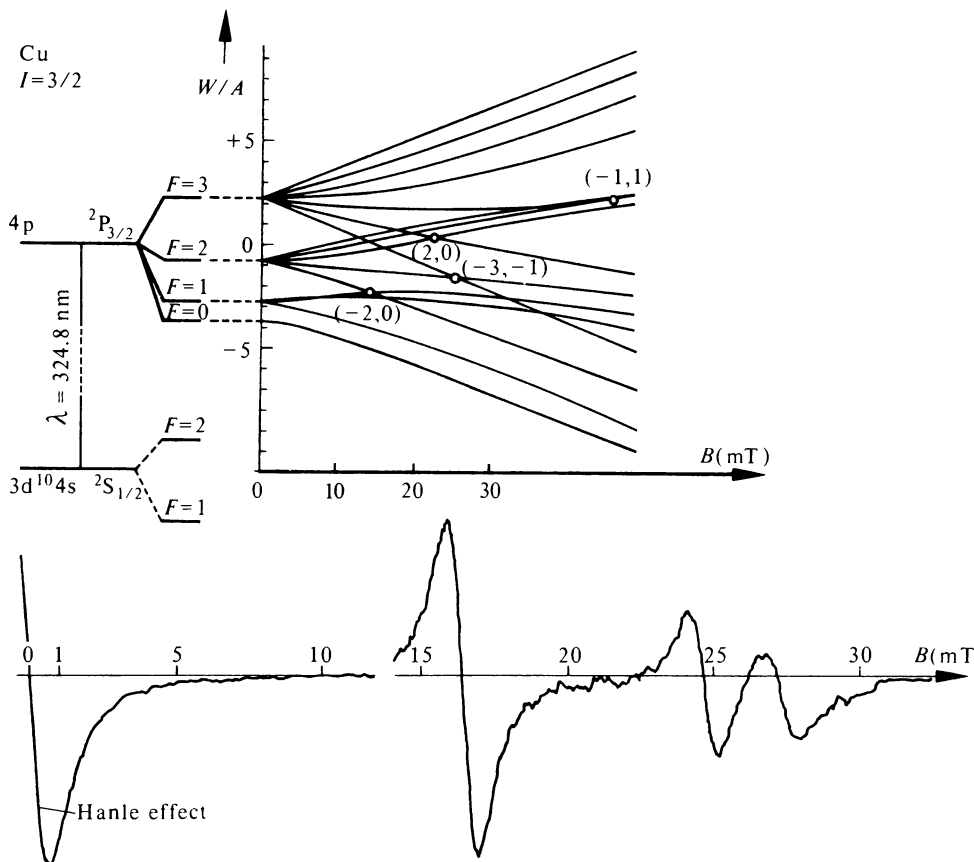


Figure 7.12 Shape of Hanle effect curves

the second term of the bracket, for $\beta = 0$, has a value of $\frac{1}{2}$ (half height of the curve). These values of ω_0 and B_0 correspond to the extrema of I for $\beta = \pi/4$.

(6) *Results.* The study of the Hanle effect and of level crossings has been very productive. Apart from lifetime determinations, many fine or hyperfine structure measurements have been obtained by taking advantage of the resolution offered by the narrow width of the observed curves which is usually of the order of several megahertz; fine or hyperfine structure separations can thus be determined to a much higher degree of accuracy than in interference spectroscopy. Most atomic levels that are accessible by optical excitation have been studied by this technique. For instance, the $2^2P_{3/2} - 2^2P_{1/2}$ fine structure of ${}^6\text{Li}$ has been found to be 10 052.76 MHz, and in figure 7.13 we show the appearance of the experimental curves obtained from experiments



Note: The observation conditions account for the dispersion shape of the curve

Figure 7.13 Level crossings observed in the $2^2P_{3/2} > 2^2S_{1/2}$ transition of copper. The energy levels are shown in the upper half of the diagram

on copper. The excited levels of helium in particular have been studied very extensively, either by stepwise optical excitation from a metastable level (the first level-crossing experiment: Franken, 1959), or by electronic excitation.

The method of magnetic depolarisation, for levels whose Landé factor is known, enables atomic lifetimes to be measured very simply. It should be noted that atomic lifetimes determined in this way are in fact 'coherence times' of the excited state, a concept that we shall discuss later, in section 7.3.4.

7.3 Radiofrequency Spectroscopy

In this section, we bring together experiments involving transitions between levels that are close enough for the frequency of the electromagnetic radiation emitted or absorbed by an atom to fall in a region usually known as the radio-frequency region. The frequency spectrum proves to be very extended and goes from several kilohertz to hundreds of thousands of megahertz; the experimental techniques therefore can be quite varied. Despite the term 'radiofrequency spectroscopy' it is important to note that the observation of some phenomena can take place by measuring a quantity unrelated to a radio-frequency wave: the displacement of an atomic beam, the change of polarisation of a light beam and so on. Some of the transitions which are observed result from an electric dipole mechanism, others from a magnetic dipole mechanism (see section 4.1).

7.3.1 General description of experiments in radiofrequency spectroscopy

(1) *Absence of the Doppler effect.* We can ascertain the main feature of radiofrequency spectroscopy straight away. The ratio v/c , where v is the mean velocity of thermal agitation, is less than 10^{-5} ; the Doppler width will therefore be $\Delta\nu_D \approx (v/c)v_0$ and since $v_0 < 10^{10}$ Hz, $\Delta\nu_D < 10^5$ Hz. It is therefore less than the natural width of an excited level. *The resolution of a radio-frequency spectroscopy experiment carried out on excited states will therefore be limited only by the natural width.*† If the transitions studied are of high frequency, and involve ground levels or long-lived metastables whose natural widths are small, these simple considerations lead to the calculation of a Doppler width greater than the natural width. However, in many experiments, the Doppler effect remains negligible for another reason: the displacement of the atom is confined to a distance less than the wavelength λ of the radio-frequency field.

This condition is realised when the atoms under study form a vapour enclosed by a cell of small dimensions or when this vapour is mixed with a foreign gas at sufficiently high pressure, thereby restricting the mean free path of the atoms. Under these conditions, a random-walk calculation for an atom must be carried out, taking account of the frequent changes of velocity. This was done by Dicke, who showed that the width obtained is much less than the Doppler width calculated by the usual formula.

† This is only a first approximation; a more complete discussion is given for a particular case in section 7.3.4, paragraph (2).

Comment A simple argument based on the elementary explanation of the Doppler effect, allows the Dicke effect to be understood intuitively. The Doppler frequency shift depends on the fact that in a given time interval the observer and the emitter do not count the same number of periods: in figure 7.14 we show the respective positions of an atom A in motion and a stationary observer O at successive times t_1 and t_2 ; the distance AO is $N_1\lambda$ at time t_1 but is only $N_2\lambda$ at time t_2 , and during the time interval $t_2 - t_1$, the observer will have counted $(N_1 - N_2)$ periods more than the atom. Now, if the atom is enclosed within a region of linear dimension less than λ , N_2 remains equal to N_1 whatever the time interval $t_1 - t_2$.

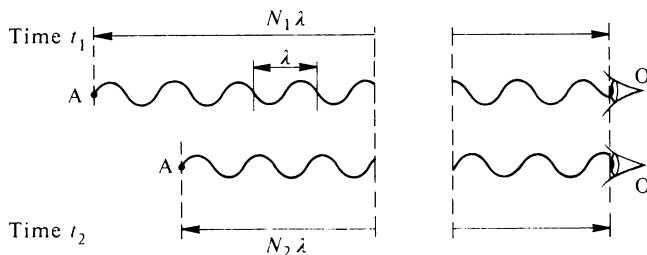


Figure 7.14

To summarise, the resolution in radiofrequency spectroscopy is limited only by the natural width of the level under study, inversely proportional to its lifetime in the wider sense. (For ground levels or metastables, this 'lifetime' is determined not by spontaneous emission, but by non-radiative transitions related to relaxation effects.)

(2) *Spontaneous emission, induced emission and absorption.* In volume 1, chapter 3, the reader was introduced to the concept of a spontaneous emission probability A_{21} , the coefficient of induced emission B_{21} and the coefficient of absorption B_{12} (level 1 is the lower energy level). It was also noted that

$$A_{21}/B_{21} = 8\pi h/\lambda^3$$

From this relationship, an order-of-magnitude calculation shows that spontaneous emission can be disregarded when radiofrequency transitions are studied. Induced emission and absorption are then the main modes of interaction between the radiation and the atomic system.

For simplicity, let us assume that the statistical weights G_1 and G_2 of the two levels are equal; therefore $B_{12} = B_{21}$. By using the notation of volume 1, chapter 3 (n_1 and n_2 are populations and u_ν is the energy density), the number of photons absorbed per unit time is $n_1 B_{12} u_\nu$ and the number of photons emitted is $n_2 B_{21} u_\nu$. The interaction between the atoms and the radiation can be observed only if these two numbers are different

$$n_1 B_{12} \neq n_2 B_{21}$$

that is to say, if $n_1 \neq n_2$.

Let us assume that the excited states have populations described by a thermal equilibrium law at an ambient temperature $T = 300$ K; if E_1 and E_2 represent the energies of states 1 and 2, the Boltzmann law may be written

$$n_2/n_1 = e^{-(E_2-E_1)/kT} = e^{-h\nu_{21}/kT}$$

Since $h\nu_{21}/kT$ is very small, we can write

$$n_2/n_1 \approx 1 - h\nu_{21}/kT$$

and we obtain for various values of ν_{21} and for $T = 300$ K

ν_{21} (Hz)	$n_2/n_1 \approx 1 - h\nu_{21}/kT$
10^3	$1 - 1.6 \times 10^{-10}$
10^6	$1 - 1.6 \times 10^{-7}$
10^9	$1 - 1.6 \times 10^{-4}$

Examination of this table shows us that the ratio n_2/n_1 is very close to unity for thermal equilibrium; the number of photons emitted by induced emission will be nearly equal to the number of photons absorbed.

Experiments on atomic levels are usually carried out on the atoms of an atomic beam or of a gas at low pressure. The number of atoms involved is therefore small (of the order of 10^8 to 10^{12}) and it proves impossible to observe the interaction between the atomic system and the radiofrequency wave with population ratios so close to unity. *A process must therefore be devised whereby the population distribution differs significantly from that obtained in an equilibrium state.* Any radiofrequency spectroscopy experiment carried out in order to study atomic levels will therefore feature a means of selectively populating certain levels.

Comment In the case of radiofrequency spectroscopy experiments carried out on solids or liquids, the number of atoms involved is much greater and it is possible to detect a difference in the rates of induced emission and absorption in thermal equilibrium. This is a special case of magnetic resonance (see volume 1, chapter 10).

(3) *Classification of radiofrequency spectroscopy experiments.* It is difficult to find a logical classification of the various experiments in radiofrequency spectroscopy carried out in the field of atomic physics so as to study them systematically. They can be distinguished by several different criteria:

(a) *By the atomic state investigated.* The state investigated may be the ground state of an atom or, on the other hand, an excited state.

(b) *By the nature of the transition studied.* This can be induced either by the electric field (electric dipole transition) or by the magnetic field (magnetic dipole transition) of the radiofrequency wave used. By confining ourselves to $L-S$ coupling, transitions between levels of different L such that $\Delta L = \pm 1$, are electric dipole transitions. Transitions within the same multiplet and transitions between hyperfine levels for which $\Delta L = 0$, are magnetic dipole transitions.

(c) *By the process that creates the population difference.* Rabi's mechanical method; excitation by polarised light; optical pumping of the ground state; electronic excitation creating a population difference as a result of different excitation cross-sections.

(d) *By the method used for detection.* A change in the number of atoms reaching a given point in the apparatus in the case of an atomic beam; a change of the light intensity or the degree of polarisation of the light emitted or absorbed by the atomic system; a change of radiofrequency amplitude.

We devote the rest of section 7.3 to describing several methods used in radiofrequency spectroscopy of the atom. In none of these do we wish to make an exhaustive study, but only to present experiments that make an important contribution to atomic physics, either due to a particular result or because of the wealth of data obtained. In this book the reader has already met some of the fundamental aspects of these techniques; we shall refer back to them in order to elaborate.

7.3.2 Measurement of the 'Lamb-shift' in the $n = 2$ level of atomic hydrogen

(1) *Principle of the experiment.* As we saw in section 4.3, the energy difference δS between the $2^2S_{\frac{1}{2}}$ and $2^2P_{\frac{1}{2}}$ levels was observed in 1940 by interferometric methods, which indicated that the order of magnitude of the effect was 0.03 cm^{-1} . In 1947 Lamb and Retherford undertook a systematic study of the $n = 2$ level of hydrogen in the presence of a magnetic field that separated the magnetic sublevels. Figure 7.15 shows the energy diagram of these sublevels.

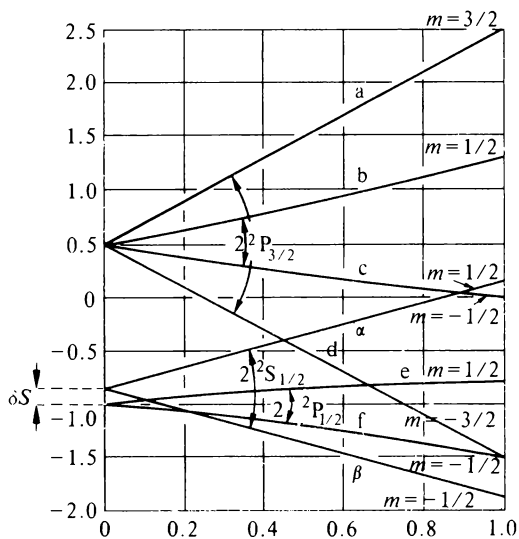


Figure 7.15 Zeeman splitting of the $n = 2$ level of hydrogen (from Lamb and Retherford). *Abscissa:* magnetic field, unity corresponding to 5214 GHz; *ordinate:* energy measured in frequency units, unity corresponding to 7300 MHz

Some properties of the hydrogen atom enable the principle of the Lamb and Retherford experiment to be understood.

- In the case of atomic hydrogen, atoms in the $2P$ state return to the $1S$ ground state by emitting the Lyman α line of wavelength 121.6 nm. The lifetime of the $2P$ state is very short (1.6×10^{-9} s).
- An atom in the $2^2S_{\frac{1}{2}}$ state is metastable and has a lifetime of the order of 10^{-4} s.
- The transitions $2^2P_{\frac{3}{2}} - 2^2S_{\frac{1}{2}}$ and $2^2S_{\frac{1}{2}} - 2^2P_{\frac{1}{2}}$ have an electric dipole character and are easy to induce by a radiofrequency electric field.

With the help of these remarks, the diagram of the experiment given in figure 7.16(a) can be understood.

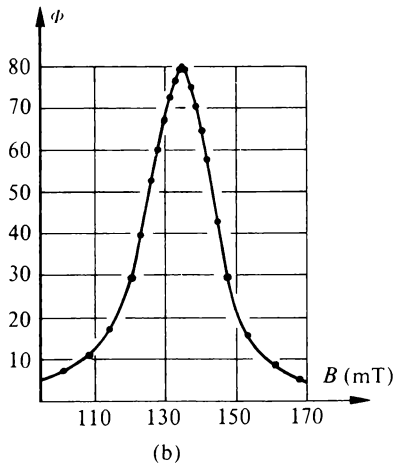
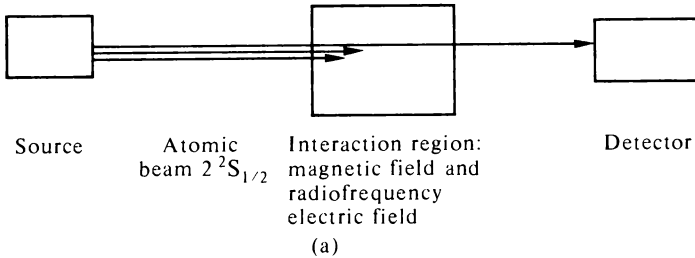


Figure 7.16 The Lamb–Retherford experiment. (a) Schematic diagram of the experiment. (b) Resonance curve observed for hydrogen at 2395 MHz. *Abcissa*: magnetic field (in GHz); *ordinate*: percentage of atoms Φ having undergone a transition (a transition between the levels α and f of figure 7.15)

A beam of hydrogen atoms in the $2^2S_{\frac{1}{2}}$ metastable state may be obtained from a source within a vacuum chamber. This beam passes into an interaction region where it is subjected to a magnetic field and to a radiofrequency electric

field. The beam finally reaches a detector which enables a quantitative measurement of the number of incident $2^2S_{\frac{1}{2}}$ atoms to be obtained.

One operates at a fixed radiofrequency and a variable magnetic field. When the Zeeman splitting corresponds to the frequency of the radiofrequency field, there is a transition from the $2^2S_{\frac{1}{2}}$ state to the $2P$ states, followed immediately by a return to the $1S$ ground state by emission of the Lyman α line. The number of atoms in the $2^2S_{\frac{1}{2}}$ state decreases and there is a drop in signal at the detector. By making use of the Zeeman effect formulae, the shift δS can be deduced from the position of the resonance.

The experiment thus described may seem simple, but it presents many difficulties. The main difficulty is due to the width of the resonance line, which is about 10 millitesla. However, the position of the resonance has been measured to nearly 10 microtesla. This requires extreme care on the part of the experimenter and, above all, a thorough study of the causes of systematic errors that result in shifts or distortions of the resonance curve.

(2) *The apparatus.* We shall give a brief description of Lamb's apparatus.

(a) *Production of the beam of atoms in the $2^2S_{\frac{1}{2}}$ state.* Thermal dissociation of molecular hydrogen produces atomic hydrogen in the $1S$ ground state. At 2770 K, the degree of dissociation is 64 per cent. Bombardment of the atomic beam by electrons allows a small fraction of the beam to reach the excited $2^2S_{\frac{1}{2}}$ metastable state.

(b) *Detection of the beam.* A beam of metastable atoms incident on a metal plate can release electrons. In the case of hydrogen atoms, the phenomenon is quantitative. An anode enables the electrons to be collected and the current is measured by means of an electrometer. Under typical experimental conditions, a current of 3 pA is measured (when the bombardment current that produces the metastable atoms is 200 μ A).

Let I_1 be the anode current when there is no radiofrequency applied, I_2 the current at resonance and I_3 the residual current when no atoms are incident on the detector. Hence, the percentage Φ of atoms having undergone a radiofrequency transition is

$$\Phi = 100 \frac{I_1 - I_2}{I_1 - I_3}$$

(see figure 7.16).

(c) *Interaction region.* The magnetic field is produced by means of an electromagnet, calibrated by nuclear resonance. The radiofrequency is fed in through a waveguide; the frequency is measured by a beats method and is compared indirectly to the 5 MHz frequency standard of a local radio station WWV.

(3) *Results.* Figure 7.16(b) shows one of the transitions observed; the shape of the line has been studied very carefully in order to define its position accurately and several corrections have had to be applied to take account of various effects. In particular, we may mention the Stark effect produced by the electric field $\mathbf{E} = (1/\kappa)\mathbf{v} \times \mathbf{B}$ seen by the atoms moving with velocity \mathbf{v} in

a magnetic field B , and the influence of the hyperfine structure of the 2S and 2P levels, not shown in the diagram of figure 7.15.

From their experiment, Lamb and co-workers† deduced the value

$$\delta S = 1057.77 \pm 0.10 \text{ MHz}$$

very close to the theoretical value deduced from quantum electrodynamics

$$\delta S_{\text{th}} = 1057.56 \pm 0.10 \text{ MHz}$$

Similar experiments have been performed on the same levels of deuterium and of ionised helium.

7.3.3 The hyperfine structure of hydrogen. The hydrogen maser

The hydrogen atom possesses a nuclear spin $I = \frac{1}{2}$ and consequently the structure of the ground state of hydrogen, in the presence of a magnetic field, is of the form shown in figure 7.17. The hydrogen maser developed by Kleppner, Goldenberg and Ramsey (1960) has enabled this hyperfine structure to be measured very accurately. We give a brief description of its principle of operation below (figure 7.18).

A beam of atomic hydrogen in the ground state is obtained by thermal dissociation of molecular hydrogen (see section 7.3.2, paragraph (2)). It is directed along Oz and enters a magnetic selector formed from magnets arranged in such a way that the magnetic field is zero along the Oz axis and increases the further one goes from the axis. The energy of the states $F = 0$ and $F = 1$, $m_F = -1$ is a decreasing function of the magnetic field; hydrogen

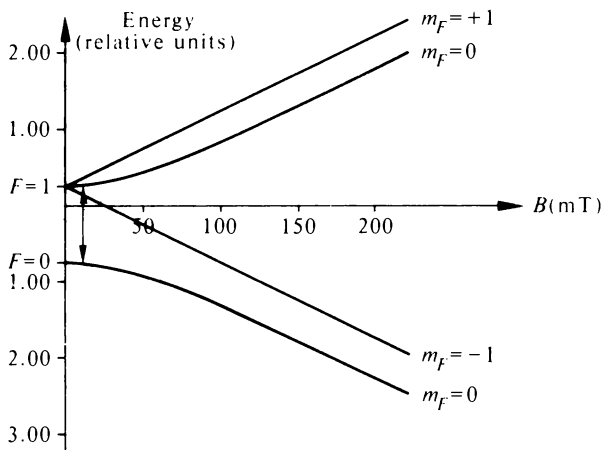


Figure 7.17 Hyperfine structure of the ground level of hydrogen in the presence of a magnetic field

† Lamb, W. E., and Retherford, R. C. (1952). *Phys. Rev.*, **86**, 1014.

Triebwasser, S., Dayhoff, E. S., and Lamb, W. E. (1953). *Phys. Rev.* **89**, 98, 106.

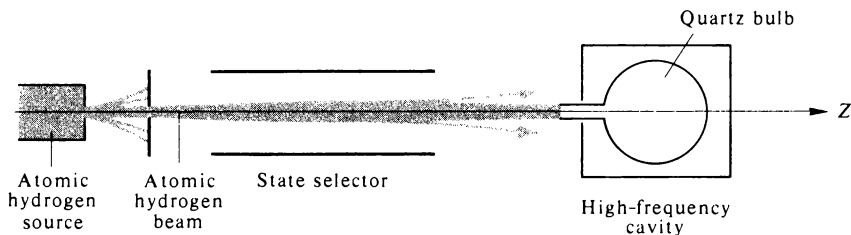


Figure 7.18 Schematic diagram of the hydrogen maser

atoms in these states therefore have a tendency to move away from the axis, the most stable state being that of minimum energy; on the other hand, atoms in the states $F = 1$, $m_F = 0$ and $m_F = 1$ will be focused towards the axis of the selector. Therefore at the exit from the selector we see that the atomic beam on the Oz axis is enriched with atoms in the $F = 1$ state. The beam then leaves the magnetic field region and enters a quartz bulb placed within a resonant cavity tuned to the frequency of the hyperfine splitting and situated in a region where the magnetic field is zero. Within the cavity the number of atoms n_2 in the $F = 1$ state is greater than the number n_1 in the $F = 0$ state; the conditions for maser oscillation are therefore satisfied. With achievable beam intensities, the power resulting from the oscillation is very low, of the order of a picowatt. The frequency stability is remarkable; by comparing the frequency with the frequency of a caesium atomic clock used as a time standard, an extremely accurate value of the hyperfine structure

$$\delta\nu_{\text{H}} = 1\,420\,405\,751.786 \pm 0.028 \text{ Hz}$$

is obtained. Similar measurements have been carried out on deuterium and tritium.

7.3.4 The spectroscopy of excited states by magnetic resonance and optical detection

(1) *Principle of the experiment.* In volume 1, section 11.4, Brossel's magnetic resonance experiment on the 6^3P_1 level of mercury was described. The reader should recall the main features of the experiment:

- selective optical excitation of the Zeeman sublevels of the 6^3P_1 level by means of polarised light at a wavelength of 253.7 nm from the transition $6^3\text{P}_1 \rightarrow 6^1\text{S}_0$;
- a transition between the Zeeman sublevels (a magnetic dipole transition) under the influence of a radiofrequency magnetic field of amplitude B_1 ;
- detection of the resonance by observation of the degree of polarisation of the emitted light: the resonance changes the populations of the Zeeman sublevels and, as a result, the polarisation state of the emitted light.

(2) *Application of the experiments.* In the simple case that has been described, the influence of the magnetic field may be described in terms of the Zeeman levels in a weak field (the experiment is carried out on an even isotope of zero nuclear spin, so there is no hyperfine structure; the fine structure separations $6^3P_2 - 6^3P_1 - 6^3P_0$ are very large—see figure 4.7). The position of the resonance line leads to the Landé factor: the excellent signal-to-noise ratio allows the line to be plotted accurately and the Landé factor can be determined with a relative precision of the order of 10^{-4} . Such a measurement proves to be a useful test of theoretical atomic structure calculations.

The shape of the resonance line is a rather complicated function of the amplitude B_1 of the radiofrequency field and of the lifetime τ of the level. If the value of B_1 is gradually reduced to zero in a series of experiments, the curves obtained have a decreasing amplitude (see volume 1, figure 11.10), but their width at half height tends towards a limiting width which depends only on the lifetime τ of the level

$$\Delta B = |\gamma| \Delta\omega = |\gamma| \frac{2}{\tau} = g \frac{e}{2m\kappa} \frac{2}{\tau}$$

(see steady-state solution of the Bloch equations, volume 1, section 9.5.3).

If the number of atoms in the cell is very small, corresponding to pressures less than 10^{-4} mm of mercury, the time τ is effectively the radiative lifetime of the level. At higher pressures, collisions take place during which the excited atoms lose their excitation energy. Their lifetime decreases, and the curves *broaden*.

Comment The preceding paragraph is valid in general. However, in Brossel's actual experiment, carried out on a resonance level by optical absorption, the situation is more complex. There is competition between the collision processes, which de-excite the atoms and thus reduce their lifetime, and the process of 'multiple scattering' which acts overall to lengthen the lifetime. Let us explain the latter process: when an atom (1) in the 6^3P_1 state is de-excited, it undergoes the transition $6^3P_1 \rightarrow 6^1S_0$ and emits a photon which can be absorbed by a neighbouring atom (2) in the ground state; this reabsorption of the photon becomes more probable as the pressure is raised. A theoretical study of this phenomenon shows that the description of excited atom (2) in terms of its wave function cannot distinguish it from excited atom (1); for the whole vapour, we see therefore that this process leads to an increase in the apparent lifetime of the 6^3P_1 state. This is a collective phenomenon; one speaks of the 'coherence time' of the 6^3P_1 level, reserving the term lifetime for phenomena related to the de-excitation of an isolated atom. It is this 'coherence time' that in fact is involved in the expression for the line width.

This process of lengthening the coherence time involves the phase properties of the wave functions. It should not be confused with another aspect of multiple scattering that we have met already: the imprisonment time of resonance radiation (see volume 1, section 3.2.2, comment). The coherence time cannot be greater than twice the radiative lifetime, whereas the imprisonment time can be tens or hundreds of times longer.

(3) *Generalisation of the method and its limitations.*

(a) The use of optical excitation with polarised light allows only levels directly connected to the ground level by an allowed transition, usually called

'resonance levels', to be reached. In addition, the transitions necessary for excitation should be in a spectral region that is easily accessible experimentally. (The resonance levels of the rare gases, for instance, decay to the ground level by emitting radiation ≈ 50 nm in the far ultraviolet region.) The element studied should be sufficiently volatile to form either a vapour or an atomic beam. Some of the levels that have been studied are the resonance levels of the various isotopes of mercury, zinc, cadmium, sodium and potassium.

While retaining the same method of detection, a population difference between the Zeeman sublevels can be created through excitation by a beam of slow electrons having a well-defined direction. This direction defines an anisotropy in the excitation, manifested by population differences in the Zeeman sublevels. The use of excitation by electrons of energy between 10 and 50 eV has permitted an extension of Brossel's resonance method to many excited levels that cannot be reached by optical excitation.

(b) The interaction time between the atom and the radiofrequency field is determined by the lifetime of the excited state. This implies that the shorter the lifetime τ , the greater must be the amplitude of this field (see volume 1, section 9.5.3). When $\tau < 10^{-8}$ s, the amplitude of the radiofrequency field B_1 , necessary to produce magnetic resonance is of the order of a millitesla, which requires a power of several tens of watts in the circuit producing B_1 ; in addition to various technical difficulties, undesirable discharges appear in the vapour under study, produced by these strong alternating fields. The method is therefore not easily applicable to levels of short lifetime.

(c) When the level under study has hyperfine structure, the experiment is usually carried out in conditions of intermediate field; the sublevels then have a complicated pattern and for a given value of the field the separations between consecutive Zeeman sublevels are no longer identical. The observed phenomena are complex; apart from the various $\delta F = 0$ transitions, some $\delta F = 1$ transitions can be detected. Analysis of the results, taking account of the Zeeman diagram in intermediate field, enables values of the hyperfine structures to be obtained, from which the value of the nuclear magnetic moment of the atom under study can be deduced.

To summarise, the method of magnetic resonance applied to excited levels has contributed a considerable amount of spectroscopic data. It has also led to several new investigations in fundamental physics: atom-radiation interactions and the study by means of line widths of collision phenomena involving excited atoms, for example.

7.3.5 Study of the ground level in an atomic beam by Rabi's method

This experiment was discussed in volume 1, section 10.5 and a diagram of the apparatus given in volume 1, figure 10.7. The population difference is obtained by means of an inhomogeneous static field B_1 which allows only atoms of a given quantum number $|m\rangle$ to reach the region of interaction with a radiofrequency field situated in the airgap of magnet (2). Magnet (3) provides an inhomogeneous field B_3 which permits only atoms having a particular value of $|m\rangle$ to reach the detector.

The Rabi method can be applied easily only to atoms in the ground state or in a metastable state because, owing to the velocity of the atomic beam, an excited atom of lifetime 10^{-7} s will travel only a fraction of a millimetre. The main use of the Rabi method is to measure hyperfine structures of ground states in order to obtain nuclear moments. For discussion of its field of application, it is convenient to amplify some of the points made in volume 1, chapter 10.

(1) The existence of hyperfine structure complicates the Zeeman diagram, and the paths of atoms of different m_F in magnets (1) and (3) must be studied by using the concept of an effective magnetic moment, as defined in section 6.7.

(2) The radiofrequency magnetic field can induce a large number of magnetic dipole transitions, as illustrated in figure 7.19 for a level with $J = \frac{1}{2}$, $I = \frac{1}{2}$:

- in a weak field, one can observe either the transitions $\delta F = 0$, $\delta m_F = \pm 1$ ('low-frequency' transitions) or $\delta F = \pm 1$, $\delta m_F = 0, \pm 1$ ('high-frequency' transitions);
- in a strong field, one can observe either the 'low-frequency' transitions $\delta m_J = 0$, $\delta m_I = \pm 1$, or the 'high-frequency' transitions $\delta m_J = \pm 1$, $\delta m_I = 0$;
- in an intermediate field, we can only provide a continuity argument: the transitions that have a large probability are those corresponding to an allowed transition between two given levels in both weak and strong fields; these are shown in figure 7.19.

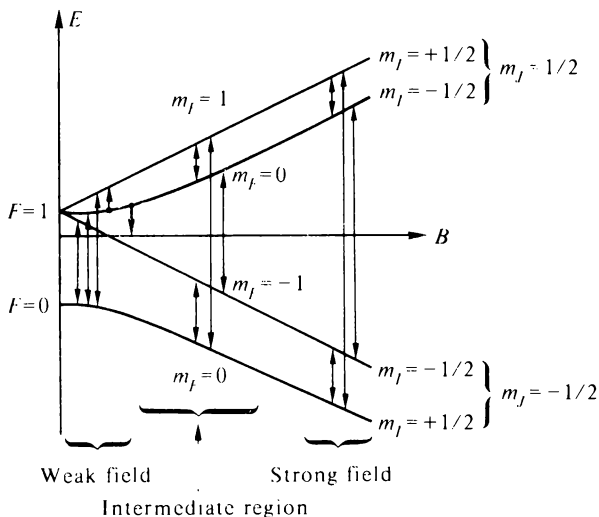


Figure 7.19 High-frequency and low-frequency allowed transitions for the case $J = \frac{1}{2}$, $I = \frac{1}{2}$

From measurements carried out on the magnetic resonance lines corresponding to these transitions, hyperfine structure separations can be calculated (for instance by using the Breit–Rabi formula, see section 6.7).

(3) The width of the resonance lines is inversely proportional to the transit time t of an atom in the region where it is subjected simultaneously to the radiofrequency magnetic field and to the static field B_2 . To obtain the greatest possible accuracy in hyperfine structure determinations, the resonance lines should be narrow and consequently the transit time t should be long. As the velocity of the atomic beam is not easily adjustable, the interaction region (2) between the atom and the radiofrequency field must be made as long as possible. This is clearly very difficult if the necessary conditions of homogeneity of the fields are to be maintained. A clever device to overcome this problem was proposed by Ramsey (figure 7.20): after passing through the inhomogeneous field B_1 , the atoms enter a region of length L in which a homogeneous magnetic field B_2 exists; towards each end of this region, the atom is subjected to a radiofrequency field over a distance l . The line then has a complicated shape (figure 7.21); the width of the envelope, drawn in dotted lines, may be inferred from the time $t = l/v$, where v is the average speed of the atoms, whereas the width of the central peak is related to the time $T = L/v$. The position of the central peak can then be determined with great accuracy.

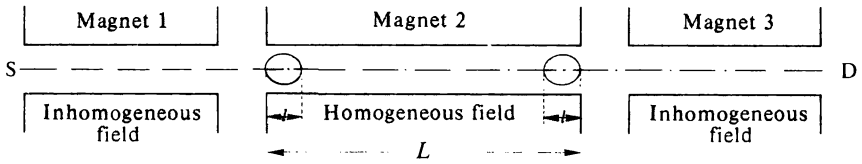


Figure 7.20 Similar to volume 1, figure 10.7. Ramsey’s arrangement: the radiofrequency field is applied in the two shaded regions each of length l

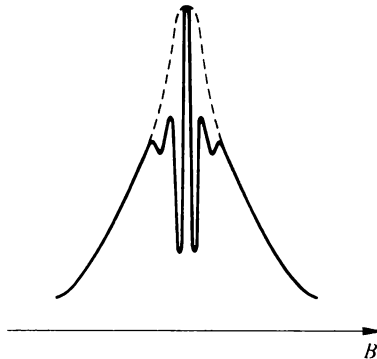


Figure 7.21 Theoretical shape of a resonance line obtained with a Ramsey arrangement (figure 7.20)

(4) Rabi's method has been widely used; most elements, both stable and radioactive, have been studied. For example, experiments have been carried out on the isotope sodium 21 with a radioactive lifetime of 23 s, and on several transuranium atoms. Figure 7.22 shows part of a table of hyperfine structures measured by the Rabi technique. The Rabi method has also been used to construct frequency standards which are then used as time standards (see section 6.2.2).

Isotope	I	Atomic state	J	F	$\Delta\nu_{F,F-1}$ (MHz)
^{87}Rb	$\frac{3}{2}$	^2S	$\frac{1}{2}$	2	6834·682614 (1)
^{89}Y	$\frac{3}{2}$	^2D	$\frac{3}{2}$	3	88·63 (60)
				2	114·72 (20)
^{90}Y	2	^2D	$\frac{3}{2}$	3	403·719 (37)
				2	293·203 (22)
				1	198·287 (24)
				0	114·515 (19)
				$\frac{1}{2}$	613·023 (34)
^{91}Y	$\frac{3}{2}$	^2D	$\frac{3}{2}$	3	410·871 (24)
				2	235·722 (26)
				1	103·0

Figure 7.22 Part of a table giving the hyperfine splitting $\Delta\nu_{F,F-1}$ between a level F and a level $F-1$ of the ground level. (In the last column, the estimated errors in the last significant figures are given in brackets.)

7.3.6 Study of the ground state by optical pumping

Optical pumping was described in volume 1, section 11.5. It enables a population difference to be created between the ground state Zeeman sublevels of an assembly of atoms, thereby permitting magnetic resonance experiments to be performed; detection of the magnetic resonance is carried out by optical analysis of this atomic vapour. In volume 1, chapter 11 a simplified scheme was used as a basis of explanation; in the case of alkali atoms, two neighbouring resonance lines, D_1 and D_2 , exist (see figure 5.8) and furthermore, the ground level has hyperfine structure due to the nuclear spin, which in volume 1, chapter 11, was deliberately overlooked, since at that stage the reader had not met this concept. The description of the pumping cycle is therefore, in general, rather complicated, but the fundamental ideas remain the same.

We shall describe below some physical aspects of the techniques that have been developed from the method of orientation of the ground level by optical pumping.

(1) *The width of a resonance curve.* We have seen several times that the width of a resonance is inversely proportional to the lifetime of an atom in the state under consideration. At first sight, by generalising the ideas developed in section 7.3.4 with regard to excited states, then, since the lifetime of a

ground state is infinite, the resonance curves should be infinitesimally narrow. However, what is important here is the lifetime of the sublevels involved in the experiment, that is to say the relaxation time which was studied in volume 1, chapter 9; the width of the resonance is therefore related to the relaxation time. Several relaxation effects can occur as discussed below.

(a) The experimental procedure itself, the pumping light preferentially emptying one of the sublevels, brings about relaxation of an atom—that is to say a limit to its lifetime. The greater the intensity of the pumping light, the shorter will be the relaxation time of an atom.

(b) The vapour has to be contained in a cell, and atoms will be disoriented on collision with the walls; after a collision, the direction of the magnetic moment of an atom will in general have changed. Early experiments showed that the line widths observed corresponded to a lifetime equal to the mean time of flight of an atom between one wall and another, this time of flight being of the order of 10^{-4} s. However, certain atoms, whose ground state is spherically symmetric, do not have an electronic magnetic moment, so their magnetic moment is of purely nuclear origin. Nuclear magnetic moments interact only weakly with the walls and they have only a small probability of being disoriented by collisions with the walls of the cell. Mercury is a particular example, for which very narrow resonance lines can be obtained (0.01 Hz in frequency units). In the case of an alkali atom, whose ground level is not spherically symmetric and which possesses electronic spin, two techniques have enabled very narrow resonance lines to be observed as follows.

(i) Certain coatings on the walls of the cell (paraffins, silicones) enable an atom to undergo collisions without being disoriented.

(ii) The introduction of a foreign gas within the cell allows the time of flight between the walls to be increased, and experiment has shown that the rate of orientation (see volume 1, chapter 11) increases correspondingly, as long as collisions with atoms of this foreign gas do not cause disorientation. A study of the influence of various gases has enabled optimum conditions for obtaining narrow lines to be defined. However, it should be pointed out that as the pressure of the foreign gas (usually called the buffer gas) increases, collisions between the excited atoms and the gas may become evident; these collisions equalise the populations of the Zeeman sublevels of the excited state and the pumping process becomes inefficient. To avoid this difficulty, Dehmelt devised a different optical pumping process for the alkali atoms: the irradiation of the vapour by circularly polarised light whose D_1 and D_2 lines have different intensities.

Comment Here a fundamental difference may be seen between an experiment of the Rabi type and an optical pumping experiment. In the Rabi experiment the atoms are isolated and the relaxation time is therefore infinite; it is the time of flight of an atom through the apparatus that limits the interaction time between the atom and the radiofrequency field.

(2) *Multiple quantum transitions in magnetic resonance.* When electromagnetic waves of high intensity are used, it can happen that an atom makes

a transition between two energy states E_1 and E_2 by absorbing several photons simultaneously.

These multiple quantum transitions are possible if they conserve energy. For example

$$E_2 - E_1 = h\nu_1 + h\nu_2$$

for two waves of different frequencies.

$$E_2 - E_1 = 2h\nu, 3h\nu, 4h\nu, \text{ etc.}$$

for a single wave.

These transitions, however, must also be able to conserve angular momentum, and they provide confirmation of the concept of angular momentum of a photon (see volume 1, chapter 11).

These multiple quantum transitions between two nearby Zeeman sublevels may be observed by magnetic resonance. With a wave of fixed frequency ν , they are produced in a magnetic field B two or three times greater than the normal transition, such that $h\nu = g\beta(B/2)$ or $g\beta(B/3)$ and so on. These transitions do not, however, occur under all conditions.

(a) If the wave is circularly polarised, these n quanta transitions cannot occur because an atom cannot absorb an angular momentum $n\hbar$ corresponding to n photons.

(b) If an oscillating field $2B_1 \cos \omega t$ is produced perpendicular to the constant field B_0 (see volume 1, section 9.5.4), it is equivalent to the sum of two fields rotating in opposite senses, that is two waves of polarisation σ^+ and σ^- ; the atom can then absorb simultaneously p σ^- -photons of angular momentum $-\hbar$ and $p + 1$ σ^+ -photons of angular momentum $+\hbar$, since the $2p + 1$ photons together contribute the necessary angular momentum. Thus only transitions with an odd number of photons are possible.

(c) If one adds an oscillating field parallel to the constant field B_0 , that is to say photons of zero angular momentum, transitions with an even number of photons become possible (the experiments of J. Winter in 1955).

Comment These transitions are not easily observable in excited states because their lifetimes are too short, and because radiofrequency fields of sufficient amplitude cannot be produced.

(3) *Detection by modulation of the absorption.* During magnetic resonance, a transverse magnetisation M_\perp is present in the vapour; this magnetisation precesses around the Oz direction of the magnetic field B_0 (figure 7.23). The M_x component of this magnetisation is therefore a sinusoidal function of time, of frequency $\omega_0 = B_0/\gamma$. Moreover, the absorption properties of a beam of light polarised by an atom are related to the direction of its magnetic moment. (In section 7.2, we used a similar property, in the case of emission, in the study of the Hanle effect.) If, therefore, besides the pumping beam (1), a second beam (2) of the same resonance wavelength is passed through the cell in the Ox direction (figure 7.23), an absorption of this beam as a function of the value of M_x is observed. After passing through the cell containing the vapour, the beam (2) will be partially modulated at the frequency ω_0 . After

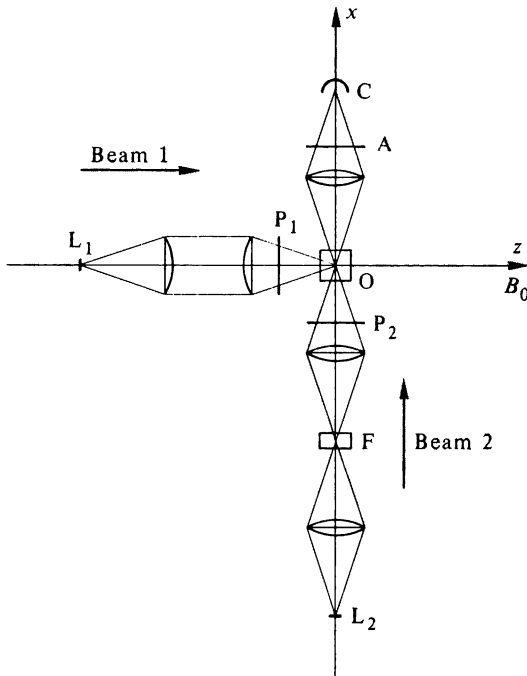


Figure 7.23 Schematic diagram of Dehmelt's crossed-beam method. Beam 1 = circularly polarised pumping beam. Beam 2 = detection beam whose intensity is modulated by the magnetic resonance. P_1 and P_2 are polarisers, F is a filter, A is an analyser and C is a photodetector

being received by a photodetector, this modulation may be amplified and displayed. This technique, introduced by Dehmelt, and known as the crossed-beam technique, has proved to be very useful in the analysis of magnetic-resonance phenomena.

(4) *Applications of optical pumping.* There are many of these, and for the most part they are related to the width of the observed lines.

(a) *Spectroscopic applications.* As in Rabi's method, hyperfine structure and nuclear magnetic moment measurements have been detected from the shape of the resonance curves. We may mention in particular:

(i) the nuclear magnetic moment measurements of

^{23}Na , ^{39}K , ^{40}K , ^{41}K , ^{65}Zn , ^{67}Zn , ^{85}Rb , ^{87}Rb , ^{107}Cd , ^{109}Cd ,
 ^{111}Cd , ^{115}Cd , ^{133}Cs , ^{134}Cs , ^{135}Cs , ^{193}Hg , ^{195}Hg , ^{197}Hg , ^{199}Hg ,
 ^{201}Hg

by an optical pumping method similar to that described above.

(ii) the use of exchange methods of orientation (described for electrons in volume 1, section 12.3): it has been possible to orient various atoms in their

ground state by collisions with alkali atoms oriented by pumping—for example, we may mention the experiments on the ground level of nitrogen;

(iii) the ground level of the isotope ^3He can be oriented by transfer of orientation produced in the 2^3S_1 metastable level by a pumping cycle involving the $2^3\text{P} - 2^3\text{S}_1$ ($1.083 \mu\text{m}$) transition.

(b) *Fundamental physics.* In the realm of fundamental physics, it has been possible to study many effects related to interactions between atoms and radiation, and it has been shown that the illumination of an atomic system can produce very small shifts of the energy levels; these have been observed thanks to the narrowness of the resonance curves (Cohen–Tannoudji, 1962).

(c) *Application to magnetometers and to frequency standards.* In the weak field Zeeman effect, the resonance frequency is proportional to the value of the field. This property has led to the construction of magnetometers for the measurement of low fields. Some of these instruments use a low frequency resonance $\delta F = 0$, $\delta m_F = \pm 1$ in one of the hyperfine sublevels of the caesium atom. Dehmelt's pumping technique is used, detection being carried out by the method of crossed beams described in paragraph (3). A rather complicated electronic arrangement adjusts the frequency of the transmitter so that resonance conditions remain satisfied during changes of the magnetic field. By measurement of the frequency, this servo-mechanism allows the resonance line to be plotted very accurately. The resonance frequency in the earth's field is of the order of 150 kHz, and the apparatus remains sensitive in a magnetic field of the order of 10^{-11} tesla.

The transitions $\delta F = 1$, $m_F = 0 \rightarrow m_F = 0$ have a frequency practically independent of magnetic field. In the cases of ^{133}Cs , ^{85}Rb and ^{87}Rb they have formed the basis of frequency standards. Two principles are used: the first consists in the construction of a servo-system similar to that described for the magnetometer, which regulates the frequency of a transmitter so that the resonance retains a maximum amplitude; the second amounts to producing a population difference within a cavity, sufficient to generate maser oscillation as in the case of the hydrogen maser (see section 7.3.3).

7.3.7 Conclusion

This brief review illustrates the wealth of spectroscopic radiofrequency experiments; they have made important contributions to the development of theoretical physics where increasingly accurate measurements are required for the interpretation of subtle effects. In addition, they have given rise to applied research problems: magnetometers, and time standards.

7.4 Lifetimes and Oscillator Strengths

The concepts of lifetime and of absorption and emission probabilities were studied in volume 1, chapter 3. In this section, we shall refine these ideas and give an account of various experimental methods.

In chapters 1 to 5, we described an atom in terms of energy levels, and in

previous sections we showed how modern experimental methods have enabled extremely accurate data to be obtained in this area. However, we have not studied the intensity of the emitted spectrum at all, nor considered the populations of the various excited levels. This information, however, expressed in the concepts of lifetime and of oscillator strength, is required in various areas of physics whenever an accurate quantitative analysis of an excited or ionised medium must be undertaken: a gas laser operates only if a 'population inversion' exists between certain excited levels (see volume 1, section 4.3), and the populations of the levels result from competition between processes creating excited states that involve 'excitation cross-sections' (to be studied in section 7.5) and decay processes that involve, in particular, the radiative lifetime of the levels. Astrophysicists obtain information about stellar and interstellar media by studying in particular the intensity of emitted lines; the values of oscillator strengths and of atomic lifetimes therefore will also be fundamental parameters for describing these media.

7.4.1 Definition of oscillator strengths and of lifetimes

In appendix 2 we review the classical results for the absorption of an electromagnetic wave of frequency ν by an assembly of N dipoles per unit volume (formed from elastically bound electrons of natural frequency ν_0). The absorption of the incident wave of intensity I_0 is described by a coefficient K such that after travelling a distance z , the intensity is given by

$$I = I_0 e^{-Kz} \quad (7.1)$$

The absorption coefficient K was calculated in the approximation where the absorption band is narrow enough to be able to write $|\omega - \omega_0| \ll \omega$. It is proportional to the number of dipoles N contained in a unit volume.

For a classical description of the absorption of an electromagnetic wave by a medium containing n atoms per unit volume, these atoms having an absorption frequency ν_0 , we assume that each atom is equivalent to f classical oscillators; f is then called the oscillator strength. Thus $N = nf$, and therefore we write the absorption coefficient

$$K(\nu) = f \frac{ne^2}{16\pi^2 m\epsilon_0 c} \left(\frac{\gamma}{(\nu_0 - \nu)^2 + (\gamma/4\pi)^2} \right) \quad (7.2)$$

(γ is a damping coefficient, see appendix 2).

If the incident wave has a continuous frequency spectrum, the total absorption is found to be (see appendix 2)

$$\mathcal{A} = \int_0^\infty K(\nu) d\nu = f \frac{ne^2}{4m\epsilon_0 c} \quad (7.3)$$

The total absorption \mathcal{A} therefore depends only on n and on the value of f ; in particular it does not involve the value of the damping coefficient γ . This has an extremely important practical application because the absorption of a continuous spectrum will permit the oscillator strength to be measured independently of any other parameter.

If the incident wave is suddenly cut off, the electrons will continue to oscillate with an amplitude which decreases owing to damping effects. Classical theory shows us that the emitted intensity can be written

$$I(t) = I_0 e^{-t/\tau}$$

where $\tau = 1/\gamma$. The parameter τ is called the lifetime.

The classical picture provides only a very elementary model; it takes account of the many possible transitions between various excited states only with difficulty, and does not express the quantum nature of the phenomena. In quantum theory, if there are n_i stationary atoms per unit volume in the state i able to absorb the radiation ν_{ij} (thereby passing into the energy level $E_j > E_i$), the shape of the absorption line is given by the Weisskopf relation, similar to the relationship (7.2)

$$K_{ij}(\nu) = \frac{n_i e^2}{16\pi^2 m \epsilon_0 c} f_{ij} \frac{\Gamma_j}{(\nu - \nu_{ij})^2 + (\Gamma_j/4\pi)^2} \quad (7.4)$$

f_{ij} represents the oscillator strength associated with absorption of the transition ν_{ij} ; it is no longer an integer and is less than unity: Γ_j is the damping coefficient. These two parameters are related to the Einstein coefficients A_{ji} , B_{ji} and B_{ij} defined in volume 1, chapter 3.

(1) To a good approximation the coefficient Γ_j can be taken as equal to

$$\Gamma_j = \sum_k A_{jk}$$

the summation over k being carried out over all levels of energy less than that of level j . Comparison between the expression (7.4) and the classical expression (7.2) indicates that with the lifetime of level j is given by

$$\tau_j = \frac{1}{\Gamma_j} = \frac{1}{\sum_k A_{jk}} \quad (7.5)$$

(2) The relationship (7.3) for the total absorption by n atoms, is always valid. It allows the oscillator strength to be related to the Einstein coefficients. Let us assume that the radiation incident on the assembly of atoms has a continuous spectrum whose differential energy density u_ν is constant over the whole region where $K_{ij}(\nu)$ is different from zero. There are n_i atoms per unit volume in the state i under consideration. From equation (7.3), we have

$$\mathcal{A} = \int_0^\infty K_{ij}(\nu) d\nu = \frac{e^2}{4m\epsilon_0 c} n_i f_{ij} \quad (7.6)$$

By using the relationship established in volume 1, section 3.1.4

$$B_{ij} = \frac{\lambda_{ij}}{h} \frac{1}{n_i} \int K_{ij}(\nu) d\nu$$

and by taking the value of the integral given by equation (7.6), we have

$$B_{ij} = \frac{e^2}{4\epsilon_0 mc} \frac{\lambda_{ij}}{h} f_{ij} = \frac{e^2}{4\epsilon_0 mh\nu_{ij}} f_{ij} \quad (7.7)$$

(3) By making use of the relations expressing B_{ij} as a function of A_{ji} (see volume 1, section 3.3), we can also relate the oscillator strength f_{ij} to the spontaneous transition probability A_{ji} . Let us denote the order of degeneracy $G = 2J + 1$ of the levels i and j by G_i and G_j respectively. (Remember that in this section the level j is the higher energy level, and the level i has the lower energy.) We have

$$A_{ji} = \frac{8\pi h}{\lambda_{ij}^3} B_{ji} = \frac{8\pi h}{c^3} \nu_{ij}^3 B_{ji} = \frac{8\pi h \nu_{ij}^3}{c^3} \frac{G_i}{G_j} B_{ij}$$

and hence from equation (7.7)

$$A_{ji} = \frac{2\pi e^2 \nu_{ij}^2}{\epsilon_0 mc^3} \frac{G_i}{G_j} f_{ij} \quad (7.8)$$

From the definitions and properties given above, the reader will note that the lifetime is a parameter characterising a given atomic level, whereas the oscillator strength characterises a transition between two levels. These two concepts are very similar however; if only two levels i and j were involved, τ would be proportional to $1/f$, from equations (7.5) and (7.8).

The quantum theory of radiation allows lifetimes and oscillator strengths to be evaluated from wave functions. Rigorous calculations are possible only in the case of the hydrogen atom and usually, therefore, theoretical determinations will require approximations and numerical solution. Consequently, experimental study is of considerable interest; apart from the fact that it can give important numerical results, it allows parameters to be obtained whose theoretical evaluation is difficult. When comparison between theory and experiment is possible, the latter can provide useful tests of suggested approximate wave functions.

Comment I The oscillator strength $f = f_{ij}$ which we have defined, relates to absorption; some authors use $f = f_{ji}$, an oscillator strength relating to emission, such that

$$f_{ji} = f_{ij} \frac{G_i}{G_j}$$

Care should therefore be taken when reading articles dealing with oscillator strengths.

Comment II When only two levels i and j are involved (this can be the case if j is one of the first excited states), the expression (7.8) gives us the inverse of the lifetime of the level j directly: $1/\tau = A_{ji}$. This may be compared with the expression calculated classically (see appendix 2)

$$\gamma = \frac{1}{\tau} = \frac{2\pi e^2 \nu_0^2}{3\epsilon_0 mc^3}$$

One converts from one to the other by replacing $(G_i/G_j) f_{ij}$ by $\frac{1}{3}$.

7.4.2 Experimental study of atomic lifetimes

(1) *Study as a function of time of the decrease of the intensity of a transition originating from a level B, after cutting off the excitation.* This is the simplest and most general method of studying the lifetime of this level B. Some aspects of this method were discussed in volume 1, chapter 3, and although the method is very attractive at first sight, two types of difficulty arise as follows.

- (a) The lifetimes of excited atomic levels are of the order of 10^{-7} to 10^{-9} s; study of the decrease of the emitted light intensity is difficult and requires the use of fast electronic techniques.
- (b) Cascade effects make the interpretation difficult. Suppose the transition $B \rightarrow A$ (figure 7.24) is observed, originating from level B. A higher level C, with a lifetime longer than that of B, can produce atoms in the state B through the transition $C \rightarrow B$. Level B, after the cut-off of excitation, will therefore be fed throughout the lifetime of level C, and the profile of the decreasing light intensity will be a function of the lifetimes of both levels B and C.

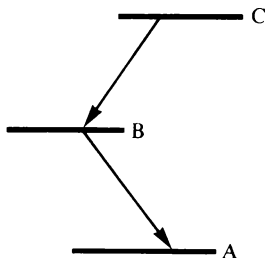


Figure 7.24 Cascading

However, the use of advanced techniques and a systematic analysis of the results enable satisfactory data to be obtained for a large number of atoms. An experiment involving this principle is illustrated in figure 7.25. The measurement cell is filled with the atomic vapour under study, at a pressure of the order of 100 torr, and a voltage pulse with a fast time rise produces excitation by electron bombardment. This starts the time sweep of a multi-channel analyser, whose channels are activated in succession; channel n of this analyser is opened between the times $n\theta$ and $(n+1)\theta$, θ being a time interval short compared with the lifetime τ . This channel receives pulses produced by the photoelectrons during this interval; their number N is proportional to the light intensity at the time $t = n\theta$. Figure 7.26 shows the results obtained (the number of pulses received in each channel) for a transition in argon. One notes first an increase of light intensity after the cut-off of the discharge, due to other modes of excitation, then a decrease which cannot be reconciled with one exponential decay since this would show as a straight-line graph on a logarithmic scale. A complex analysis, bearing in mind the

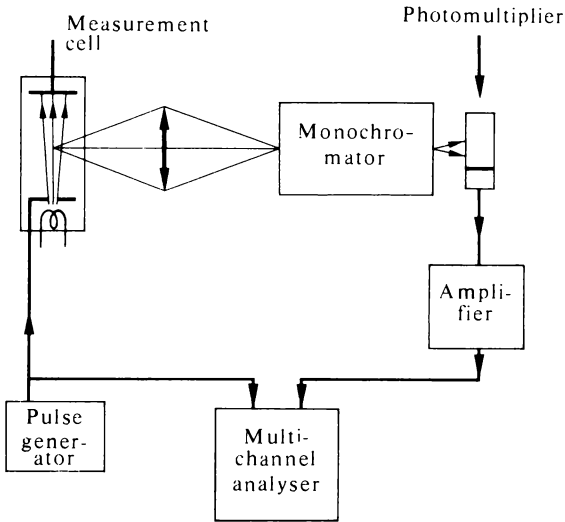


Figure 7.25 An apparatus for measuring lifetimes of excited states

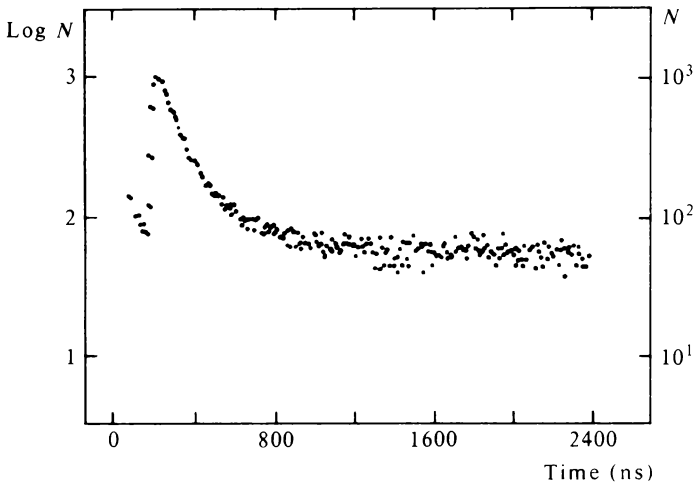
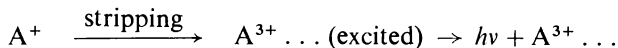


Figure 7.26 Decrease of intensity of the 451.1 nm transition of argon

observation of a large number of transitions, results in attributing a lifetime of 95 ± 2 ns to the upper level of the transition.

(2) *Beam-foil spectroscopy*. This recently developed technique is based on a principle very similar to that of experiments involving instantaneous excitation of an atomic beam (see volume 1, figure 3.7). It has enabled the lifetimes of many excited states of ions to be determined. The apparatus is illustrated

in figure 7.27. A beam of ions, accelerated by a potential difference of 10^5 to about 10^6 volts, passes through a target formed from a very thin carbon foil, whose thickness is of the order of a micrometre. The drop in velocity caused by this foil is only a few per cent, but because of 'stripping' reactions (see section 7.5), multiply ionised species of the incident ion are formed in excited states. By means of emission transitions, they will return to the ground state of the corresponding ion:



As a result of the high velocity of the ions (of the order of 10^6 m/s), light emission will be observed over a considerable length of the beam, of the order of several tens of centimetres for a lifetime of 10^{-6} s. Analysis of the emitted light with a spectrograph allows different transitions to be isolated, and the

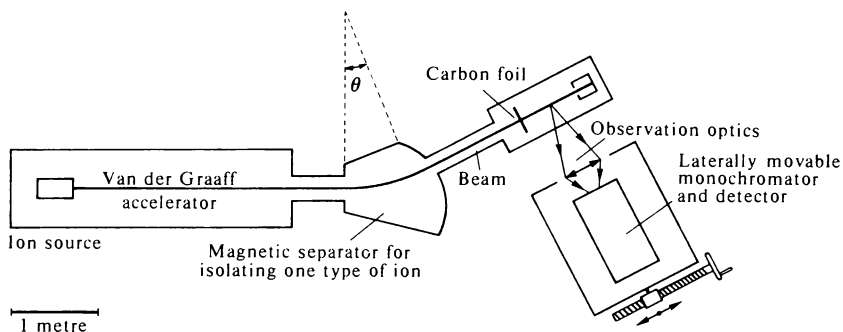


Figure 7.27 Diagram showing the principal features of a beam-foil spectroscopy experiment

measurement of the emitted intensity as a function of the distance from the carbon foil enables an analysis to be carried out which, by taking account of possible cascade effects, gives a value of the lifetime. Results have been obtained with ions such as those of iron, sodium, nitrogen, xenon and so on. The main difficulty is the construction of the ion source that must be attached to the accelerator.

(3) *From the widths of lines.* In section 7.2 we described level-crossing experiments and in section 7.3, radiofrequency spectroscopy experiments. *The widths of the lines* observed are related to the natural width of the level and when such experiments on an excited level are possible, a study of the width of the curves leads to accurate results for its lifetime; they are usually free from cascade effects, because the phenomenon observed is generally specific to the level under study (the position of a resonance line depending on the Landé factor). Unfortunately, as discussed in section 7.3, the conditions

necessary for the observation of radiofrequency transitions mean that these techniques cannot be applied to all levels. However:

- (a) magnetic resonance experiments on levels excited optically or by electronic excitation have led to the determination of lifetimes of an appreciable number of atomic levels that can be studied in the form of a vapour (alkalis, mercury, zinc, cadmium, rare gases);
- (b) the zero-field level-crossing method (Hanle effect) has been applied especially to resonance levels excited optically—many experiments have been carried out on such excited levels, both of neutral atoms and of ions.

7.4.3 Experimental study of oscillator strengths

(1) *From absorption measurements.* Equation (7.6) enables the value of the oscillator strength f to be determined from these measurements. However, to obtain the value of the total absorption

$$\mathcal{A} = \int_0^{\infty} K(\nu) d\nu$$

it would be necessary to have a spectrometer of sufficient resolution to follow the variation of K with ν , that is, a resolution enabling the line profile to be traced. The problem is simplified considerably if the absorption is weak; expression (7.1) can then be written

$$I \approx I_0(1 - Kz)$$

and the total absorption over the spectrum $\int_0^{\infty} (I_0 - I) d\nu$ measured experimentally, can then be simply related to \mathcal{A}

$$\int_0^{\infty} (I_0 - I) d\nu \approx I_0 z \int_0^{\infty} K(\nu) d\nu = I_0 z \mathcal{A}$$

In order to separate the transition under study from other transitions, all that is necessary is to isolate a band of the spectrum with a low-resolution spectrometer since the contribution to the integral $\int_0^{\infty} K(\nu) d\nu$ of frequencies far from the absorption line centre is negligible.

Depending on the element under study, the experimental factors in constructing an absorption cell and a convenient source can be quite different and can lead to a variety of arrangements.

(2) *From the intensity of a transition ν_{ij} in emission.* The power P emitted spontaneously at a frequency ν_{ij} , within a solid angle Ω , can be calculated as a function of the total number N_j of excited atoms present in the luminous source. (If a resonance line is involved, the source is assumed to be thin enough to disregard the process of self-absorption (see volume 1, section 3.1.4, comment).)

$$P = N_j A_{j1} h\nu_{ij} \frac{\Omega}{4\pi}$$

If the total number of excited atoms N_j is known, an absolute intensity measurement can lead to the value of A_{ji} and thus to the value of f_{ij} by using the relationship (7.8).

(3) *From dispersion measurements.* In section 7.4.1, we reviewed only the laws concerning the absorption of electromagnetic radiation by an atomic vapour. Dispersion phenomena are also involved (see appendix 2); the refractive index of the vapour varies in conjunction with the absorption, and involves the oscillator strength f . Refractive-index measurements in the neighbourhood of an absorption band can then be used to obtain oscillator strengths.

7.5 Electronic and Atomic Collisions

In this book, we have focused our attention for the most part on the properties of an isolated atom: the description of excited levels, the description of the emitted radiation and so on. However, atoms are not usually isolated and in most problems it is necessary to study the interactions between an atom and another particle (atom, electron, ion, and so on). Sometimes these interactions can lead to the formation of a stationary bound state (molecule, ion, and so on), but they always appear in a transitory fashion as particles approach each other during the complicated evolution of a system. The branch of physics devoted to the study of these transitory phenomena is called the physics of electronic and atomic collisions. Many physicists work in this area, and the results they obtain provide important data for plasma physics and astrophysics.

This branch of physics is vast; here we can give only a brief insight into a particular aspect. The concept of a 'cross-section', which we shall review next, is very important; it is a fundamental parameter, and its value is of interest to experimental collision physicists and theoreticians.

7.5.1 The collision cross-section

The reader has already come across the concept of a collision cross-section in volume 1, chapter 3, in the model of collisions between hard spheres, and in volume 1, chapter 5, during the discussion of Rutherford's experiment. Here, we bring together the main ideas concerning the concept of a cross-section.

The various collision processes may be classified essentially as elastic collisions and inelastic collisions (see volume 1, chapter 2).

(a) In an elastic collision, the total kinetic energy of the system of interacting particles is the same before and after the collision; there is no change in the internal energy of the particles. Therefore the collision is manifested mainly by a change of trajectories. This is often described as an elastic scattering process. Results will be sought to express these changes of trajectory.

They can be described either in a laboratory reference frame or in the centre-of-mass frame. They will often be described in terms of a 'differential cross-section'.

(b) In an inelastic collision, the momentum is conserved, but the total kinetic energy of the system is changed as a result of a change of internal energy of one or more of the particles taking part. As in the case of an elastic collision, the study of the geometry of the trajectories can be of interest, and leads to a differential cross-section, but usually the objective is to find the probability of a certain change of state occurring in one of the particles present. This is done by means of the total cross-section.

(1) *The differential cross-section.* A beam of incident projectile particles is directed along the Oz axis in the laboratory frame, and the experiment involves the passage of N_{proj} projectiles. The N_{targ} target particles form a cloud and are at rest in the region of the origin O . Let us suppose that the collisions are only elastic. Furthermore, we shall assume that the density of the target particles is sufficiently low to be able to disregard the screening of one target particle by another.

Let $N(\theta, \phi)d\Omega$ be the number of projectile particles scattered during the experiment within the solid angle $d\Omega$ around the direction θ, ϕ (see figure 7.28). The integral over all space of this quantity will give the total number of scattered particles, which must be equal to N_{proj} .

By generalising the relationship given in volume 1, section 3.1.1, we can write that the probability of scattering projectiles within the solid angle $d\Omega$ is

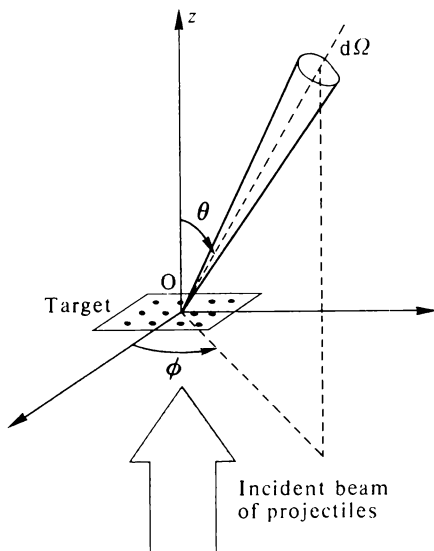


Figure 7.28 Geometry used in the discussion of differential cross-sections

proportional to this solid angle $d\Omega$ and to the number of targets per unit cross-sectional area

$$\frac{N(\theta, \phi) d\Omega}{N_{\text{proj}}} = F(\theta, \phi) d\Omega \frac{N_{\text{target}}}{S} \quad (7.9)$$

where S is the cross-sectional area common to the target and beam.

The coefficient of proportionality $F(\theta, \phi)$, a function of θ and ϕ , is called the 'differential cross-section'. Henceforth we write it by using the usual notation $(d\sigma/d\Omega)(\theta, \phi)$ or, more simply, $d\sigma/d\Omega$.

From equation (7.9), we see immediately that $F(\theta, \phi) d\Omega \equiv (d\sigma/d\Omega) \cdot d\Omega$ has the dimensions of area. Let us give a physical interpretation of $d\sigma/d\Omega$; from (7.9) the quantity

$$p(\theta, \phi) d\Omega = \frac{d\sigma}{d\Omega} d\Omega \times \frac{1}{S}$$

represents the probability of an incident particle being scattered within the angle $d\Omega(\theta, \phi)$ by *one* target particle.

Therefore we shall interpret $(d\sigma/d\Omega)d\Omega$ as an area associated with the target particle such that any incident particle crossing this area is scattered in the direction defined by θ and ϕ , and within the solid angle $d\Omega$. Any incident particle crossing the total area S of the target outside the area $(d\sigma/d\Omega)d\Omega$ will be scattered in a direction different from θ, ϕ . (Volume 1, figure 5.3, illustrates this property for the special case of Rutherford scattering.)

(2) *The total microscopic cross-section.* This will be obtained by integration of the differential cross-section over all angles θ and ϕ

$$\sigma = \int_{\phi=0}^{\phi=2\pi} \int_{\theta=0}^{\theta=\pi} \frac{d\sigma}{d\Omega}(\theta, \phi) \sin \theta d\theta d\phi$$

In certain cases the above integral does not converge and the discussion can be complicated. If we ignore this difficulty, we note that σ represents an area, associated with a target particle, such that any incident particle crossing this area undergoes a deflection with respect to its initial motion. In a collision problem, σ may be thought of as the 'size' of a target particle.

Let us return briefly to the question of convergence. In the interpretation of a collision phenomenon in classical mechanics, the reader may readily appreciate the following points.

(a) The total cross-section of an elastic scattering process is infinite (unless one imagines a law of force acting only at a finite distance). Whatever the value of the impact parameter, the particle is deflected, the deflection clearly tending to zero as the impact parameter tends to infinity. This is the situation in Rutherford's experiment (volume 1, chapter 5).

(b) If the process is inelastic, energy must be exchanged between the target particle and the projectile particle. For this to happen, the impact parameter must be sufficiently small, since beyond a certain value no energy exchange will occur. In this case, the total cross-section has a finite value.

We shall not deal with the quantum description.

(3) *The total microscopic cross-section and the absorption coefficient.* Let us consider an inelastic collision process. We wish to know only the total probability of the process, and are not interested in the trajectories of the particles after the collision. By calling N_{coll} the number of projectiles having undergone the process, integration of equation (7.9) will lead to the same relationship as in volume 1, chapter 3

$$\frac{N_{\text{coll}}}{N_{\text{proj}}} = \sigma \frac{N_{\text{targ}}}{S} \quad (7.10)$$

σ being the total microscopic cross-section.

Let us introduce the intensity \mathcal{D} of the beam of projectiles (that is, the number of projectiles per unit area per second). The beam enters the target at $z = 0$; if $\mathcal{D}(z)$ is the intensity of particles not having interacted at a distance z , equation (7.10) leads to:

$$\mathcal{D}(z) = \mathcal{D} e^{-n\sigma z} \quad (7.11)$$

(see volume 1, section 3.1.2) n being the number of target particles per unit volume.

We see, therefore, that the total microscopic cross-section (sometimes called the 'atomic cross-section' or simply the 'cross-section') can also describe the macroscopic evolution of a system in terms of the intensity of particles. The quantity $n\sigma = K$, representing an absorption coefficient and having dimensions of inverse length, is often used (some authors call K , rather inadvisably, the macroscopic cross-section).

Comment Cross-sections having the dimensions of an area can be expressed by means of a variety of units:

(a) in centimetres squared;

(b) in units of a_1^2 or πa_1^2 , a_1 being the radius of the first circular Bohr orbit:

$$a_1 = 0.5292 \times 10^{-8} \text{ cm} \quad a_1^2 = 2.803 \times 10^{-17} \text{ cm}^2$$

$$\pi a_1^2 = 8.806 \times 10^{-17} \text{ cm}^2$$

(c) in 'barns', the barn being equal to 10^{-24} cm^2 (used for collisions with nuclei or elementary particles).

7.5.2 The various collision processes

There are clearly a great number of collision processes involving a variety of interactions between two or more of the following atomic entities:

neutral atom (0)—excited atom (0')—singly ionised atom (1)—multiply ionised atom (1, 2, 3, . . .)—negative ion (1)—electron (e).

The symbols in brackets are used by some authors to describe an interaction process symbolically. For example, the excitation of an atom by an electron would be represented by the expression

$$e0/e0'$$

where the particles in the initial state are on the left and the particles in the final state on the right. Similarly, ionisation by electron impact will be denoted by

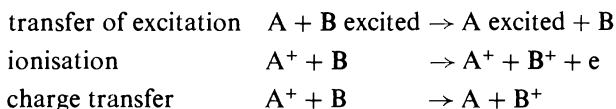
$$e^0/eel$$

In this section we list only the most important processes.

(1) *Elastic scattering of electrons and of atoms in a gas.* Understanding this is of fundamental importance; this phenomenon, which should be analysed in every collision problem, becomes dominant when the particles involved have insufficient energy to produce inelastic collisions.

(2) *Ionisation and excitation of atoms by electron impact.* This type of collision will be studied in detail later (section 7.5.3).

(3) *Inelastic collisions between heavy particles (atoms, molecules).* Collisions of this type are very common in electric discharges and plasmas; some examples are



Under this type of collision, we must also classify 'stripping' phenomena, mentioned in the description of beam-foil spectroscopy experiments



where the atom A may also be obtained in stages of multiple ionisation.

(4) *Recombination.* These processes, the inverse of certain processes mentioned above, contribute to the achievement of steady states in electric discharge phenomena. They can occur in several forms

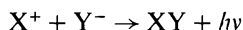
radiative recombination



dissociative recombination involving a molecular ion XY^+

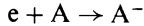


ion-ion recombination which can occur in different ways



(5) *Formation of negative ions.* The phenomenon of attachment of an electron to a neutral atom to form a negative ion takes place with ease in the

case of atoms having a nearly complete electronic shell (F, Cl, I, etc.) (see section 2.4.2)



When this attachment occurs in an ionised medium, the number of electrons will diminish, which will have an important bearing on the macroscopic electrical characteristics.

In this list, deliberately abbreviated, we have not mentioned collisions involving three particles, nor those where unstable intermediate stages are involved in a transitory fashion, for example, states where two electrons from the shells of an atom are in excited states and whose energy is greater than the ionisation threshold (auto-ionising levels). The reader will appreciate the importance of a specific study of these different types of collision; the actual description of an ionised gas will result from the competition between processes that often oppose one another.

7.5.3 Ionisation and excitation of atoms by electron impact

Amongst all the possible processes, we shall merely provide some information about experimental methods of studying ionisation phenomena and of excitation by electron impact. In these rather simple experimental situations, related to phenomena studied in previous chapters, the reader should be able to appreciate the experimental difficulties and the different orders of magnitude of the results obtained.

(1) *Ionisation.* The general experimental arrangement is shown in figure 7.29. An electron gun E provides a beam of electrons with as well-defined an energy as possible. This constitutes a severe constraint and permits only beams of very low intensity, of the order of 10^{-8} A, to be obtained. The beam then passes into the collision chamber C where the atoms to be studied are in the form of a gas at a pressure of the order of 10^{-4} torr. The ions formed are collected by an electrode P_1 charged to a negative potential; the intensity of the electron beam is determined by means of a collector F. The experimental

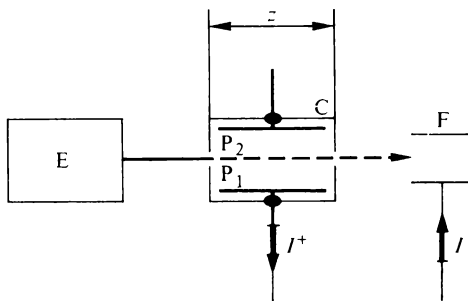


Figure 7.29 Diagram of an experiment to study ionisation cross-sections: E = electron gun; C = collision chamber; F = electron collector

conditions are chosen so that all the ions formed can be collected by P_1 and, moreover, so that the number of electrons involved in collisions is small compared with the total number transported in the beam; only in this case will the measurement of the current at F have any meaning. Let I^+ be the current collected by P_1 , I the current transported by the electron beam, n the number of atoms per unit volume in the chamber C and z the thickness of the gaseous target in C; the ionisation cross-section σ_i may easily be obtained from equation (7.10).

$$I^+ = I\sigma_i nz$$

The basic difficulty is the production of a mono-energetic electron beam despite the energy spread related to thermionic emission. Two techniques are normally used, as follows.

(a) *The electrostatic selector.* The electron gun is illustrated in figure 7.30. The electron beam, after passing through electrode (a), enters a cylindrically

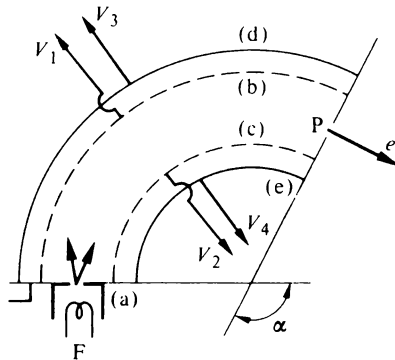


Figure 7.30 Electrostatic selector

symmetric electrostatic field whose magnitude is proportional to $1/r$, produced by electrodes (b), (c), (d) and (e), charged to potentials that can be adjusted. The theory of the arrangement shows that there is a refocusing of the electrons emitted at (a) at various angles, if the angle α has a value of 127° . For a radial field of given magnitude, focusing occurs at the point P for electrons of a particular energy only.

By paying careful attention to the geometry of the apparatus, it is possible to obtain at the exit slit P, electrons having an energy of several electronvolts, with an energy spread of 0.02 eV. These experiments require careful work on the part of the experimenter.

(b) *The r.p.d. (retarding potential difference) method.* A special technique allows a beam with an energy spread of less than 0.1 eV to be obtained quite simply. The apparatus, reduced to its essential elements, is shown in figure 7.31(a). First we ignore the electrode R; the electron beam is accelerated by the potential difference between the collision chamber at

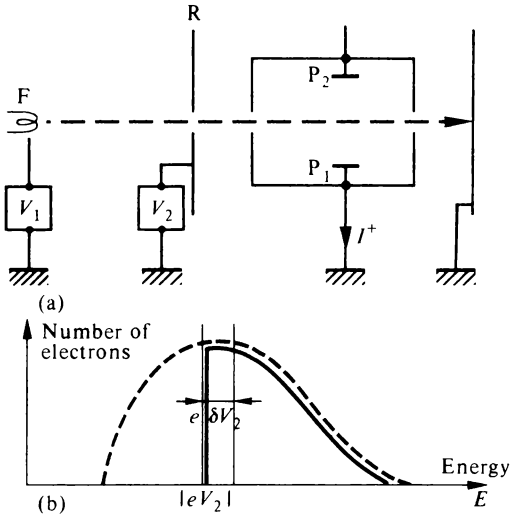


Figure 7.31 The r.p.d. method

zero potential and the filament F at a negative potential V_1 . Because of the fluctuations in the initial thermal energy of the electrons, and space charge phenomena, the velocities of the electrons collected in the collision chamber are characterised by a certain spread; figure 7.31(b) shows the energy spectrum of these electrons in dotted lines.

Let us now consider the electrode R charged to a potential V_2 slightly lower than V_1 . It slows the electrons and only those whose initial energy is sufficiently high can pass through it; it stops all electrons whose initial velocity is too small. Among the electrons received in the collision chamber, the slowest are those that were able to pass through the electrode R with zero velocity; their kinetic energy at the entrance to the chamber is $|eV_2|$. The energy spectrum of the electrons collected then displays a rather sharp cut-off at the value $|eV_2|$ (see curve in thick lines in figure 7.31(b)). Let us now increase V_2 by δV_2 ; the ion current collected in the ionisation chamber will change by δI^+ . It is easy to show that δI^+ corresponds to the number of ions created by a mono-energetic beam of electrons of energy $|eV_2|$ and of energy spread $e\delta V_2$.

Many experimental results have been obtained by the above techniques. Figure 7.32 shows ionisation cross-sections of mercury. The existence of ionisation thresholds and the existence, as a rule, of maximum cross-sections will be noted, as will be the orders of magnitude of the cross-sections. The use of a beam of well-defined energy enables a 'fine structure' to be observed in certain cases, an example of which is given in figure 7.33. This structure corresponds, on the one hand, to the existence of structure in the ground level of the ion and, on the other hand, to the presence of the several processes leading to ionisation. The contribution of these elementary processes is

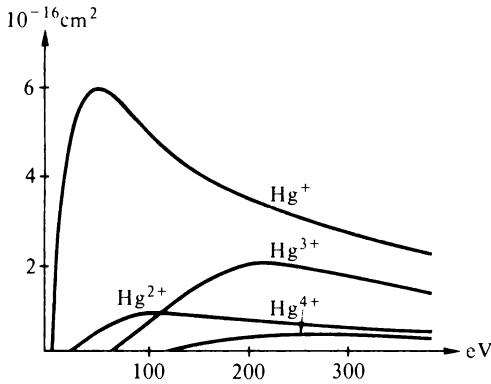


Figure 7.32 Ionisation cross-sections of mercury (the scale is in 10^{-21} m^2 for Hg^{3+} and Hg^{4+})

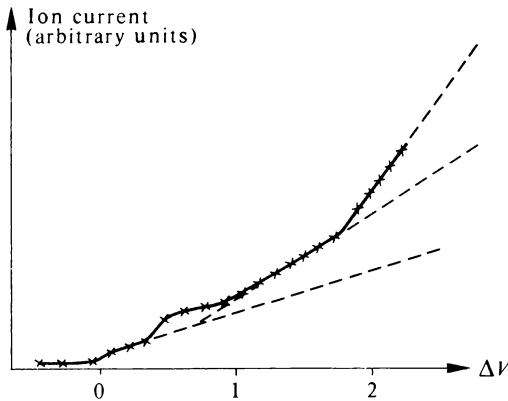


Figure 7.33 Ionisation of krypton near threshold. At the ionisation threshold, $\Delta V = 0$. The ordinate is in arbitrary units (the crosses denote experimental points)

illustrated in figure 7.33 by extrapolations in broken lines. Apart from direct ionisation by electron collision, account should be taken of indirect processes where the atom is excited to an intermediate state (an ‘autoionising state’) of energy greater than the ionisation threshold.

(2) *Excitation.* The study of excitation cross-sections of excited atomic levels is also very important for many problems. The experimental situation is more difficult because the excited levels may be studied only by means of optical measurements on the emitted radiation. We outline the principle of an excitation cross-section measurement: radiation emitted in a collision chamber is analysed by a spectrograph, followed by a detector which is usually a photomultiplier. An ancillary experiment enables the apparatus to be calibrated against a standardised incandescent source in order to

be able to determine the number of photons emitted. Figure 7.34 shows the variation of the excitation cross-section of the 2p level of hydrogen as a function of the energy of the incident electrons.

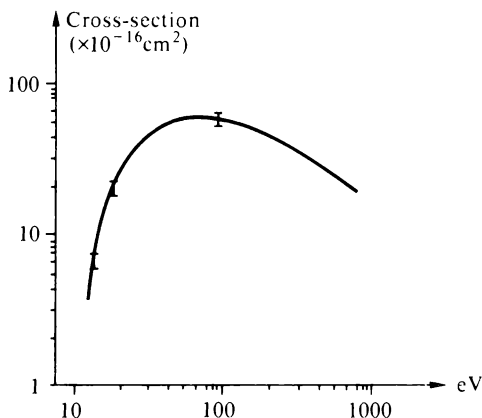


Figure 7.34 Excitation cross-section of the 2p level of hydrogen (logarithmic scale)

7.6 The Electric Dipole Moment of the Neutron and of the Electron

7.6.1 Aim of the experiments

For a particle having an angular momentum, the existence of an electric dipole moment is not compatible with the symmetry rules that express the conservation of parity and incorporate time reversal. However, some experiments (decay of the K meson) have shown that these symmetry principles can be violated. Taking account of experimental results, and calculating the order of magnitude of these violations, theoreticians have evaluated a possible order of magnitude of the electric dipole moments of the neutron and the electron. In particular, in the case of the neutron, the ratio of the dipole moment p_N to the charge e of the electron should have an upper limit between 10^{-21} and 10^{-24} metres, depending on the author.

The experiments are therefore relevant to the discussions of the symmetry laws. They have been undertaken especially in the case of the neutron since its total charge of zero is a simplifying factor in the interpretation of the results.

7.6.2 The electric dipole moment of the neutron

(1) *The principle.* Basically the experiments are very simple. In figure 7.35 the energy levels of the neutron in a magnetic field are represented by thick lines. Since the spin equals $\frac{1}{2}$, then

$$W = \pm \frac{1}{2} g B$$

(g is the Landé factor of the neutron).

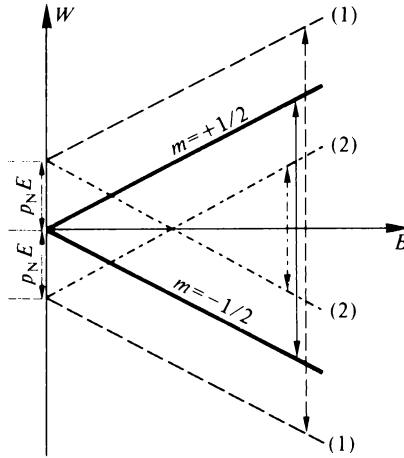


Figure 7.35 Energy, as a function of magnetic field \mathbf{B} , of a neutron with a dipole moment \mathbf{p}_N in an electric field \mathbf{E}

Let us impose an electric field in the same direction as \mathbf{B} ; since the electric dipole moment vector \mathbf{p}_N is parallel to the spin vector, there is an additional energy

$$W_e = \pm p_N E$$

The \pm sign depends not only on the state $m = \pm \frac{1}{2}$, but also on the sense of \mathbf{E} in relation to \mathbf{B} and the sense of \mathbf{p}_N in relation to the spin. The total energy in the presence of \mathbf{E} and \mathbf{B} is therefore represented by the set of curves (1) or (2) in dotted lines, according to the orientations defined above. If the sense of \mathbf{E} in relation to \mathbf{B} is changed, we pass from diagram (1) to (2) or vice versa.

Suppose we carry out a magnetic resonance experiment, such as described in volume 1, chapter 8, on a beam of polarised neutrons, in the presence of an electric field \mathbf{E} , parallel to a magnetic field \mathbf{B} . The frequency of the transition $m = +\frac{1}{2} \rightarrow -\frac{1}{2}$ will depend on the sense of \mathbf{E} in relation to \mathbf{B} , as illustrated by the two arrows in figure 7.36. The shift of the magnetic resonance in the presence of the field \mathbf{E} will then allow p_N to be determined.

(2) *A difficulty.* The neutron moves with velocity \mathbf{v} in the electric field \mathbf{E} . Besides the applied field \mathbf{B} , it will also see a 'motional' field, in accordance with the results obtained in electromagnetism by a change of reference frame (section 3.2.1)

$$\mathbf{B}_m = \frac{\kappa}{c^2} \mathbf{E} \times \mathbf{v}$$

(see figure 7.36).

When \mathbf{B} and \mathbf{E} are exactly parallel to Oz and \mathbf{v} is directed along Oy , \mathbf{B}_m is directed along Ox ; the magnitude of the field $\mathbf{B} + \mathbf{B}_m$ seen by the neutron is, to a good approximation, equal to B .

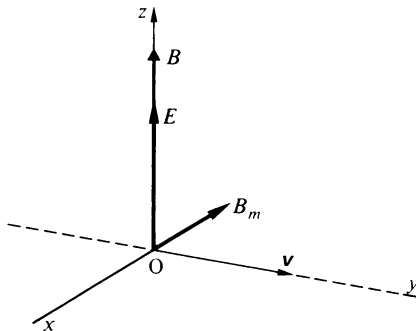


Figure 7.36 Direction of 'motional' electric field

On the other hand, if B and E are not perfectly colinear, E for example being in the xOz plane, a component of B_m in the Oz direction will appear. A change of E will then produce a change of magnitude of the total magnetic field seen by the neutron. The observed shift of the resonance will not then be related exclusively to the influence of the electric dipole moment, but will result also from the variation of the coupling energy between the magnetic moment and the magnetic field.

To demonstrate the importance of this effect, let us carry out an order-of-magnitude calculation. We take the following approximate values

applied electric field: $E = 10^7$ V/m

velocity of thermal neutrons at ordinary temperatures: $v = 2 \times 10^3$ m/s

magnetic moment of the neutron:

$$\mathcal{M}_n = 1.913\beta_N = 1.913 \times 5.05 \times 10^{-27} \text{ SI} \approx 10^{-26} \text{ SI}$$

The magnitude of the motional field is

$$|B_m| = \frac{\epsilon_0 \mu_0}{\kappa} vE = \frac{\kappa}{c^2} vE = 2.2 \times 10^{-7} \text{ T}$$

Let us assume that the electric field E makes an angle $\alpha = 10^{-3}$ radian with the y axis; then the change of magnitude of B as a result of the appearance of B_m will be of the order of

$$\delta B = \alpha B_m \approx 2 \times 10^{-10} \text{ T}$$

Let us calculate the electric dipole moment p which, when placed in the field E , would cause the same energy change as a nuclear magnetic moment \mathcal{M}_N experiencing a change of field δB , in other words such that

$$pE = \mathcal{M}_n \delta B$$

Taking account of the value of \mathcal{M}_n (see chapter 6)

$$p \approx 2 \times 10^{-43} \text{ SI} \text{ so } p/e \approx 10^{-24} \text{ m}$$

The error introduced is of the order of magnitude of the effect sought.

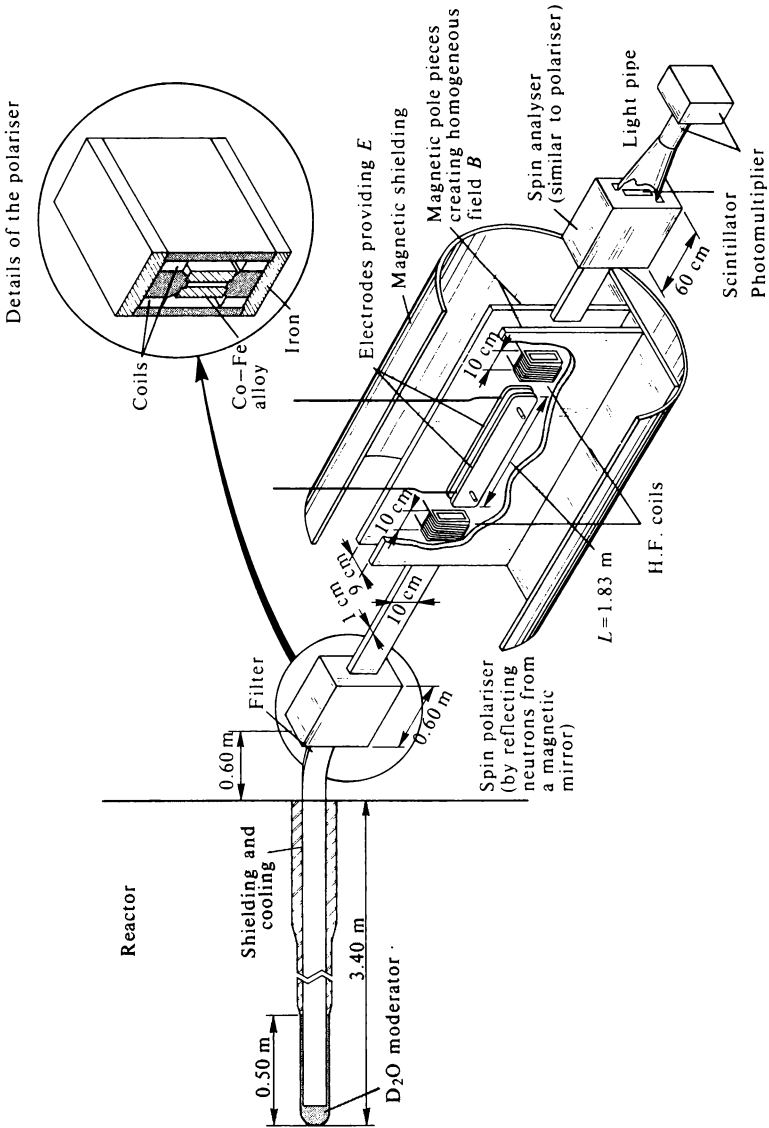


Figure 7.37 Measurement of the electric dipole moment of the neutron. Diagram of Ramsey's apparatus

(3) *The experimental procedure.* This proves to be difficult. From the outset, it is advisable to use conditions allowing the best possible magnetic resonance signal to be obtained:

- (a) a resonance curve as narrow as possible which requires a neutron-magnetic field interaction region as long as possible, as in Rabi's experiments on atomic beams (see section 7.3);
- (b) a good signal-to-noise ratio, and therefore the use of an intense and strongly polarised neutron beam.

To minimise the effect of the motional field, it is also advisable to use very slow neutrons and to pay careful attention to the geometry of the apparatus. Figure 7.37 shows the arrangement used by Ramsey and his associates at Oak Ridge. The reader should ascertain the purpose of the various components and appreciate the difficulty of the experiment. The velocity of the neutron beam is 136 m/s. The magnetic resonance is carried out in a field B of 1.8×10^{-3} T. The uncertainty in the results confirms only that $p_N/e < 2 \times 10^{-25}$ m.

Several experiments are now in the process of being undertaken and from them a better resolution is anticipated.

7.6.3 The electric dipole moment of the electron

The principle of these experiments is similar; they have been performed on atomic beams of alkali atoms in an apparatus resembling Rabi's arrangement with the addition of an electric field E parallel to the static field B . The shift of a magnetic resonance line is studied as a function of the applied electric field E . The discussion is more complicated because, as a result of the charge of the electron, the electric field E interacts with the atom independently of any dipole moment, and produces a shift of the level (the Stark effect). In the last few years, a number of experiments have been carried out and the most recent have led to attributing an electric dipole moment to the caesium atom p_{Cs} such that

$$p_{Cs}/e = (0.8 \pm 1.8) \times 10^{-24} \text{ m}$$

This result allows an upper limit to be defined for p_{Cs} and hence an upper limit for the electric dipole moment of the electron

$$p_e/e \lesssim 3 \times 10^{-26} \text{ m}$$

7.7 Muonium, Mesic Atoms and Positronium

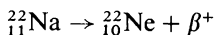
These are related systems involving positrons and μ mesons. The main properties of these two particles are summarised in table 7.1.

(a) Positronium is formed by the association of an electron and a positron rotating around one another. It was discovered in 1951 by M. Deutsch, and is formed mainly when a beam of positrons of energy of the order of one MeV is stopped by a gas. It is often produced by placing a source of sodium 22 in

Table 7.1

	Positron	μ^+ or μ^- Meson
Mass	$m_e = 0.9109 \times 10^{-30}$ kg	$m_\mu = (206.767 \pm 0.003) m_e$
Charge	$+e$	$+e$ or $-e$
Spin quantum number	$\frac{1}{2}$	$\frac{1}{2}$
Gyromagnetic ratio	$\gamma_p = -\gamma_e = +1.001159 (e/m_e)$	$+1.001167 (e/m_\mu)$
Lifetime	Stable (but annihilated on an encounter with an electron)	2.2×10^{-6} s

an atmosphere of argon. The disintegration of sodium 22 produces positrons according to the reaction



(β^+ is the positron emitted by the nucleus).

(b) Muonium is the positive μ meson–electron system. It is obtained by stopping a beam of μ^+ mesons in a gaseous target. It was discovered by V. W. Hughes in 1960.

(c) Mesic atoms are formed by the capture of a μ^- meson by a nucleus. They are produced when a beam of high-energy mesons is stopped by a target of dense material (Wheeler, 1953).

The study of these systems turns out to be extremely important; they permit certain parameters to be ascertained in conditions often far more favourable than in conventional atomic systems. The construction of accelerators with increasingly improved performance (an energy of at least several tens of MeV is necessary to obtain μ mesons) gives rise to the expectation of more intense beams of mesons as well as important developments in the physics of mesic atoms.

7.7.1 Positronium

Positronium can be considered as a light isotope of hydrogen (the positron is 1836 times lighter than the proton). An elementary quantum study will then lead qualitatively to the same results as for the hydrogen atom; quantitative results will be obtained by taking the reduced mass of the electron equal to half the mass of the electron. The energy differences between levels will therefore be very nearly equal to half those of hydrogen and the expected wavelength of the various transitions will therefore be twice as long.

A more detailed study, especially of the fine structure, gives rise to considerable differences when compared to hydrogen. The reasons are as follows.

(1) The magnetic moment of the positron is equal in magnitude to that of the electron, and consequently is much greater than that of the proton. Spin–spin interactions will have a much greater influence than in the case of the hydrogen atom.

(2) Particle–antiparticle annihilation interactions existing between the

positron and the electron will enter into the fine structure calculations, involving the methods of quantum electrodynamics.

In particular, the description of the ground level, involving coupling of the electron and positron spins, will be completely different from that of hydrogen. The experimental study of positronium, therefore, would appear to be extremely important, as a test of a rather complex theory.

The ground level of positronium. Depending on the relative directions of the electron and positron spins, we obtain two states, of total spin $S = 0$ and $S = 1$; the ground state is said to have a fine structure Δv_0 . (Qualitatively the effect is similar to the hyperfine structure of the ground level of hydrogen resulting from the coupling between the magnetic moment of the electron and the magnetic moment of the proton; but in the case of positronium, this coupling involves two electronic magnetic moments, as in the fine structure effects of an atom: hence the term 'fine structure'.)

This coupling between the electron and the positron has an influence on the electron-positron annihilation process:

- (a) In the $S = 1$ state, the lifetime of positronium before annihilation is 1.4×10^{-7} s; it is manifested by the emission of three γ photons.
- (b) In the $S = 0$ state, the lifetime is 1.25×10^{-10} s; annihilation occurs with the emission of two γ photons.

These quite different properties have led some authors to consider these two states as different species: parapositronium, $S = 0$ (1S_0) and orthopositronium, $S = 1$ (3S_1). In a steady-state regime of continuous creation of positronium, the much shorter lifetime of parapositronium will lead to a smaller population of the 1S_0 state. Therefore a population difference will exist between the two states.

Figure 7.38 shows the Zeeman diagram of the ground state. It may be shown theoretically that the levels $m = \pm 1$ of orthopositronium are degenerate

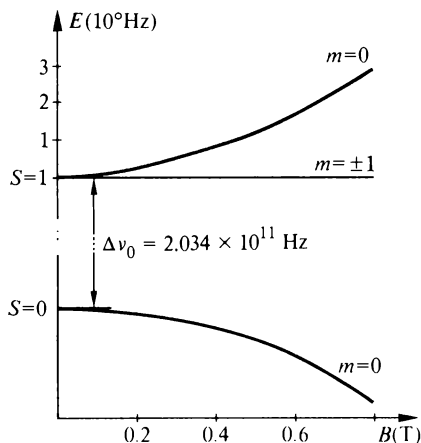


Figure 7.38 Zeeman diagram of the ground level of positronium

and independent of B . Furthermore, it may be shown that in the presence of a magnetic field, the states $m = 0$ are mixtures of the 3S_1 and 1S_0 wave functions; since the states $m = \pm 1$ have a pure 3S_1 wave function, it may be seen that the decay modes will differ for the states $m = 0$ and $m = \pm 1$ and consequently population differences will exist between these states. It is then possible to induce a transition between different Zeeman sublevels by means of a radio-frequency field. The fine-structure separation $^1S_0 - ^3S_1$ in zero field, $\Delta\nu_0$, is of the order of 2×10^5 MHz, corresponding to a wavelength of 1.5 mm; this makes the experiment difficult. On the other hand, the separation $m = 0 \leftrightarrow m = \pm 1$ at 0.8 T is about 3000 MHz ($\lambda = 10$ cm), and thus in a region where the dimensions of tuned cavities makes the experiment easier. In order to induce this transition a strong radiofrequency field, requiring powers of the order of a hundred watts, is necessary. This transition will be manifested by a change of population of the two sublevels and thus a change in the annihilation mode (since one is a pure 3S_1 state and the other a mixed $^1S_0 - ^3S_1$ state) as detected by two coincidence scintillation counters. Figure 7.39 gives the arrangement of the experimental apparatus. From the theoretical shape of the Zeeman diagram, and knowing the frequency and the field B_0 corresponding to the resonance, $\Delta\nu_0$ can be deduced. The experimental value is found to be

$$\Delta\nu_0 = (2.03398 \pm 0.00011) \times 10^5 \text{ MHz}$$

whereas the theoretical value is

$$2.03380 \times 10^5 \text{ MHz}$$

This slight disagreement hardly exceeds the experimental uncertainties.

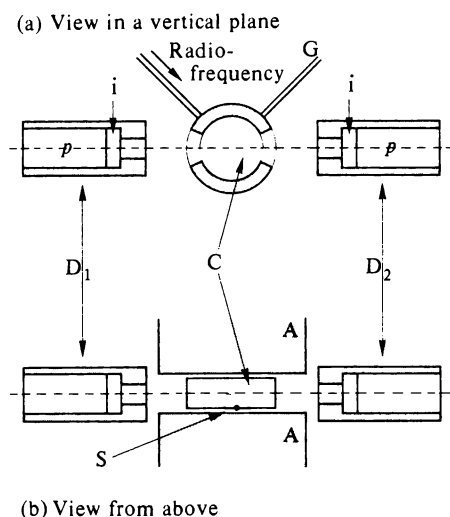


Figure 7.39 Measurement of the fine structure of the ground level of positronium. Diagram of the apparatus: A: Pole pieces of the electromagnet; B: Resonant cavity; C: Gas inlet; S: source of sodium 22—positronium is produced within the resonant cavity; D₁ and D₂: Detectors formed from a crystal scintillator (sodium iodide) i and a photomultiplier. These two detectors are connected in coincidence, enabling *ortho*- and *para*-positronium to be distinguished by their mode of disintegration

Comment The study of excited levels of positronium would also be of great interest, but unfortunately the density of positronium obtained is too small to allow the excited levels to be investigated by means of optical transitions in emission.

7.7.2 Muonium

Muonium can also be regarded, in terms of its energy levels, as a light isotope of hydrogen. The absence of annihilation phenomena, and the magnetic moment of the μ meson, much smaller than that of the positron (about 200 times smaller), make the study rather similar to that of hydrogen. This two-particle system can be treated rigorously; in particular, the hyperfine structure of the ground level can be expressed in the form of terms dependent on the fine-structure constant α . The experimental studies, which act as tests of the theory, are also very important. The transitions between ground-state sub-levels can be investigated by means of the positrons resulting from the decay of the μ meson.

Accelerators now being planned will enable far more intense beams of μ mesons to be obtained than those available presently: the higher number of muonium atoms that could then be obtained in the ground state might permit the study of the excited levels of muonium.

7.7.3 Mesic atoms

The radius of a Bohr orbit of an electron (see volume 1, chapter 6) is inversely proportional to its mass m . An atom formed from a meson moving around a nucleus will therefore have Bohr radii 207 times smaller. In addition, it is subjected to the total charge Ze of the nucleus. The probability of finding a meson within the nuclear charge distribution is therefore very high (figure 7.40); it constitutes one of the main reasons for studying mesic atoms—the

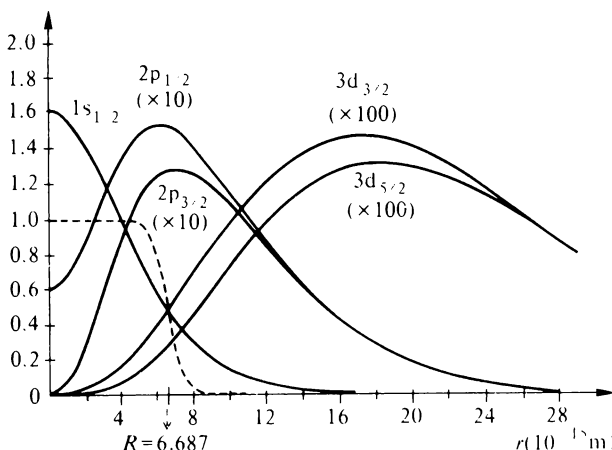


Figure 7.40 Continuous line: position probability of the meson in various orbits. Broken line: nuclear charge distribution. The figure represents the case of lead, $Z = 82$. (nuclear radius $R = 6.687 \times 10^{-15}$ m)

study of the various interactions with the nucleus. A mesic atom retains its electron cloud with changes, if necessary, to conserve the average charge neutrality. However, since the orbits of the μ meson are much smaller than the electronic orbits, in most cases it is unnecessary to consider the electrons in the study of mesic atoms.

The energy levels of a mesic atom. Let us assume that a meson is captured by a nucleus. As there is only one meson, all the muonic states except one are empty; if we suppose that it was captured in a level corresponding to $n = 7$, it will cascade to lower-energy levels, each of these transitions being characterised by the emission of electromagnetic radiation. The observed lines also correspond to the pattern of the hydrogen spectrum. Their energy is of the order of 10^5 to 10^7 eV, in the X-ray and γ -ray region. Figure 7.41 shows the

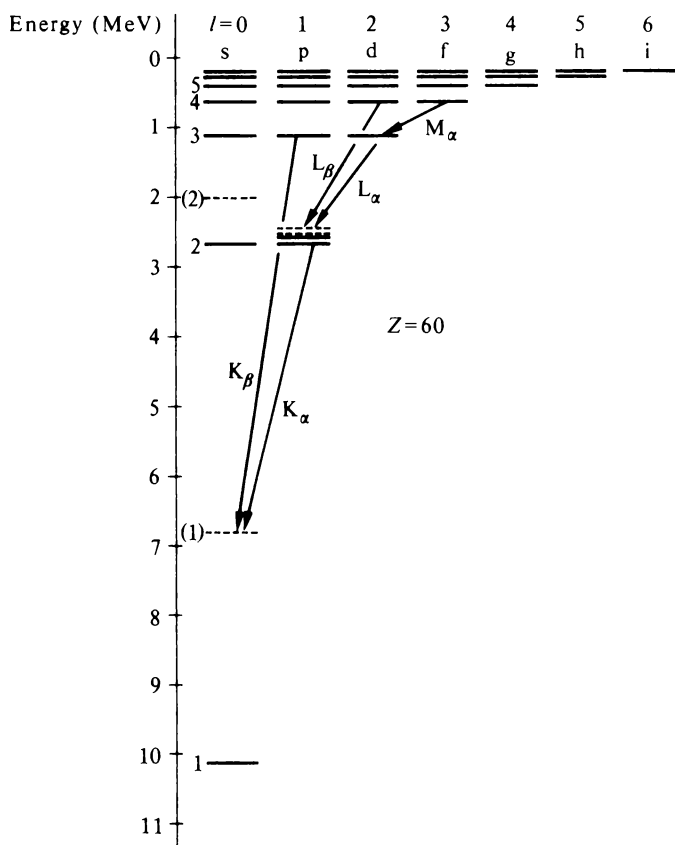


Figure 7.41 Mesic level diagram for $Z = 60$. Levels drawn with a solid line correspond to the assumption of a point nucleus. Levels drawn with a dotted line take account of the finite size of the nucleus. The importance of the effect for $1s$ and $2s$ levels should be noted; this is consistent with the data of figure 7.40

energy-level diagram and figure 7.42 shows some of the observed transitions. The reader will find many similarities between the spectrum of a mesic atom and the X-ray spectrum of an atom. The radiation emitted during mesic transitions may be analysed by means of photon detectors, as in nuclear physics, the amplitude of the pulses received being a function of the wavelength. The trace of a spectrum is obtained by using an amplitude selector. Until 1964, sodium iodide scintillators attached to a photomultiplier were used as detectors, and their energy resolution did not allow the various fine structures to be resolved. The discovery of Ge(Li) detectors has improved the resolution considerably, and 1 keV can be achieved.

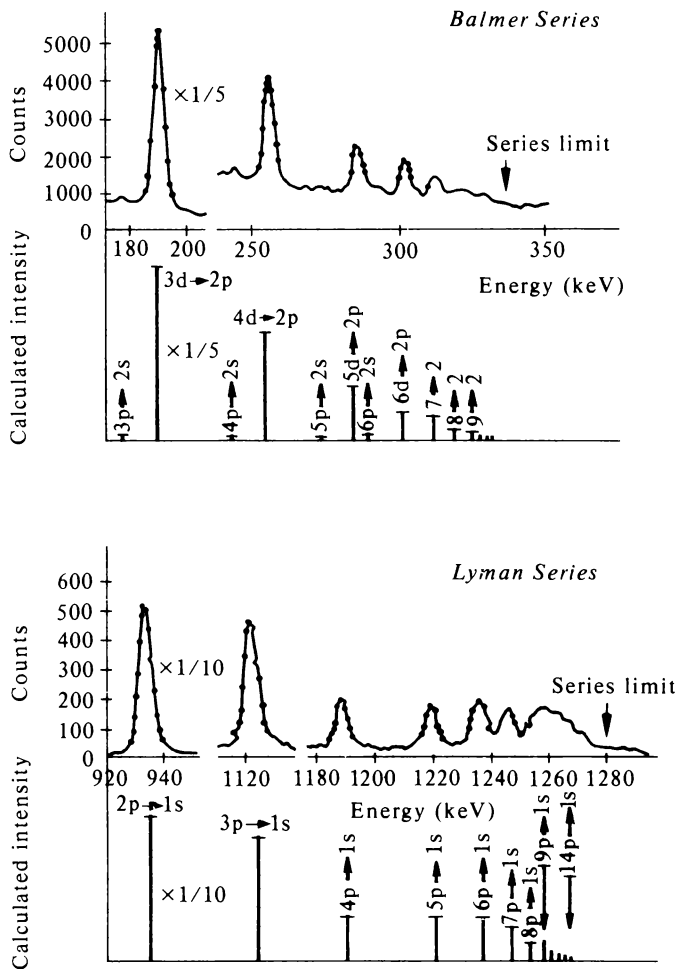


Figure 7.42 Mesic transitions in titanium: Lyman series ($np \rightarrow 1s$) and Balmer series ($nd \rightarrow 2p$) (from D. Kessler and co-workers)

Isotope shifts. The considerable localisation of the meson within the nuclear charge distribution gives rise to large level shifts related to the finite size of the nucleus. Figure 7.43 shows the shifts that result for the K_{α_1} and K_{α_2} transitions relating to the different isotopes of neodymium. A considerable amount of experimental data has been collected, providing nuclear-structure

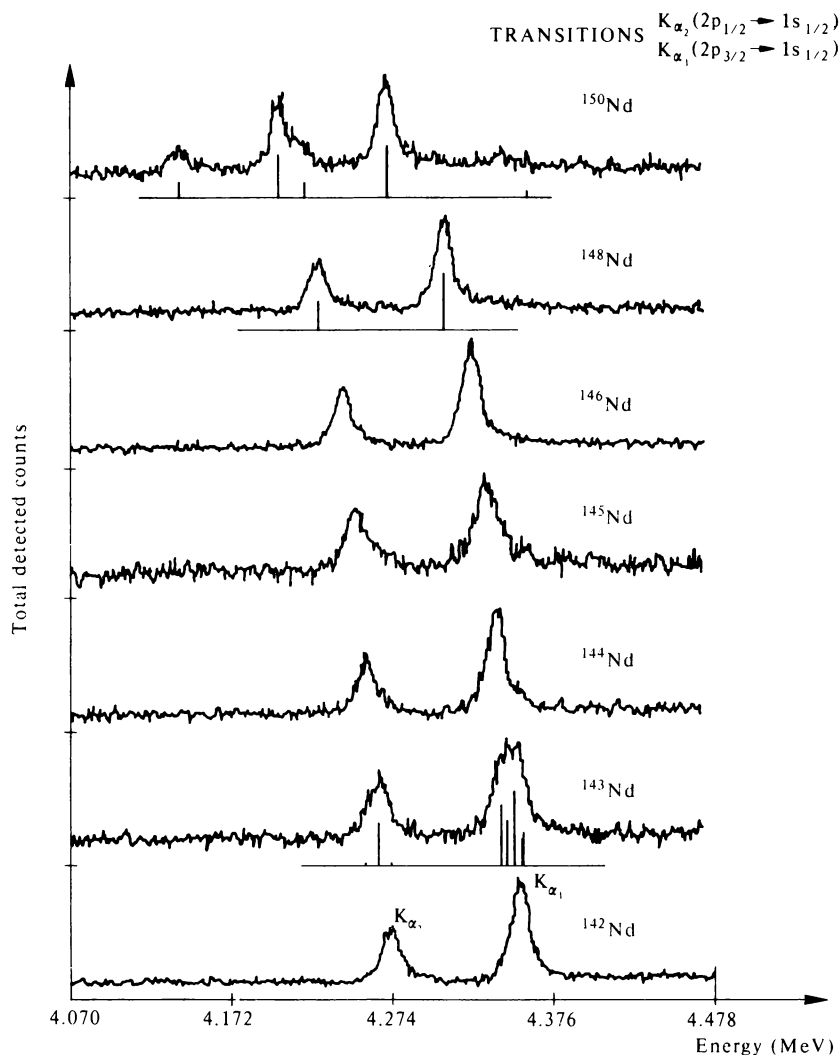


Figure 7.43 Mesic transitions K_{α_1} and K_{α_2} of various isotopes of neodymium. The reader should note: the isotope shifts; the broadening of the odd isotope and 150 isotope lines due to hyperfine interactions (the vertical lines represent the calculated position and relative intensity of the various components); the resolution obtainable by amplitude selection with Ge(Li) detectors

theorists with important information. It should be noted that isotope shifts observed in optical transitions of a normal atom include the screening action of the internal electrons and consequently their interpretation is more complicated than that of mesic transitions where this effect is not involved. Once again we discover a direct link between atomic physics and nuclear physics.

Appendix 1

Electromagnetic Formulae

adaptable to all the usual systems of units

The formulae are rationalised, but from the coefficients ϵ_0 , μ_0 and from the velocity of light c , we introduce a coefficient κ such that

$$\epsilon_0 \mu_0 c^2 = \kappa^2$$

In the SI system

$$\kappa = 1 \quad 4\pi\epsilon_0 = \frac{1}{9 \times 10^9} \quad \frac{\mu_0}{4\pi} = 10^{-7}$$

In the gaussian system (electric units of the c.g.s. electrostatic system and magnetic units of the c.g.s. electromagnetic system)

$$\kappa = c \quad 4\pi\epsilon_0 = 1 \quad \mu_0/4\pi = 1$$

Definition of the fields

$$\mathbf{f} = q\mathbf{E} + \frac{1}{\kappa} q\mathbf{v} \times \mathbf{B}$$

Maxwell's equations

$$(I) \begin{cases} \text{curl } \mathbf{E} + \frac{1}{\kappa} \frac{\partial \mathbf{B}}{\partial t} = 0 \\ \text{div } \mathbf{B} = 0 \end{cases} \quad \text{general solution} \quad \begin{cases} \mathbf{E} = -\text{grad } V - \frac{1}{\kappa} \frac{\partial \mathbf{A}}{\partial t} \\ \mathbf{B} = \text{curl } \mathbf{A} \end{cases}$$

$$(II) \begin{cases} \text{curl } \mathbf{B} - \frac{\epsilon_0 \mu_0}{\kappa} \frac{\partial \mathbf{E}}{\partial t} = \frac{\mu_0}{\kappa} \mathbf{j} \\ \text{div } \mathbf{E} = \rho / \epsilon_0 \end{cases}$$

By adopting the Lorentz gauge

$$\text{div } \mathbf{A} + \frac{\epsilon_0 \mu_0}{\kappa} \frac{\partial V}{\partial t} = 0$$

Hence *equations of propagation of the potentials* are found which justify the relation between ϵ_0 , κ and c

$$\Delta \mathbf{A} - \frac{\epsilon_0 \mu_0}{\kappa^2} \frac{\partial^2 \mathbf{A}}{\partial t^2} = -\frac{\mu_0}{\kappa} \mathbf{j}$$

$$\Delta V - \frac{\epsilon_0 \mu_0}{\kappa^2} \frac{\partial^2 V}{\partial t^2} = -\frac{\rho}{\epsilon_0}$$

The retarded potentials (general solution of the propagation equations)

$$\mathbf{A}(t, \mathbf{r}) = \frac{\mu_0}{4\pi\kappa} \iiint \frac{\mathbf{j}(t-r/c)}{r} d\mathcal{V}, \quad V(t, \mathbf{r}) = \frac{1}{4\pi\epsilon_0} \iiint \frac{\rho(t-r/c)}{r} d\mathcal{V}$$

Hence, for the static or quasi-static case (\mathbf{j} and ρ vary slowly with time):

$$\mathbf{B} = \frac{\mu_0}{4\pi\kappa} \iiint \frac{\mathbf{j} \times \mathbf{r}}{r^3} d\mathcal{V} \quad \text{or} \quad \frac{\mu_0}{4\pi} \int \frac{I d\mathbf{l} \times \mathbf{r}}{r^3} \quad (\text{Laplace's law})$$

$$\mathbf{E} = \frac{1}{4\pi\epsilon_0} \iiint \frac{\rho \mathbf{r}}{r^3} d\mathcal{V} \quad \text{or} \quad \frac{1}{4\pi\epsilon_0} \frac{q\mathbf{r}}{r^3} \quad (\text{Coulomb's law})$$

Appendix 2

Review of the Classical Theory of Radiation

The theory of dipole radiation is of considerable importance in physics. First, it allows a simple interpretation of many phenomena related to the interactions between radiation and matter, to be given in terms of classical models. Furthermore, it is the starting point for the quantum interpretation. Some of the simpler aspects of the theory which arose in the course of the book are reviewed below.

A2.1 The Radiation from an Oscillating Dipole

A2.1.1 Assumptions

A dipole is formed from two charges $+Q$ and $-Q$ at the extremities of a small linear element l centred at the origin, and lying along the Oz axis (see figure A2.1(a)). The charges Q are assumed *to occupy fixed positions* but their magnitudes vary with time; to assure charge conservation, it must be assumed in addition that a current of magnitude $I = \partial Q / \partial t = (1/l) \partial p / \partial t = (1/l) p'(t)$ passes through the linear element l , where p is the algebraic value of the electric dipole moment $p = Ql$ along Oz and p' is its derivative with respect to time. The dipole is oscillating, that is to say the dipole moment will be assumed to vary sinusoidally with time; using imaginary notation, $p = p_0 e^{i\omega t}$.

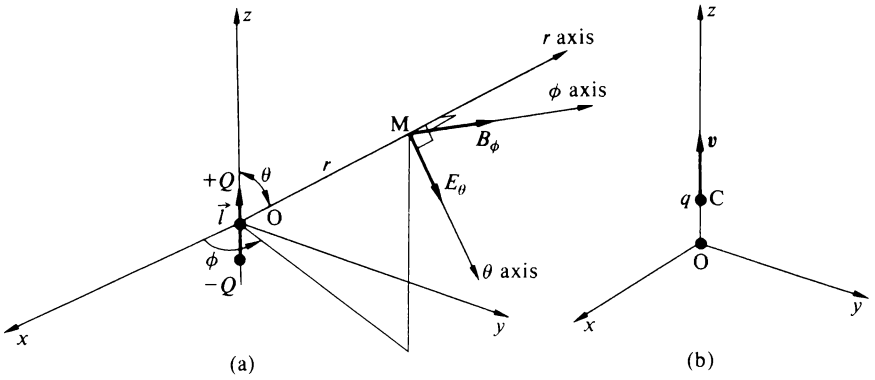


Figure A2.1

This problem is interesting from three points of view:

- (1) it leads to relatively simple calculations;
- (2) it allows an *exact* account of the theory of radiofrequency antennae to be given;
- (3) it may be applied as a *first approximation* to an isolated charge C of constant magnitude q moving with a non-relativistic velocity $v = dz/dt$ (see figure A2.1(b)); it is sufficient to put $p = qz$. The exact theory for the case of an isolated charge in motion utilises the Lienart–Wiechert potentials, but it is complicated and contains many correction terms in v/c .

A2.1.2 Retarded potentials

We calculate retarded potentials at a point M defined by the spherical coordinates r, θ, ϕ (see figure A2.1(a)).

(1) The vector potential

$$A(M, t) = \frac{\mu_0}{4\pi\kappa} \frac{I(t - r/c)}{r} \quad I = \frac{\mu_0}{4\pi\kappa} \frac{1}{r} p' \left(t - \frac{r}{c} \right)$$

This may be reduced to its component along the Oz axis

$$A_z(M, t) = \frac{\mu_0}{4\pi\kappa} \frac{1}{r} p' \left(t - \frac{r}{c} \right)$$

(2) The scalar potential may be obtained most simply from the Lorentz condition:

$$\frac{\partial V}{\partial t} = - \frac{\kappa}{\epsilon_0 \mu_0} \operatorname{div} A = - \frac{\kappa}{\epsilon_0 \mu_0} \frac{\partial A_z}{\partial z} = - \frac{\kappa}{\epsilon_0 \mu_0} \cos \theta \frac{\partial A_z}{\partial r}$$

By taking account of the fact that A_z depends on r both through the factor $1/r$ and through the factor $p(t - r/c)$, then integrating with respect to time, one obtains

$$V(M, t) = \frac{1}{4\pi\epsilon_0} \cos \theta \left[\frac{1}{r^2} p \left(t - \frac{r}{c} \right) + \frac{1}{rc} p' \left(t - \frac{r}{c} \right) \right]$$

A2.1.3 The radiation fields

Calculation of the fields may be carried out using the two equations

$$\mathbf{E} = -\text{grad } V - \frac{1}{\kappa} \frac{\partial \mathbf{A}}{\partial t}$$

and

$$\mathbf{B} = \text{curl } \mathbf{A}$$

In spherical co-ordinates, one obtains the components

$$\begin{cases} E_r(M, t) = \frac{1}{4\pi\epsilon_0} \cos \theta \left[\frac{2}{r^3} p \left(t - \frac{r}{c} \right) + \frac{2}{r^2 c} p' \left(t - \frac{r}{c} \right) \right] \\ E_\theta(M, t) = \frac{1}{4\pi\epsilon_0} \sin \theta \left[\frac{1}{r^3} p \left(t - \frac{r}{c} \right) + \frac{1}{r^2 c} p' \left(t - \frac{r}{c} \right) + \frac{1}{rc^2} p'' \left(t - \frac{r}{c} \right) \right] \\ E_\phi(M, t) = 0 \\ B_r(M, t) = 0 \\ B_\theta(M, t) = 0 \\ B_\phi(M, t) = \frac{\mu_0}{4\pi\kappa} \sin \theta \left[\frac{1}{r^2} p' \left(t - \frac{r}{c} \right) + \frac{1}{rc^2} p'' \left(t - \frac{r}{c} \right) \right] \end{cases}$$

At a sufficiently great distance r , the terms in $1/r$ in the expressions for E_θ and B_ϕ dominate. These terms are proportional to p'' , the second derivative of the electric dipole moment, and thus for an isolated charge, to its acceleration $a = d^2 z/dt^2$.

For sinusoidal motion, complex quantities are introduced

$$p(t) = p_0 e^{i\omega t}, \quad p'(t) = i\omega p, \quad p''(t) = -\omega^2 p$$

and hence the terms in $1/r$ become dominant when

$$r \gg c/\omega = \lambda/2\pi$$

(where λ is the wavelength corresponding to the frequency ω).

Making use of this condition, the radiation fields at large distances may be

written

$$\begin{cases} E_r \approx 0 \\ E_\theta \approx \frac{1}{4\pi\epsilon_0} \frac{\sin\theta}{rc^2} p'' \left(t - \frac{r}{c} \right) = -\frac{1}{4\pi\epsilon_0} \frac{\sin\theta}{r} \frac{\omega^2}{c^2} p_0 e^{i\omega t} e^{-i(\omega/c)r} \\ E_\phi = 0 \end{cases}$$

$$\begin{cases} B_r = 0 \\ B_\theta = 0 \\ B_\phi \approx \frac{\kappa}{c} E_\theta \end{cases}$$

It may easily be verified that in this approximation the fields at the point M are similar to those of a plane wave propagating in the direction of the radius vector r , the term in $e^{-i(\omega/c)r}$ representing the dephasing due to propagation.

Comment It can be shown that the same formulae are applicable in the non-relativistic approximation ($v \ll c$) to an isolated charge in any type of motion (non-rectilinear, and non-periodic), provided that the position of the charge is taken as the origin and the direction of its acceleration vector a at the time $(t - r/c)$ is taken as the Oz axis. It is then permissible to write $p''(t - r/c) = qa(t - r/c)$. The emission of a radiation field (of amplitude in $1/r$, relatively important at large distances) occurs every time an electric charge has an acceleration vector. This happens for instance when high energy electrons are suddenly stopped by collision in a metal (deceleration radiation or 'bremsstrahlung', see volume 1, section 7.3.1) or when high velocity electrons in a magnetic field are in uniform circular motion (synchrotron radiation).

A2.1.4 Total radiated power

The total power P radiated throughout space may be obtained by calculating by means of Poynting's vector the flux emerging from a sphere Σ (of large radius r)

$$\frac{\kappa}{\mu_0} \mathbf{E} \times \mathbf{B} \approx \frac{\kappa}{\mu_0} E_\theta B_\phi \frac{\mathbf{r}}{r} = \epsilon_0 c E_\theta^2 \frac{\mathbf{r}}{r}$$

At every point on the sphere Σ this vector is perpendicular to an element of area

$$dS = r^2 \sin\theta \, d\theta \, d\phi$$

and directed outwards such that

$$P = \iint_{\Sigma} \epsilon_0 c E_\theta^2 r^2 \sin\theta \, d\theta \, d\phi = \frac{1}{16\pi^2 \epsilon_0 c^3} \left[p'' \left(t - \frac{r}{c} \right) \right]^2 \int_0^{2\pi} d\phi \int_0^\pi \sin^3\theta \, d\theta$$

The product of the two integrals is $8\pi/3$, and one obtains

$$P = \frac{1}{6\pi\epsilon_0 c^3} p''^2 = \frac{1}{6\pi\epsilon_0 c^3} \omega^4 p^2 = \frac{1}{6\pi\epsilon_0 c^3} q^2 a^2$$

depending on whether p'' is replaced by $-\omega^2 p$ (the so-called oscillating dipole case) or by qa (as for an isolated charge q of acceleration a).

The power thus calculated is independent of the radius r of the sphere Σ ; whatever its size, the same quantity of energy crosses its surface in a given time interval.

A2.2 Application to an Elastically Bound Electron—Damping of Free Oscillations

The classical theory of radiation is based mainly on the results for the dipole reviewed above. We shall now go on to discuss some elementary aspects of the theory. We assume that an atomic electron whose position is defined by the radius vector r is bound by an elastic force proportional to r (the Thomson model; see comments in volume 1, sections 1.3.2 and 5.2.3)

$$f = -kr$$

If such an electron happens to be displaced from its equilibrium position, it carries out a spontaneous oscillatory motion, or free oscillation, with a natural frequency determined by the attractive force

$$\omega_0 = \sqrt{\left(\frac{k}{m}\right)}$$

(m is the mass of the electron)

We consider, for simplicity, linear motion in only one dimension; in imaginary notation

$$z = z_0 e^{i\omega_0 t}$$

Since this electron is accelerating, it generates an electromagnetic wave that is a function of its acceleration $a = d^2z/dt^2$, and that continuously carries away energy to infinity.

Using the results of the preceding section, we can calculate the *mean value* in time of the power transported by the wave

$$\bar{P} = \frac{1}{6\pi\epsilon_0 c^3} q^2 \omega_0^4 \bar{z}^2 = \frac{1}{6\pi\epsilon_0 c^3} q^2 \omega_0^4 \frac{z_0^2}{2}$$

On the other hand, it is known that an oscillator of mass m , of natural frequency ω_0 and of amplitude z_0 , stores an energy

$$W = \frac{1}{2} m \omega_0^2 z_0^2$$

(This result may be obtained by writing, for example, the kinetic energy of an oscillator as it passes through its equilibrium position, where the potential energy corresponding to the attractive force is zero.) To satisfy the principle of conservation of energy, the amplitude z_0 of the oscillations must gradually

decrease with time in such a way that the loss of energy W is exactly counter-balanced by the energy carried away by the wave

$$\frac{dW}{dt} = -\bar{P} = -\frac{1}{6\pi\epsilon_0 c^3} q^2 \omega_0^4 \frac{z_0^2}{2} = -\frac{q^2 \omega_0^2}{6\pi\epsilon_0 c^3 m} W$$

Thus the energy W obeys the differential equation

$$\frac{1}{W} \frac{dW}{dt} = -\frac{q^2 \omega_0^2}{6\pi\epsilon_0 c^3 m} = -\frac{1}{\tau}$$

where the constant representing the second term has been called $1/\tau$ with the dimensions of an inverse time.

Integration of this well-known differential equation shows that the energy W decreases exponentially with a time constant

$$W = W_0 e^{-t/\tau}$$

and by taking the square root of the energy, the variation of amplitude may be deduced

$$z_0 = C e^{-t/2\tau}$$

The amplitude decreases with twice the time constant. The oscillatory motion practically stops after a time of the order of τ , the time τ being called the lifetime of the oscillator.

The complete equation of motion of the electron, including this damping phenomenon, leads to a third-order differential equation. A simplified solution may be obtained to a good approximation by describing the damping as a viscous friction term; the differential equation for the free oscillation may then be written

$$\frac{d^2 z}{dt^2} + \gamma \frac{dz}{dt} + \omega_0^2 z = 0$$

which leads to the solutions

$$z = C \exp \left\{ \left[-\frac{\gamma}{2} \pm \sqrt{\left(\frac{\gamma^2}{4} - \omega_0^2\right)} \right] t \right\} \approx C \exp \left[\left(-\frac{\gamma}{2} \pm i\omega_0 \right) t \right] \quad \text{if } \gamma \ll \omega_0$$

in agreement with the results found above when $\gamma = 1/\tau$.

A2.3 Forced Oscillations of an Elastically Bound Electron

A2.3.1 Steady-state motion of the electrons

The differential equation written at the end of the preceding section is the same for the three co-ordinates of the electron and can be applied directly to the vector \mathbf{r} defining the position of the electron in space.

When the electron is subjected to the influence of an external sinusoidal electric field $\mathbf{E} = \mathbf{E}_0 e^{i\omega t}$, of fixed direction and frequency ω , different from ω_0 , the differential equation describing its motion becomes

$$\frac{d^2 \mathbf{r}}{dt^2} + \gamma \frac{d\mathbf{r}}{dt} + \omega_0^2 \mathbf{r} = \frac{q}{m} \mathbf{E} = \frac{q}{m} \mathbf{E}_0 e^{i\omega t}$$

From this the *steady-state* solution may be found directly

$$\mathbf{r} = \frac{1}{\omega_0^2 - \omega^2 + i\omega\gamma} \frac{q}{m} \mathbf{E}_0 e^{i\omega t} = \frac{q}{m} \frac{1}{\omega_0^2 - \omega^2 + i\omega\gamma} \mathbf{E}$$

If the electromagnetic wave of frequency ω propagates in a material medium containing N electrons per unit volume (all elastically bound and having the same natural frequency ω_0), an oscillating current density \mathbf{j} appears in this medium, such that

$$\mathbf{j} = Nq \frac{d\mathbf{r}}{dt} = \frac{Nq^2}{m} \frac{1}{\omega_0^2 - \omega^2 + i\omega\gamma} \frac{\partial \mathbf{E}}{\partial t}$$

A2.3.2 The complex refractive index and the coefficient of absorption

The Maxwell–Ampère equation

$$\text{curl } \mathbf{B} = \frac{\mu_0}{\kappa} \left(\epsilon_0 \frac{\partial \mathbf{E}}{\partial t} + \mathbf{j} \right)$$

may be written to take account of the motion of the electrons

$$\text{curl } \mathbf{B} = \frac{\mu_0}{\kappa} \epsilon_0 \left(1 + \frac{Nq^2}{m\epsilon_0} \frac{1}{\omega_0^2 - \omega^2 + i\omega\gamma} \right) \frac{\partial \mathbf{E}}{\partial t} = \frac{\mu_0}{\kappa} \epsilon_0 \epsilon_r \frac{\partial \mathbf{E}}{\partial t}$$

where we have put

$$\epsilon_r = 1 + \frac{Nq^2}{m\epsilon_0} \frac{1}{\omega_0^2 - \omega^2 + i\omega\gamma}$$

Thus we have expressed the Maxwell–Ampère equation in a form equivalent to that describing a dielectric medium with a complex relative dielectric constant ϵ_r . The theory of propagation of electromagnetic waves thus leads to the introduction of a complex refractive index $(n - ik)$ such that

$$\epsilon_r = (n - ik)^2 = n^2 - k^2 - 2ink \approx n^2 - 2ik$$

where we have made the following approximations

$$\begin{cases} \text{the real part of the refractive index } n \approx 1 \\ \text{the imaginary part of the refractive index } k \ll 1. \end{cases}$$

Equating real and imaginary parts of ϵ_r , then allows one to write

$$\left\{ \begin{array}{l} \text{real refractive index} \\ \text{imaginary refractive index} \end{array} \right. \quad \begin{array}{l} n = 1 + \frac{Nq^2}{2m\epsilon_0} \frac{\omega_0^2 - \omega^2}{(\omega_0^2 - \omega^2)^2 + \omega^2 \gamma^2} \\ k = \frac{Nq^2}{2m\epsilon_0} \frac{\omega\gamma}{(\omega_0^2 - \omega^2)^2 + \omega^2 \gamma^2} \end{array}$$

The curves of figures A2.2(a) and A2.2(b) show the changes of n and of k respectively as a function of the frequency ω of the incident electromagnetic

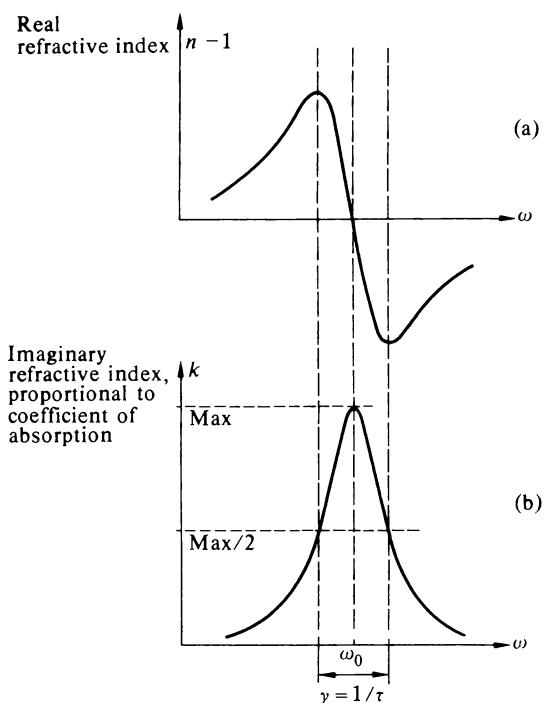


Figure A2.2

wave. The real refractive index n enables the phase velocity of the propagating waves to be calculated; it represents the normal refractive index. It should be noted that at high frequencies ($\omega > \omega_0$) the refractive index n becomes less than unity; this may be confirmed experimentally in the propagation of X-rays. The imaginary refractive index k enables the absorption coefficient of the electromagnetic wave in the medium under study to be calculated. We summarise this calculation as follows.

If one starts from the Maxwell–Ampère equation expressed in the form above and applies the theory of wave propagation, a solution may be obtained for a plane wave propagating parallel to the Ox axis

$$E(x, t) = A \exp\{i\omega[t - (n - ik/c)x]\}$$

or, by rearranging the terms

$$E(x, t) = A \exp[-k(\omega/c)x] \exp\{i\omega[t - (n/c)x]\} = E_0 \exp\{i\omega[t - (n/c)x]\}$$

where

$$E_0 = A \exp[-(\omega/c)kx]$$

This equation represents a wave that propagates with a phase velocity c/n and with a decreasing amplitude E_0 .

Its intensity E_0^2 is damped according to the exponential law

$$E_0^2 = A^2 \exp[-2(\omega/c)kx] = A^2 \exp^{(-Kx)}$$

with an absorption coefficient (see volume 1, section 3.1.2)

$$K = \frac{2\omega}{c} k = \frac{Nq^2}{m\epsilon_0 c} \frac{\omega^2 \gamma}{(\omega_0^2 - \omega^2)^2 + \omega^2 \gamma^2}$$

Thus we obtain a theoretical expression for the absorption coefficient K as a function of frequency. This description must be considered only as an outline; it can be improved by introducing several types of electrons having different natural frequencies.

A2.3.3 The absorption coefficient in the region of a natural frequency

The expression obtained for K can be simplified by making the following additional assumption

$$\gamma \ll \omega_0$$

This assumption is often true (it signifies that the oscillator has time to carry out many oscillations before dying away); under these conditions the absorption coefficient K is practically zero except in a narrow frequency interval around ω_0 . We can then make the approximation

$$|\omega_0 - \omega| \ll \omega_0$$

and

$$\omega_0 + \omega \approx 2\omega_0$$

Hence

$$K = \frac{2\omega k}{c} \approx \frac{Nq^2}{m\epsilon_0 c} \frac{\gamma}{4(\omega_0 - \omega)^2 + \gamma^2} = \frac{Nq^2}{16\pi^2 \epsilon_0 cm} \frac{\gamma}{(\nu_0 - \nu)^2 + (\gamma/4\pi)^2}$$

If the incident electromagnetic radiation has a continuous frequency spectrum, each frequency band is absorbed with a different coefficient $K(\nu)$. Some theories (see volume 1, section 3.1.4) involve what is called the total absorption, proportional to the area bounded by the curve in figure A2.2(b)

$$\int_0^{\infty} K(\nu) d\nu$$

To facilitate the evaluation of this definite integral, it should be noted that the coefficient $K(\nu)$ is practically zero when the frequency ν differs from the natural frequency ν_0 ; although having no physical meaning, we can write

$$\int_0^{\infty} K(\nu) d\nu \approx \int_{-\infty}^{+\infty} K(\nu) d\nu = \frac{Nq^2}{4\pi\epsilon_0 cm} \int_{-\infty}^{+\infty} \frac{(\gamma/4\pi) d\nu}{(\nu - \nu_0)^2 + (\gamma/4\pi)^2}$$

The latter integral may be evaluated by standard techniques in terms of an arctan, and may be shown to be equal to π . Hence the *total absorption* may be found

$$\int_0^{\infty} K(\nu) d\nu \approx \frac{Nq^2}{4\epsilon_0 cm}$$

This expression is utilised in section 7.4 to define oscillator strengths. It should be especially noted that the damping coefficient $\gamma = 1/\tau$ does not appear; this coefficient is a measure of the frequency width at half height of the absorption curve (see figure A2.2(b)); the area under the curve $K(\nu)$ has the same value whatever the causes of damping determining its width.

A2.3.4 Thomson scattering of X-rays

While investigating the laws for reflection of X-rays, Imbert and Bertin Sans, in 1896, demonstrated the existence of omnidirectional X-ray scattering. J. J. Thomson interpreted this effect as due to radiation from the electrons of the material, forced into oscillation by the incident radiation. In the case of X-rays, the frequency of the incident wave is far greater than the resonance frequency of the electrons, and thus the motion of the electrons can be written by simplifying the equation in section A2.3.1

$$\omega \gg \omega_0 \rightarrow \mathbf{r} = -\frac{q}{m\omega^2} \mathbf{E}$$

Each electron in motion behaves as an oscillating dipole of moment $\mathbf{p} = q\mathbf{r}$ and emits a radiation field. The electrons are distributed randomly in space and their separations are of the order of magnitude of the wavelength of the X-rays; under these conditions the phase differences between these various radiated fields are completely random and it is their intensities that are added. (These results are in complete contrast with those relating to the scattering of visible light by a condensed solid or liquid medium.)

Therefore, we obtain the total power P_s scattered by all the oscillating electrons simply by multiplying the contribution calculated for one of them as if it were isolated, by their total number $\mathcal{V}N$ (\mathcal{V} is the volume of a sample containing N electrons per unit volume)

$$P = \mathcal{V}N \frac{1}{6\pi\epsilon_0 c^3} \omega^4 q^2 r^2 = \mathcal{V}N \frac{q^4}{6\pi\epsilon_0 c^3 m^2} E^2$$

Let us assume that there are n atoms per unit volume in the scattering material and that each atom contains Z electrons (the atomic number), so that $N = Zn$.

Let us also assume that the incident beam of X-rays is a parallel beam of cross-sectional area S , so that the incident power transported is $P_i = S\epsilon_0 cE^2$.

Hence the ratio of energy scattered to energy incident is

$$\frac{P_s}{P_i} = \frac{\mathcal{V}}{S} Zn \frac{q^4}{6\pi\epsilon_0^2 c^4 m^2}$$

This ratio can be determined experimentally and, knowing n , the number of electrons per atom, Z can be deduced. Barkla in 1909 was the first to determine the value of Z by this method.

Comment I This result can be expressed in a slightly different way in terms of the absorption coefficient K . The scattered power P_s is equal and opposite to the change δP_i in the incident power as a result of passing through the scattering sample. If the latter fills the cross-section S of the incident beam over a distance δx (its volume is therefore $\mathcal{V} = S\delta x$), one finds

$$K = -\frac{1}{P_i} \frac{\delta P_i}{\delta x} = \frac{1}{\delta x} \frac{P_s}{P_i} = Zn \frac{q^4}{6\pi\epsilon_0^2 c^4 m^2}$$

The same formula can be calculated from the expression for K obtained at the end of section A2.3.2, by simplifying it using the assumption $\omega \gg \omega_0$

$$K \approx \frac{Nq^2}{\epsilon_0 cm\omega^2} \gamma$$

and then replacing γ by the expression calculated in section A2.2 for the case where the radiation is the only cause of damping of the electronic motion

$$\gamma = \frac{1}{\tau} = \frac{\omega^2 q^2}{6\pi\epsilon_0 c^3 m}$$

Comment II *Spatial distribution and polarisation of the scattered wave.* The wave radiated by each electron is not distributed isotropically; the amplitude of the field obeys the $\sin\theta$ law derived in section A2.1; thus the intensities obey a $\sin^2\theta$ law (θ being the angle between the dipole moment \mathbf{p} and the direction of observation). Hence the scattered power P_s must be distributed among the various directions of observation according to a $(1 + \cos^2\alpha)$ law, where α is the angle between the direction of observation and the direction of propagation Ox of the incident wave. This law is in excellent agreement with experimental measurements.

Besides this intensity variation, a greater variation in polarisation of the scattered wave is also observed, depending on the angle α , which may be explained completely by the classical theory. We shall consider only a simple case where the direction of observation Oy is perpendicular to the direction of propagation Ox of the incident wave: the forced oscillations are produced in the yOz plane. Dipoles in the Oz direction radiate in the Oy direction an electric field parallel to Oz , and dipoles in the Oy direction emit no waves in the Oy direction. This explains why the wave scattered in the Oy direction is 100 per cent linearly polarised: since half the dipoles do not contribute to this emission the wave is half as intense as it is in the forward or backward directions.

Comment III The case where $\omega \ll \omega_0$, on the other hand, is called Rayleigh scattering (in contrast with Thomson scattering). An example of this is the scattering of visible light by air molecules in the atmosphere. By simplifying the equation in section A2.3.1, a radius vector r is obtained independent of ω . The scattered power is then proportional to ω^4 .

Appendix 3

Multipole Moments

A3.1 Stationary Charges—Electric Multipole Moments

Statement of the problem and notation. A collection of charges q_n situated at points C_n are all in the region of a point C which will be taken as the origin (see figure A3.1):

$$CC_n = r_n \quad (\text{with components } x_n, y_n, z_n); \quad r_n = |r_n|$$

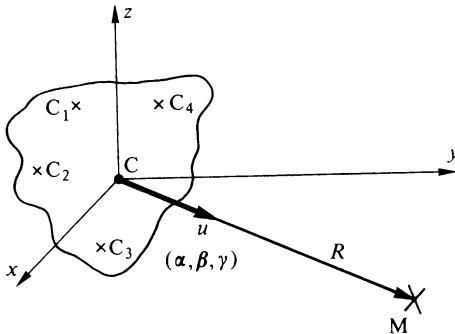


Figure A3.1

We investigate the interaction between the collection of charges C_n and other charges situated at points M at a great distance from C:

$$\mathbf{CM} = \mathbf{R} \quad (\text{with components } X, Y, Z); \quad R = |\mathbf{R}|$$

We shall assume that $R \gg$ all the r_n . The unit vector $\mathbf{u} = \mathbf{R}/R$ along CM will be introduced, the components of which are the direction cosines of the line CM: $\alpha = X/R$, $\beta = Y/R$, $\gamma = Z/R$.

A3.1.1 Calculation of the potential at M created by the collection of charges

$$V(\mathbf{M}) = \frac{1}{4\pi\epsilon_0} \sum_n \frac{q_n}{C_n \mathbf{M}}$$

To evaluate $1/C_n \mathbf{M}$, we form an expansion in terms of the small quantities x_n, y_n, z_n

$$\begin{aligned} \frac{1}{C_n \mathbf{M}} &= \frac{1}{\sqrt{[(X - x_n)^2 + (Y - y_n)^2 + (Z - z_n)^2]}} = f(X - x_n, Y - y_n, Z - z_n) \\ &= f(X, Y, Z) - x_n \frac{\partial f}{\partial X} - y_n \frac{\partial f}{\partial Y} - z_n \frac{\partial f}{\partial Z} + \frac{1}{2} x_n^2 \frac{\partial^2 f}{\partial X^2} + x_n y_n \frac{\partial^2 f}{\partial X \partial Y} \\ &\quad + \dots, \text{ etc.} \end{aligned}$$

$$f(X, Y, Z) = (X^2 + Y^2 + Z^2)^{-1/2} = 1/R$$

$$\left. \begin{aligned} \partial f / \partial X &= -X(X^2 + Y^2 + Z^2)^{-3/2} = -\alpha/R^2 \\ \partial f / \partial Y &= -Y(X^2 + Y^2 + Z^2)^{-3/2} = -\beta/R^2 \\ \partial f / \partial Z &= -Z(X^2 + Y^2 + Z^2)^{-3/2} = -\gamma/R^2 \end{aligned} \right\} \text{These are the components of the} \\ \text{vector } \text{grad } f = -\mathbf{u}/R^2$$

$$\partial^2 f / \partial X^2 = -(X^2 + Y^2 + Z^2)^{-3/2} + 3X^2(X^2 + Y^2 + Z^2)^{-5/2} = (3\alpha^2 - 1)/R^3$$

$$\partial^2 f / \partial X \partial Y = +3XY(X^2 + Y^2 + Z^2)^{-5/2} = 3\alpha\beta/R^3, \text{ etc.}$$

$$\frac{1}{C_n \mathbf{M}} = \frac{1}{R} \left[1 + \frac{r_n}{R} \mathbf{u} + \frac{x_n^2}{R^2} \left(\frac{3\alpha^2 - 1}{2} \right) + \frac{x_n y_n}{R^2} 3\alpha\beta + \dots, \text{ etc.} \right]$$

This form of the expression emphasises the order of magnitude of the successive terms. By adding the contributions of all the charges, one obtains

$$\begin{aligned} 4\pi\epsilon_0 V(\mathbf{M}) &= \frac{1}{R} (\sum q_n) + \frac{\mathbf{u}}{R^2} \cdot \left(\sum q_n \mathbf{r}_n \right) + \\ &\quad \frac{1}{2R^3} [(3\alpha^2 - 1)(\sum q_n x_n^2) + 6\alpha\beta(\sum q_n x_n y_n) + \dots, \text{ etc.}] \end{aligned}$$

Interpretation of the result

(1) When $\sum q_n \neq 0$, there exists a centre of gravity of the charges q_n at which the origin C can be placed; then $\sum q_n \mathbf{r}_n = 0$ and the second-order terms cancel out. The first term after the term in $1/R$ is the term in $1/R^3$ (a particular example is the nucleus of an atom).

(2) When $\sum q_n = 0$, the sum $\sum q_n \mathbf{r}_n$ is independent of the choice of origin C (from the theory of the centre of gravity) and therefore characterises the charge system completely.

This vector $\mathbf{p} = \sum q_n \mathbf{r}_n$ is called the electric dipole moment because the simplest way to set up such a system of charges is to choose two equal charges of opposite sign. (It is then possible to choose the origin and orientation of the axes such that the terms in $1/R^3$ cancel out.)

(3) When $\sum q_n = 0$ and $\sum q_n \mathbf{r}_n = 0$ simultaneously, the first non-zero terms are those in $1/R^3$. It may be easily shown that the coefficients of these six terms are then independent of the choice of origin C. The symmetric tensor of second order formed from these six coefficients $\sum q_n x_n^2$, $\sum q_n x_n y_n$ and so on, is called the electric quadrupole moment because the simplest example of one is to arrange four charges, equal in magnitude, placed at the corners of a parallelogram so as to form two dipoles in opposition (see figure A3.2). In section A3.3 we present a more detailed discussion of the quadrupole moment.

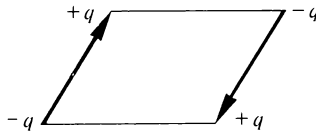


Figure A3.2

(4) Generally speaking, the set of coefficients expressing the term in $1/R^{n+1}$ is called the electric multipole moment of order 2^n , because the simplest way of cancelling the set of preceding terms is to choose a system of 2^n charges suitably positioned.

A3.1.2 Calculation of the forces applied to the collection of charges

This calculation is in some respects analogous to the preceding one. It enables the same multipole moments to be found in a slightly different way, but does not introduce any new fundamental concept.

It is well known that forces can be calculated by the method of virtual work, by deriving the interaction energy (see textbooks on classical electromagnetism). Here we shall merely calculate the interaction energy W between the collection of charges C_n and the other charges situated at points M far removed from C (all the $R \gg$ all the r_n). If we let $U(C_n)$ be the potential created at each point C_n by all the other charges, this interaction energy is $W = \sum q_n U(C_n)$.

Since the charges creating the potential U are all far from C, the potential U varies very little from one point C_n to another, and we can express $U(C_n)$ as an expansion around the origin C

$$U(C_n) = U(C) + x_n \frac{\partial u}{\partial x} + y_n \frac{\partial u}{\partial y} + z_n \frac{\partial u}{\partial z} + \frac{1}{2} x_n^2 \frac{\partial^2 u}{\partial x^2} + x_n y_n \frac{\partial^2 u}{\partial x \partial y} + \dots, \text{ etc.}$$

Summing over all the charges C_n , one obtains

$$W = U(C) (\sum q_n) + \text{grad } U \cdot (\sum q_n \mathbf{r}_n) + \frac{1}{2} \frac{\partial^2 u}{\partial x^2} (\sum q_n x_n^2) + \frac{\partial^2 u}{\partial x \partial y} (\sum q_n x_n y_n) \\ + \dots, \text{ etc.}$$

Consider orders of magnitude: U goes as $1/R$, $\text{grad } U$ goes as $1/R^2$ and the second-order derivatives in U go as $1/R^3$ and so on. As in the preceding section, the expansion is found to converge rapidly, and this expansion may be expressed in terms of components of the multipole moments that have already been defined.

A3.1.3 Field corresponding to the dipole term

We must calculate the gradient of the potential obtained in section A3.1.1, case (2)

$$V(M) = \frac{1}{4\pi\epsilon_0} \frac{\mathbf{p} \cdot \mathbf{u}}{R^2} = \frac{1}{4\pi\epsilon_0} \frac{\mathbf{p} \cdot \mathbf{R}}{R^3}$$

The vector $\mathbf{p} = \sum q_n \mathbf{r}_n$ is independent of M and hence: $\text{grad}(\mathbf{p} \cdot \mathbf{R}) = \mathbf{p}$. Furthermore,

$$\text{grad} \left(\frac{1}{R^3} \right) = -\frac{3}{R^4} \text{grad } R = -\frac{3}{R^4} \mathbf{u} = -\frac{3\mathbf{R}}{R^5}$$

$$\mathbf{E} = -\text{grad } V = \frac{1}{4\pi\epsilon_0} \left(\frac{3\mathbf{p} \cdot \mathbf{R}}{R^5} \mathbf{R} - \frac{1}{R^3} \mathbf{p} \right)$$

Hence, in particular, the interaction energy of the dipole \mathbf{p} with another dipole \mathbf{p}' placed at M is given by

$$W = \mathbf{p}' \cdot \text{grad } V = -\mathbf{p}' \cdot \mathbf{E} = -\frac{1}{4\pi\epsilon_0} \left[\frac{\mathbf{p} \cdot \mathbf{p}'}{R^3} - \frac{3(\mathbf{p} \cdot \mathbf{R})(\mathbf{p}' \cdot \mathbf{R})}{R^5} \right]$$

The latter formula has many applications in atomic physics.

A3.2 Charges in Motion—Magnetic Multipole Moments

Assumptions and notation. We shall consider the same collection of charges q_n as in section A3.1 but we shall assume that each of them has a velocity \mathbf{v}_n ; we propose to calculate the magnetic field created at a very distant point M ($R \gg r_n$ for all n).

This is a magnetostatics problem, that is to say (1) the velocities v_n are all much less than c , the velocity of light; (2) the mean distribution of the electrostatic charges is unchanged by this motion. (In the formalism of continuous functions, the equation for charge conservation relating the current density

\mathbf{j} to the charge density ρ may be written: $\text{div } \mathbf{j} = -\partial\rho/\partial t = 0$.) In the case of point charges, one may write that the various electric multipole moments of the charge collection are independent of time, or that their derivatives with respect to time are zero.

The following derivations can also be generally applied to systems of charges that do not obey the usual assumptions of magnetostatics, *provided that mean values in time are considered. One need then only assume that the charges remain enclosed within a bounded volume.*

Let $f(t) = \sum q_n x_n y_n$ be a function of the type we have to use (a component of an electric multipole moment). Let us calculate the mean value in time of its derivative with respect to time

$$\left(\overline{\frac{df}{dt}}\right) = \frac{1}{t_2 - t_1} \int_{t_1}^{t_2} \frac{df}{dt} dt = \frac{1}{t_2 - t_1} (f_2 - f_1)$$

Taking account of the additional assumption (bounded volume) the function f varies within finite limits; the quantity $f_2 - f_1$ is therefore finite and by lengthening the time interval $t_2 - t_1$, the mean value (df/dt) can be made as small as required. Hence, provided that mean values in time are considered, the derivative of the function f is zero and therefore the function f is constant in time. *In other words, any system of charges that remain enclosed in a bounded volume conforms on average with the assumptions of magnetostatics.*

This may be applied in particular to an atom or to a molecule. In this case, the time interval $t_2 - t_1$ over which an average must be calculated is of the order of a period of orbital motion of the electrons.

A3.2.1 Calculation of the magnetic field created by the system of charges

To calculate this from the vector potential

$$\mathbf{A}(\mathbf{M}) = \frac{\mu_0}{4\pi\kappa} \sum \frac{q_n \mathbf{v}_n}{C_n \mathbf{M}}$$

we use the same expansion of $1/C_n \mathbf{M}$ as in section A3.1, but the greater complexity of the calculation necessitates concentration on the first two terms

$$\frac{4\pi}{\mu_0} \mathbf{A}(\mathbf{M}) = \frac{1}{R} \left(\sum \frac{q_n \mathbf{v}_n}{\kappa} \right) + \frac{1}{R^2} \sum \left[\frac{q_n \mathbf{v}_n}{\kappa} (\mathbf{r}_n \cdot \mathbf{u}) \right] + \dots, \text{ etc.}$$

In the earlier electrostatic calculation, the second term in $1/R^2$ was found to have the simple form of a product between a part depending only on \mathbf{M} (that is, on \mathbf{u} and R) and another part depending only on the charge collection (that is, on q_n , \mathbf{r}_n , \mathbf{v}_n); but this is no longer the case—now we cannot take the vector \mathbf{u} outside the summation. However, a special technique allows this separation into two independent parts to be carried out.

Consider the vector identity

$$\mathbf{v}_n (\mathbf{r}_n \cdot \mathbf{u}) + \mathbf{r}_n (\mathbf{v}_n \cdot \mathbf{u}) = \frac{d\mathbf{r}_n}{dt} (\mathbf{r}_n \cdot \mathbf{u}) + \mathbf{r}_n \left(\frac{d\mathbf{r}_n}{dt} \cdot \mathbf{u} \right) = \frac{d}{dt} [\mathbf{r}_n (\mathbf{r}_n \cdot \mathbf{u})]$$

By choosing the Ox axis parallel to CM , that is, to \mathbf{u} , the three components of this vector may be written

$$\frac{d}{dt}(x_n^2), \quad \frac{d}{dt}(y_n x_n), \quad \frac{d}{dt}(z_n x_n)$$

By summing all these vectors multiplied by q_n , the three components

$$\frac{d}{dt}(\sum q_n x_n^2), \quad \frac{d}{dt}(\sum q_n x_n y_n), \quad \frac{d}{dt}(\sum q_n x_n z_n)$$

are obtained. According to our assumptions, these three components are zero (constancy of the quadrupole moment in time); therefore

$$\sum q_n \mathbf{v}_n(\mathbf{r}_n \cdot \mathbf{u}) + \sum q_n \mathbf{r}_n(\mathbf{v}_n \cdot \mathbf{u}) = 0$$

Furthermore, the difference between these same two vectors is a double-vector product

$$\sum q_n [\mathbf{v}_n(\mathbf{r}_n \cdot \mathbf{u}) - \mathbf{r}_n(\mathbf{v}_n \cdot \mathbf{u})] = \sum q_n (\mathbf{r}_n \times \mathbf{v}_n) \times \mathbf{u}$$

Hence

$$\sum q_n \mathbf{v}_n(\mathbf{r}_n \cdot \mathbf{u}) = \frac{1}{2} \sum q_n (\mathbf{r}_n \times \mathbf{v}_n) \times \mathbf{u} = \frac{1}{2} [\sum q_n \mathbf{r}_n \times \mathbf{v}_n] \times \mathbf{u}$$

In the double-vector product thus introduced we can take the vector \mathbf{u} outside the summation. Finally

$$\frac{4\pi}{\mu_0} \mathbf{A}(\mathbf{M}) = \frac{1}{R} \sum \frac{q_n \mathbf{v}_n}{\kappa} - \frac{\mathbf{u}}{R^2} \times \frac{1}{2} \sum \frac{q_n \mathbf{r}_n \times \mathbf{v}_n}{\kappa} + \dots, \text{ etc.}$$

Interpretation of the result

(1) When $\sum q_n \mathbf{v}_n \neq 0$, that is to say, where the charge collection is equivalent to a current element, an origin C' can be found such that the term in $1/R^2$ is zero.

Let us take the point C' as the origin such that $CC' = \mathbf{s}$. With this origin, the radius vectors become $\mathbf{r}_n' = \mathbf{r}_n - \mathbf{s}$ and we require $\sum q_n \mathbf{r}_n' \times \mathbf{v}_n = 0$, that is to say

$$\sum (q_n \mathbf{r}_n \times \mathbf{v}_n) - \mathbf{s} \times (\sum q_n \mathbf{v}_n) = 0$$

By projecting the above vector equation on to the axes, a system of three equations is obtained with three unknowns, s_x , s_y , s_z , components of the vector \mathbf{s} , which can thus be determined.

(2) When $\sum q_n \mathbf{v}_n = 0$, it may be shown that the vector $\sum q_n \mathbf{r}_n \times \mathbf{v}_n$ is independent of the choice of origin C . With C' as the origin, such that $\mathbf{r}_n' = \mathbf{r}_n - \mathbf{s}$, one obtains

$$\sum q_n \mathbf{r}_n' \times \mathbf{v}_n = \sum q_n \mathbf{r}_n \times \mathbf{v}_n - \mathbf{s} \times \sum q_n \mathbf{v}_n = \sum q_n \mathbf{r}_n \times \mathbf{v}_n$$

The vector

$$\mathcal{M} = \frac{1}{\kappa} \sum \frac{1}{2} q_n \mathbf{r}_n \times \mathbf{v}_n$$

is therefore a characteristic of the system of charges in motion. It is called the *magnetic dipole moment* of the system of charges.

This may be applied in particular to any isolated system of charges contained within a limited volume (as in an atom or molecule, for example) because the quantity

$$\sum q_n \mathbf{v}_n = \frac{d}{dt} (\sum q_n \mathbf{r}_n)$$

is the derivative of a quantity that remains fixed; the argument given above therefore shows that the *average value* of $\sum q_n \mathbf{v}_n$ is zero.

Comment The formula enabling the vector potential \mathcal{A} to be calculated from the vector \mathcal{M} is identical to that found in volume 1 when calculating the vector potential created at a large distance from a small electric circuit having a magnetic moment $\mathcal{M} = (1/\kappa) ISN$ (I is the current, S the area of the circuit and N a unit vector normal to the plane of the circuit).

(3) The expansion can be continued; in a similar way to the electrostatic calculation, a magnetic multipole moment of order 2^n may be defined from the term in $1/R^{n+1}$ of the expansion.

A3.2.2 Calculation of the magnetic forces applied to a system of charges in motion

This calculation is analogous to the preceding one; we assume that distant charges in motion create a magnetic induction $\mathbf{B}(C_n)$ at each charge C_n . Each charge C_n is subjected to a force

$$\mathbf{f}_n = \frac{1}{\kappa} q_n \mathbf{v}_n \times \mathbf{B}(C_n)$$

This set of forces has

$$\begin{cases} \text{a resultant } \mathbf{F} = \sum \mathbf{f}_n \\ \text{a resultant moment } \mathbf{\Gamma} = \sum \mathbf{r}_n \times \mathbf{f}_n \end{cases}$$

\mathbf{F} and $\mathbf{\Gamma}$ can be calculated by using the following expansion to express the induction $\mathbf{B}(C_n)$ at each charge C_n

$$\mathbf{B}(C_n) = \mathbf{B} + (\mathbf{r}_n \cdot \text{grad}) \mathbf{B} + \dots, \text{ etc.}$$

where \mathbf{B} is the value of the induction at the point C chosen as origin.

Here we shall calculate only the resultant moment. To calculate $\mathbf{\Gamma}$ to first order, only the first term of this expansion need be considered

$$\mathbf{\Gamma} \approx \sum \mathbf{r}_n \times \left(\frac{q_n}{\kappa} \mathbf{v}_n \times \mathbf{B} \right)$$

We wish to transform this expression in such a way as to be able to take \mathbf{B} outside the summation, and to do this we use a technique identical to that of the derivation in section A3.2.1.

$$\begin{aligned}\mathbf{r}_n \times (\mathbf{v}_n \times \mathbf{B}) &= \mathbf{v}_n(\mathbf{r}_n \cdot \mathbf{B}) - \mathbf{B}(\mathbf{r}_n \cdot \mathbf{v}_n) \\ \mathbf{v}_n \times (\mathbf{r}_n \times \mathbf{B}) &= \mathbf{r}_n(\mathbf{v}_n \cdot \mathbf{B}) - \mathbf{B}(\mathbf{r}_n \cdot \mathbf{v}_n)\end{aligned}$$

Subtracting

$$\mathbf{r}_n \times (\mathbf{v}_n \times \mathbf{B}) - \mathbf{v}_n \times (\mathbf{r}_n \times \mathbf{B}) = \mathbf{v}_n(\mathbf{r}_n \cdot \mathbf{B}) - \mathbf{r}_n(\mathbf{v}_n \cdot \mathbf{B}) = (\mathbf{r}_n \times \mathbf{v}_n) \times \mathbf{B}$$

Furthermore

$$\begin{aligned}\mathbf{r}_n \times (\mathbf{v}_n \times \mathbf{B}) + \mathbf{v}_n \times (\mathbf{r}_n \times \mathbf{B}) &= \mathbf{r}_n \times \left(\frac{d\mathbf{r}_n}{dt} \times \mathbf{B} \right) + \frac{d\mathbf{r}_n}{dt} \times (\mathbf{r}_n \times \mathbf{B}) \\ &= \frac{d}{dt} [\mathbf{r}_n \times (\mathbf{r}_n \times \mathbf{B})]\end{aligned}$$

By summing over n , the last term becomes

$$\frac{d}{dt} \sum_n [\mathbf{r}_n \times (\mathbf{r}_n \times \mathbf{B})]$$

which from our assumptions is zero. Therefore

$$\begin{aligned}\sum_n \mathbf{r}_n \times (\mathbf{v}_n \times \mathbf{B}) + \sum_n \mathbf{v}_n \times (\mathbf{r}_n \times \mathbf{B}) &= 0 \\ \sum_n \mathbf{r}_n \times (\mathbf{v}_n \times \mathbf{B}) - \sum_n \mathbf{v}_n \times (\mathbf{r}_n \times \mathbf{B}) &= (\mathbf{r}_n \times \mathbf{v}_n) \times \mathbf{B}\end{aligned}$$

Hence

$$\sum_n \mathbf{r}_n \times (\mathbf{v}_n \times \mathbf{B}) = \frac{1}{2} (\mathbf{r}_n \times \mathbf{v}_n) \times \mathbf{B}$$

and consequently, to first order, $\mathbf{I} = \mathcal{M} \times \mathbf{B}$. We have derived a formula well known in the case of small electric circuits.

A3.3 A Detailed Study of the Electric Quadrupole Moment

Sections A3.1 and A3.2 set out the main ideas concerning multipole moments. In the series expansions, we have concentrated principally on the terms in $1/R^2$ corresponding to electric or magnetic dipole moments, since use is made of these most often. However, the concept of an electric quadrupole moment is important in the characterisation of atomic nuclei and for this reason we are expanding our treatment of the subject.

Nuclei have very small but nevertheless finite dimensions. In many problems, they can be considered to a first approximation as point charges, but sometimes it is necessary to take account of the volume distribution of the nuclear charges. In such calculations the nucleus may be represented as a superposition of (1) a point charge placed at its centre of gravity (and therefore the term

corresponding to the dipole moment is zero: $\sum q_n \mathbf{r}_n = 0$); (2) an electric quadrupole. It is the quadrupole part that we discuss below.

A3.3.1 General definition and properties of the electric quadrupole tensor

(1) In section A3.1, we calculated the *potential created by a quadrupole* at a distance R in a direction having direction cosines α, β, γ ; it had the form

$$4\pi\epsilon_0 V = \frac{1}{2R^3} [(3\alpha^2 - 1)(\sum q_n x_n^2) + (3\beta^2 - 1)(\sum q_n y_n^2) + (3\gamma^2 - 1)(\sum q_n z_n^2) \\ + 6\alpha\beta(\sum q_n x_n y_n) + 6\beta\gamma(\sum q_n y_n z_n) + 6\gamma\alpha(\sum q_n z_n x_n)]$$

Since $x_n^2 + y_n^2 + z_n^2 = r_n^2$, one obtains

$$4\pi\epsilon_0 V = \frac{1}{2R^3} [3\alpha^2(\sum q_n x_n^2) + 3\beta^2(\sum q_n y_n^2) + 3\gamma^2(\sum q_n z_n^2) - \sum q_n r_n^2 \\ + 6\alpha\beta(\sum q_n x_n y_n) + \dots, \text{etc.}]$$

This expression is not homogeneous with respect to the direction cosines α, β, γ ; to make it homogeneous, the term $\sum q_n r_n^2$ is multiplied by the quantity $\alpha^2 + \beta^2 + \gamma^2 = 1$. The terms in α^2, β^2 and γ^2 can then be rearranged, and one obtains

$$4\pi\epsilon_0 V = \frac{1}{2R^3} [\alpha^2 \sum q_n (3x_n^2 - r_n^2) + \beta^2 \sum q_n (3y_n^2 - r_n^2) + \gamma^2 \sum q_n (3z_n^2 - r_n^2) \\ + 2\alpha\beta \sum (3q_n x_n y_n) + 2\beta\gamma \sum (3q_n y_n z_n) + 2\gamma\alpha \sum (3q_n z_n x_n)]$$

The six summations \sum that enter into this expression form the nine components of a symmetric tensor $\|Q\|$ of second order, defined as follows

$$\begin{cases} Q_{xx} = \sum q_n (3x_n^2 - r_n^2) \\ Q_{yy} = \sum q_n (3y_n^2 - r_n^2) \\ Q_{zz} = \sum q_n (3z_n^2 - r_n^2) \end{cases} \quad \begin{cases} Q_{xy} = Q_{yx} = \sum 3q_n x_n y_n \\ Q_{yz} = Q_{zy} = \sum 3q_n y_n z_n \\ Q_{zx} = Q_{xz} = \sum 3q_n z_n x_n \end{cases}$$

This tensor is usually called the electric quadrupole moment. The electric potential created by a system of charges can be written as a function of its components

$$4\pi\epsilon_0 V = \frac{1}{2R^3} (\alpha^2 Q_{xx} + \beta^2 Q_{yy} + \gamma^2 Q_{zz} + 2\alpha\beta Q_{xy} + 2\beta\gamma Q_{yz} + 2\gamma\alpha Q_{zx})$$

The matrix representing a tensor can be diagonalised, that is, new axes XYZ can be found, called the principal axes of the tensor, such that the off-diagonal components of the tensor are zero

$$Q_{XY} = Q_{YZ} = Q_{ZX} = 0$$

and the potential created by the charge system may be written simply

$$4\pi\epsilon_0 V = \frac{1}{2R^3} (\alpha^2 Q_{xx} + \beta^2 Q_{yy} + \gamma^2 Q_{zz})$$

(2) The electric quadrupole tensor also has the following properties

$$(a) \quad Q_{xx} + Q_{yy} + Q_{zz} = \sum q_n(3x_n^2 + 3y_n^2 + 3z_n^2) - 3 \sum q_n r_n^2 = 0$$

The sum of the diagonal components is zero whatever the co-ordinate axes. Of the nine components of the tensor, only five are independent: three parameters determine the orientation of the charge system in space, and only two parameters characterise the 'shape' of the charge distribution.

(b) If the charges q_n have a spherically symmetric distribution

$$\sum q_n x_n^2 = \sum q_n y_n^2 = \sum q_n z_n^2 = \frac{1}{3} \sum q_n r_n^2$$

and hence $Q_{xx} = Q_{yy} = Q_{zz} = 0$; the other components of the tensor are also zero. *The electric quadrupole tensor measures to some extent the departure from spherical symmetry of a collection of charges.*

(c) When a collection of charges is reduced to a pure electric quadrupole, that is when $\sum q_n = 0$ and $\sum q_n r_n = 0$ simultaneously, it may be shown that *the components of the tensor $\|Q\|$ are independent of the origin chosen for their calculation:*

Let C' be a new origin relative to which the co-ordinates are x_n', y_n', z_n' . The components of the vector CC' are denoted by a, b and c

$$\begin{aligned} \sum q_n x_n'^2 &= \sum q_n (x_n - a)^2 = \sum q_n x_n^2 - 2a \sum q_n x_n + a^2 \sum q_n = \sum q_n x_n^2 \\ \sum q_n x_n' y_n' &= \sum q_n (x_n - a)(y_n - b) = \sum q_n x_n y_n - a \sum q_n y_n - b \sum q_n x_n \\ &\quad + ab \sum q_n = \sum q_n x_n y_n \end{aligned}$$

(3) The components of the tensor also allow an expansion to be found for the interaction energy W between the collection of charges q_n and other external charges that create a potential U . In section A3.1, we found

$$\begin{aligned} W &= \frac{1}{2} \frac{\partial^2 U}{\partial x^2} (\sum q_n x_n^2) + \frac{1}{2} \frac{\partial^2 U}{\partial y^2} (\sum q_n y_n^2) + \frac{1}{2} \frac{\partial^2 U}{\partial z^2} (\sum q_n z_n^2) \\ &\quad + \frac{\partial^2 U}{\partial x \partial y} (\sum q_n x_n y_n) + \frac{\partial^2 U}{\partial y \partial z} (\sum q_n y_n z_n) + \frac{\partial^2 U}{\partial z \partial x} (\sum q_n z_n x_n) \end{aligned}$$

To extract the diagonal components of the tensor, a special property is used based on the fact that the laplacian of the electric potential is zero outside the charges which create this potential: $\Delta U = 0$.

Therefore we can omit from the expression for W , the quantity

$$0 = \Delta U (\sum q_n r_n^2) = \frac{1}{6} \frac{\partial^2 U}{\partial x^2} (\sum q_n r_n^2) + \frac{1}{6} \frac{\partial^2 U}{\partial y^2} (\sum q_n r_n^2) + \frac{1}{6} \frac{\partial^2 U}{\partial z^2} (\sum q_n r_n^2)$$

as it is zero. One then obtains

$$W = \frac{1}{6} \left(\frac{\partial^2 U}{\partial x^2} Q_{xx} + \frac{\partial^2 U}{\partial y^2} Q_{yy} + \frac{\partial^2 U}{\partial z^2} Q_{zz} + 2 \frac{\partial^2 U}{\partial x \partial y} Q_{xy} + 2 \frac{\partial^2 U}{\partial y \partial z} Q_{yz} + 2 \frac{\partial^2 U}{\partial z \partial x} Q_{zx} \right)$$

If the principal axes of the tensor, XYZ , are taken as co-ordinate axes, the off-diagonal components are zero and

$$W = \frac{1}{6} \left(\frac{\partial^2 U}{\partial X^2} Q_{XX} + \frac{\partial^2 U}{\partial Y^2} Q_{YY} + \frac{\partial^2 U}{\partial Z^2} Q_{ZZ} \right)$$

A3.3.2 Special case of rotational symmetry

(1) If the charge distribution has rotational symmetry around the OZ axis

$$\sum q_n X_n^2 = \sum q_n Y_n^2$$

and hence

$$Q_{XX} = Q_{YY} = -\frac{1}{2} Q_{ZZ}$$

The 'shape' of the charge distribution is now characterised only by a single parameter. In practice, it is useful to factorise the elementary charge $e = 1.6 \times 10^{-19}$ C out of the expression for Q_{ZZ} ; one then writes

$$Q_{ZZ} = \sum q_n (3Z_n^2 - r_n^2) = eQ$$

Rotational symmetry is met very frequently in practice and the parameter Q thus defined is usually called a quadrupole moment. It has the dimensions of area, and since the dimensions of nuclei are of the order of 10^{-14} m, it has a magnitude of the order of 10^{-28} m² (see end of this appendix and figure A3.5). The quadrupole moments Q are often measured in terms of a practical unit: 1 barn = 10^{-28} m².

Q can be positive or negative.

(a) For example, $Q > 0$ is obtained with a uniform density of positive charge within a prolate ellipsoid, that is, a nucleus elongated in the shape of a cigar.

(b) On the other hand, $Q < 0$ is obtained with a uniform density of positive charge within an oblate ellipsoid, that is a nucleus flattened into an oval shape (see figure A3.3).

(2) Taking account of rotational symmetry, the expressions given above for the potential V or the interaction energy W can be simplified still further, by taking as axes the principal axes XYZ of the quadrupole tensor.

(a) The potential V created at a distance R in a direction having direction

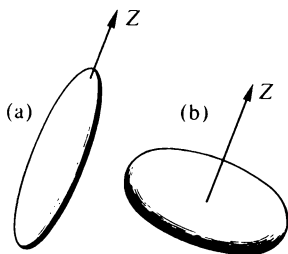


Figure A3.3

cosines α, β, γ may be simplified by taking account of the fact that $\alpha^2 + \beta^2 + \gamma^2 = 1$

$$4\pi\epsilon_0 V = \frac{eQ}{2R^3} \left(\gamma^2 - \frac{\alpha^2 + \beta^2}{2} \right) = \frac{eQ}{4R^3} (3\gamma^2 - 1) = \frac{eQ}{4R^3} (3 \cos^2 \theta - 1)$$

where θ is the angle between the symmetry axis OZ of the system of charges and the direction in which V is measured.

(b) The interaction energy W with other distant charges which create a potential U may be simplified by taking account of the fact that

$$\Delta U = \partial^2 U / \partial X^2 + \partial^2 U / \partial Y^2 + \partial^2 U / \partial Z^2 = 0$$

$$W = \frac{eQ}{6} \left[\frac{\partial^2 U}{\partial Z^2} - \frac{1}{2} \left(\frac{\partial^2 U}{\partial X^2} + \frac{\partial^2 U}{\partial Y^2} \right) \right] = \frac{eQ}{4} \frac{\partial^2 U}{\partial Z^2} = -\frac{eQ}{4} \frac{\partial E_z}{\partial Z}$$

where E_z is the component along the symmetry axis OZ of the electric field E created by the distant charges.

(3) The second derivatives of the potential U to which the quadrupole is subjected also form a symmetric tensor of second order. In many problems it is convenient to take as axes the principal axes of this new tensor related to the external potential U , that is axes xyz such that

$$\partial^2 U / \partial x \partial y = \partial^2 U / \partial y \partial z = \partial^2 U / \partial z \partial x = 0$$

If α, β, γ now denote the direction cosines of the quadrupole's symmetry axis OZ with respect to the axes xyz , it may be shown readily that

$$\frac{\partial}{\partial Z} \equiv \alpha \partial / \partial x + \beta \partial / \partial y + \gamma \partial / \partial z$$

(Note that α, β, γ here have a meaning different from that used previously.) Taking account of the fact that the second derivatives of U with respect to two different co-ordinates are zero, then

$$\partial^2 U / \partial Z^2 = \alpha^2 \partial^2 U / \partial x^2 + \beta^2 \partial^2 U / \partial y^2 + \gamma^2 \partial^2 U / \partial z^2$$

and it follows that the interaction energy is

$$W = \frac{eQ}{4} \left(\alpha^2 \frac{\partial^2 U}{\partial x^2} + \beta^2 \frac{\partial^2 U}{\partial y^2} + \gamma^2 \frac{\partial^2 U}{\partial z^2} \right)$$

Since the laplacian of U is zero, its three second derivatives depend only on two independent parameters. The usual choice is to express $\partial^2 U/\partial x^2$ and $\partial^2 U/\partial y^2$ as a function of $\partial^2 U/\partial z^2$ by means of a parameter η defined as follows

$$\frac{\partial^2 U}{\partial x^2} - \frac{\partial^2 U}{\partial y^2} = \eta \frac{\partial^2 U}{\partial z^2}$$

(η is zero if the function U has rotational symmetry around Oz ; η is to some extent a measure of the departure of the function U from rotational symmetry.)

Knowing that $\partial^2 U/\partial x^2 + \partial^2 U/\partial y^2 = -\partial^2 U/\partial z^2$, then

$$\frac{\partial^2 U}{\partial x^2} = -\frac{1-\eta}{2} \frac{\partial^2 U}{\partial z^2}; \quad \frac{\partial^2 U}{\partial y^2} = -\frac{1+\eta}{2} \frac{\partial^2 U}{\partial z^2}$$

By substituting into W and remembering that $\alpha^2 + \beta^2 + \gamma^2 = 1$ one obtains

$$W = \frac{eQ}{4} \frac{\partial^2 U}{\partial z^2} \left(\gamma^2 - \frac{\alpha^2 + \beta^2}{2} + \eta \frac{\alpha^2 - \beta^2}{2} \right) = \frac{eQ}{8} \frac{\partial^2 U}{\partial z^2} [3\gamma^2 - 1 + \eta(\alpha^2 - \beta^2)]$$

This expression is used in several problems. It may be simplified if the potential U also has rotational symmetry around Oz , because then $\eta = 0$ and one obtains

$$W = \frac{eQ}{8} \frac{\partial^2 U}{\partial z^2} (3\gamma^2 - 1) = \frac{eQ}{8} \frac{\partial^2 U}{\partial z^2} (3 \cos^2 \theta - 1)$$

where θ is the angle between the symmetry axis OZ of the quadrupole and the symmetry axis Oz of the potential U in which it is situated. It should not be forgotten that in the latter part of this section, the symbols α , β and γ do not have the same meaning as in paragraph (2) and all previous sections.

A3.3.3 Equivalence between a quadrupole moment and a system of four point charges

A system of charges may be reduced to a quadrupole moment if two conditions are fulfilled simultaneously

$$\begin{cases} \sum q_n = 0 & \text{(zero total charge)} \\ \sum q_n \mathbf{r}_n = 0 & \text{(zero dipole moment)} \end{cases}$$

The simplest way of fulfilling these two conditions is to take four charges arranged in a parallelogram so as to form two equal and opposite dipoles.

If the XYZ axes are to be the principal axes of the quadrupole tensor, it is

simplest to place these four charges on the axes: thus each of the charges has two co-ordinates equal to zero, thereby ensuring that the products $X_n Y_n$, $Y_n Z_n$, $Z_n X_n$ are all zero, and therefore that $Q_{XY} = Q_{YZ} = Q_{ZX} = 0$. This leads to a diamond-like arrangement of the charges as in figure A3.4:

- (1) two equal charges on the OZ axis, each of magnitude q and situated at the same distance c on either side of the origin;
- (2) two equal charges on the OX axis, each of magnitude $-q$ and situated at the same distance a on either side of the origin.

One then finds

$$Q_{XX} = -2q(2a^2 + c^2), \quad Q_{YY} = 2q(a^2 - c^2), \quad Q_{ZZ} = +2q(a^2 + 2c^2)$$

(It may be verified that $Q_{XX} + Q_{YY} + Q_{ZZ} = 0$.)

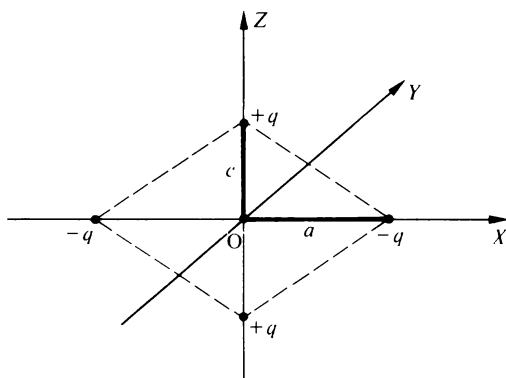


Figure A3.4

When values are given to Q_{XX} , Q_{YY} and Q_{ZZ} , the OY axis is selected such that the corresponding component has a value intermediate between the two others ($Q_{XX} \leq Q_{YY} \leq Q_{ZZ}$); the three equations above then provide two independent linear equations with two unknowns a^2 and c^2 , which can thus be determined

$$a^2 = -\frac{2Q_{XX} + Q_{ZZ}}{6q} \quad c^2 = \frac{Q_{XX} + 2Q_{ZZ}}{6q}$$

With our chosen convention, the two quantities $2Q_{XX} + Q_{ZZ}$ and $Q_{XX} + 2Q_{ZZ}$ have opposite signs and the solution of the system of equations is always possible (the magnitude of q remains arbitrary). Thus it is always possible to find four point charges equivalent to a given quadrupole moment. (An infinite number of systems of four charges corresponding to the same quadrupole moment can be found. The one we have studied is the simplest to calculate.)

When the charge system has rotational symmetry, we have seen that

$$Q_{XX} = -\frac{1}{2}Q_{ZZ}$$

It may then be shown that $a = 0$. In other words, two of the four point charges are coincident midway between the two others, in such a way that all the charges are aligned along the symmetry axis OZ . If the absolute value of the point charges is chosen to be equal to the elementary charge e , one obtains

$$Q_{zz} = eQ = \pm 4ec^2$$

The \pm sign depends on the sign of Q_{zz} and Q ; the two cases are illustrated in figure A3.5. It will be noted that in both cases the absolute value $|Q|$ of the quadrupole moment is equal to the area of the square whose side is the separation $2c$ of the two charges furthest apart.

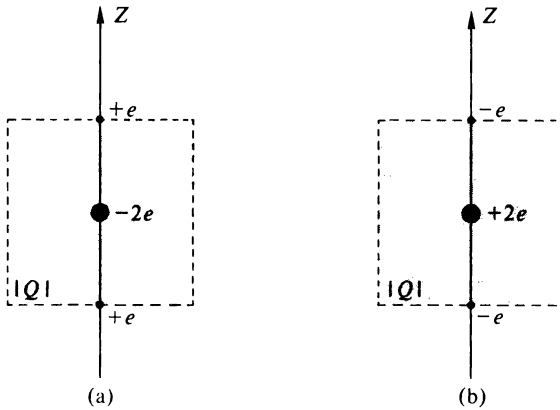


Figure A3.5 (a) $Q > 0$ (nucleus elongated like a cigar); (b) $Q < 0$ (nucleus flattened like a pancake)

Appendix 4

Non-Relativistic Elastic Collisions

Two particles that interact during a collision form an isolated system to which the laws of conservation of energy and momentum may be applied. It may easily be shown that these laws are valid in all galilean frames; they are particularly simple to apply in the centre of mass frame because the total momentum there is zero. We reviewed the properties of the centre of mass C at the beginning of volume 1, section 5.1.1 and we retain the same notation.

	Radius vectors of the two particles		Velocities of the two particles	
In the laboratory	OM_1	OM_2	$V_1 = v_1 + V$	$V_2 = v_2 + V$
In the centre of mass frame	$r_1 = -\frac{m_2}{m_1 + m_2} r$	$r_2 = \frac{m_1}{m_1 + m_2} r$	$v_1 = -\frac{m_2}{m_1 + m_2} v$	$v_2 = \frac{m_1}{m_1 + m_2} v$

{ where $r = r_2 - r_1$ and $v = dr/dt = v_2 - v_1 = V_2 - V_1$ (relative velocity),
and where V is the velocity of the centre of mass in the laboratory frame.

From conservation of kinetic energy (the collisions are *elastic*)

$$m_1 v_1^2 + m_2 v_2^2 = \text{constant}$$

From conservation of momentum

$$m_1 \mathbf{v}_1 + m_2 \mathbf{v}_2 = 0$$

$$\left. \begin{array}{l} \left. \begin{array}{l} v_1 = \text{constant} \\ v_2 = \text{constant} \end{array} \right\} \right\} \begin{array}{l} \text{in magnitude } m_1 v_1 = m_2 v_2 \\ \text{the direction of } \mathbf{v}_1 \text{ is} \\ \text{always opposite to } \mathbf{v}_2 \end{array}$$

Hence the magnitude v of the relative velocity also remains constant. Figure A4.1 summarises the results obtained in the centre of mass frame. In it, quantities after the collision are labelled with a 'prime': $v_1 = v'_1$; $v_2 = v'_2$ and $v = v'$.

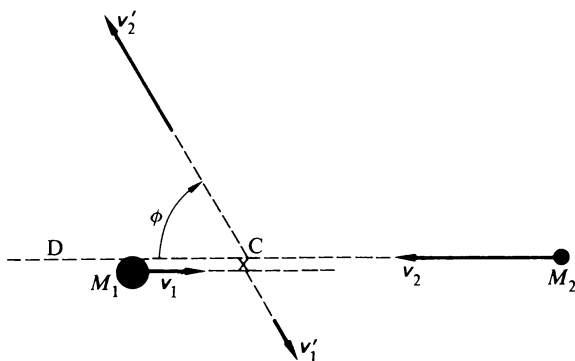


Figure A4.1

The only quantity that remains undetermined is the angle of deviation ϕ . This may be calculated as a function of the impact parameter (the distance between the two lines colinear with the vectors \mathbf{v}_1 and \mathbf{v}_2) if the interaction law between the two particles is known (see volume 1, chapter 5, Rutherford's experiment).

Special case where a projectile meets a stationary target. The initially stationary target is particle number 1. Since $\mathbf{V}_1 = 0$ one finds

$$\left\{ \begin{array}{l} v = V_2 \\ \mathbf{V} = \frac{m_2}{m_1 + m_2} \mathbf{V}_2 = \frac{m_2}{m_1 + m_2} \mathbf{v} \end{array} \right.$$

After the collision, the velocities in the laboratory are
for the target

$$\mathbf{V}'_1 = \mathbf{v}'_1 + \mathbf{V} = \frac{m_2}{m_1 + m_2} (\mathbf{v} - \mathbf{v}')$$

for the projectile

$$V'_2 = v'_2 + V = \frac{m_1}{m_1 + m_2} v' + \frac{m_2}{m_1 + m_2} v$$

It should be remembered that the two vectors v' and $v = V_2$ have the same magnitude.

(1) If the target is much heavier than the projectile

$$m_1 \gg m_2 \rightarrow \begin{cases} V'_1 \approx 0 \\ V'_2 \approx v', \text{ with a relative error of the order of } m_2/m_1 \end{cases}$$

the projectile keeps almost all of its kinetic energy and its angle of deviation in the laboratory frame is nearly equal to ϕ .

(2) If the masses of the target and of the projectile are of the same order of magnitude, the angle of deviation χ observed in the laboratory frame must be determined. To do this, we project the velocity vectors on to a line D parallel to the initial velocity V_2 and on to a perpendicular line (see figure A4.2).

	Initial relative velocity v	Final relative velocity v'	Final velocity of projectile V'_2
Projection on D (parallel to V_2)	v	$v \cos \phi$	$\frac{m_1}{m_1 + m_2} v \cos \phi + \frac{m_2}{m_1 + m_2} v$
Projection on a perpendicular line	0	$v \sin \phi$	$\frac{m_1}{m_1 + m_2} v \sin \phi$

Hence the angle of deviation χ in the laboratory frame is given by

$$\tan \chi = \frac{m_1 \sin \phi}{m_1 \cos \phi + m_2} = \frac{\sin \phi}{\cos \phi + m_2/m_1}$$

It is confirmed that $\chi \approx \phi$ when $m_2/m_1 \ll 1$.

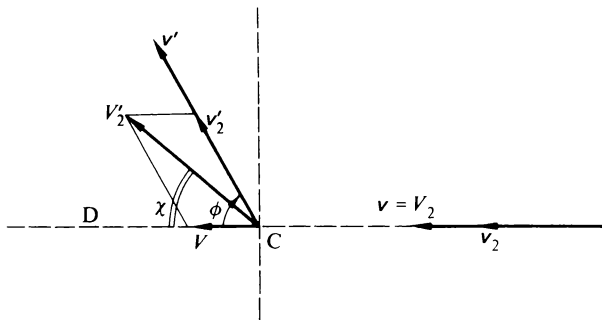


Figure A4.2

Appendix 5

The Representation of Vector and Scalar Operators. The Wigner–Eckart Theorem

Here we state the important properties of the matrix elements of scalar or vector operators. We use the $\{J^2, J_z\}$ representation, the basis vectors being denoted by $|Jm\rangle$.

The commutator $[A, B]$ will be taken as

$$[A, B] = \frac{AB - BA}{i}$$

A5.1 The Matrix Elements of a Scalar Operator A

A scalar operator A is by definition invariant under rotation. Let \mathcal{R} be a rotation operator. A system previously described by a basis state $|a\rangle$ is described after rotation by a basis state $|a'\rangle$. Rotational invariance implies that

$$\langle a|A|a\rangle = \langle a'|A|a'\rangle \quad \text{where} \quad |a'\rangle = \mathcal{R}|a\rangle$$

This relationship may be rewritten

$$\langle a|A|a\rangle = \langle a|\mathcal{R}^{-1}A\mathcal{R}|a\rangle$$

Hence

$$A = \mathcal{R}^{-1} A \mathcal{R} \quad \text{or} \quad \mathcal{R} A = A \mathcal{R} \quad (\text{A5.1})$$

Let us take \mathcal{R} as an infinitesimal rotation through an angle $\delta\omega$ around an axis defined by the unit vector \mathbf{u} . \mathcal{R} may then be written (see a textbook on quantum mechanics, for example, Messiah, page 531)

$$\mathcal{R} = 1 - i(\mathbf{J} \cdot \mathbf{u}) \delta\omega \quad (\text{A5.2})$$

Equation (A5.1) becomes

$$A \mathcal{R} = \mathcal{R} A \quad (\text{A5.3})$$

The scalar operator A commutes with the angular momentum operator, and in particular

$$A J_z = J_z A \quad (\text{A5.4})$$

which in matrix form may be written

$$\langle J m' | A J_z | J m \rangle = \langle J m' | J_z A | J m \rangle$$

Let us evaluate these matrix elements by using the matrix multiplication rule

$$\sum_{J'' m''} \langle J m' | A | J'' m'' \rangle \langle J'' m'' | J_z | J m \rangle = \sum_{J'' m''} \langle J m' | J_z | J'' m'' \rangle \langle J'' m'' | A | J m \rangle$$

Since the matrix of J_z is diagonal

$$\langle J'' m'' | J_z | J m \rangle = m \delta_{m'' m} \delta_{J'' J}$$

the above expression reduces to

$$\langle J m' | A | J m \rangle (m' - m) = 0$$

Therefore the matrix elements of A will be different from zero only if $m = m'$.

By considering the operator $J_+ = J_x + iJ_y$, equation (A5.3) leads to

$$A J_+ = J_+ A$$

which in matrix form can be written, for particular elements

$$\langle J, m+1 | A J_+ | J m \rangle = \langle J, m+1 | J_+ A | J m \rangle$$

Evaluating this relationship by using the matrix multiplication rule and taking account of the value of the matrix elements of J_+ (refer to a textbook on quantum mechanics), this equation may be reduced to

$$\langle J, m+1 | A | J, m+1 \rangle = \langle J m | A | J m \rangle$$

Therefore all the diagonal elements of the matrix A are equal and consequently independent of m .

To summarise, the matrix of a scalar operator A is diagonal, and all its elements are equal (spherical matrix).

A5.2 The Matrix Elements of a Vector Operator \mathbf{A}

A5.2.1

Let us consider a vector \mathbf{A} with components A_x, A_y, A_z . By applying a rotation of angle $\delta\omega$ around the direction of a unit vector \mathbf{u} , we obtain the vector

$$\mathbf{A}' = \mathbf{A} + \delta\omega(\mathbf{u} \times \mathbf{A}) \quad (\text{A5.5})$$

If we denote the matrix elements of the operator \mathbf{A} before rotation by $\langle a|\mathbf{A}|a\rangle$ and after rotation by $\langle a'|\mathbf{A}|a'\rangle$, equation (A5.5) may be written

$$\langle a'|\mathbf{A}|a'\rangle = \langle a|\mathbf{A}|a\rangle + \delta\omega \cdot \mathbf{u} \times \langle a|\mathbf{A}|a\rangle$$

From this, one deduces that

$$\mathcal{R}^{-1}\mathbf{A}\mathcal{R} = \mathbf{A} + \delta\omega(\mathbf{u} \times \mathbf{A}) \quad (\text{A5.6})$$

For the infinitesimal rotation defined by (A5.2), the first term in equation (A5.6) may be written

$$\mathcal{R}^{-1}\mathbf{A}\mathcal{R} = (1 + i\mathbf{J} \cdot \mathbf{u} \delta\omega) \mathbf{A} (1 - i\mathbf{J} \cdot \mathbf{u} \delta\omega) = \mathbf{A} - i\delta\omega[\mathbf{A}(\mathbf{J} \cdot \mathbf{u}) - (\mathbf{J} \cdot \mathbf{u})\mathbf{A}]$$

which, after simplification, becomes

$$\boxed{[\mathbf{A}, \mathbf{J} \cdot \mathbf{u}] = \mathbf{u} \times \mathbf{A}} \quad (\text{A5.7})$$

Several commutation relations may be deduced from (A5.7). Let us illustrate this with respect to the component A_z . For this component, (A5.7) may be written

$$[A_z, \mathbf{J} \cdot \mathbf{u}] = u_x A_y - u_y A_x \quad (\text{A5.8})$$

This relationship must be true for any unit vector \mathbf{u} ; hence

$$[A_z, J_z] = 0 \quad (\text{A5.9a})$$

$$[A_z, J_x] = A_y \quad (\text{A5.9b})$$

$$[A_z, J_y] = -A_x \quad (\text{A5.9c})$$

Similar commutation relations may be obtained with A_x and A_y .

A5.2.2

Let us write the relation (A5.9a) $A_z J_z - J_z A_z = 0$ in matrix form

$$\langle Jm'|A_z J_z|Jm\rangle = \langle Jm'|J_z A_z|Jm\rangle \quad (\text{A5.10})$$

After multiplying the matrices and taking account of the values of the matrix elements of J_z , equation (A5.10) may be written

$$\langle Jm'|A_z|Jm\rangle(m - m') = 0$$

Therefore A_z is a diagonal matrix.

A5.2.3

Let us consider the vector operator $A_+ = A_x + iA_y$; from equation (A5.7) it may be shown without difficulty

$$[A_+, J_z] = [A_x + iA_y, J_z] = -A_y + iA_x = iA_+$$

Thus

$$A_+ J_z - J_z A_+ = -A_+ \quad (\text{A5.11})$$

After multiplying the matrices and taking account of the value of the matrix elements of J_z , we obtain

$$\langle Jm' | A_+ | Jm \rangle (m - m' + 1) = 0$$

The only non-zero matrix elements of A_+ are elements such that

$$m' = m + 1$$

A5.2.4

From equation (A5.7), we can evaluate the commutator $[A_+, J_+]$

$$[A_+, J_+] = [A_x + iA_y, J_x + iJ_y] = -A_z + A_z = 0$$

so that

$$A_+ J_+ = J_+ A_+ \quad (\text{A5.12})$$

Using the property of the matrix elements of A_+ derived in section A5.2.3 and the values of the matrix elements of J_+ , equation (A5.12) may be written

$$\begin{aligned} \langle J, m + 2 | A_+ | J, m + 1 \rangle \langle J, m + 1 | J_+ | J, m \rangle &= \langle J, m + 2 | J_+ | J, m + 1 \rangle \\ &\times \langle J, m + 1 | A_+ | J, m \rangle \end{aligned}$$

so that

$$\frac{\langle J, m + 2 | A_+ | J, m + 1 \rangle}{\langle J, m + 1 | A_+ | J, m \rangle} = \frac{\langle J, m + 2 | J_+ | J, m + 1 \rangle}{\langle J, m + 1 | J_+ | J, m \rangle} \quad (\text{A5.13})$$

Equation (A5.13) is true only if the matrix elements of A_+ and J_+ are proportional to each other; if a is a constant of proportionality, we may write

$$\boxed{\langle J, m + 1 | A_+ | J, m \rangle = a \langle J, m + 1 | J_+ | J, m \rangle} \quad (\text{A5.14})$$

A5.2.5

From equation (A5.7) we can also write

$$[A_z, J_+] = -iA_+$$

so that

$$A_z J_+ - J_+ A_z = A_+$$

Using equation (A5.14) this leads to the equation

$$\begin{aligned} &\langle J, m+1 | A_z | J, m+1 \rangle \langle J, m+1 | J_+ | J, m \rangle - \langle J, m+1 | J_+ | J, m \rangle \\ &\quad \times \langle J, m | A_z | J, m \rangle = a \langle J, m+1 | J_+ | J, m \rangle \end{aligned}$$

Simplified, this expression may be written

$$\langle J, m+1 | A_z | J, m+1 \rangle - \langle J, m | A_z | J, m \rangle = a \quad (\text{A5.15})$$

Equation (A5.15) can be satisfied only if the matrix element $\langle Jm | A_z | Jm \rangle$ is of the following form

$$\langle Jm | A_z | Jm \rangle = am + b$$

where b is a scalar. Let us prove that b is zero, by evaluating the trace of A_z

$$\text{Tr } A_z = \sum_{m=-J}^{m=+J} \langle Jm | A_z | Jm \rangle = \sum_{-J}^{+J} (am + b) = (2J + 1)b$$

However, from equation (A5.7), we can write

$$A_z = [A_x, J_y] = \frac{1}{i} (A_x J_y - J_y A_x)$$

As a result of a general property of the trace of a product

$$\text{Tr } AB = \text{Tr } BA$$

from which $\text{Tr } A_z = 0$ and thus $b = 0$.

Therefore we have $\langle Jm | A_z | Jm \rangle = am$, which can be written

$$\langle Jm | A_z | Jm \rangle = a \langle Jm | J_z | Jm \rangle \quad (\text{A5.16})$$

To summarise, the relationships (A5.14) and (A5.16) may be stated as follows.

In the $\{J^2, J_z\}$ representation, in a subspace corresponding to a given value of J in which the basis vectors are represented by $|Jm\rangle$, the matrix elements of the components of vector operators are proportional, the coefficient of proportionality being the same for the various components; this may be written

$$\langle Jm' | A | Jm \rangle = a \langle Jm' | J | Jm \rangle \quad (\text{A5.17})$$

A5.3 The Wigner–Eckart Theorem

This theorem generalises the property we have just established in the case of vector operators to that of ‘irreducible tensor operators’, entities that cannot be defined here, but of which vector operators are a particular case.

The Wigner–Eckart theorem states (see, for example, A. Messiah, *Quantum Mechanics*, page 489):

In a standard representation $\{J^2, J_z\}$ whose basis vectors are represented by $|\tau J, m\rangle$, the matrix element $\langle Jm | T_q^k | J'm' \rangle$ of the q th standard component of an irreducible tensor operator T^k of given order k is equal to the product

of the Clebsch–Gordan coefficient $\langle J' km' q | Jm \rangle$ and a quantity independent of m, m' and q

$$\langle \tau Jm | T_q^k | \tau' J' m' \rangle = \langle \tau J \| T^k \| \tau' J' \rangle \langle J' km' q | Jm \rangle$$

The quantity $\langle \tau J \| T^k \| \tau' J' \rangle$ is the reduced matrix element of the tensor operator. The factor $1/\sqrt{(2J+1)}$ introduced by Messiah has been deliberately suppressed here by adopting a different normalisation.

Vector operators are irreducible tensor operators of order $k=1$; the components q (an index that can take the values $-1, 0, +1$) are the standard components of vector operators, that is to say, if A is a vector operator

$$A_{-1} = -\frac{1}{\sqrt{2}}(A_x + iA_y) \quad A_0 = A_z \quad A_1 = \frac{1}{\sqrt{2}}(A_x - iA_y)$$

Applied in this way, the reader may easily verify that the relationship (A5.17) is a particular case of the general theorem stated above, the quantity independent of m, m' and q being a constant.

A5.3.1

Application of the Wigner–Eckart theorem: for example, property (2) stated in section 5.3.2. Let us successively apply the Wigner–Eckart theorem to the components A_q and J_q of the vector operators A and J

$$\begin{aligned} \langle \tau Jm | A_q | \tau' J' m' \rangle &= \langle \tau J \| A \| \tau' J' \rangle \langle J' 1m' q | Jm \rangle \\ \langle \tau Jm | J_q | \tau' J' m' \rangle &= \langle \tau J \| J \| \tau' J' \rangle \langle J' 1m' q | Jm \rangle \end{aligned}$$

The reduced matrix element of J is zero when $J \neq J'$, in contrast to the reduced matrix element of A . When $J = J'$, we can compare the matrix elements of A and J by using the above relations

$$\langle \tau Jm | A_q | \tau' Jm' \rangle = \frac{\langle \tau J \| A \| \tau' J \rangle}{\langle \tau J \| J \| \tau' J \rangle} \langle \tau Jm | J_q | \tau' Jm' \rangle \quad (\text{A5.18})$$

The reduced matrix element $\langle \tau J \| A \| \tau' J \rangle$ is a scalar quantity, completely independent of m . It may be written as proportional to the various matrix elements of the scalar operator $J \cdot A$ which are all equal to one another for $m = m'$, and equal to zero for $m \neq m'$ (see section A5.1); thus

$$\langle \tau J \| A \| \tau J \rangle = c \langle \tau Jm \| J \cdot A \| \tau Jm \rangle \quad (\text{A5.19})$$

the coefficient c being independent of A .

To determine the value of c , we apply the Wigner–Eckart theorem to the particular matrix element $\langle \tau J J | J_z | \tau' J J \rangle$ which has the value J

$$J = \langle \tau J J | J_z | \tau' J J \rangle = \langle \tau J \| J \| \tau' J \rangle \langle J 1 J 0 | J J \rangle$$

Using the value of the Clebsch–Gordan coefficient

$$\begin{aligned}\langle J1J0|JJ\rangle &= \sqrt{\left(\frac{J}{J+1}\right)} \\ \langle \tau J \| J \| \tau' J \rangle &= \sqrt{[J(J+1)]}\end{aligned}\tag{A5.20}$$

Now let us apply equation (A5.19) to the case $\mathbf{A} \equiv \mathbf{J}$; since the matrix elements of \mathbf{J}^2 are equal to $J(J+1)$, we deduce the value of c :

$$c = \frac{1}{\sqrt{[J(J+1)]}}\tag{A5.21}$$

By substituting into equation (A5.18) the reduced matrix element of \mathbf{J} given by (A5.20) and the reduced matrix element of \mathbf{A} given by (A5.19), and taking account of the expression for c , equation (A5.21), we obtain

$$\boxed{\langle \tau J m | \mathbf{A}_q | \tau' J m' \rangle = \frac{\langle \tau J m | \mathbf{J} \cdot \mathbf{A} | \tau' J m \rangle}{J(J+1)} \langle \tau J m | J_q | \tau' J m' \rangle}\tag{A5.22}$$

This formula, (A5.22), provides us with an expression for the coefficient of proportionality a in equation (A5.17), as a function of the scalar operator $\mathbf{J} \cdot \mathbf{A}$.

Appendix 6

Historical Summary of Atomic Physics

A6.1 The Existence of the Atom and Avogadro's Number

Proust's law of definite proportions, 1801.

Dalton's law of multiple proportions, 1807.

Gay-Lussac's law of combination by volume, 1808.

Avogadro's hypothesis, 1811.

The Avogadro–Ampère law, 1814

Interpretation of Boyle's law by Bernoulli, 1738.

Brownian motion, 1827.

Clausius' kinetic theory of gases, 1857; Maxwell, 1860.

Scattering of light: Tyndall, 1868; Rayleigh, 1871.

Boltzmann's law, 1896.

Atomic beams: Dunoyer, 1911; Stern, 1920.

Measurements of \mathcal{N}

(1) From statistical laws

The interpretation of Van der Waals equation and the viscosity of gases, 1875.

Thermal radiation: Planck, 1900.

Brownian motion: Jean Perrin, 1907.

Critical opalescence: Smoluchowski, 1908.

Scattering of light by a gas: Cabannes, 1913.

(2) From the charge of the electron $-e$ compared to 1 faraday: Millikan, 1908.

(3) By counting α -particles and measuring simultaneously:
 the volume of helium liberated } Rutherford, Geiger, Regener, Mme.
 the period of disintegration } Curie, about 1910.

(4) From atomic dimensions

Diffraction of X-rays: Röntgen, 1895; von Laue, 1912; Bragg, 1914;
 Debye-Scherrer, 1915; Siegbahn, Compton, 1925.

Monomolecular surface layers: Devaux, Langmuir, 1917; Marcellin.

A6.2. Identification of the Electron

Volta's battery, 1800.

Laws of electrolysis: Faraday, 1833.

(Maxwell's equation, 1855.)

Cathode rays: Hittorf, 1869; canal rays: Goldstein, 1886.

The theory of ions: Arrhenius, 1887.

Transport of negative charge by cathode rays: Jean Perrin, 1895.

The Zeeman effect ($\Delta\omega = eB/m$), 1896.

Direct measurement of e/m for cathode rays: J. J. Thomson, 1897.

Lorentz's theory of the electron, 1897.

Direct measurement of e : Millikan, 1908.

Thermionic diode: Fleming, 1904. Triode: Lee de Forest, 1907; improved by
 Langmuir, 1915.

Measurement of e from fluctuations in thermionic emission: Hull and Williams,
 1925 (from Schottky's formula, 1918).

Measurement of e by counting particles and measurement of the charge
 transported.

Measurement of e/m for free electrons within a metal: Tolman and Stewart,
 1916.

Measurement of e/m from the cyclotron frequency ($\omega = eB/m$): the Lawrence
 cyclotron, 1933; Purcell and Gardner, 1950; Sommer, Thomas and Hipple,
 1950.

Measurement of e/m by electron magnetic resonance: Rabi, 1938; Zavoisky,
 1945.

A6.3 Quantisation of Radiated Energy

(The measurements of h are marked with an asterisk.)

Kirchhoff's laws of thermal radiation, 1859.

Stefan's law (1879); theoretical justification by Boltzmann, 1884.

The photoelectric effect: Hertz, 1887; Halbwachs, 1888.

The spectral distribution of thermal radiation: Wien, 1893.

Quantum explanation by Planck, 1900.

*Confirmation by Lummer and Pringsheim, 1901 (volume 1, section 1.1).

Einstein's explanation of the photoelectric effect, 1905 } volume 1,

*Confirmation and measurement of h : Millikan, 1915 } section 1.2.

(Quantum theory of specific heats: Einstein, 1907; Debye-Born and von Karman, 1912.)

*(Specific heats of solids at low temperatures: Keesom and Kamerlingh Onnes.)

*The limit of the continuous spectrum in X-ray emission: Duane and Hunt, 1915 (volume 1, section 7.3).

*The Compton effect, 1922; Gingrich's measurements, 1930 (volume 1, section 2.3).

*Wavelength for annihilation of an electron and a positron: Du Mond, 1952.

A6.4 Atomic Structure

(The measurements of h are marked with an asterisk.)

Periodic table, 1869 (section 2.4).

Balmer's hypothesis, 1885, transformed by Rydberg, 1889 (volume 1, section 1.3).

Lenard's observation of cathode rays passing through apertures, 1894.

The Zeeman effect, 1896 (volume 1, sections 8.4 and 11.3 and volume 2, chapter 5).

Ionisation potentials: Lenard, 1902 (volume 1, section 1.4).

The theory of paramagnetism: Langevin, 1905 (volume 1, sections 9.2 and 10.4).

Wood's optical resonance experiment, 1905 (volume 1, section 1.3).

The combination principle: Ritz, 1908 (volume 1, section 1.3).

Measurement of the atomic number by scattering of X-rays: Barkla, 1909 (appendix 2).

Existence of the nucleus: Rutherford, Geiger and Marsden, 1911 (volume 1, section 5.2).

The existence of isotopes: J. J. Thomson, 1913. The mass spectrograph: Aston, 1920.

*The Bohr atom (interpretation of Rydberg's constant), 1913 (volume 1, section 6.1).

*Resonance potentials: Franck and Hertz, 1913 (volume 1, section 1.4).

Moseley's law, 1913 (volume 1, section 7.4).

X-ray absorption spectra: Maurice de Broglie, 1916 (volume 1, section 7.1).

The theory of X-ray emission spectra: Kossel, 1917 (volume 1, section 7.3).

X-ray photoelectrons: Maurice de Broglie, 1921; Robinson, 1923 (volume 1, section 7.2).

Gyromagnetic experiments: Barnett, 1914; Einstein-de Haas, 1915 (volume 1, section 9.3).

*The Stern and Gerlach experiment, 1921 (volume 1, section 10.1).

The Paschen–Back effect, 1921 (section 5.4).

The Landé factor, 1923 (volume 1, section 10.2 and section 5.3).

The hypothesis of spin: Uhlenbeck and Goudsmit, 1925 (volume 1, chapter 12).

Pauli's exclusion principle, 1925 (volume 1, section 7.3 and section 2.3).

The direct measurement of the spin magnetic moment of free electrons

- | | |
|--|----------------------------|
| (1) in an electron beam, polarised by scattering: Louisell,
Pidd and Crane, 1954; | } volume 1,
chapter 12. |
| (2) by magnetic resonance: Dehmelt, 1958. | |

A6.5 Nuclear Magnetism

Existence of the hyperfine structure of spectral lines: Michelson, 1891;
Fabry and Perot, 1897; Lummer and Gehrcke, 1903.

The hypothesis of a nuclear magnetic moment: Pauli, 1924; Russel, Meggers
and Burns, 1927.

A detailed explanation of hyperfine structure in terms of nuclear spin: Back
and Goudsmit, 1927 (section 6.5).

The hypothesis of neutron spin: Heisenberg, 1932.

Measurement of the magnetic moment of the proton: Stern, 1933 (section 6.1).

Nuclear magnetic resonance on atomic beams: Rabi, 1938 (volume 1,
section 10.5).

Measurement of the magnetic moment of the neutron: Alvarez and Bloch,
1940 (section 6.1).

Electronic detection of nuclear magnetic resonance: Bloch, 1946; Purcell,
1946 (volume 1, section 9.5).

A6.6 Wave Mechanics and Quantum Mechanics

Bohr's correspondence principle, 1923.

Matter waves $\lambda = h/mv$: Louis de Broglie, 1923 (volume 1, section 4.4).

Schrödinger's equation, 1925.

Heisenberg's matrix mechanics, 1925.

Commutation laws: Born and Jordan, 1925.

Probabilistic interpretation: Born, 1926.

The uncertainty principle: Heisenberg, 1927 (volume 1, section 4.2).

Diffraction of electrons by a crystal: Davisson and Germer, 1927.	} (volume 1, section 4.4)
Diffraction of molecules: Stern, 1932.	

Fresnel diffraction of electrons: Boersch, 1940.

The relativistic wave theory of the electron: Dirac, 1928.

The anomalous spin magnetic moment: Kusch and Foley, 1947 (volume 1,
sections 12.1 and 12.2).

Energy difference between the $2S_{1/2}$ and $2P_{1/2}$ levels of hydrogen: Lamb and
Retherford, 1947 (chapter 4).

Bibliography

Historical

Perrin, J. *Les Atomes*, Presses universitaires, Paris (1924).

General Books Covering Experimental History and Theory

Jacquinet, P. *Optique quantique*, Hermann.

Rouault, M. *Physique atomique*, Armand Colin.

Lopes, L. *Fondements de la physique atomique*, Hermann.

Born, M. *Atomic Physics*, Blackie, London. 8th ed. (1969).

Peaslee, D. C., and Mueller, H. *Elements of Atomic Physics*, Prentice Hall, New York (1955).

Fano, U., and Fano, L. *Physics of Atoms and Molecules: an Introduction to the Structure of Matter*, University of Chicago Press (1972).

Richtmyer, F., Kennard, E., and Cooper, J. *Introduction to Modern Physics*, 6th ed., McGraw-Hill, New York (1969).

Theoretical Books

Matthews, P. T. *Introduction to Quantum Mechanics*, McGraw-Hill, New York. 2nd ed. (1968).

- Ayant, Y., and Belorizky, E. *Cours de Mécanique quantique*, Dunod.
- Messiah, A. *Quantum Mechanics*, North-Holland, Amsterdam (1961–2).
- Barchewitz, P. *Spectroscopie atomique et moleculaire*, Masson.
- Durand, E. *Mécanique quantique*, Masson.
- Merzbacher, E. *Quantum Mechanics*, Wiley. 2nd ed. (1970).
- Eyring, H., Walter, J., and Kimball, G. E. *Quantum Chemistry*, Wiley, New York (1954).
- Bohm, D. *Quantum Theory*, Prentice Hall, London (1960).

Discussions of the Significance of Quantum Mechanics

- Bohr, N. *Atomic Physics and Human Knowledge*, Wiley, New York (1958) (Articles).
- d'Espagnat, B. *Conception de la physique contemporaine*, Hermann.
- Margenau, H. *The Nature of Physical Reality*, McGraw-Hill, New York (1950).

Specialised Books Giving Fuller Explanations of the Ideas Presented in This Book

The corpuscular and wave nature of light (volume 1) :

Selected reprints of the American Institute of Physics :

Quantum and Statistical Aspects of Light

Mössbauer Effect

Masers and Optical Pumping

Emission and absorption of photons (volume 1, chapter 3) :

Mitchell, A., and Zemansky, M. *Resonance Radiation and Excited Atoms*, Cambridge (1934).

X-rays and the spectroscopy of electrons (volume 1, chapter 7) :

Compton, A., and Allison, S. *X-Rays in Theory and Experiments*, Macmillan, London (1935).

Guinier, A. *Cristallographie*, Dunod.

Siegbahn, K. *Alpha, Beta and Gamma Ray Spectroscopy*, North-Holland, Amsterdam (1965), 2 vols.

Siegbahn, K., and collaborators, ESCA. *Atomic, Molecular and Solid State Structure by means of Electron Spectroscopy*, Amqvist and Wiksell, Uppsala (1967).

Magnetism in general and magnetic resonance (volume 1) :

Herpin, A. *Theorie du magnetisme*, P.U.F.

de Broglie, L. *La spectroscopie en radiofrequences*, Revue d'Optique, Paris.

- Freymann, R. and Soutif, M. *Spectroscopie hertzienne*, Dunod.
Grivet, P. *Resonance magnetique nucléaire*, C.N.R.S.
Andrew, E. R. *Nuclear Magnetic Resonance*, Cambridge (1955 and 1958).
Abragam, A. *The Principles of Nuclear Magnetism*, Clarendon Press, Oxford (1961).
Pake, G. E. *Paramagnetic Resonance*, Benjamin, New York (1962).
Selected reprints of the American Institute of Physics: *Atomic and Molecular Beam Spectroscopy*.

Atomic and molecular spectroscopy (volume 2) : n.m.r. and e.p.r.

- Bousquet, P. *Instrumental Spectroscopy*, Dunod, Paris (1969).
Bruhat, G., and Kastler, A. *Optique*, Masson.
Bopp, E., and Kleinpoppen, H. *Physics of One and Two Electron Atoms*, North-Holland, Amsterdam (1969).
Kuhn, H. G. *Atomic Spectra*, Longmans, London (1969).
White, H. E. *Introduction to Atomic Spectra*, McGraw-Hill, New York (1934).
Herzberg, G. *Molecular Spectra and Molecular Structure*, Volume I: *Spectra of Diatomic Molecules*, Van Nostrand, New York (1939), 2nd ed., Toronto (1950).

Two Series Presenting Modern Developments in Atomic Physics (chapter 7) :

- Advances in Atomic and Molecular Physics* (Edited by D. Bates and I. Estermann) (five published volumes), Academic Press, New York (1965).
Methods of Experimental Physics (Edited by L. L. Marton) (eight published volumes), Academic Press, New York (1959-).

Index

Numbers in roman refer to pages in *Fundamental Principles*; numbers in italic refer to pages in *Quantum Theory and its Applications*.

- Absorption, classical theory of 208
 coefficient of 68
 cross-section 66, 177
 of γ -rays 58
 of X-rays 169
 optical resonant 18, 56
 self- 73
- Alkali atoms, effective quantum numbers 19
 quantum model of 17
 spectroscopy of 61
 Zeeman and Paschen-Back effects in 105
- Alkaline earth atoms, spectroscopy of 65
- Alpha particles, scattering of 145
- Alvarez and Bloch 115
- Amplification of a wave 110
- Angular momentum, as a characteristic of an atomic state 39, 53
 composition of 40, 119
 for motion due to a central force 144
 in a centre of mass frame 143
 of a complete sub-shell 42
 of a ground state 42
 of a nucleus 113
 of a photon 273, 168
 of radiation 266
 orbital 159, 164, 245, 40
 quantisation of 159, 164, 245, 40
 quantum number 246
 relationship of, to magnetic moment 208
 spin 291, 41
- Angular part of a wave function 3
- Atomic beam, as a light source 145
 speed of 263
 suppression of the Doppler effect in 145
 used in, measurement of lifetimes 77
 population inversion (maser) 112
 Rabi's experiment 257, 163
 Stern and Gerlach experiment 239
- Atomic number, and periodic (Mendeleev) table 37
 Barka's measurement of 212
 Chadwick's measurement of 154
 Moseley's law of 186
- Auger effect 175, 182
- Avogadro's number 36
- Back and Goudsmit effect 118
- Balmer 14, 15, 17, 160, 197
- Barkla 48, 212
- Barnett 219
- Basov and Prokhorov 113
- Beam-foil spectroscopy 175
- Beth 271
- Binding energy of atomic electrons 171, 184
- Black-body radiation 3, 85
- Bloch and Alvarez 115
- Bloch equations (magnetic resonance) 226
- Bloch method of detection (magnetic resonance) 232
- Bloembergen 113
- Bohr-Coster diagram 187
- Bohr hypothesis 14, 257
- Bohr magneton 248
- Bohr model of an atom 158, 13
- Boltzmann constant 36
- Boltzmann proof of Stefan's law 44
- Boltzmann thermal equilibrium 83, 111, 212, 251, 156
- Brackett 17, 161
- Bragg diffraction of X-rays 136, 169
- Bragg and Pierce, experimental law of 171
- Breit 292, 136
- Bremsstrahlung 62, 177, 205
- Brillouin 251
- de Broglie, Maurice (X-rays) 172
- de Broglie wavelength 129
- Brossel 284, 161
- Brück 78
- Carrara 273
- Casimir, equation of 126
- Central potential or force, motion under a 144
 quantum mechanical treatment of 1
- Centre of mass 142
- Chadwick 154
- Chemical properties of elements 35
- Circular polarisation (of a wave), angular momentum 270
 in magnetic resonance 273
 in the Zeeman effect 282
 interaction of, with a crystalline plate 266
- Classical theory, of diamagnetism 201
 of magnetic resonance 223
 of multipole moments 214
 of radiation 79, 202
 of radiation pressure 37
 of the elastically bound electron 206
 of the Zeeman effect 203
 planetary model 141
- Coherence, of atomic excitation 148
 spatial, of a wave 123
 temporal, of a wave 126
- Coherence time 126, 154, 162
- Collisions, elastic and inelastic 27
 non-relativistic elastic 229
 of electrons 24-34, 183-7
 of hard spheres 66
 of photons 48-64
 probability of 67
 various types of, process 181
- Collision cross-section 66, 178
- Combination principle 14
- Compton 48
- Configuration, electronic 25-38

- Conservation, of angular momentum 215
of energy 3-36
of momentum 270-90
- Constant, Curie 253, 256
fine-structure 161
fundamental 34-6
Rydberg; *see* Rydberg
screening 186
- Contact potential 10
- Contact term 124
- Core polarisation 20, 124
- Correspondence principle 162
- Coster, Bohr and 187
- Coulomb, law of 201
non-, potential 16
- Coulomb potential 151, 2
- Coupling, hyperfine (I - J) 119, 132
j-*j* 51, 73
L-*S* 48, 53, 68
spin-orbit 43
- Crane 295
- Critical potentials 32
- Cross-section, and absorption coefficient 68, 181
and transition probability 70
differential 148, 179
hard-spheres collision 66
total 68, 180
- Crystal diffraction 135, 169
- Crystalline plate, interaction of, with a polarised wave 266
- Curie (law and constant of) 253, 258
- Cyclotron frequency 201, 297
- Damped wave train 79, 101
- Damping, of an oscillator 206
radiation 207
- Deceleration radiation 177, 205
- Degeneracy 164, 250, 8, 16, 19, 30
- Dehmel 299, 167, 169
- Deuteron (nucleus of deuterium) 116
- Deutsch 191
- Diamagnetism 201
- Dicke 154
- Diffraction, of electrons 136
of neutrons 136
of X-rays 169
- Dipole, electrostatic 216
magnetic 220
oscillating (classical theory) 202
transition; *see* Transition
- Dipole moment; *see* Electric dipole moment
and Magnetic moment
- Dirac 292, 78
- Dispersion (classical theory of) 207
- Doppler effect, in γ -ray spectroscopy 60
in optical spectroscopy 21, 144
in radiofrequency spectroscopy 154
- Duality, wave-corpucle 87
- Doublet (energy level) 50
- Duane and Hunt 177
- Dunoyer 240
- Einstein and de Haas experiment 213
- Einstein equation (photoelectric effect) 8
- Einstein theory of radiation 80
- Elastic collisions, and inelastic 27, 63
non-relativistic 229
of photons 48
- Elastically bound electron; *see* Electron
- Electric dipole moment, of the electron and of the neutron 187
general discussion of 216
- Electric quadrupole moment, general discussion of 216, 221
of a nucleus 125
- Electromagnetism, absorption and dispersion 208
general formulae of 200
multipole moments 214
oscillating dipole (radiating) 202
oscillator strength 73, 170
polarised wave passing through a crystalline plate 266
radiation pressure 37
Thomson and Rayleigh scattering 211, 213
- Electrostatic selector 184
- Electrons, associated wavelength of 129
collisions of, with atoms 24-34
collisions of, with photons 50
conduction (or free) 27
elastically bound 20, 79, 80, 206, 207
interference of 129
mass of 36
outer 17, 61
valence 36
- Electron bombardment 24-34, 183-7
- Electron diffraction 136
- Electron paramagnetic (or spin) resonance (e.p.r. or e.s.r.) 234
- Electron spin 291
- Electron volt 34
- Electronic configuration 25-38
- Electronic orbit; *see* Orbit
- Electronic shell and sub-shell 27, 29
- Elliptic orbits 164
- Emission, in cascade 76, 174
induced or stimulated 80, 108, 260, 155
of γ -rays 58
resonant 15, 31, 57
spontaneous 73, 173
superradiant 118
thermal 3, 13, 83
- Energy, binding, of atomic electrons 171, 184
Bohr's quantisation of 159
exchanged, in collisions 27, 53, 62
extraction or escape 8, 171
hyperfine coupling 119, 122
ionisation 12, 24, 34
magnetic 195
photon 5, 8
resonance 29, 56
spin-orbit coupling 43, 62, 66
units of 34
- Energy density, and number of photons 68, 87
and radiation pressure 41, 42
and transition probabilities 71, 72
of thermal radiation 3
- Energy level diagram, of hydrogen 17
of mercury 72
of sodium 64

- Energy levels, crossing of 105, 147
 deep (X-rays) 182, 82
 enumeration of 53
 excited 20
 experimental evidence for 31
 ground 19
 of hydrogen (Bohr's theory) 14, 17, 158
 of hydrogen (in quantum mechanics) 8
 hyperfine 118
 of mercury 72
 of sodium 64
 theoretical discussion of 47
- Equivalent electrons 54
- Esterman, Frisch and Stern 113
- Exchange, effect of 24, 74
- Excitation, by collisions with electrons 24, 183
 by optical resonance 18, 56
 coherent 148
 probability and cross-section 71, 178
- Exclusion principle 183
- Extraction energy (or escape energy) 8, 9, 171
- Fabry-Perot (use in lasers) 117, 120
- Faget and Fert 129
- Fermi, contact term 124
- Field, induced 109
 'intermediate' 104, 135
 'motional' 188
 radiation (classical theory) 202
 relativistic transformation 43
- Fine structure 164, 189, 49
 of hydrogen 164
- Fine-structure constant 161
- Fluorescence optical 18, 19
 X-ray 175
- Foley and Kusch 293
- Fourier transform 98
- Frame of reference; *see* Reference frame
- Franck and Hertz 27, 28, 32
- Franken 150, 154
- Frequency, cyclotron 201, 297
 Larmor 200, 210
 of orbital motion 162
 resonance 18, 56
 threshold; *see* Threshold
- Frisch, Esterman and Stern 113
- Fundamental constants 34, 35
- Gamma rays, absorption of 59
 and the Mössbauer effect 58
 emission of 58
- Gaussian system of units xiv, 200
- Geiger and Marsden 153
- Gerlach, Stern and 239, 137
- Gorter, de Haas and Vanden Haendel 255
- Goudsmit, Back and 118, 135
 Uhlenbeck and 292
- Gozzini 275
- Grotrian diagrams 283
- Ground state 19, 31, 161, 287, 166
- Gyromagnetic ratio, in terms of the Landé factor 248
 manifestation of, by a mechanical effect 213
 measurement of, by magnetic resonance 234
 nuclear 116
 orbital 209
 relativistic expression for 296
 spin 291
- Gyroscopic effect (or diamagnetic effect) 209
- Hamiltonian, of a many-electron atom 23
 of an electron in a magnetic field 89
 of the hydrogen atom 2
- Hanle 150
- de Haas, Einstein and 213
 Gorter and Vanden Haendel 255
- Half-life 75
- Half-width 102
- Helium, exchange interaction in 74
 ion spectrum of 164
- Hertz; *see* Franck
- Holbourn 271
- Hollow cathode 145
- Hund 256, 56
- Hunt, Duane and 177
- Hydrogen, Balmer-Rydberg law for 14
 Bohr model of 158
 energy-level diagram of 17
 fine structure of 75
 ortho and para 113
 quantum theory of 2
- Hydrogen maser 160
- Hydrogen-like ions 162
- Hyperfine structure 112
- Hyperfine splitting data 121
- Identical particles 26
- I-J* coupling 119, 132
- Imprisonment (of a resonance line) 79
- Independent electron approximation 22
- Induced (stimulated) emission 80, 108, 260, 155
- Inelastic collisions, and elastic 27, 63
 of electrons 24, 182
 of photons 54
- Interactions within an atom 22
- Intercombination lines 71
- Interference, between two lasers 127
 of electrons 129
 of single photons 94, 128
- Inversion of population 112, 290
- Ionisation, by collisions with electrons 24, 181, 183
 light-induced 12
 of alkali atoms and rare gases 27
- Ionisation cross-section 185
- Ionisation potential and energy 12, 24, 34
- Isotope shift 127, 198
 in mercury 129
- Javan 116
- j-j* coupling 51, 73, 109
- Kastler 287
- Kepler's law 156
- Keyser (unit of wavenumber) 34

- Kinetic energy, exchanged in collisions 28, 63
 relativistic 47
 Kossel 168
 Kusch and Foley 293
- Lagrange equations 86
 Lagrangian of an electron in a magnetic field 87
 Laguerre polynomials 6
 Lamb shift 80, 157
 Landé factor, definition of 248
 for electron spin 292
 measurement of, by Zeeman effect 277
 nuclear 117
 quantum theory of 94
 sign of 118
 Landé interval rule 69, 121
 Langevin theory of magnetisation 250
 Laplacian in spherical polar co-ordinates 2
 Larmor angular frequency 210
 Larmor angular velocity 199
 Larmor explanation of Zeeman effect 203
 Larmor precession 208
 Larmor theorem 197
 Laser, gas 115, 117
 general description of 108
 ruby 115
 use of, in spectroscopy 146
 Lebedew 44
 Legendre polynomials 4
 Lenard 24
 Level-crossing 105, 147
 Lifetime, classical theory of 79, 207
 coherence 126, 154, 162
 imprisonment 79
 of an excited state 73, 170
 Linear oscillator 202
 Lineshape 144
 Linewidth, absorption 71
 Doppler 21, 144, 154
 emission 21
 in magnetic resonance 229, 165, 166
 natural 23, 100, 144, 149, 154
 Stark 23
L-S coupling 48, 66, 68, 93
 Lorentz curve 102
 Louisell, Pidd and Crane 295
 Lummer and Pringsheim 5
 Lyman series 17, 20, 160, 197
- Magnetic field and induction 193
 Magnetic quantum number 246
 Magnetic sublevel 249, 97
 Magnetic moment (dipole), anomalous, of the electron 293, 297
 classical microscopic definition of 194, 220
 effective 136
 nuclear 116
 of the proton and of the neutron 113, 114
 quantisation of 248
 relationship of, to angular momentum 208
 resultant, in *I-J* coupling 131
 resultant, in *L-S* coupling 93, 98
 spin 291, 43
 subjected to an inhomogeneous field 240
 subjected to a uniform field 209
 Magnetic resonance, and circular polarisation 273
 Bloch equations for 226
 Bloch method of detection of 232
 classical explanation of 223
 detection of, in an atomic beam (Rabi's method) 257, 163
 mechanical 275
 multiple quantum transitions in 167
 nuclear 234
 on free-electron spins 299
 optical detection of 284, 287, 161, 166
 quantum explanation of 257
 radiofrequency detection of 231, 260
 Magnetisation, diamagnetic 202
 due to orbital motion 213, 219
 longitudinal and transverse 213
 paramagnetic 211
 rotating (in magnetic resonance) 229
 Magnetometer 234
 Magnetron, Bohr 248
 nuclear 114
 Magyar and Mandel 127
 Maiman 115
 Mandel and Pfligor 128
 Marsden, Geiger and 154
 Maser, general description of 108
 hydrogen 160
 three-level 113
 Townes's 112
 Mass, centre of 142
 of the electron and of the proton 36
 reduced 143
 units of 34, 35
 Mass effect (in spectroscopy) 127
 Matrix element, of a scalar operator 232
 of a vector operator 234
 Maxwell's equations 39, 201
 Mendeleev (periodic) table 37
 Mercury, energy-level diagram of 72
 hyperfine structure of 129
 isotope shift of 129
 isotopes of 130
 magnetic resonance in an excited state of 284
 Mesic atoms 192, 195
 Metastable state 33, 73, 158
 Millikan (photoelectric effect) 10
 MKSA (SI) system of units xiii, 200
 Model, Bohr 158
 notion of a 166
 planetary (Rutherford's) 141, 151, 154
 shell *chapter 2*
 Thomson 153, 157
 vector 66, 95, 98, 102, 111
 Momentum, conservation of 42, 46
 expressed in terms of a wave vector 97
 generalised, of a charge in a magnetic field 87, 89
 of a photon 46
 of radiation 37, 42
 Moseley's law 186
 Mössbauer effect 58

- Multiplet level 50
 Multiplicity 49
 Multipoles (in classical theory) 214
 μ -mesons 192
 Muonium 191, 195
- Natural width 23, 100, 144, 149, 154
 Neutron, electric dipole moment of 187
 spin and magnetic moment of 114
 Noise, signal-to-, ratio 141
 Normal Zeeman effect 203, 282
 Nuclear magnetic resonance (n.m.r.) 234
 Nucleus, angular momentum and magnetic moment of 113
 electric quadrupole moment of 125
 existence of (Rutherford) 145
 mass and volume effects 127
- Optical pumping 115, 287, 166
 Optical resonance 18
 Optics, non-linear 125
 Orbit, Bohr 161
 penetrating 189, 16, 195
 Sommerfeld 164
 spin-, interaction 43
 Orbital angular velocity 162
 Orbitals 13
 Order of degeneracy, of a configuration 29
 of energy levels in j - j coupling 52
 of energy levels in L - S coupling 50, 53
 of the levels of hydrogen 8
 in the theory of radiation 83
 Orientation, of angular momenta or polarisation 212, 250, 288, 300, 114
Ortho-hydrogen 113
 Oscillator, linear 202
 strength of 173, 170
- Para*-hydrogen 113
 Paramagnetic magnetisation 211, 250
 Paramagnetic resonance 234
 Paschen series 17, 160
 Paschen-Back effect 99
 total 111
 Pauli principle 183, 28, 53
 Penetrating orbit 189, 16, 195
 Periodic table 37
 Perturbation theory, application of, to the problem of an external field 96, 99
 to the problem of electronic interactions 23
 to the problem of magnetic interactions 47
 principle of 93
 Pflugor and Mandel 128
 Pfund series 17, 161
 Photoelectric effect, in metals 5
 photoionisation 12, 62
 X-ray 171
 Photomultiplier 90
 Photon, angular momentum of 273
 energy of 5, 8, 15
 interference 92
 momentum of 46
 Photon absorption 66
 Photon counting 90
 Photon collisions 48-64
 Pickering 164
 Pierce, Bragg and 171
 Planck constant 5, 35
 Planck formula (radiation) 5, 85
 Planetary model 141, 151, 154
 Polarisation of angular momenta; *see* Orientation
 Populations of atomic states, in an optical-resonance experiment 82
 in magnetic resonance 259
 in paramagnetism 251
 in thermal equilibrium 83, 111, 212, 251, 156
 inversion of 112, 290
 spontaneous evolution of 74
 Positron 62, 192
 Positronium 192
 Potential, central (in classical theory) 144
 central (in quantum theory) 3
 contact 10
 critical 32
 extraction or escape 8
 ionisation 12, 24, 34
 non-coulomb 16
 resonance 28
 Precession, Larmor 208
 Principal quantum number 159
 Pringsheim, Lummer and 5
 Probability, and amplitude of a wave 92
 and cross-section 68
 of a collision 66
 of a transition 70, 257
 of spontaneous emission 73
 of stimulated emission 82
 position, of an electron in an atom 9
 Probability density, angular 12
 radial 11
 of the sodium atom 21
 Prokhorov 113
 Proton, mass of 36
 resonance 234, 114
 spin and magnetic moment 113
 Pumping, optical 115, 287, 166
 radiofrequency 113
 Purcell 232
- Quadrupole; *see* electric quadrupole moment
 Quadrupole tensor 222
 Quantisation, of angular momenta 159, 245, 40
 of energy chapter 1
 spatial 239
 Quantum number, and Pauli's principle 28
 angular momentum 246
 effective 19
 half-integral 246
 magnetic 246, 4
 principal 159, 165, 6
 spin 291
 Quantum efficiency 11
 Quenching 83
- Rabi 257, 136, 163
 Radial wavefunction 5

- Radiation, classical theory of 202
 deceleration (Bremsstrahlung) 62, 177, 205
 Einstein theory of 80
 laser 123
 scattered 211
 spectral 13
 spontaneous 73
 stimulated (or induced) 108
 thermal (black body) 3, 13, 85
- Radiation pressure, and momentum 42
 classical theory of 37
 experimental evidence for 43
- Radiative corrections 79
- Radiofrequency spectroscopy 154
- Radiometer 44
- Radius (mean) of the hydrogen atom 162, 15
- Radloff 128
- Ramsey 160, 165, 191
- Rare earths 34, 36
- Rayleigh scattering 213
- Recoil, absence of (Mössbauer) 61
 of an electron (Compton) 53
 of a nucleus (γ -emission) 58
- Reduced mass 143
- Reference frame, centre of mass 142
 Larmor 198
 rotating (in magnetic resonance) 224
- Refractive index (real and imaginary parts) 208
- Relativistic energy-momentum relationship 47
- Relativistic field transformation 43
- Relaxation, longitudinal and transverse 213
 in magnetic resonance 226, 261, 167
 magnetic 211
 paramagnetic 211
 time 213
- Resonance, energy 31
 line 19, 31, 72
 optical 18, 56, 81, 185
 paramagnetic 234
 potential 28
- Retherford, Lamb and 80, 157
- Reversal; *see* Self-reversal
- Ritz 16, 178
- Roth 256
- R.P.D. (retarding potential difference) 184
- Rutherford's model of the atom 154
- Rutherford's scattering experiment 145
- Rydberg constant 14, 158, 160, 186
- Rydberg law 14, 158
- Saturation, of magnetic resonance 229, 262
 of magnetisation 253
- Scattering, Bragg 135
 classical Rayleigh 213
 classical Thomson 54, 211
 Compton 48
 multiple 79, 162
 of electrons 293
 of particles (Rutherford) 145
- Schawlow 117, 81
- Schrödinger's equation 2
- Screening effect and coefficient of 188
- Screening separation 84
- Selection rules, for magnetic quantum number 276
 general 59
 in j - j coupling 74
 in L - S coupling 71
 in X-ray spectra 181, 84
- Self-reversal of a resonance line 73
- Series (of spectral lines) hydrogen 17, 160
 X-ray 178
- Shells (electronic) 27, 29
- SI system of units xiii, 200
- Singlet level 50
- Sodium, energy-level diagram for 64
 ground state configuration of 42
 probability density of electrons in 21
- Sommerfeld, Bohr-, comparison with quantum mechanics 13
- Sommerfeld elliptic orbits 164
- Spectral term 15, 178, 75
- Spectroscopic notation 50
- Spectroscopy, level-crossing 147
 of alkalis 61
 of atoms with two electrons 65
 of hydrogen 14, 158, 75
 of X-rays 168, 81
 optical 13
 radiofrequency 154
- Spectrum, continuous 14
 line 14, 177
 photoelectron velocity 172
 X-ray absorption 169
 X-ray emission 175
- Specular reflection 20
- Spin, nuclear 117
 of the free electron 291
- Spin magnetic moment 292
- Spin-orbit coupling 43
- Spin quantum number 292
- Spontaneous emission 73, 173
- Standards of frequency and of time 121, 161, 170
- Stark effect 23
- States, excited 20
 ground 19, 32, 161, 287, 166
- Statistical weight; *see* Order of degeneracy
- Stefan's law 44
- Stern, and Gerlach 239, 137
 Estermann and Frisch 113
- Stimulated (induced) emission 80, 108, 260, 155
- Stripping 176
- Structure, fine 188, 49
 constant 161
 of hydrogen 164, 75
 of the alkalis 61
 hyperfine 112 (chapter 6)
- Superradiance 118
- Susceptibility, diamagnetic 201, 203
- Temperature, negative 112, 290
- Tensor, quadrupole 222
- Tensor operator 236
- Thomas 45
- Time, imprisonment, of a resonance line 79
 relaxation 213
- Thermal emission, radiation 3, 13
- Thermal equilibrium 85, 111, 212, 251, 156

- Thermoelectric effect 8, 24
 Thomson scattering 54, 211
 Thomson model of the atom 20, 153, 157
 Threshold frequency, for photoelectric effect in metals 7
 photoionisation 12, 26
 X-ray absorption 171
 Townes 112, 113, 117
 Transition, electric dipole 60
 magnetic dipole 226, 61, 156
 multiple quantum 167
 spectral or radiative 16, 31, 65, 59
 Transition element 34, 36
 Transition probability 70, 257
 Triplet level 50
- Uhlenbeck and Goudsmit 292
 Uncertainty principle 96
 Units, of energy 35
 systems of xiii, 200
- Valence 36
 Van Leeuwen 238
 Vector model 66, 95, 98, 102, 111
 Vector operator 234
 Velocity, cyclotron angular 201, 297
 in a vapour 21, 28
 in an atomic beam 263
 Larmor angular 199
 orbital 162
 Volume effect (in spectroscopy) 127
- Wave, and corpuscle 87
 de Broglie, of a particle 128
 Fourier components of 98, 101
 induced (stimulated) 108
 polarised; *see* Circular polarisation
 Wave functions, angular 3, 10
 radial 5, 9
 Wavelength, Compton 53
 de Broglie 128
 of spectral lines 14
 Wavenumber 14, 32
 Wave vector 96
 Weisskopf 172
 Wigner-Eckart theorem 60, 94, 232
 Wilkinson 296
 Wood 18
- X-rays, absorption spectra of 169
 and Auger effect 182
 Bremsstrahlung 176
 diffraction of (Bragg's law) 169
 discontinuities in absorption of 170
 Moseley's law for 186
 photoelectric effect 171
 scattering (Thomson, Barkla) of 211
 selection rules for 179, 84
 X-ray emission lines 175, 81
- Young's slits 92
- Zavoisky 232
 Zeeman components 276
 Zeeman effect, anomalous 207
 classical explanation of 203
 including nuclear spin 131
 quantum explanation of 276
 Zeeman sublevels 249